भारतीय प्रौद्योगिकी संस्थान मुंबई
पवई, मुंबई-400 076, भारत
Indian Institute of Technology Bombay
Powai, Mumbai-400 076, India

दूरभाष/Phone : (+91-22) 2572 2545
फैक्स/Fax : (+91-22) 2572 3480
वेबसाईट/Website : www.iitb.ac.in

IIT Bombay

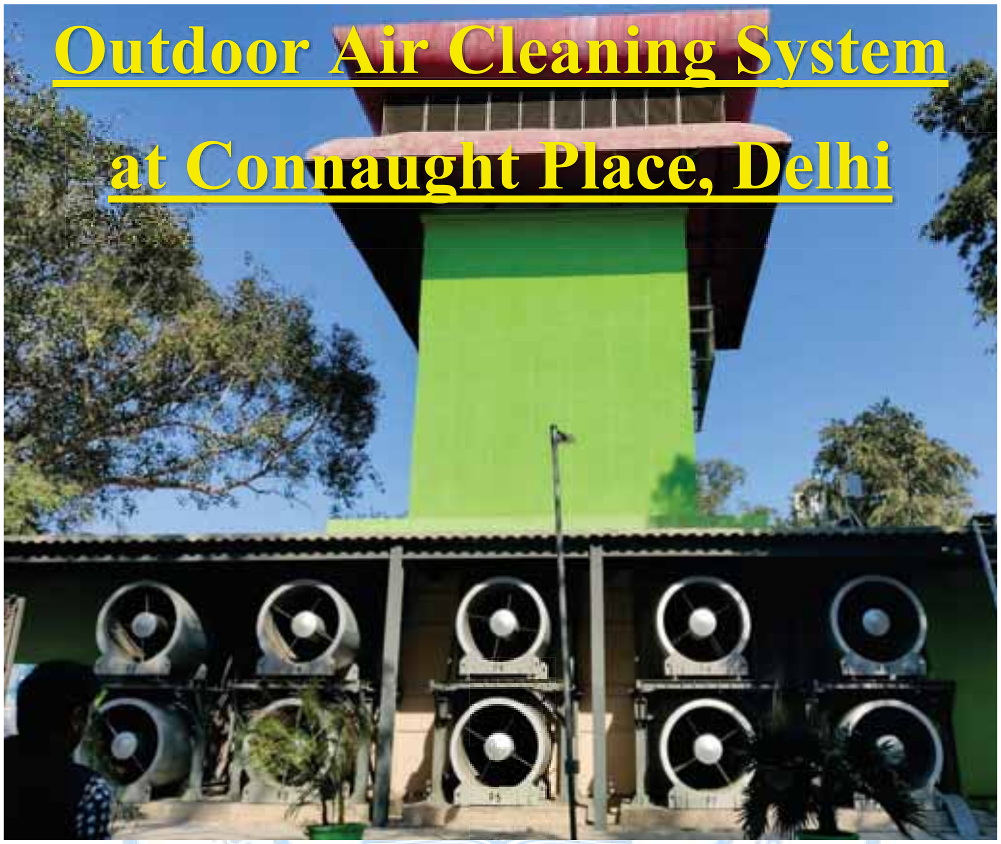

"Pilot Study for Assessment of Reducing Particulate Air Pollution in Urban Areas by Using Medium Scale Air Cleaning System (sometimes called as Smog Tower)"

Funded by Delhi Pollution Control Committee (DPCC)

(In respect of Indian Institute of Technology Bombay (IITB) roles and responsibilities as outlined in MoU)

Prepared by

Indian Institute of Technology Bombay

30th September 2023

BLANK PAGE

Team Members

S. No.	Name	Designation	Institute/ Organization name
1	Prof. Manoranjan Sahu	Principal Investigator (PI)	IITB
2	Prof. V. S. Vamsi Botlaguduru	Co-PI	IITB
3	Prof. Partha Sarathi Goswami	Co-PI	IITB
4	Prof. Abhishek Chakraborty	Co-PI	IITB
5	Prof. Swatantra Pratap Singh	Co-PI	IITB
6	Prof. Tabish Nawaz	Co-PI	IITB
7	Prof. M. V. Rane	Co-PI	IITB
8	Prof. Y. S Mayya	Technical Advisor/ Consultant	IITB

Members contributed to the report

S. No.	Name	Designation	Institute/ Organization name
1	Prof. Manoranjan Sahu	Principal Investigator (PI)	IITB
2	Prof. Y. S Mayya	Technical Advisor/ Consultant	IITB
3	Dr. Veerendra Sahu	Project Research Scientist	IITB
4	Dr. Rohit Kumar	Project Research Scientist	IITB
5	Mr. Kamlesh Dehariya	Senior Research Fellow	IITB
6	Miss Riya Parikh	Senior Research Fellow	IITB
7	Miss Labhini Pagarware	Junior Research Fellow	IITB
8	Mr. Anwar Hameed Banday	Project Assistant	IITB
9	Mr. Ashok Bishnoi	Project Assistant	IITB
10	Mr. Aditya Sharma	Former Project Assistant	IITB
11	Mr. Prashant Nawale	PhD student	IITB
12	Mr. Mohd Zaid	PhD Student	IITB

Preamble

This is the final report of the outdoor Air Cleaning System project at Connaught Place titled "**Pilot Study for Assessment of Reducing Particulate Air Pollution in Urban Areas by Using Air Cleaning System (sometimes called as Smog Tower)".** A Tripartite MoU between IITB, TPL & DPCC was signed on 7th August 2020, effective from 29th October 2020 for the execution of the project.

This final report is subsequent to the submission of the Inception Report, Interim Report-1 and Interim Report-2 of the project at Connaught Place. This report deals with the activities carried out by IITB in accordance with the roles namely, scientific advice, technical guidance, and assistance to PMC in performing technical coordination with all partners, performance evaluation of the air cleaning system through field experiments after commissioning, analysis of the data and validation of numerical models.

As per the MoU, the Inception Report included three important aspects: (1) Literature review on Air cleaning technologies (2) Status of placing of indents of monitoring system (3) Modelling status report. This report was submitted on 6th January 2021 after two months of project start up. Subsequent to the inception report, as per MoU, the first Interim Report-1 submitted on 4th September 2021 consisted of four important aspects (1) Status of acquisition of monitoring equipment (2) Protocol development (monitoring, validation, etc.) (3) Pre-operational measurements (4) Intrinsic data (flow rate, etc.) of the air cleaner system along with particle size distribution. In the Interim Report-2, as per MoU, a report was submitted on 15th September 2022 that included 1) One-year concentration data around the tower system, 2) First analysis of results including particle size distribution profile, 3) Optimization of operating parameters using numerical modelling results and 4) Presentation of interim results. As per the MoU, the final report now submitted includes the following activities: 1) Two-year concentration data, 2) Comprehensive analysis of air cleaning effectiveness, 3) Data on zone of influence, 4) Comparison with numerical modelling, 5) Summary and Conclusions and 6) Over all recommendations. It is also expected as per MoU that there will be a final presentation from IITB.

It may be noted that in the interest of successful execution of the project, IIT Bombay has worked beyond the strict confines of the MoU for smooth execution and functioning of the MSACS for comprehensive evaluation, considering that no prior information/knowledge was available on this type of air cleaner. Some of these new aspects are: theoretical developments, troubleshooting and commissioning, development of Standard Operating Procedures (SOPs) for various troubleshooting activities, evaluation of indigenous filters supplied by local vendors.

The present report completes the pilot study of MSACS at Connaught Place. It provides the basic performance evaluation data in considerable depth and detail, its validation through modelling and provides summary takeaways regarding the impact of the system in the ambient domain through summary and conclusions and suggests future recommendations.

Table of Contents

List of Figures

List of Tables

1 Background of the Project

Technological solutions for creating clean air zones in human confluence regions should be considered important supplementary options among the portfolio of measures to combat severe air pollution episodes. This forms the core philosophy behind setting up outdoor air cleaners. These are also sometimes referred to as large-scale or medium-scale air cleaners, as the case may be.

Large-scale outdoor air cleaning is a novel concept that received the attention of scientists and technologists less than ten years ago. It was first designed on a viable scale by the University of Minnesota/Clean-Care Limited (UoM/CCL), and its demonstration was done by setting up a solar-assisted unit in Xian City, China. To explore the suitability of such technological solutions in the Indian context, IIT Bombay (IITB) formulated, after consideration of various mentions of air cleaners in the public domain, a way forward by entering into technical discussions with the UoM/CCL and then making a joint proposal to Delhi Pollution Control Committee (DPCC). It is to be noted that the original proposal was put up to Central Pollution Control Board (CPCB) to establish such an air cleaning system in Delhi. Subsequently, based on the request from DPCC, the same proposal with suitable modifications was submitted to DPCC to install a similar system at Connaught Place. This eventually led to a multi-institutional collaborative project involving the UoM/CCL, IITB, IIT Delhi (IITD) and Tata Projects Limited (TPL), with funding from DPCC with well demarcated roles and responsibilities. The project was envisaged as a pilot study in which TPL will acquire design and component details from the CCL upon payment, build the structure and install the components making the system ready for commissioning. A Tripartite MoU was signed between IITB, Tata Projects and DPCC and the role of IITB was (i) to offer scientific and technical suggestions during the TPL-UoM discussions to ensure that the intended components with the right specifications are acquired for the system (ii) to help evolve methodology for intrinsic parameter monitoring and to acquire field measurement equipment for performance evaluation (iii) to build a computational fluid dynamics approach to pre-assess the potential impact (iv) to conduct field surveys for performance evaluation of the system for two years after installation (v) to validate the model and fine-tune it for future applications.

The medium-scale air cleaning system based on UoM/CCL design was installed at Connaught Place in Delhi in August 2021. This is envisaged as a zonal air cleaning device to deliver clean air within a limited range during severe pollution situations for places of confluence of significant populations in connection with their day to day activities in urban settings. Subsequent to installation, elaborate post-commissioning tests such as the ejected air flow rates, clean air delivery rates, filtration efficiencies, pressure drops, filter rigidity and leaks through gaps within the installed system were conducted. The purpose of this study was to critically assess the performance of a medium-scale air cleaning system (MSACS) aiming to create clean air zones in the Indian ecosystem for efficient air pollution management and its impacts on human health & the environment. To the best of our knowledge, such an approach to provide air purification in the Indian scenario is second of its kind (first one being at Anand vihar Delhi).

In this backdrop, the previous report (Inception Report) discussed the literature review, the monitoring instrumentation, concepts of CADR, first-level models and rationale for CFD modelling. In the Interim Report-1, progress in terms of freezing the components such as the filters and fans by TPL and the progress in performance evaluation preparatory strategies in monitoring and modelling were discussed in detail. The Interim Report-2 covered post-commissioning operational experiences that includes, commissioning and start-up experience, early observation in the system and fan operating philosophies followed by measurement-based performance evaluation results and CFD modelling studies that were conducted.

After initial commissioning and start-up, post-installation performance evaluation of the tower and operational testing were conducted under different scenarios. Systematic protocols were developed to assess the intrinsic performance of MSACS as well as its performance in the ambient domain. Simultaneously, CFD numerical models were developed, analysed, and comparisons were made with respect to monitoring results. As the MSACS is basically meant for high air pollution loads or scenarios such as winter, operation and measurements during the winter season along with other seasons were conducted systematically to assess the realistic efficiency of the system. During the 2nd year operation period, data were collected systematically under various operating and environmental conditions for arriving at definite conclusions about its performance during periods of high pollution episodes. The performance data were compared with CFD modelling results and are discussed in detail in this report. Future recommendations have been made based on the analysis of the data generated over the past 2-years post installation of the system.

1.1 Location of the Tower

The location for installation of MSACS system during the site visit by IIT Bombay and TPL in February 2020 that was finalized is shown in Figure 1 and marked with a square in green. The pictures taken during the same site visit are shown in Figure 2 and Figure 3. The visuals show garden and Gurudwara near the site.

1.1.1 Coordinates of the location

The MSACS is located in an area adjacent to the traffic training park (28.62827°, 77.21051°), Baba Kharak Singh Rd, near Gurudwara Bangla Sahib, Hanuman Road Area, Connaught Place, New Delhi, Delhi, India 110001. To the northeast (NE), 50 m is the junction of the Bangla Sahib lane to the Baba Kharak Singh road. In East-northeast (ENE), within 150 m is the ONGC Shivaji Maharaj Stadium station. At ~300 m in SouthWest (SW) from MSACS Bangla Sahib Gurudwara is loacted.

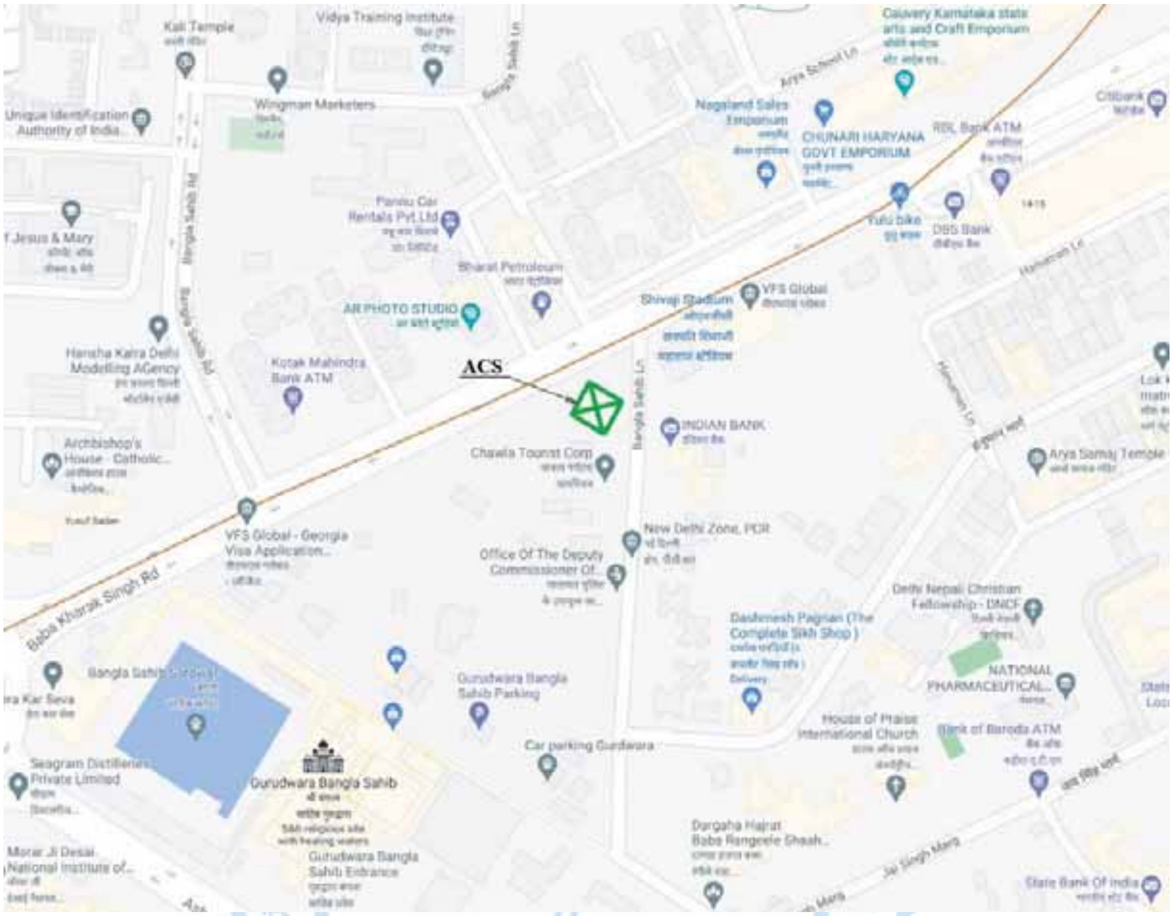

Figure 1. The proposed site location of MSACS in google map.

The topographic features around the MSACS site include: Traffic training school towards South at 29 m distance, a Residential building towards South-East at 43m distance, VFS Visa office towards North-East at 47 m distance, Residential Building towards North-west & North at 150 m distance, Church of Height approx. 22 m towards West at 360 m distance, and NDMC Building of Height approx. 75 m towards East at 445 m distance. Figure 1 shows a map view of the site location of the MSACS rotated around 50 degrees.

The residential buildings are located towards North-West and West-NorthWest with other structures near the MSACS. The presence of a lot of building structures around the tower and the traffic movement had three distinct consequences: (i) The buildings provided obstruction to the clean air flow, (ii) buildings also affected the airflow travel length and reduced clean air velocity, (iii) Introduced difficulty in performance evaluation.

Figure 2. Proposed site visuals before construction of MSACS.

Figure 3. Site visuals (with Gurudwara around) before construction of MSACS.

The location of the MSACS chosen is shown in Figure 4. The site pictures after the completion of construction of MSACS are shown in Figure 5 and Figure 6.

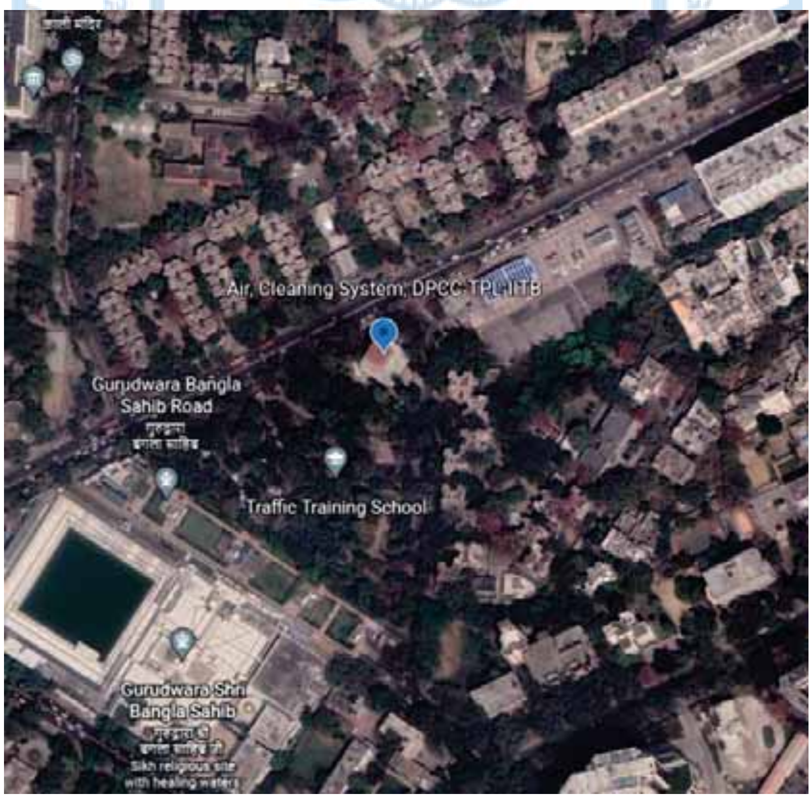

Figure 4. Google map of the site after MSACS construction.

Figure 5. MSACS constructed at Connaught Place, Delhi.

Figure 6. MSACS site view after completion of the construction.

2 Activities Conducted Post-Replacement of the Filters

After the successful commissioning of the MSACS in October 2021, and its operation for the period of one year, the filters were found to be loaded to their full capacity and required to be replaced with fresh filters. This was carried out during the second week of September 2022. The activities undertaken by IITB to render the system operational in different scenarios are presented below.

2.1 Operational Trouble Shooting and System Rectification

A total of 4800 pre-filters and 4800 fine filters were installed in the filter bank of the Medium Scale Air Cleaning System (MSACS). These filters need to be replaced from time to time based on their dust loading over the period of time. After the successful commissioning of the MSACS in October 2021, efforts were made for filter strengthening and operating the system as per the designed capacity. IITB has evolved the measurement strategy with the experience gained in the field since its construction and commissioning. Through multiple site visits, various leak points were identified, which were reported to Operation & Maintenance (O & M) team. IIT Bombay developed strategies/diagnostics tools to identify the leaks in the system. Several experiments were conducted from October 2021 to July 2022 to assess the system performance. The system pressure drop reached ~ 1.15 in-H_2O in July 2022, and the dust-loaded filters were replaced. As per the UoM experts, theoretically, the filters need to be replaced when the pressure drop reaches ~ 1.1 in-H_2O at 100% fan capacity. The old filters were replaced by one set of new filters (pre-filters and fine filters) in the middle of October 2022. The MSACS was kept ready for the winter period study after reinstalling one new set of filters. The system was kept again in operation from the last week of October 2022 and the field sampling was continued to assess the MSACS performance.

2.2 Filter replacement and reversing pre-filter directions to minimize filter dislodging

The filter installation work is crucial since all the leaks need to be addressed properly from the beginning of the filter installation work. After evaluating the system's internal performance over the previous year, it was found that the leaks and gaps between the pre-filters, and the gap between the filter frame and filters, were the major constrain for leak-proofing the system. Based on the dislodging experience gained at Anand Vihar MSACS, the system at Connaught Place was operated at 50% fan capacity. To operate at higher fan capacities it was advised to reverse the pre-filter direction, as shown in Figure 7 (a), as IIT Bombay professors and UoM experts suggested to minimize the gaps between the pre and fine filters to avoid filter dislodging and reduce the leaks from the system. The pre-filter direction, as previously installed in the system, is illustrated in Figure 7 (b). By reversing the direction of the filter, the gaps between the pre-filter and fine filter were reduced, and it was anticipated that it would help reduce the leaks.

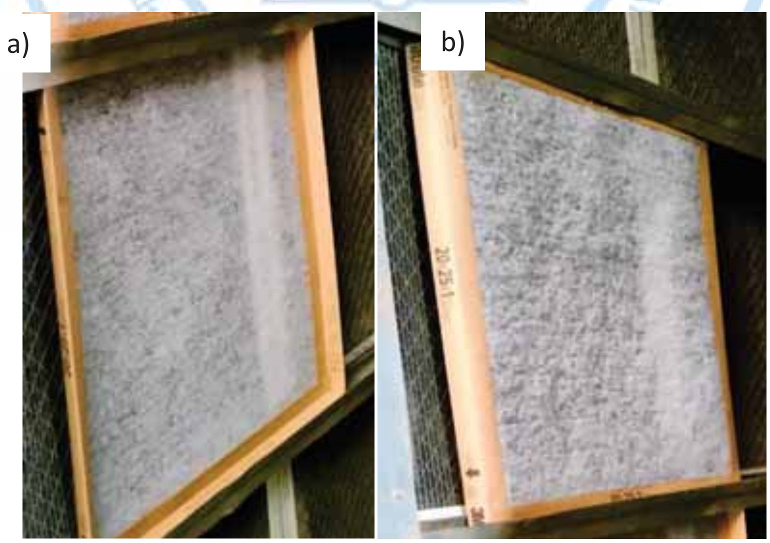

Figure 7. (a) Pre-filter placed in reversed direction (b) Pre-filter initial placement direction.

2.3 Institution of Standard Operating Procedure for filter replacement

Based on the previous year's operational experience after filter replacement, it was found that leaks still exists and the leak rate changes over a period of time. It is important to address all the possible leaks during the filter replacement period. Based on the experience, the following detailed Standard Operating Procedure (SOP) was developed in consultation with the TPL O&M team for the replacement of filters to maintain consistency in workmanship by the external vendors.

Standard Operating Procedure for Replacement of Filters

- **Objective**
  To lay down a procedure for replacing the pre-filters of the Air Cleaning system.

- **Scope**
  This Standard Operating Procedure is applicable for the replacement of the MSACS filters.

- **Responsibility**
  The site in-charge or executive will be in charge of carrying out this procedure.

Procedure for filter replacement:

First, it must be ensured that the new pre-filters are checked for their condition. The damaged or distorted filters need to be identified from the stored lot, i.e. received earlier.

- The quality of all the adhesive tape samples needs to be checked.
- All required materials should be stored at the site before starting the replacement works.
- Before removing the end plates of the filter bank assembly, the surrounding area needs to be cleaned properly with the help of a vacuum cleaner.
- After removing the filters, all filter frames should be cleaned properly with the help of cloths & vacuum cleaners.

- During each stage of work, keep in mind to have protection from dust.
- Before placing the new filters, all filter frames should be cleaned properly.
- All filters should be installed as per the direction shown in Figure 8.
- The foam adhesive tape should be fixed properly on the filter frame.
- All the gaps should be filled with thick-foam adhesive tape & locked with brown adhesive tape.
- All filters should be fixed properly in the frame to avoid leaks.
- The gaps between the filters and the filter frame must be adequately sealed.
- The damaged fine filters also need to be replaced with new fine filters.
- All filters' end plates should be appropriately tightened and leak-proof.
- Check all the leaks and seal all the possible leaks before the test run.
- Continuous checking and sealing of the leaks should be conducted throughout the system's operation.

Figure 8. Pre-filter installation.

2.4 Observations of leaks and gaps, rectification of the filters: seek and seal approach

After the reinstallation of one new set of filters (Pre-filter and Fine filter) in October 2022, the IIT Bombay field team examined the MSACS during the initial test run.

The observations regarding the possible leaks in the system were as follows:

- The cascade tapes between the filters and the filter frame were found to be removed from various frames (Figure 9 and Figure 10).
- The gaps were also created between the pre-filters when system was operated at higher fan capacity, i.e., 75% and 100% (Figure 11).
- The gaps were developed between the pre-filters and the filter frame (Figure 12).
- Some pre-filters were found dislodged, and fine filters were also found vibrating at 100% fan capacity.
- The unfiltered air was observed to be escaping from the gaps at the end-plates of the fine-filter assembly.

The early observations for possible leaks in the system are shown in Figure 11-8 (leak points are marked in blue boxes and arrows in the pic). These leaks needed to be addressed regularly by the O&M team on a priority basis by seeking and sealing approach, as suggested by IITB.

Figure 9. Cascade tape detached from fine filters.

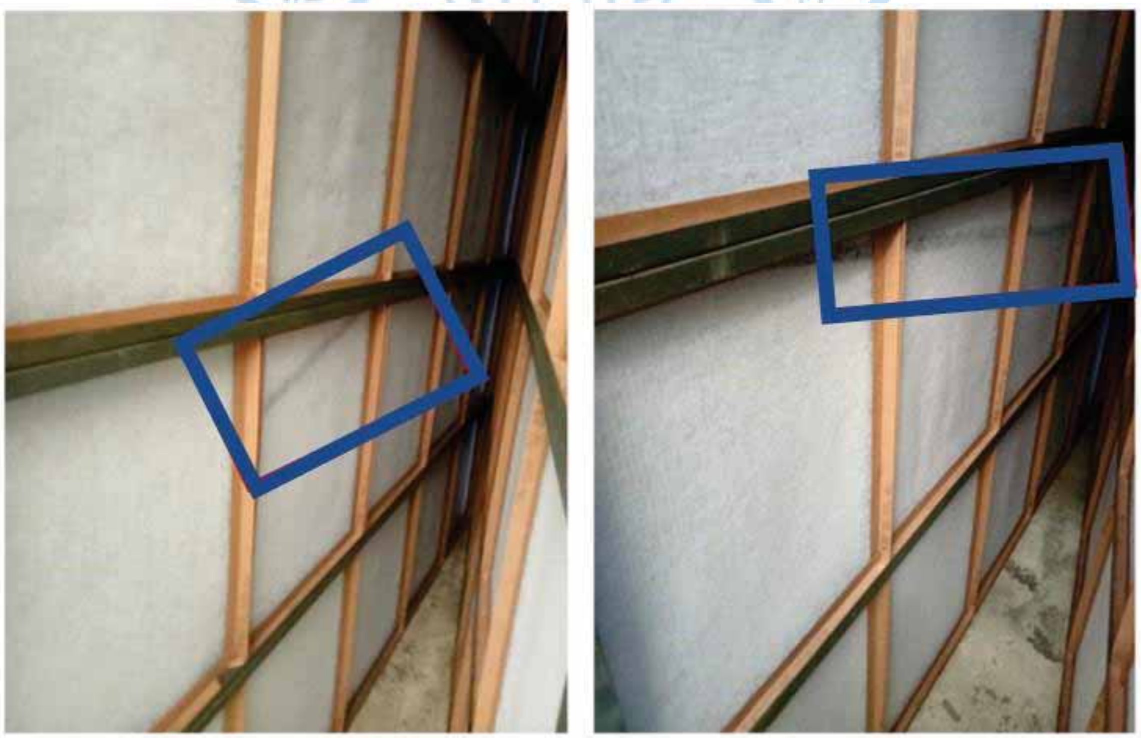

Figure 10. Cascade tape detached from pre-filters.

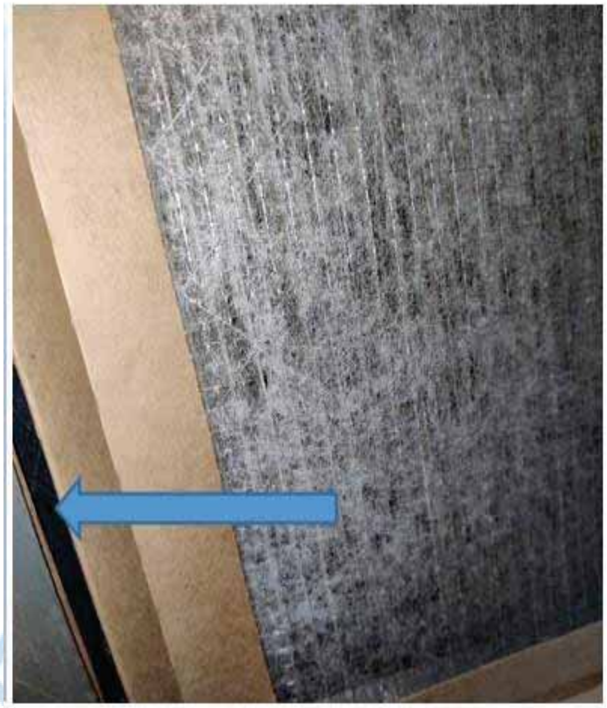

Figure 11. Gaps spotted between the pre-filters.

Figure 12. Gaps created between the pre-filters and filter frame.

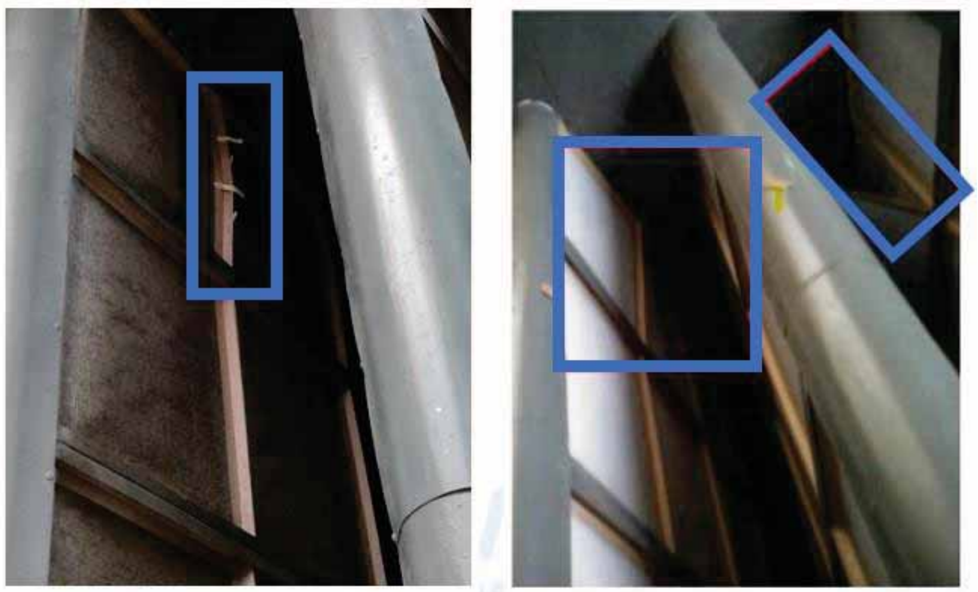

Figure 13. Dislodged pre-filters spotted at 100% fan capacity.

Figure 14. Leaks in the structural joints.

2.5 Assessment of performance improvement post rectification of leaks

The IITB team was rigorously involved in operational troubleshooting in system operations and identified several issues and various leaks in the system. It must be noted that, the unfiltered air enters into the buffer zone through all the possible leaks in the system and the gaps between the filters. Thereafter, the filtered air escaping out from the filter banks gets mixed with the polluted air, resulting in a decrease in the system efficiency. Thus, resolving these leaks is important to ensure that the MSACS deliver only filtered air to the surrounding area. Therefore, the possible leaks needed to be identified on a regular basis and required measures were needed to improve the system's efficiency. The IIT Bombay team suggested several corrective measures to the TPL O&M team to address the identified leaks in the system. The corrective measures suggested are as follows:

1- The pre-filters need to be joined side by side using adequate quality adhesive tape to avoid gaps between the pre-filters.
2- A good quality cascade tape needs to be used to seal the gaps between the filter frame and the filters.
3- Proper sealing of all joints in the frame using silicon.
4- All the structural leaks and cracks need to be repaired.

The corrective measures taken to address the leaks in the system are shown in Figure 15 and Figure 16.

Figure 15. Pre-filters are joined side by side using good-quality adhesive tapes to arrest the leaks/gaps between the filters.

Figure 16. Structural joint sealing using silicon for arresting the system leaks.

In a properly sealed, leak-proof system, the efficiency in the buffer zone should be very similar to intrinsic zone efficiency. The methodology to assess the buffer zone and intrinsic zone efficiency was already discussed in detail in the Interim Report-2 and other previous reports. However, it is not feasible to seal all the leaks in such a large system to achieve a leak-proof state. The system's efficiency in arresting the unfiltered air can be assessed by analysing the system leaks, which are responsible for escaping the unfiltered air. The percentage reduction in the overall leaks after system rectification and arresting the possible leaks is shown in Figure 17.

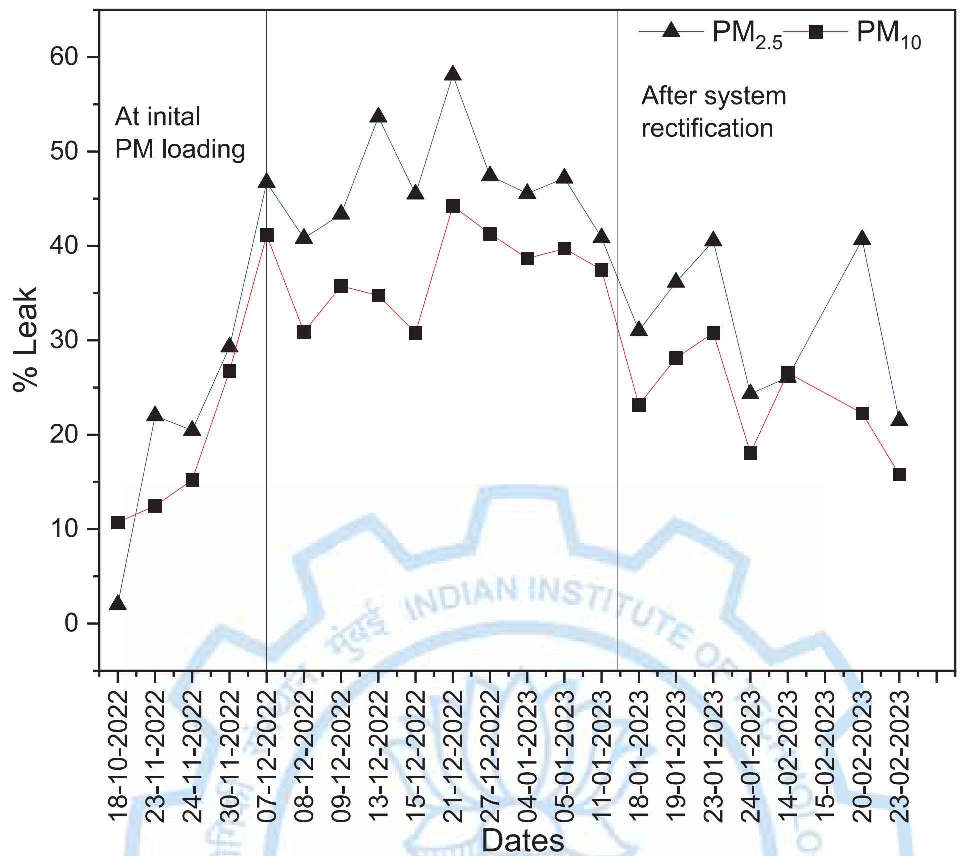

Figure 17. Percentage reduction in the leaks after system rectification.

Overall, the leaks in the system need to be addressed from time to time as new leaks were observed throughout the system operation. As the system operational time increases, more dust is deposited on the filters and pressure drop increases. Due to the rise in pressure drop, the unfiltered air will try to find the least resistance pathway to escape. Therefore, regular maintenance by diagnosing leaks is essential in this system. Considering the scale of the structure, it may not be possible to completely seal the system for unfiltered air. However, it was observed that the system could be rendered leakproof to 80-85% for arresting the unfiltered air.

2.6 Visual observation of filter condition during the operation period

After the reinstallation of one new set of filters (Pre-filter and Fine filter) in MSACS, the performance assessment was initiated for the winter period (October 2022 to February 2023). The filter visuals were captured for pre and fine-filter from time to time throughout the MSACS operation during winter to observe the filters' condition and are shown in Figure 18 to Figure 21. The pre and fine filters in fresh filter conditions are shown in Figure 18. Since a high pollution loading was observed in Delhi during the winter, a significant amount of particulate matter/dust started depositing on the pre-filters and fine filters in November 2022 (Figure 19). It was observed that initially, the fine filters have shown a higher dust loading compared to the pre-filters, as shown in Figure 19. Thereafter, the pre-filters have shown a higher amount of dust loading as compared to the fine filters, as shown in Figure 20, indicating the cake formation phenomenon on pre-filters. A detailed description regarding the dust loading on pre and fine filters is mentioned in section 4.6. The pre-filters were completely loaded with dust in the middle of February 2022, as shown in Figure 21, indicating that pre-filters started approaching their maximum dust loading capacity. The quantitative details for the dust loading on the pre and fine filters in g/m^2 on each filter are mentioned in Table 12. Further details about the change in dust loading throughout the MSACS operation during the studied winter period are discussed in section 4.6.

Figure 18. Visual observations of the filters at fresh conditions (a) Fine filters and (b) Pre-filters, October 2022.

Figure 19. Visual observations on the condition of filters in November 2022 (a) Pre-filters and (b) Fine filters.

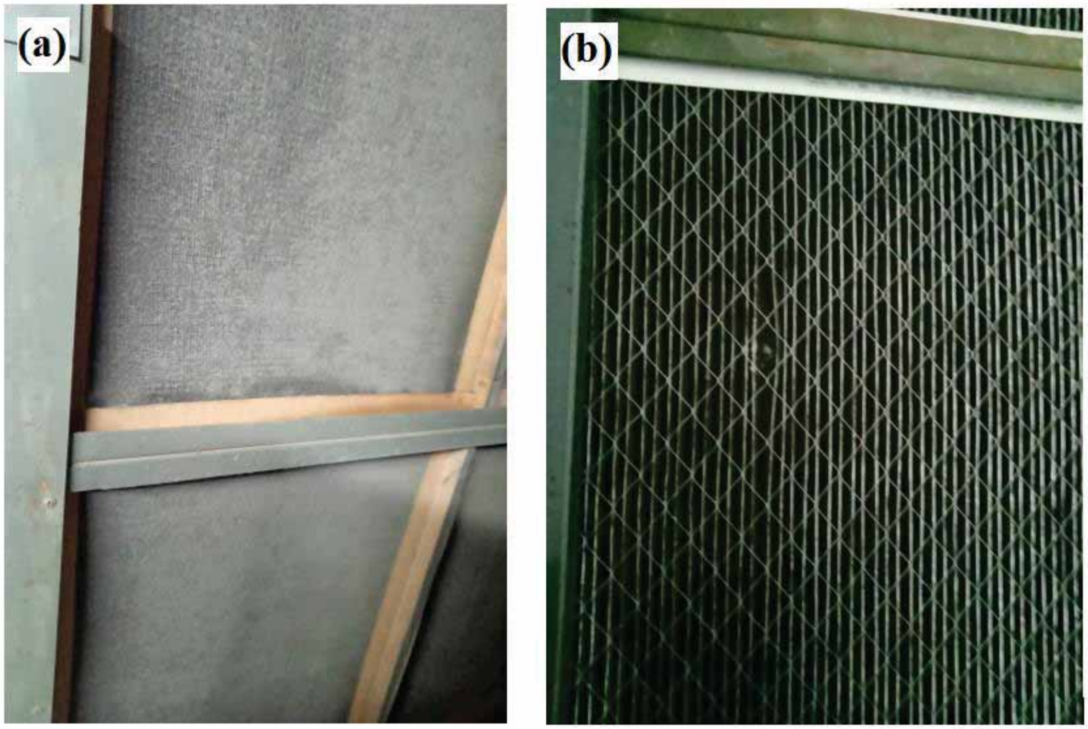

Figure 20. Visual observations on the condition of filters in January 2023 (a) Pre-filters and (b) Fine filters.

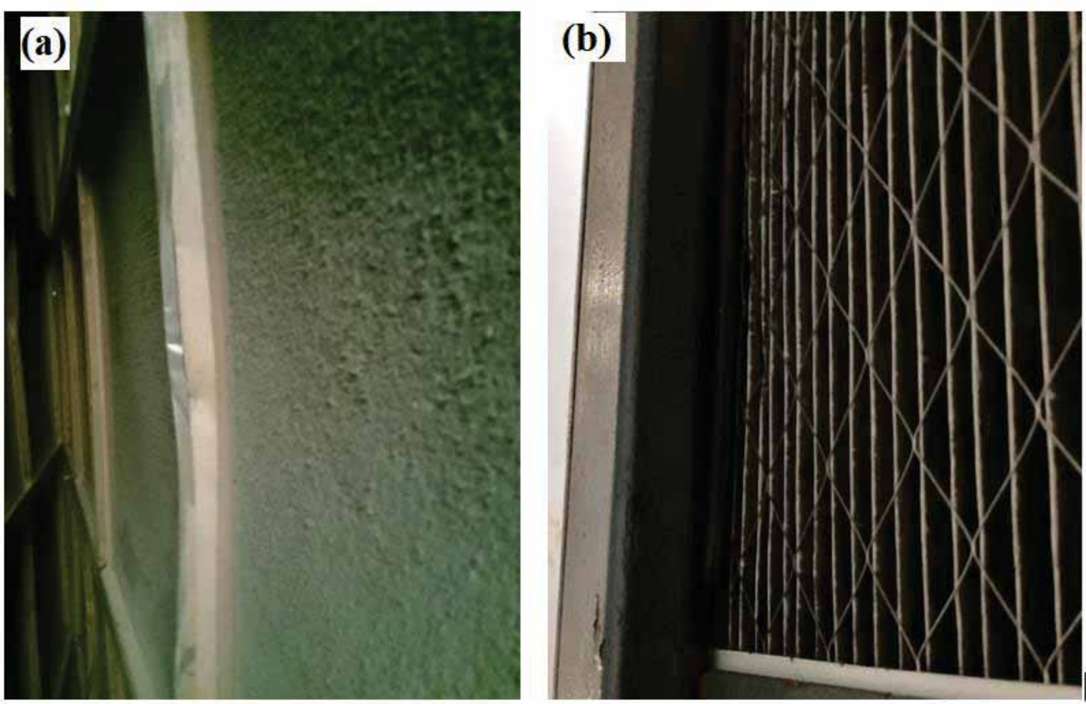

Figure 21. Visual observations on the condition of filters in February 2023 (a) Pre-filters and (b) Fine filters.

2.7 Quality control measures for data recording using monitoring instruments

The regular exposure of the monitoring instruments to the high pollution load in Delhi may affect the instrument's performance in quality data recording. Therefore, the optical chamber of the monitoring instruments was cleaned regularly once in two weeks to ensure that the instruments performed at their best during field measurements. The regular maintenance of the devices, i.e., DustTrak aerosol monitors, Optical Particle Sizer (OPS) and Environmental Beta Attenuation Monitor (E-BAM) was performed as mentioned in the instruments' guidebooks. The regular maintenance procedure for the instruments is shown in Figure 22 to Figure 28. Instruments from both the MSACS projects were calibrated simultaneously at one place.

The 'zero calibration' (calibration tests before starting the measurements) was performed prior to each use for all the DustTrak aerosol monitors (Figure 22). Further, all the DustTrak aerosol monitors and Optical Particle Sizers (OPS) were cleaned from time to time according to the amount of aerosol drawn through the instrument and dust load to keep the instrument in a good operating condition. The regular maintenance was done by following the maintenance guidebook and with prior guidance from the service engineer. The following actions were taken for the regular maintenance of the DustTrak aerosol monitors and OPS.

1- Instrument Cleaning:

   The inlet nozzle and inlet ports were cleaned properly using the dry cotton swab and an isopropanol-damped cotton swab, followed by blowing the air.

2- Internal Filter replacement:

   The 37-mm filter cassette and screen mesh were cleaned, and the exhausted filters were replaced with new filters.

The instrument was screwed properly after the maintenance. For DustTrak aerosol monitors', the filter counter was reset, and zero calibration was performed after the maintenance. The flow calibration was performed for OPS after the maintenance.

Figure 22. Zero calibration for DustTrak aerosol monitors.

Figure 23. Inlet nozzle and inlet port cleaning for DustTrak.

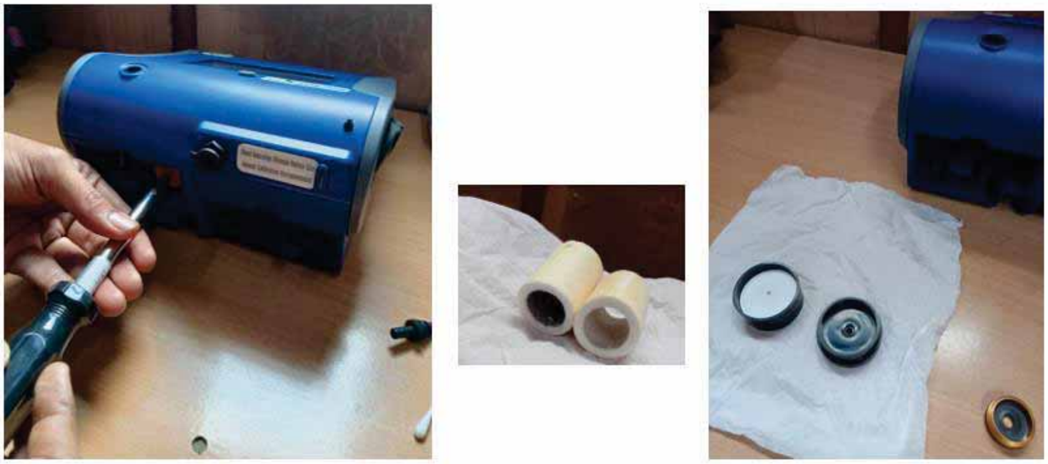

Figure 24. Internal filter replacement for DustTrak.

Figure 25. Internal cleaning of OPS.

Figure 26. OPS flow calibration.

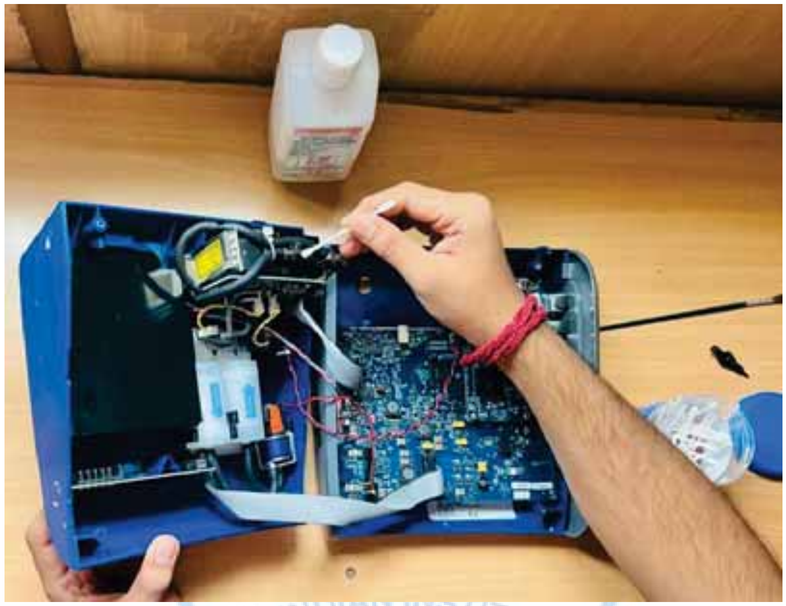

Figure 27. DustTrak internal cleaning.

The DustTrak aerosol monitors were cleaned from the inside with support from the TSI service engineer, as shown in Figure 27. The internal HEPA filters in the external pump modules were also changed once as recommended for the DustTrak aerosol monitors being used in a highly polluted environment.

The following actions were taken for the regular maintenance of E-BAM, as shown in Figure 28.

1- The suction head was cleaned.
2- $PM_{2.5}$ sharp cut cyclone was cleaned.
3- Weatherproof fitting, short inlet tube and other parts were cleaned.

The E-BAM filter tape was replaced from time to time once the filter tape was exhausted. The internal battery was replaced when required, and the instrument was also examined for calibration using a MetOne BX-302 filter kit to set it for local conditions.

Figure 28. Regular maintenance and cleaning of the reference grade instrument: E-BAM.

Along with the regular maintenance, the monitoring instruments were also corrected and serviced by the service engineers as and when required at the time of instrument failure. Since multiple devices were used for monitoring the mass and number concentration of the PM, from time to time, a colocation factor was also developed. The colocation for the DustTrak and OPS is shown in Figure 29.

Figure 29. Colocation of the DustTrak and OPS.

2.7.1 Correlation with different instruments

Timely maintenance and correlation of the same instrument were conducted to have information on the deviation between the instruments. A correction factor was applied to the deviating instruments to bring all the instruments on the same level. The instrument was properly cleaned, and due maintenance was done from time to time if a good correlation (R^2>0.7) was not obtained.

DustTrak

A correlation between different DustTrak (DT) instruments is shown in Figure 30. The scatter plots were analysed to assess the correlation between the DustTrak instruments. The reference DustTrak instrument used was DT 1 i.e., the latest calibrated from the manufacturer's laboratory. The black square box shows the correlation between DT 2 and DT 1. The red circle shows the correlation between DT 4 and DT 1. While the blue triangle shows the correlation between DT 5 and DT 1. It was found that all three instruments were correlating well, and a correction factor, i.e., the slope, is multiplied by the respective DustTrak.

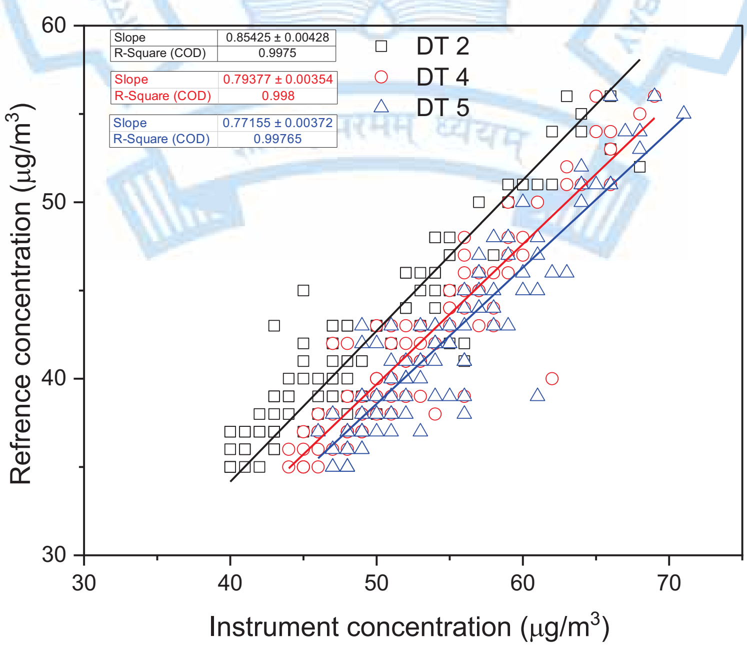

Figure 30. Correlation between DustTrak instruments.

Inter-comparison between two E-BAM

An inter-comparison study was performed to check the variability between the two instruments. Both instruments were located nearby (~ 4 m), and PM_{10} concentrations were measured. Both E-BAMs recorded the data at the 15-minute interval, and the colocation was performed for ten days. The error values were removed from the data as an outlier. The study showed an R^2 of 0.94 with a slope value of 1.22, as shown in Figure 31. A time series graph is shown in Figure 32; it was observed that the trend for both the E-BAMs was similar, and E-BAM 2 overestimates the value by ~ 20%. The variability between both the E-BAMs was found to be within the acceptable range recommended by the instrument manufacturer. The timely maintenance were conducted by service engineer for both the E-BAMs to avoid deviation between instruments.

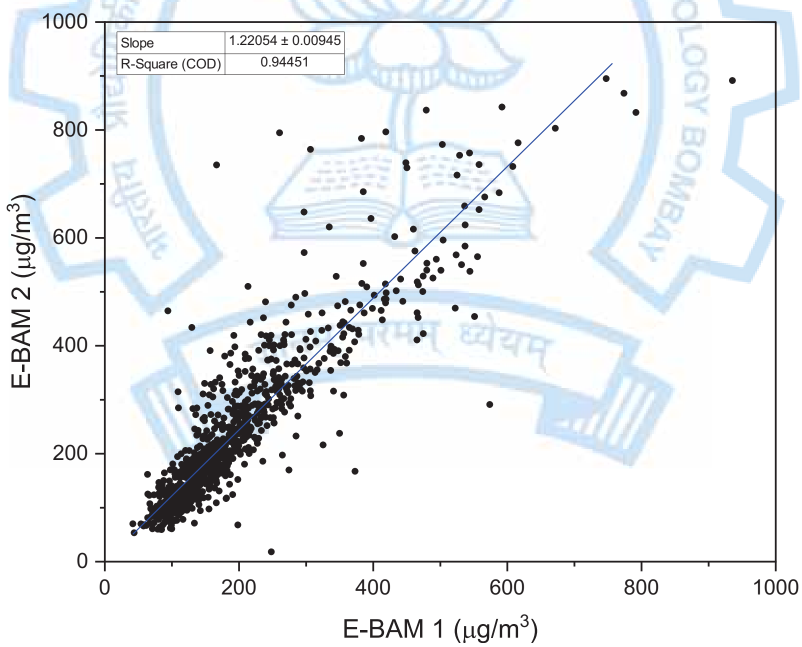

Figure 31. Correlation between E-BAM instruments.

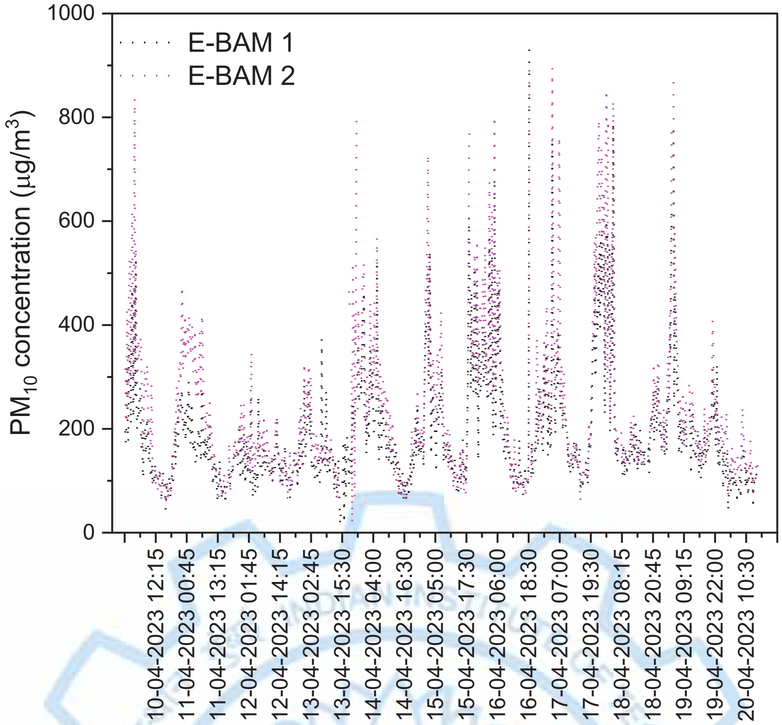

Figure 32. Time series for both the E-BAMs.

3 Indigenous Filter Development Efforts for the MSACS

The fine and pre-filters used in the MSACS were imported from 3M USA. The procurement process for these filters is quite complex and time-consuming. Following the similar schedule provided by CPCB, the calculations based on the PM concentration for 2019 Mandir Marg data, it was found that 5-6 sets of pre-filter and 2 sets of fine filters replacement was required. These filters are quite expensive also. In view of this, efforts were made to find Indian suppliers that can supply the filters for the MSACS on a continuous basis. One important point to note is that the filters should match or have similar characteristics to the 3M filter to achieve a similar level of performance. The detailed specification was supplied to TPL for identifying various Indian suppliers. The details are described below.

3.1 Characteristics of filters used in MSACS and comparison of filters supplied by Indian companies

The two types of filters (Pre-filter and Finefilter) used in MSACS has unique media characteristic that enhances the capture of Particulate Matter (PM). The pre-filter (MERV-2) used in the system is capable of capturing coarser size particles (while the fine-filter (MERV-13) captures coarser size particles (<95% efficiency for 3.0-10.0 µm). The fine filters are made up of electrostatically charged fibre media which captures finer particles with an efficiency of >65% for particle size 0.3-1.0 µm and ~90% for particle size 1.0-3.0 µm.

The important criterion considered for the selection of filter/filter media is a low initial pressure drop, as a high initial pressure drop would not be cost-efficient. Another criterion that was considered is the filtration efficiency at different dust loadings. As observed, depending on the filter media used, the efficiency differs with an increase in the dust loading (Explained in section 4.2). Dust holding capacity is an important criterion to be considered, as this will determine the replacement period of the filters used in the system. As the filters used in the system are already tested and supported by several published research, 3M filters were considered to be the basis for evaluating other companies' filters. Table 1 describes the specifications for the 3M pre-filters. The initial pressure drop for pre-filter at 1000 m^3/hr and 0.65 m/s face velocity, a 3M 20×25×1 inch, was 9.6 Pa.

One of the important characteristics of the fine filter media is its' electrostatic charged fibre, which enhances the filtration capacity with less initial pressure drop. The media is pleated for increasing its surface area and for reducing its face velocity. All the testing on the filter media was done as per the standard testing method mentioned in ASHRAE (The American Society of Heating, Refrigerating and Air-Conditioning Engineers) 52.2.

Table 2 describes the specifications for the 3M fine filters. The initial pressure drop of 3M fine filter at 1000 m^3/hr and 0.65 m/s face velocity of 20×25×1 inch was 19 Pa and the filter efficiency was >65% for 0.3-1.0 µm, 90% for 1.0-3.0 µm, and >95% for 0.3-1.0 µm.

Table 1. Technical specifications for the 3M pre-filter.

Sr. No.	Specifications	Range/ Required (3M pre-filter)
1	**Name**	Flat Panel Air Filter
2	**Nominal Length**	25 inch
3	**Overall Thickness**	1 inch
4	**Overall Width**	20 inch
5	**Filter Media Size**	18 in x 23 in
6	**Testing**	ASHRAE 52.2
7	**MERV Rating**	2
8	**Filter frame**	1 inch x1 inch x 1 inch (Cardboard)
9	**Construction**	Non- Electrostatic/ electrostatic filter media surrounded by a cardboard frame
10	**Filter Efficiency**	~20% efficiency for average particle size for 3.0-10.0 µm
11	**Captures**	Lint, Household Dust, PM_{10}

12	**Filter loading vs pressure drop**	20×25×1	290	430	575	720	970	Air Flow (CFM)
			0.04	0.07	0.10	0.14	0.21	Initial Resistance (inches H_2O)

Table 2. Technical specifications for the 3M fine filter.

Sr. No.	Specifications	Range/ Required (3M fine-filter)
1	**Name**	Premium Allergen & Home Pollutants Air Filter
2	**Nominal Length**	25 inch
3	**Overall Thickness**	1 inch
4	**Overall Width**	20 inch
5	**MERV**	13
6	**Filter Media Size**	18 inch x 23 inch
7	**Testing**	ASHRAE 52.2
8	**Filter frame**	1 inch x1 inch x 1 inch (cardboard)
9	**Solidity (1-porosity)**	0.090 - 0.095
10	**Pressure drop for face velocity of 14 cm/s (mm H_20)**	1.2-1.3
11	**Flow Rate (m^3/hr)**	1000
12	**HVAC filters**	YES
13	**Effective Fibre diameter**	17-17.5 μm
14	**Thickness of filter media**	0.7-0.75 mm
15	**Construction**	Pleated polyolefin filter media surrounded by a cardboard frame and supported by polyolefin strands on one side. The finished product should contain 42 pleats per foot.
16	**Captures**	Lint, Household Dust, Dust Mite Debris, Mold Spores, Pollen, Pet Dander, Smoke, Smog, Cough & Sneeze particles, Bacteria, Viruses, Candle Soot, $PM_{2.5}$ & Exhaust Particles
17	**Electrostatic charged; charging density.**	Electrostatically charged filter media with a significant microscopic bipolar charge on the fibres with charging density between 70-120 μC/m^2

<table>
<tr>
<td>18</td>
<td>Filter Performance and Filter Efficiency</td>
<td>Filter Flow Rate and Pressure Drop
<table>
<tr><td rowspan="2">20×25×1</td><td>515</td><td>770</td><td>1025</td><td>1280</td><td>1735</td><td>Air Flow (CFM)</td></tr>
<tr><td>0.06-0.08</td><td>0.12-0.14</td><td>0.18-0.20</td><td>0.27-0.29</td><td>0.41-0.43</td><td>Initial Resistance (inches H_2O)</td></tr>
</table>
Filter Efficiency (%)
<table>
<tr><td>e1</td><td>e2</td><td>e3</td></tr>
<tr><td>>65</td><td>90</td><td>>95</td></tr>
</table>
</td>
</tr>
</table>

3.2 Evaluation of filters quoted by local suppliers

The filters installed in the MSACS are of 3M, USA made. As these filters are exported from the USA, their procurement is time-consuming. It would take at least four-six months for a private vendor to acquire the filters. The pre-filters installed in the system are non-electrostatic filters, and the Indian suppliers can be consulted to procure the filter media. Each 3M pre-filter costs approximately Rs. 300-500 (overall cost required to get it on the site). Considering the dislodging problems which may occur when operated at higher fan capacities and PM loading in the system, and the high cost of the filters purchased from the USA, it was decided to look for suppliers who could provide strong filter frames. After inquiring with multiple local suppliers, it was suggested that the filter frame could be made reusable, either made up of aluminium or plastic. Buying the indigenous filter media would be more cost-effective as compared to importing the filters.

Few suppliers have submitted their specifications for either pre-filter and/or fine filter, and the IITB team has tried to evaluate the filters based on the available knowledge, even if the evaluation of the filter vendors is beyond the scope of the IITB research team. Multiple Indian suppliers like Spectrum, Airth, AFI and Camfil have submitted the specifications. Various aspects of filter requirements were discussed by the respective Indian suppliers. The comments and the remarks suggested by the IITB are given in Table 3 for pre-filters and Table 4 for fine filters.

3.2.1 Spectrum

Pre-filters and fine filter specifications were submitted by the Spectrum. A detailed comparison of the specifications is shown in Table 3 and Table 4. The company was ready to provide the MERV5 filter, a higher rating filter media than 3M. The fine filters provided by the company are non-electrostatic. However, the spectrum filter frame is made up of recyclable plastic, which can minimize the leaks in the system. The weight of both filters is quite heavy when compared to 3M.

Table 3. Spectrum: Technical specifications for the Spectra Pre "Blue Series".

Sr. No.	Specifications	Spectra Pre "Blue Series"	Remarks by IITB
1	**Name**	Spectra Pre "Blue Series"	
2	**Nominal Length**	25 in	Complied
3	**Overall Thickness**	1 in	
4	**Overall Width**	20 in	
5	**Filter Media Size**	18 in x 23 in	
6	**Testing**	ASHRAE 52.2	
7	**MERV Rating**	5	Currently using 3M filter of MERV 2 rating
8	**Filter frame**	1 in x1 in x 1 in	PP
9	**Construction**	Synthetic high loft washable media	Non-electrostatic thermal bonded polyester media
10	**Filter Efficiency**	As per MERV 5 rating, the efficiency should be higher than MERV 2, which is 3 to 10 µm	30% < **Spectra Pre " Blue Series"** > 20% efficiency for average particle size for 3.0-10.0 µm
11	**Captures**	The filter is constructed robustly and is suited for use in Comfort HVAC systems (Offices, Hospitals, Hotels, Educational Institutes) Filter	

		Towers, Clean Rooms (Food processing, pharmaceutical manufacturing, etc.)	
12	**Filter loading vs pressure drop**		Max Pressure drop (inch of H_2O): 0.07, 0.10, 0.14, 0.17, 0.23 Air Flow (CFM): 515, 770, 1025, 1280, 1735
13	**Filter loading vs efficiency**		30% <=E3 (3 to 10 µm)> 20%
14	**Critical replacement Loading**		
15	**Actual filter area per frame**		
16	**Weight of the filter per unit area**		1.0 Kg - Approx. Weight of pre-filter
17	**Pressure drop at the specified velocity**		
18	**The material of the filter media**		
19	**Summary:** More information on filter loading vs pressure drop and filter loading vs efficiency is helpful for evaluation.		

Table 4. Spectrum: Technical specifications for the Spectra Pre "Blue Series" pleated panel.

Sr. No.	Specifications	Spectra Pre "Blue Series"	IITB Remarks	Spectrum Comments
1	**Name**	Spectra Pre "Blue Series" Pleated Panel		
2	**Nominal Length**	25 in	Complied	
3	**Overall Thickness**	1 in		
4	**Overall Width**	20 in		
5	**MERV**	13		
6	**Filter Media Size**	18 in x 23 in	Filter surface area?	Filter surface area? - 1 m^2
7	**Testing**	ASHRAE 52.2	Complied	
8	**Filter frame**	1 in x1 in x 1 in	Plastic 100% recyclables frame to be provided by Spectraco	OK
9	**Solidity (1-porosity)**	NA	More information on solidity fraction is required. Another information is required on the weight of the filter per unit area	Not available
10	**Pressure drop for face velocity of 14 cm/s (mm H_20)**	1 mm H_20	What is the pressure drop at a flow rate of 750 m^3/hr?	We have provided the media pressure drop vs velocity data.
11	**Flow Rate (m^3/hr)**	3000	Clarify the flow rate provided w.r.t velocity?	Velocity considered at 1000 m^3/hr is 0.86 m/s. Velocity considered at 3000 m^3/hr is 2.59 m/s
12	**HVAC filters**	YES	Complied	

<table>
<tr><td>13</td><td>Effective Fibre diameter</td><td>NA</td><td>More information is required</td><td>Not available</td></tr>
<tr><td>14</td><td>Thickness of filter media</td><td>NA</td><td>NA</td><td>1.7 mm</td></tr>
<tr><td>15</td><td>Construction</td><td>NA</td><td>Spectraco (Electrostatic nonwoven)</td><td></td></tr>
<tr><td>16</td><td>Captures</td><td>The filter is constructed robustly and is suited for use in Comfort HVAC systems (Offices, Hospitals, Hotels, Educational Institutes), Filter Towers, and Clean Rooms (Food processing, pharmaceutical manufacturing etc.)</td><td>Nominal Volume Flow: At 3000 m^3/h</td><td></td></tr>
<tr><td>17</td><td>Electrostatic charged; charging density</td><td>High-performance electrostatic nonwoven</td><td>The charge density range is required</td><td></td></tr>
<tr><td>18</td><td>Filter Performance and Filter Efficiency</td><td></td><td></td><td>
<table>
<tr><td>Max Pressure drop (inch of H_2O)</td><td>0.10</td><td>0.19</td><td>0.26</td><td>0.38</td><td>0.58</td></tr>
<tr><td>Air Flow (CFM)</td><td>515</td><td>770</td><td>1025</td><td>1280</td><td>1735</td></tr>
</table>
<table>
<tr><td>e1</td><td>e2</td><td>e3</td></tr>
<tr><td>≥50</td><td>≥85</td><td>≥90</td></tr>
</table>
</td></tr>
</table>

19	**Filter loading vs pressure drop**		More information is required.	This test is done for the pre-filter. Fine-filter tests can be done at request.
20	**Critical replacement Loading**			
21	**Actual filter area per frame**			1 m^2
22	**Weight of the filter per unit area**			1.3 Kg Approx. - Weight of fine filter
23	**Pressure drop at specified velocity**			As shown in table above
24	**The material of the filter media**			Material of the filter media - Polyester
25	**Effect of moisture on filter media**			Moisture - No impact on filter performance
Summary: More information on solidity, fibre diameter, thickness of the filter media, filter media material, filter loading vs pressure drop and filter loading vs efficiency are required for comparison with the 3M filter. (Confirmation on pleats per foot)				

A few critical parameters for evaluation: filter efficiency, pressure drop, and pressure drop with respect to the PM loading were found missing in the details provided by the vendor. The vendor failed to submit any testing certificates, as it is important for evaluation. As per their claim, the pre-filter works better when compared to the 3M filter. The filter frame provided was oversized, and it was decided not to use the filters provided by the Spectrum.

3.2.2 Airth

Airth pre-filters were designed for the removal of microorganisms; their filter frame is made up of metallic which can be reused. Specifications provided for the pre-filters by the Airth are shown in Table 5, along with IITB comments. The company is ready to provide a pre-filter with a capturing efficiency of ~50% for particle sizes 3.0-10.0 µm.

Table 5. Airth: Technical specifications for the Airth Pre-filter.

Sr. No.	Specifications	Airth Specifications	IITB Remarks
1	**Name**	Flat panel air filter	
2	**Nominal Length**	25 in	Complied
3	**Overall Thickness**	1 in	
4	**Overall Width**	20 in	
5	**Filter Media Size**	18 in x 23 in	
6	**Testing**	ASHRAE 52.2	
7	**MERV Rating**	5	Currently using 3M filter having 2 rating for MERV
8	**Filter frame**	1 in x1 in x 1 in (Metallic "reusable" frame)	Material of filter frame
9	**Construction**	Non- Electrostatic/ electrostatic filter media surrounded by a metallic frame	Provide more information related to synthetic high loft.
10	**Filter Efficiency**	~50% efficiency for average particle size for 3.0 – 10.0 µm	More information is required
11	**Captures**	Lint, Household Dust, PM_{10}	

<table>
<tr><td>12</td><td>Filter loading vs pressure drop</td><td rowspan="7">
<table>
<tr><td>Flow (LPM)</td><td>400</td><td>200</td><td>100</td></tr>
<tr><td>Pressure (Pa)</td><td>50.88</td><td>14.10</td><td>3.06</td></tr>
</table>
<table>
<tr><td>Filter Name</td><td>Size (µm)</td><td>Reference Data (Counts) (Upstream)</td><td>Reference Data (Counts) (Upstream)</td><td>Efficiency (%) of double layer</td></tr>
<tr><td rowspan="3">MERV 5</td><td>1.0</td><td>5657960</td><td>4333000</td><td>23</td></tr>
<tr><td>5.0</td><td>44058</td><td>17149</td><td>81</td></tr>
<tr><td>10.0</td><td>780</td><td>141</td><td>82</td></tr>
</table>
</td><td rowspan="7">More information is required.</td></tr>
<tr><td>13</td><td>Filter loading vs efficiency</td></tr>
<tr><td>14</td><td>Critical replacement Loading</td></tr>
<tr><td>15</td><td>Actual filter area per frame</td></tr>
<tr><td>16</td><td>Weight of the filter per unit area</td></tr>
<tr><td>17</td><td>Pressure drop at specified velocity</td></tr>
<tr><td>18</td><td>The material of the filter media</td></tr>
<tr><td colspan="4">Summary: More information on filter loading vs pressure drop and filter loading vs efficiency are helpful for evaluation.</td></tr>
</table>

A detailed report on filter testing suggested that the instrument used for the testing is not a standard instrument, and a report from the standard instrument or recognised national testing facility was not provided by the vendor. Since the frames are made up of metallic, it is expected that the leaks would be minimised. Information on the filter loading and the efficiencies were found missing in the report.

3.2.3 Camfil

The Camfil technical specifications and the comments of the IITB team are shown in Table 6 and Table 7. As per the information provided by the Camfil Company, the capture efficiency of the pre-filters is more compared to 3M pre-filters. However, the company's dimensions of the filters were not matching with our requirement size. These fine filters are made up of glass fibre filters which have more initial pressure drop than 3M fine filters. The capture efficiency of the fine filters was found to be less as compared to the 3M filters.

Table 6. Camfil: Technical specifications for the Camfil Pre-filter.

Sr. No.	Specifications	Camfil Specifications (Filter Model: MHF 30/30)	IITB Comment
1	**Name**	Box/Panel Type Pre-Filter	
2	**Nominal Length**	610mm	The dimensions are not compatible with our system. Can filters be customized as per our system requirements?
3	**Overall Thickness**	50mm	
4	**Overall Width**	610mm	
5	**Filter Media Size**	580x580x40mm	
6	**Testing**	ISO 16890:2016 / IS 17570-2021	The testing method is different
7	**MERV Rating**	8	Provide test reports from a certified laboratory
8	**Filter frame**	610x610x50mm	Filter frame dimensions are not matching
9	**Construction**	Imported Blended Polyester Media	
10	**Filter Efficiency**	50% initial efficiency for PM_{10} particle size (ISO Rating: ePM_{10} 50%)	Good
11	**Captures**	PM_{10} Particles	
12	**Filter loading vs pressure drop**	Available	Please provide the report

13	**Filter loading vs efficiency**	Not Clear	We need information on the filter efficiency as the dust collected on the filters increases. So, dust loading (g/m^2) vs efficiency (%) is required.
14	**Critical replacement Loading**	At Recommended FPD - 25 mmWG (250 Pa)	
15	**Actual filter area per frame**	610x610x50, 610x305x50, 305x610x50, 305x305x50 (WxHxD)mm	Filter frame dimensions are not matching
16	**Weight of the filter per unit area**	610x610x50mm Filter Weight - 1.300 Kgs	
17	**Pressure drop at specified velocity**	For 610x610x50mm - 80 Pa at 3400CMH (8 mmWG at 2000CFM)	
18	**The material of the filter media**	Imported Blended Polyester Media	
Summary: More information on filter loading vs pressure drop and filter loading vs efficiency are critical for evaluation		Life cycle cost (LCC) analysis report is available.	

Table 7. Camfil: Technical specifications for the Camfil fine filter.

Sr. No.	Specifications	Camfil Remarks (Filter Model: EcoPleat)	IITB Comment
1	**Name**	EcoPleat MERV 13 / ePM_1 55% Filter	
2	**Nominal Length**	610mm	The dimensions are not compatible with our system. Can filters be customized as per our system requirements?
3	**Overall Thickness**	50mm	
4	**Overall Width**	610mm	
5	**MERV**	13	
6	**Filter Media Size**	580x580x40mm	
7	**Testing**	ASHRAE 52.2 - 2017 / ISO 16890 2016	If complied, please provide a report
8	**Filter frame**	610x610x50mm	Filter frame dimensions are not matching
9	**Solidity (1-porosity)**	NA	

10	**Pressure drop for face velocity of 14 cm/s (mm $H_2$0)**	10 mmWG / 100Pa	Provide test reports from a certified laboratory
11	**Flow Rate (m^3/hr)**	1700CMH / 1000CFM	Clarify the flow rate provided w.r.t velocity?
12	**HVAC filters**	Yes	Complied
13	**Effective Fibre diameter**	Imported Glass Fibre Media	
14	**Thickness of filter media**	NA	
15	**Construction**	Fine-filter in glass fibre media having mini-pleat construction for better efficiency	Provide the pleats per foot.
16	**Captures**	PM_1, $PM_{2.5}$ & PM_{10} particles (ISO Rating - ePM_1 55%)	
17	**Electrostatic charged; charging density**	Not applicable for these filters	
18	**Filter Performance and Filter Efficiency**	Life cycle cost (LCC) analysis report is available.	Provide test report from certified laboratory
19	**Filter loading vs pressure drop**	Performance graph available.	Provide test report from certified laboratory
20	**Critical replacement Loading**	At Recommended FPD - 35 mmWG (350 Pa)	
21	**Actual filter area per frame**	NA	
22	**Weight of the filter per unit area**	610x610x50mm Filter Weight - 2.100 Kgs	Filter frame dimensions are not matching
23	**Pressure drop at specified velocity**	For 610x610x50mm - 100 Pa at 1700CMH (10 mmWG at 1000CFM)	Provide the PD at specific face velocity
24	**The material of the filter media**	Imported Glass Fibre Media	
25	**Effect of moisture on filter media**	No effect.	
26	**Cost/unit in INR**		Please provide the quotation
Summary: More information on filter loading vs pressure drop and filter loading vs efficiency are critical for evaluation. The designed pressure of the Air Cleaning System is ~1.5 in WC. The PD of Camfil Filters is 2.4 in WC that means we have to replace Camfil filters before even it's completely loaded as we cannot exceed designed Pressure Drop.			

To check the efficiency of the pre-filters Camfil has followed ISO testing, but no certification was provided. A Life Cycle Cost Analysis was claimed to be available for their filters, but no detailed report or certificate was provided by the vendor.

3.2.4 AFI

The AFI specifications and the comments of the IITB team are shown in Table 8 and Table 9. The proposed cost of each pre-filter is ~Rs. 675 and the fine filter is Rs. 3000, ~2.5 and ~2.8 times higher than the 3M pre-filter and fine filter. As compared to the 3M, even the initial pressure drop of the filters is also high.

Table 8. AFI: Technical specifications for the AFI Pre-filter.

Sr. No.	Specifications	AFI Specifications	IITB Comments
1	**Name**	Flat Panel Air Filter	
2	**Nominal Length**	25 in	Complied
3	**Overall Thickness**	1 in	Complied
4	**Overall Width**	20 in	Complied
5	**Filter Media Size**	18 in x 23 in	Complied
6	**Testing**	ASHRAE 52.2	Provide testing report
7	**MERV Rating**	2	The quotation and the technical specification document are not matching
8	**Filter frame**	1 in x1 in x 1 in	Complied
9	**Construction**	Non-Electrostatic Media	Complied
10	**Filter Efficiency**	~20% efficiency for average particle size for 3.0-10.0 μm	Complied

<table>
<tr><td>11</td><td>Captures</td><td>Lint, Household Dust, PM_{10}</td><td>Complied</td></tr>
<tr><td>12</td><td>Filter loading vs pressure drop</td><td><table><tr><td>Air Flow (CFM)</td><td>515</td><td>770</td><td>1025</td><td>1280</td><td>1735</td></tr><tr><td>DP (mm of WC)</td><td>1.4</td><td>2.2</td><td>3</td><td>3.5</td><td>5</td></tr><tr><td>DP (inch of WC)</td><td>0.055</td><td>0.087</td><td>0.118</td><td>0.138</td><td>0.197</td></tr></table></td><td>Certification required</td></tr>
<tr><td>13</td><td>Filter loading vs efficiency</td><td><table><tr><td>Particle size</td><td>0.3-1 µm</td><td>1-3 µm</td><td>3-10 µm</td></tr><tr><td>Efficiency</td><td>NA</td><td>NA</td><td>~20%</td></tr></table></td><td>Provide test report from certified laboratory</td></tr>
<tr><td>14</td><td>Critical replacement Loading</td><td>Upto FPD 12-15 mm of WC</td><td>Max up to 0.6 in of WC; certification required</td></tr>
<tr><td>15</td><td>Actual filter area per frame</td><td>6.25 Sq ft (0.58 sq m) Media Area per filter</td><td></td></tr>
<tr><td>16</td><td>Weight of the filter per unit area</td><td>Approx. 145 Per sq ft</td><td>Unit is not clear, Provide weight of 1 filter</td></tr>
<tr><td>17</td><td>Pressure drop at specified velocity</td><td>3-4 mm of WC at 200 FPM</td><td></td></tr>
<tr><td>18</td><td>The material of the filter media</td><td>Synthetic/Cotton Supported with Metallic Mesh</td><td></td></tr>
<tr><td>19</td><td>Cost/unit (Rs)</td><td>675 per unit</td><td>~2.5 times cost than 3M</td></tr>
<tr><td colspan="4">Summary: More information on filter loading vs pressure drop and filter loading vs efficiency are critical for evaluation. As per the information provided, the pre-filters are not washable.</td></tr>
</table>

Table 9. AFI: Technical specifications for the AFI fine filter.

Sr. No.	Specifications	AFI Specifications	IITB Comments
1	**Name**	Premium Allergen & Home Pollutants Air Filter	Complied
2	**Nominal Length**	25 in	Complied
3	**Overall Thickness**	1 in	Complied
4	**Overall Width**	20 in	Complied
5	**MERV**	13	Complied
6	**Filter Media Size**	18 in x 23 in	Complied
7	**Testing**	ASHRAE 52.2	Provide testing report from certified laboratory
8	**Filter frame**	1 in x1 in x 1 in	complied
9	**Solidity (1-porosity)**	0.090 - 0.095	Provide testing report from certified laboratory
10	**Pressure drop for face velocity of 14 cm/s (mm H_20)**	1-1.2	Provide testing report from certified laboratory
11	**Flow Rate (m^3/hr)**	1150	Clarify the flow rate provided w.r.t velocity?
12	**HVAC filters**	YES	
13	**Effective Fibre diameter**	17-17.5 µm	
14	**Thickness of filter media**	0.7-0.75 mm	
15	**Construction**	Pleated Glass Fibre filter media supported by Hot Melt Glue on each side housed in cardboard frame. The finished product contains 50-55 pleats per feet.	The quotation and the technical specification document are not matching on pleats per feet
16	**Captures**	Lint, Household Dust, Dust Mite Debris, Mold Spores, Pollen, Pet Dander, Smoke, Smog, Cough & Sneeze particles, Bacteria, Virus, Candle Soot, $PM_{2.5}$ & Exhaust Particles	

<table>
<tr><td>17</td><td>Electrostatic charged; charging density</td><td>Electrostatic charged filter media with a significant microscopic bipolar charge on the fibres with charging density between 70-120 $\mu C/m^2$</td><td></td></tr>
<tr><td>18</td><td>Filter Performance and Filter Efficiency</td><td><table><tr><td>Particle size</td><td>0.3-1 µm</td><td>1-3 µm</td><td>3-10 µm</td></tr><tr><td>Efficiency</td><td><75%</td><td>>90%</td><td>>90%</td></tr></table></td><td>~2.5 times pressure drop is higher Provide testing report from certified laboratory</td></tr>
<tr><td>19</td><td>Filter loading vs pressure drop</td><td><table><tr><td>Air Flow (CFM)</td><td>515</td><td>770</td><td>1025</td><td>1280</td><td>1735</td></tr><tr><td>DP (mm of WC)</td><td>8.8</td><td>13.2</td><td>17.6</td><td>21.95</td><td>29.75</td></tr><tr><td>DP (inch of WC)</td><td>0.346</td><td>0.520</td><td>0.693</td><td>0.864</td><td>1.171</td></tr></table></td><td>Information is Required</td></tr>
<tr><td>20</td><td>Critical replacement Loading</td><td>Up to Differential pressure of 45 mm of WC</td><td>Our system is designed for maximum PD of 1.1 in WC (Complied)</td></tr>
<tr><td>21</td><td>Actual filter area per frame</td><td>Media area 31.28 sq ft (2.92 sq m) per filter</td><td></td></tr>
<tr><td>22</td><td>Weight of the filter per unit area</td><td>Approx. 285 Per sq ft</td><td>Unit is not clear, Provide weight of 1 filter</td></tr>
<tr><td>23</td><td>Pressure drop at specified velocity</td><td>12-14 mm of WC at 200 FPM</td><td>Provide testing report from certified laboratory</td></tr>
<tr><td>24</td><td>The material of the filter media</td><td>Glass Fibre Paper + Hot Melt Glue</td><td></td></tr>
<tr><td>25</td><td>Effect of moisture on filter media</td><td>No effect.</td><td></td></tr>
<tr><td>26</td><td>Cost/unit (Rs)</td><td>3000 per unit</td><td>~3 times cost than 3M (Note: Additional 3% charges of packing to be paid to AFI)</td></tr>
</table>

27	Summary: filter loading vs pressure drop and filter loading vs efficiency are critical information required for evaluation with certifications from certified laboratories. Additional information on solidity, fibre diameter, thickness of the filter media, and filter media material.	Glass fibre paper is non electrostic media proves to be having better dust loading, more stability at higher-rated flows.	Contradiction in point 17 Electrostatic charged is mentioned and in point 26 glass fibre paper non-electrostatic charged media is mentioned. Please clarify

There are some contradicting statements provided in the data sheet and the specification sheet provided. No testing reports are provided for the AFI filter and information on the pressure drop and the efficiency provided by the vendor was not found sufficient.

The information on filters proposed by the Indian suppliers who had shown interest in providing the indigenous filters for MSACS was examined. After evaluating all the suppliers, it was found that the filters provided by these Indian suppliers did not qualify for deployment in the MSACS.

4 Evaluation of MSACS: Internal Performance (2021-2023)

The internal performance of the MSACS was examined by measuring the air flow rate, pressure drop across the filters, dust load on the filters and filtration efficiency for reducing the PM concentrations. The MSACS was operated at different fan capacities, namely 50%, 75%, and 100% and the corresponding performance of the system was continuously analysed at different dust loading conditions. The details are given below.

4.1 Flow rate and Pressure drop in the system

The pressure drop and flow rates in the system for November 2021 - July 2022 are shown in Figure 33. It was observed that if the pressure drop increased, the flow rate decreased, and this was due to the increase in dust loading on the filters. In December 2021, a maximum flow rate of ~450 m^3/s was observed. Filters were found torn due to running at 100% fan capacity in September - October 2021. A decrease in pressure drop was observed in March 2022 after the completion of filter strengthening, indicating the dust loss occurred on the filters during the filter's strengthening work carried out in March 2022. A flow rate of ~330 m^3/s and a pressure drop of ~0.35 in-H_2O was observed in July 2022.

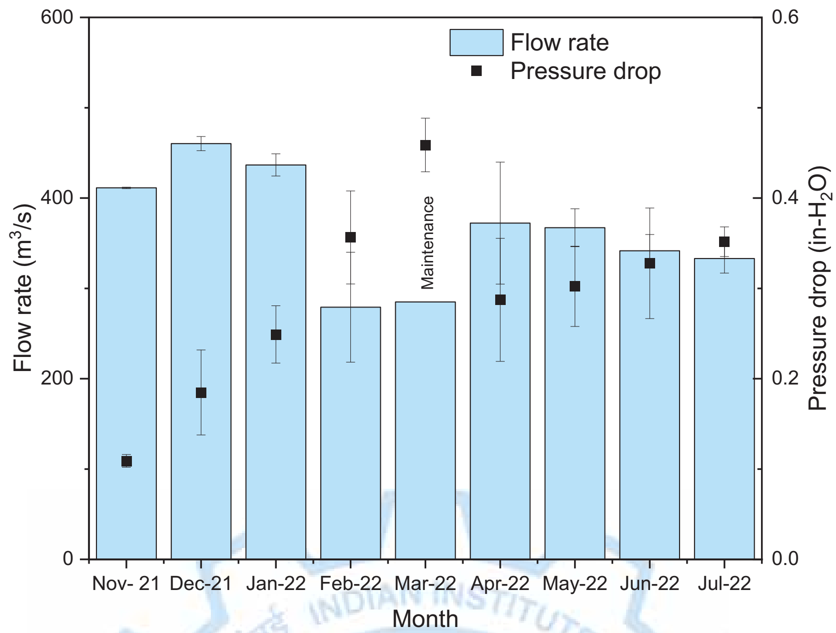

Figure 33. Pressure drop and flow rate at 50% fan capacity for months (November 2021-July 2022).

The MSACS pressure drop reached ~1.15 in-H_2O in July 2022 at 100% fan capacity. Therefore, IIT Bombay had suggested for replacement of the dust-loaded filters. Since, as per the UoM experts, theoretically, filters need to be replaced when the pressure drop reaches ~1.1 in-H_2O at 100% fan capacity (Refer technical dossier shared by UoM). The old filters were replaced by one set of new filters (pre-filters and fine filters), and the filter replacement work was completed in the middle of October 2022. The MSACS was kept ready for the winter period study after reinstalling one new set of filters. The system was kept again in operation from the last week of October 2022. During the initial testing phase, the system was operated at 50% fan capacity to check the leaks and dislodging of the filters, if any. Thereafter, the fan capacity was slowly increased to 75% and 100%. Multiple measurements were conducted at different fan capacities to assess the flow rate and pressure drop in the system. Information on fan operating capacities and flow rates is shown in Table 10. It was observed that the MSACS had delivered the flow rate at different fan capacities in accordance with the designed flow rate

(1000 m^3/s at 100% fan capacity). This is a clear indication that the system was performing well in delivering the desired flow rate.

Table 10. MSACS average flow rate at different fan capacities (2022-2023).

Fan Capacity	**Average flow rate (m^3/s)**
50%	505±31
75%	777±58
100%	1005±73

The pressure drop and flow rate at 50% fan capacity for October 2022 to January 2023 are shown in Figure 34. It was observed that the pressure drop across the filter bank was increased with the increased dust load on the filters while MSACS was in operation. At the beginning of the system, the average pressure drop for October 2022 was ~0.063 in-H_2O, and the flow rate was ~460 m^3/s at 50% fan capacity. After 1205 hours of operation at different operating fan capacities, the average pressure drop was increased to ~0.46 in-H_2O, while the flow rate was ~490 m^3/s at 50% fan capacity. This clearly indicates that dust loading has a significant influence in reducing the flow rate.

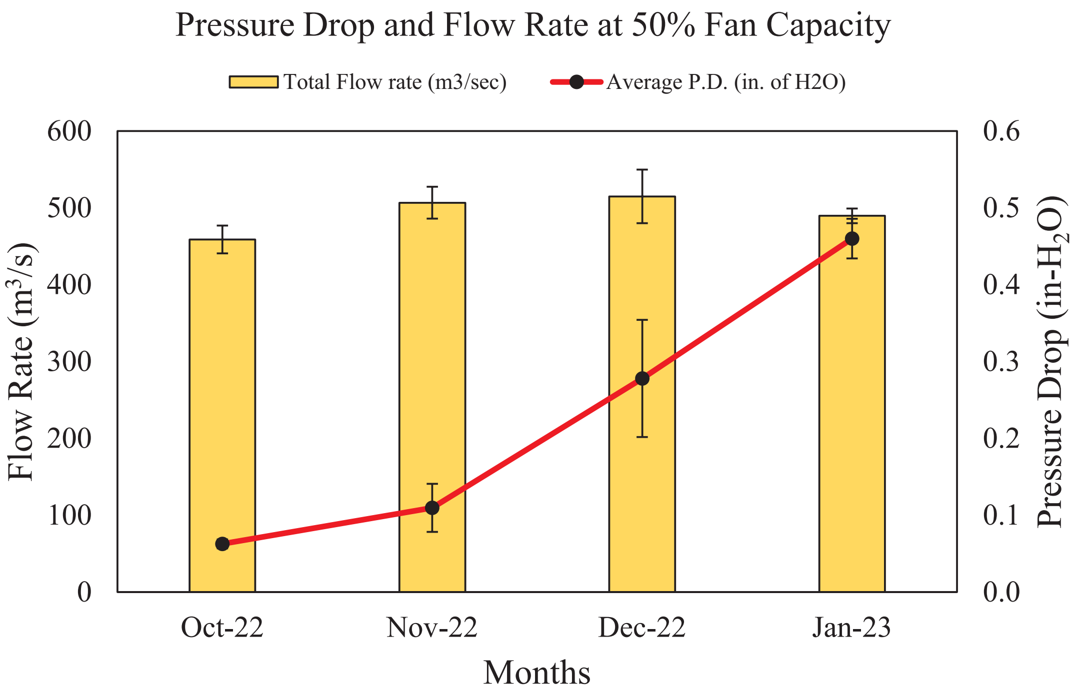

Figure 34. Pressure drop and flow Rate at 50% fan capacity (October 2022 to January 2023).

A gradual increase was observed in the average pressure drop across the filter bank with continuous operation as shown in Figure 34. The continuous MSACS operation leads to increasing dust load on the filters. A sudden increase was also observed in pressure drop in December 2022, indicating higher dust loading of the filters. The high dust loading on filters is due to the increase in overall ambient PM concentration and the increase in the operational hours of MSACS compared to October and November (Figure 50). Theoretically, the pressure drop should increase with the accumulated dust on filters, which has also been observed in the system.

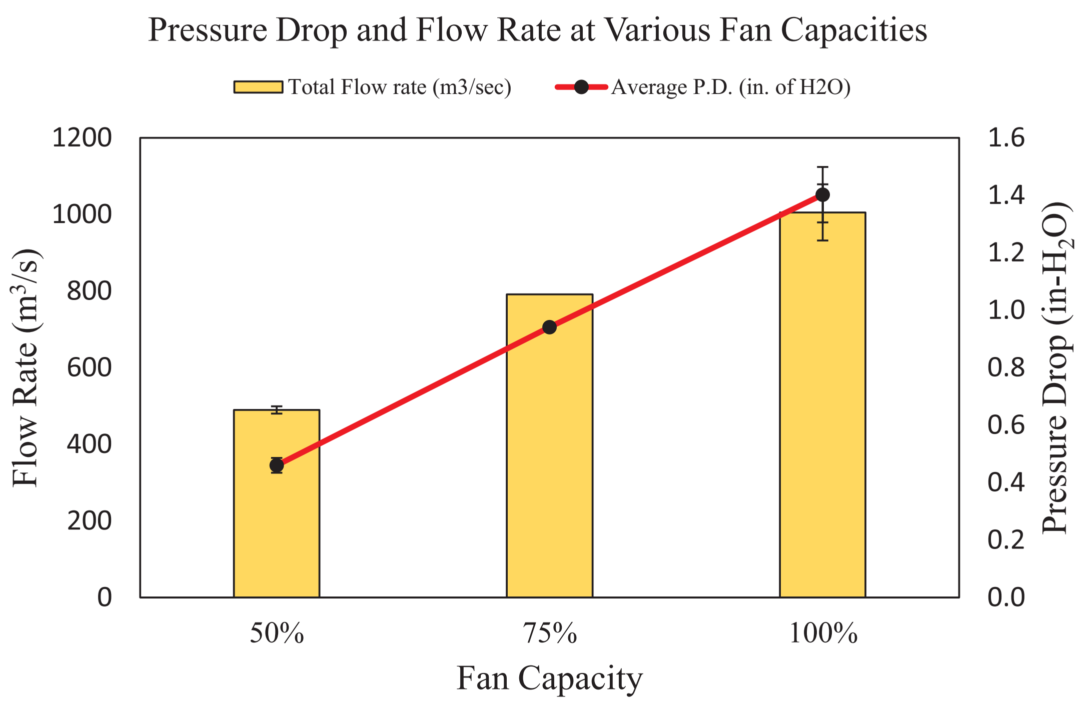

Figure 35. Pressure drop and flow rate at various fan capacities.

The dust-loaded filter data was analysed to assess the filter performance at various fan capacities. A linear relationship was observed, as shown in Figure 35, which represents the pressure drop and flow rate at various fan capacities. Overall, the system flow rate obtained was in accordance with the system design. This clearly indicates that the system was performing well in delivering the desired flow rate. For 100% fan capacity, an average flow rate of 1005 m^3/s and 1.4 in-H_2O pressure drop across the filter were observed.

4.2 Filter performance

Two types of filters (i.e., Pre-filter and Fine filter) were installed in the system. Pre-filter and Fine filter have different characteristics. The purpose of installing the pre-filter (MERV-2) is to capture the coarser-sized particles. To capture the finer particles with less initial pressure drop, electrically charged MERV-13 filters (fine filters) are installed in the MSACS. Both the filters used in MSACS are manufactured by 3M Company, USA.

The filter performance was examined in terms of the percentage reduction of PM concentrations in the downstream side of the filter bank after filtering the ambient air. One set of dust-loaded filters of MSACS was replaced by the new sets of filters (pre-filters + fine filters) in the middle of October 2022. After the initial test run, a decreasing trend was observed in the filter efficiency from November 2022, as shown in Figure 36 and Figure 37. The intrinsic efficiency of the filters in October was ~85-95% in the fresh filter conditions. Thereafter, a decrease in intrinsic efficiency was observed in middle of November. The decrease in intrinsic efficiency after the initial period may be related to the intrinsic property of filters and also due to the impact of different compositions of particulate matter under changing meteorological conditions.

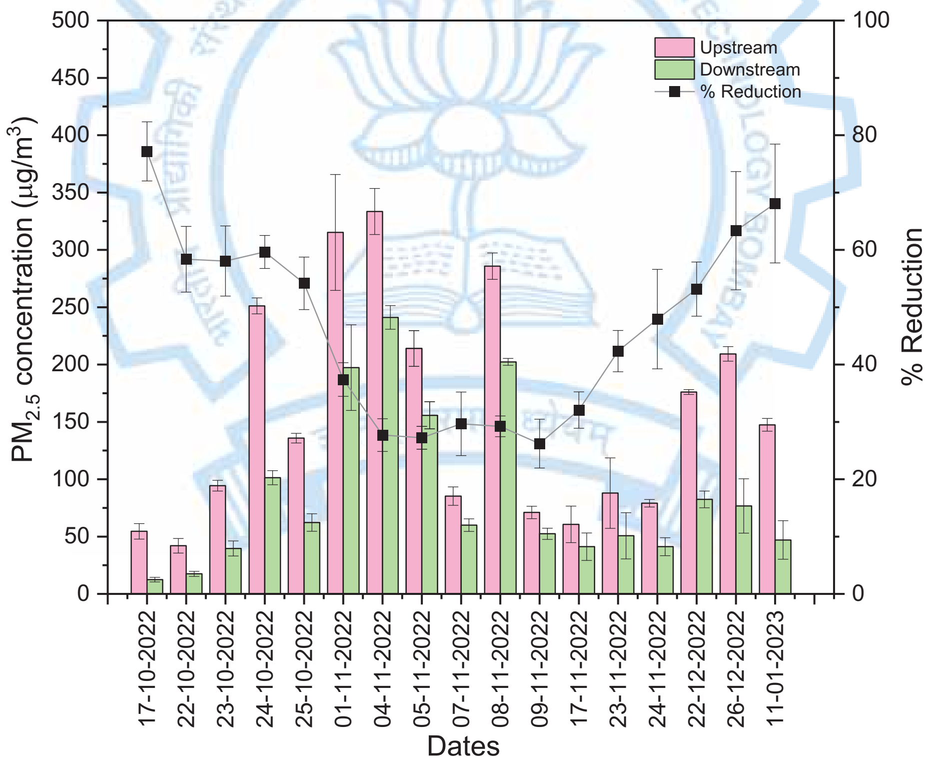

Figure 36. Percentage reduction $PM_{2.5}$ at 50% fan capacity for the old filter lot installed in the system.

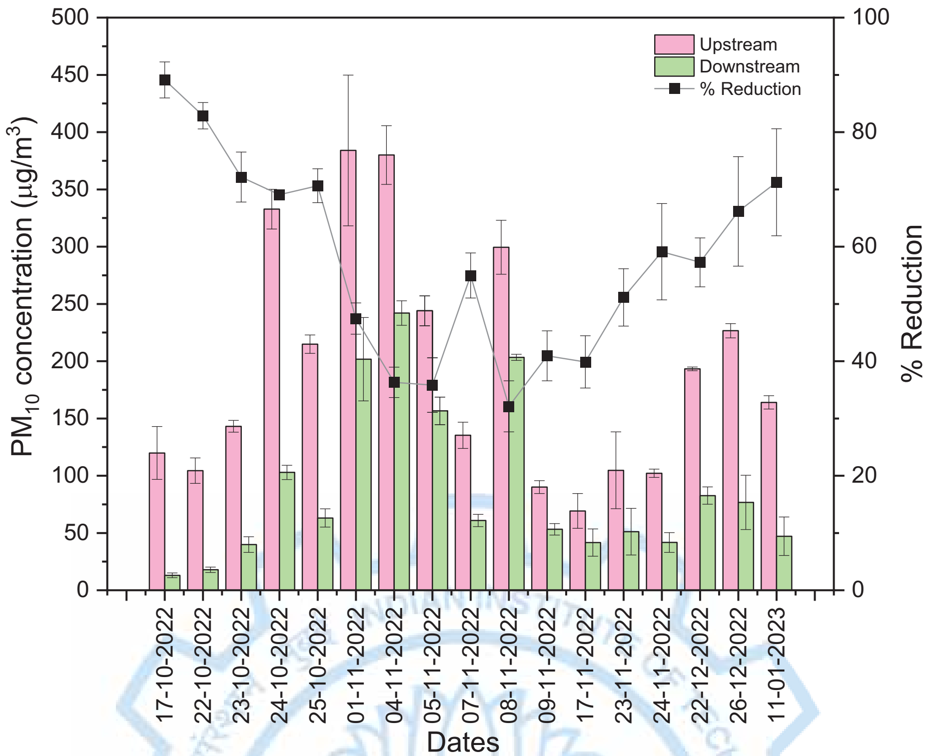

Figure 37. Percentage reduction of PM_{10} at 50% fan capacity for the old filter lot installed in the system.

The filters installed in October 2022 were taken from filters previously purchased and stored in the warehouse in July 2021. To confirm that the decreasing trend in the filter efficiency in the system was due to the phenomenon of the filters and not because of the filter degradation with time, some new pre and fine filter samples were installed in the system, which were purchased in September 2022. The filter efficiency in terms of percentage reduction of $PM_{2.5}$ and PM_{10} concentrations for the new filters installed in the system is shown in Figure 38 and Figure 39. The initial filter efficiency for $PM_{2.5}$ and PM_{10} was found to be ~70. The efficiency after one month of the system operation was found to be ~50% for $PM_{2.5}$ and ~60% for PM_{10}. A similar trend has also been observed in the previously installed filters, as shown in Figure 36 and Figure 37, which indicated that the decrease in efficiency after the initial run was due to the characteristic of the filter.

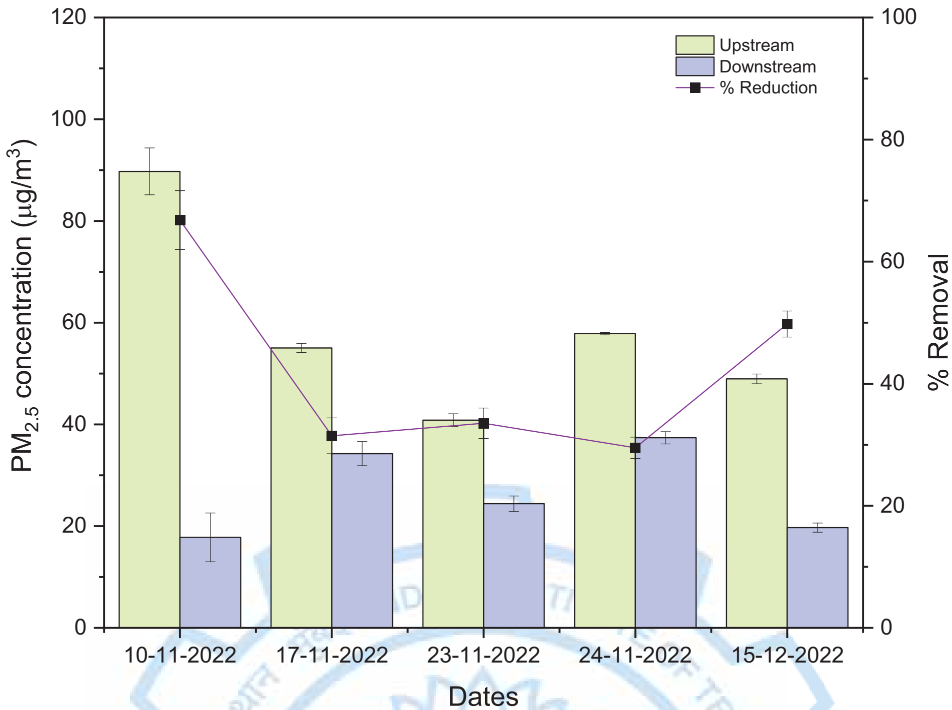

Figure 38. Percentage reduction of $PM_{2.5}$ at 75% fan capacity for the new filter lot installed in the system.

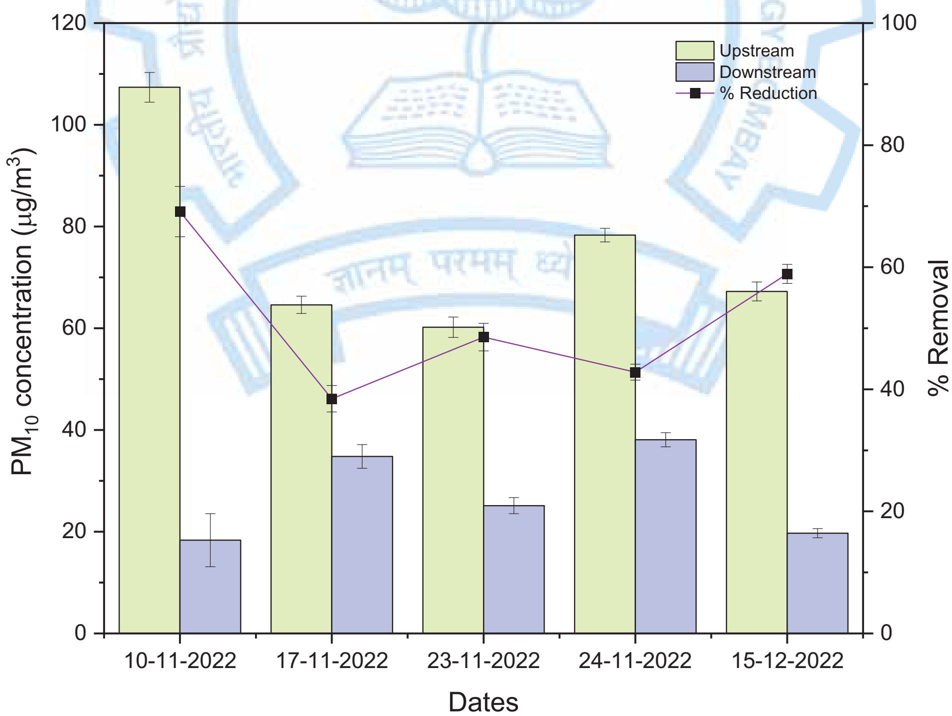

Figure 39. Percentage reduction in PM_{10} at 75% fan capacity for the new filter lot installed in the system.

Several published literature have also reported a similar phenomenon. Since the pre-filters are non-charged, the working principle of this filter is based on a traditional mechanical media filter. Tien et al. (2020) reported three special particle deposition cases on the filter depending on the type of filter media, as shown in Figure 40. Illustration (a) in Figure 40 shows the surface filtration type media (PFTE and PCTE) with small pore size; when particles approach these high-grade filters, it retains most of the particles. Once a layer is deposited on the media, fewer particles can pass through this built-up filter cake. For a depth filtration media (Glass Fibre), the particles have the capability to reach the deeper layer. However, a reducing deposition trend along the depth of the filter is observed in Figure 40 Illustration (b). Whereas, for charge fibre filters (i.e., fine filter), a uniformly deposited particle along the depth of media is observed (Figure 40 Illustration (c)). Due to the successive loss of the fibre charge of the electret media along with the loading process, it allows the lower layer to expose to the higher concentration of the incoming particles. Since the charge is lost on the fibre in the upper layer, the lower layer of the fibre still contains the charge, and thus these charged filters have the efficiency in collecting more particles (Tien et al., 2020).

It was found that the initial efficiencies of the filter media cannot represent the efficiencies of their whole life cycle (Chang et al., 2015). The filtering efficiency is supposed to increase with an increase in particle loading. However, the efficiency of the electret filter decreases as the fibre loses its charge, but again it increases with the cake filtration (Shi et al., 2013). Similar findings with respect to the dust loading and filter efficiencies were also observed for the MSACS, as shown in Figure 38 and Figure 39.

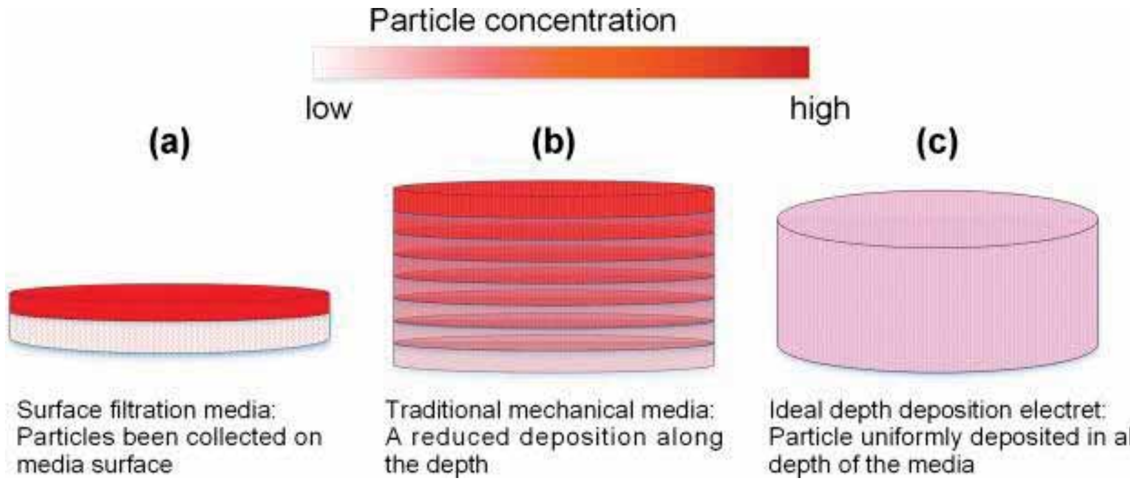

Figure 40. Three special cases of particle spatial deposition distributions in surface filtration media (a), in traditional fibrous mechanical media (b), and in perfect electret media (c). The colour bar indicates the concentration of deposited particles (Tien et al., 2020).

Tien et al. (2020) and other studies conducted experiments for various filter media and calculated the efficiency at different dust loading conditions (g/m^2). These studies reported that at an initial loading of 0 g/m^2, the filter efficiency was approximately 95% for 800 nm particles for MERV-13 filters. It was also reported that a drop-in efficiency was observed as the loading increased to 3.8 g/m^2. However, the initial filter efficiency reaches, once the filter loading increases and reaches up to 8 g/m^2. Likewise, the MSACS has also shown that once dust loading reaches ~8 g/m^2 at the end of November 2022, the filter efficiency starts to increase (from weighing the filter as described in section 4.6 of the report). Therefore, it is expected that the filter efficiency will increase once a sufficient dust load is collected on the filters. The trend for increasing filter efficiency during the winter period is shown in Figure 36 and Figure 37.

In summary, the efficiency of the new filters for $PM_{2.5}$ and PM_{10} concentrations was found to be ~80% and ~85% respectively. The intrinsic efficiency of the system was found to be decreasing after the initial test run till the dust loading on the filters was 3.8 g/m^2. Once the dust loading on the pre-filters reached up to 8 g/m^2, the system's intrinsic efficiency was found to be increasing. The intrinsic efficiency of the system was found to be increasing and it reaches again ~70% for $PM_{2.5}$ and PM_{10}, in January 2023.

4.3 Intrinsic Efficiency

To assess the performance of the MSACS, intrinsic efficiency (i.e., Efficiency of the filters at/close to the filter surface) was evaluated. The intrinsic efficiency of the system was assessed by calculating the percentage reduction of PM concentrations from the filters. The measurement strategy for the assessment of the system's internal performance was already described in detail in the Interim Report-2 and previously submitted reports.

4.3.1 Intrinsic Efficiency (January 2022- July 2022)

The intrinsic efficiency of the system for the operation period (January 2022- July 2022) is shown in Figure 41 and Figure 42, for $PM_{2.5}$ and PM_{10} at different fan capacities respectively. The system intrinsic efficiencies for $PM_{2.5}$ and PM_{10} at 50% fan capacities after operating the MSACS for approximately three months were found to be ~ 60% and ~ 65%, respectively. The intrinsic efficiency for $PM_{2.5}$ and PM_{10} at 50% fan capacities was found to be significantly increased up to 95%, after the filter strengthing, arresting the system leaks and sufficient dust loading on the filters. The detailed analysis of the system's intrinsic efficiency from Jan 2022 to July 2022 was presented in the Interim Report-2.

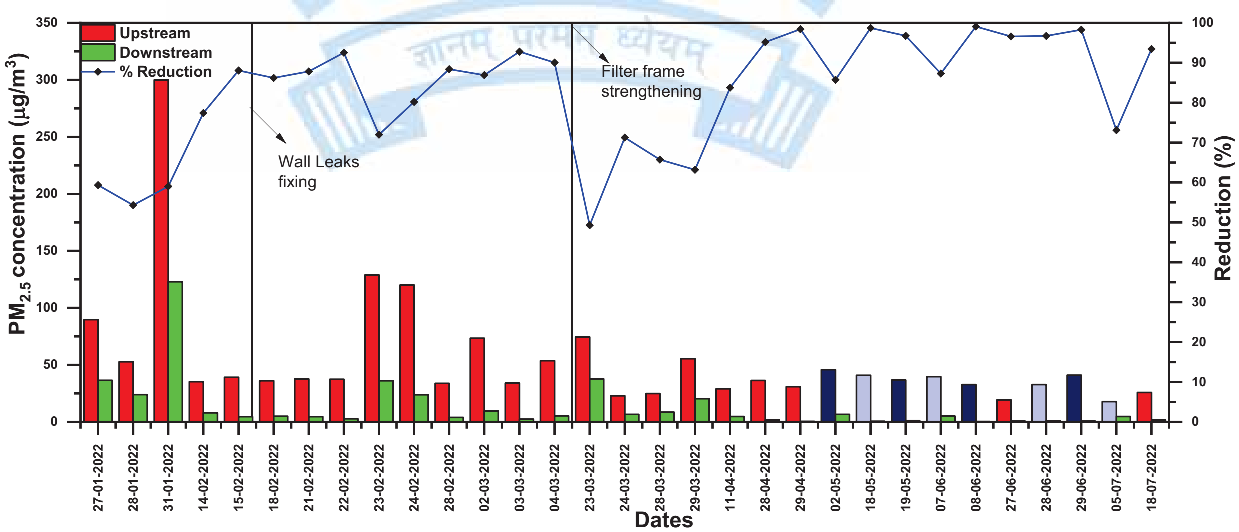

Figure 41. Intrinsic efficiency of MSACS for reducing $PM_{2.5}$ concentrations at different fan capacities (Dark blue: 100%, light blue 75%, Red: 50%).

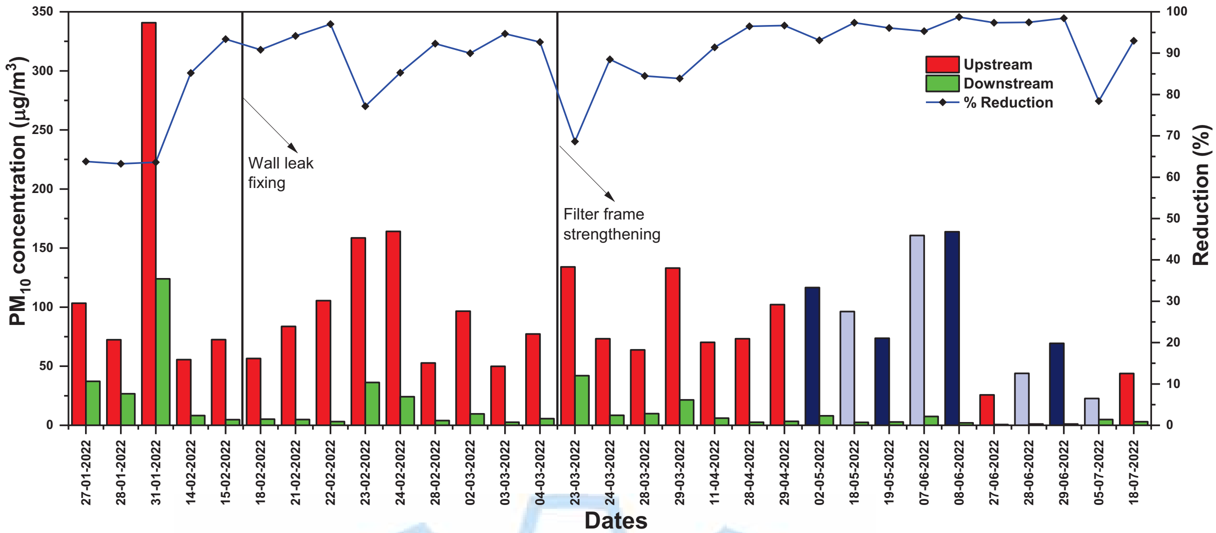

Figure 42. Intrinsic efficiency of MSACS for reducing PM_{10} concentrations at different fan capacities (Dark blue: 100%, light blue 75%, Red: 50%).

The MSACS started operating in October 2021; the filters were installed, and fan testing started. During the initial test run of the MSACS, the filters were dislodged, and a gap between the two filters and other leaks were observed in the system. The IITB team made several site visits for operational troubleshooting of the system and the corrective actions were suggested to the TPL O&M team. With corrective actions, the system performance was found to improve gradually.

4.3.2 Intrinsic Efficiency (October 2022- February 2023)

A new set of filters were installed in October 2022 for the system operation in the winter season (2022-2023). The system's intrinsic efficiency for reducing $PM_{2.5}$ and PM_{10} concentrations at different fan capacities is shown in Figure 43 and Figure 44. The system efficiencies during the initial test run for $PM_{2.5}$ at 50, 75 and 100% fan capacities were found to be approximately 77%, 66%, and 60% respectively. Similarly, the system efficiencies for reducing the PM_{10} at 50, 75, and 100% fan capacities were approximately 89%, 81%, and 78% respectively.

Table 11. Efficiencies for the filter at various fan capacities (October 2022- February 2023).

Fan Capacity (%)	Initial Efficiency (%)		Efficiency after one month (%)		Maximum efficiency at the end of the winter period (%)	
	$PM_{2.5}$	PM_{10}	$PM_{2.5}$	PM_{10}	$PM_{2.5}$	PM_{10}
50	77	89	32	42	-	-
75	67	81	40	54	-	-
100	60	78	-	-	74	86

- indicates data not available at that fan capacity.

It was observed that the system intrinsic efficiency at 50% fan capacity started to decrease to 40% for $PM_{2.5}$ and PM_{10}, during the operation in November 2022 (as explained in section 4.2). Thereafter, from December 2022 the system efficiency started to increase as expected after sufficient dust loading on the filters. It must be noteworthy that the system regained its initial efficiencies for $PM_{2.5}$ and PM_{10} in January 2023 after sufficient dust loading on the filters. It was observed that at 100% fan capacity, some new leaks were generated and thus corrective measures were taken as discussed in section 2.5. Thereafter, intrinsic efficiency at 100% fan capacity was found to be increasing in the mid of January 2023.

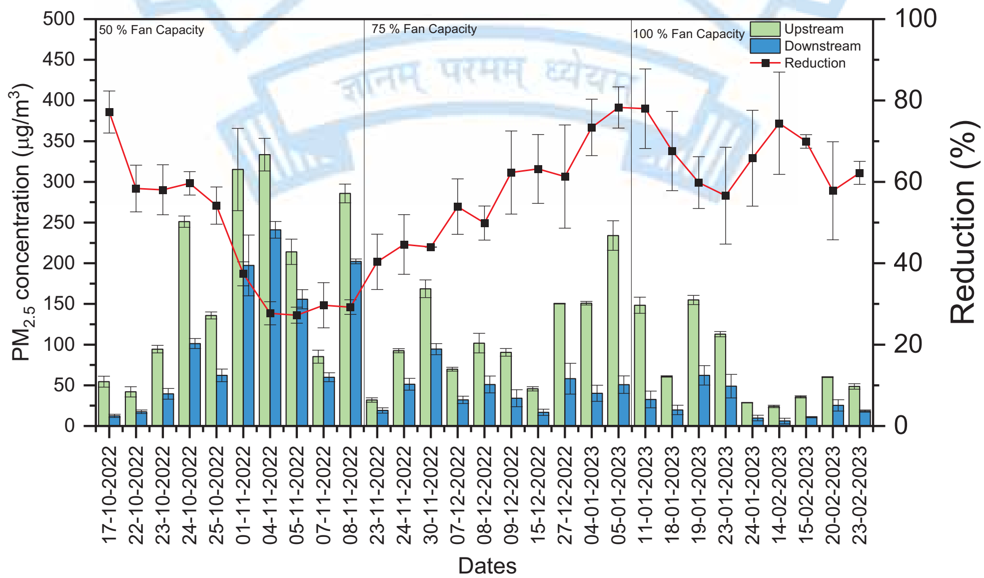

Figure 43. Intrinsic efficiency of MSACS for reducing $PM_{2.5}$ concentrations at different fan capacities.

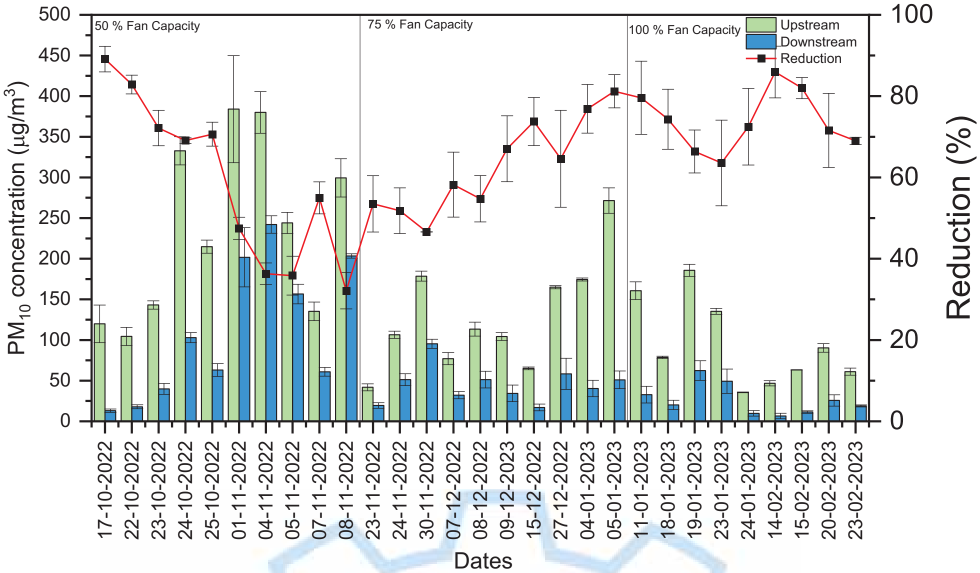

Figure 44. Intrinsic efficiency of MSACS for reducing PM_{10} concentrations at different fan capacities.

4.4 PM size distribution at different fan capacity

The MSACS was operated at various fan capacities during the initial phase (October 2022) of the testing to determine the initial efficiency of the filters after the installation of new sets of filters. To assess the system efficiency for various particle sizes, the particle number concentration was measured on the upstream and downstream sides of the system using OPS-3330 (TSI, USA). The system efficiency for various particle sizes was analysed by calculating the percentage reduction of the number concentration of each particle size. The initial efficiency of the filters at 25, 50, and 75% fan capacity is shown in Figure 45, Figure 46 and Figure 47. It was observed that the filter efficiency for the smaller size particles (0.31 µm) was ~ 80% for 25% fan capacity and ~ 70% for 50% and 75% fan capacity at the initial phase of the filter. It was also observed that as the particle size increases, the capturing efficiency also increases to >90% for 25%, 50% and 75% for fan capacity. As the testing was done during the initial phase (New filters) the filters are expected to work at higher efficiency. Similar results were observed for filter efficiencies with respect to the mass concentrations of the particles also, as shown in Figure 43 and Figure 44.

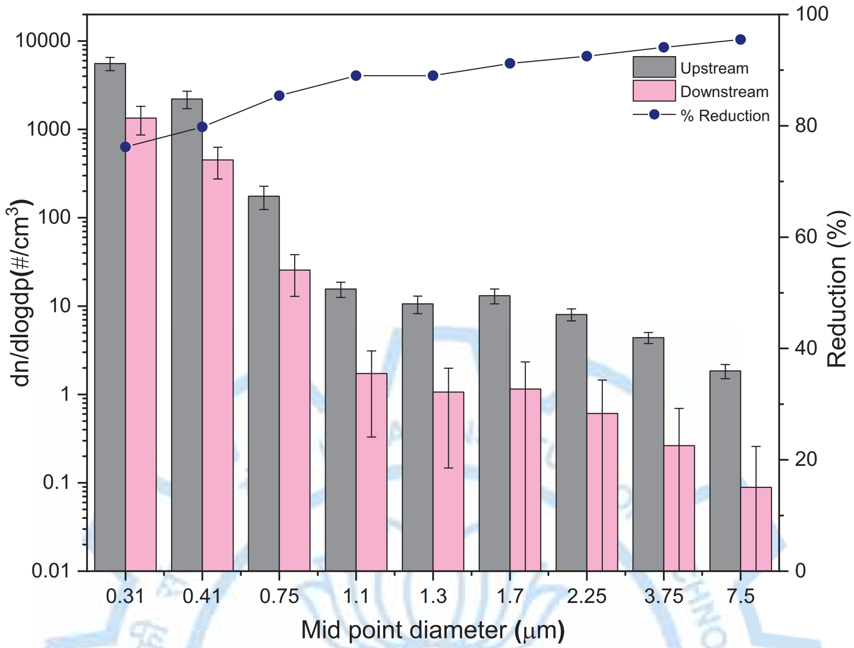

Figure 45. Percentage reduction for Particulate Matter at initial phase for 25% fan capacity.

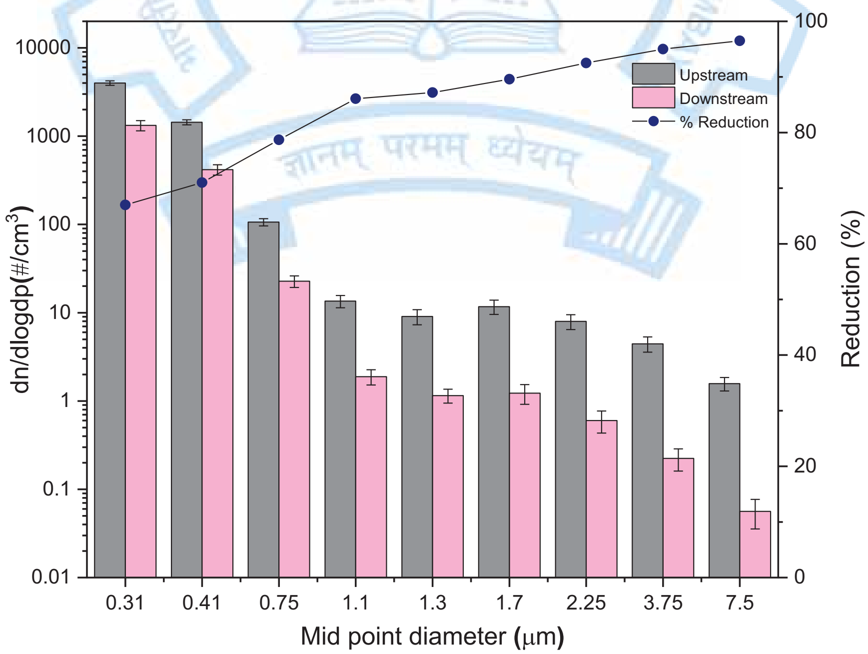

Figure 46. Percentage reduction for Particulate Matter at initial phase for 50% fan capacity.

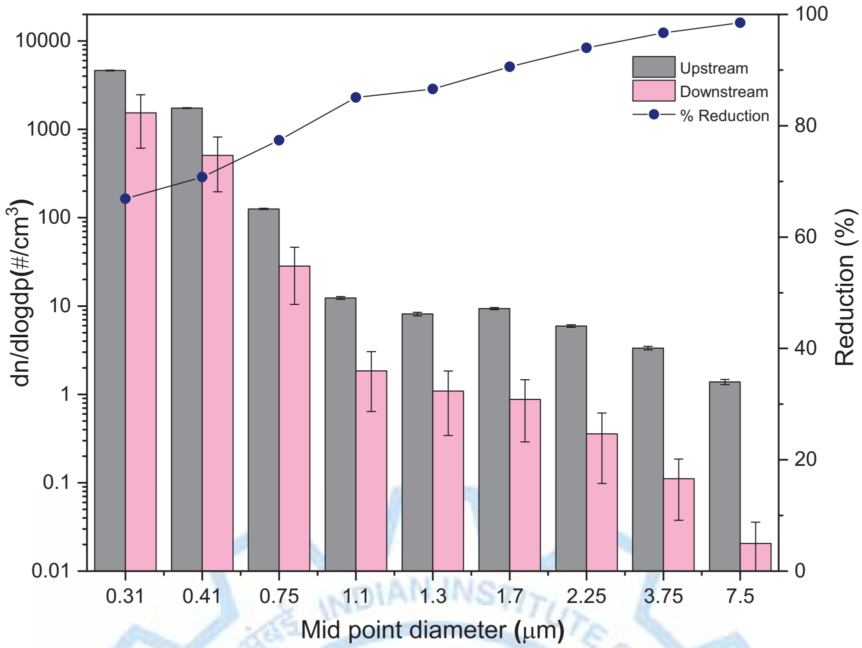

Figure 47. Percentage reduction for Particulate Matter at initial phase for 75% fan capacity.

In Figure 45, Figure 46 and Figure 47, the reduction of 70-90% of PM is due to the fine-filters as in the beginning all the particles escape pre-filter. Once the dust is accumulated on the pre-filter, a reduction in the capture of the smaller size particles is observed due to the electret fibre charge and accumulation of the dust particles.

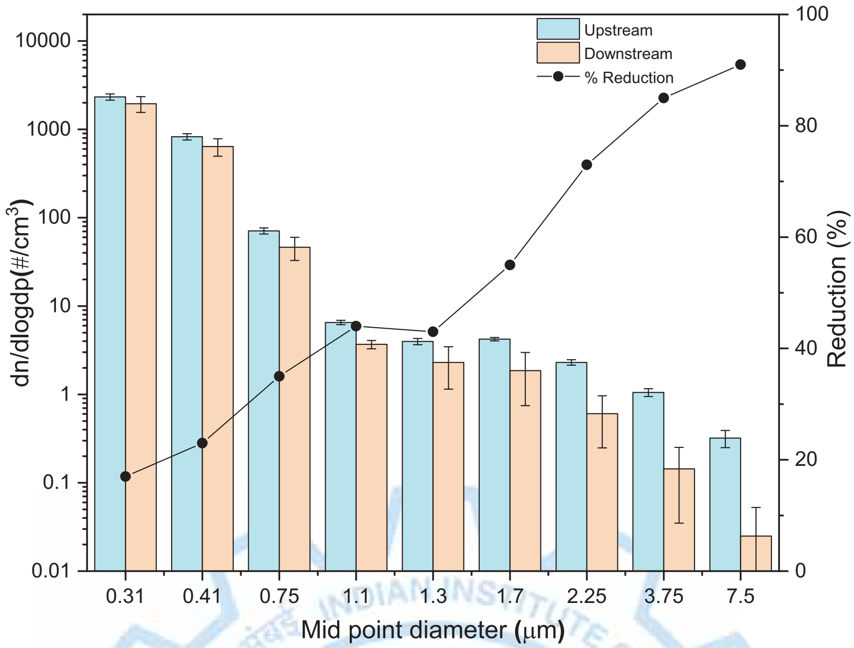

Figure 48. Percentage reduction for Particulate Matter after a few days of operation (slightly loaded) at 75% fan capacity.

A set of measurements were performed at 75% fan capacity when the filters were loaded, as shown in Figure 48. It was observed that initially the system efficiency to capture smaller size particles decreased significantly, i.e., ~ 20% as compared to the fresh filters conditions, i.e., ~ 70% (Refer Figure 47). The initial decrease in the system efficiency was due to the characteristic of the filter, which is explained in section 4.2. However, the system efficiency for bigger size particles (>2.5 μm) decreased slightly from 90% to 75%, compared to fresh filter condition. The system efficiencies for particle size are also expected to increase after sufficient dust is collected on the filters. As the fine filters have lost the charge, the reduction in efficiency is due to the cake formation on the filters. Once a sufficient amount of dust is collected on the filters, it is expected that the smaller size particles will also be captured more effectively.

4.5 Diagnostic tool for the leak

To evaluate the leaks[1] in the system, buffer zone measurements were conducted (between the filter bank and the fan). The detailed measurement strategy for system internal performance was described in Interim Report-2. The percentage of leaks in the system was calculated using Equation 1.

$$\% \text{ Leak} = 1 - \frac{\text{Buffer Efficency}}{\text{Intrinsic Efficency}} \times 100 \ldots\ldots\ldots\ldots\ldots\ldots\ldots\ldots \text{Equation 1}$$

The experiments were conducted at 50%, 75% and 100% fan capacity to assess the leaks in the system. During the system operation, continuous maintenance is required in the system to avoid the bypass of the unfiltered air. The system leakage was significantly reduced during the operation period of October 2022- February 2023, compared to the operation period of October 2021- September 2022. It was found that the average pressure drop in the system at average flow rate of 1005 m^3/s for 100% fan capacity was 1.4 in-H_2O, which is a clear indication of lesser leaks in the system. The continuous effort in leak sealing of the system based on the leak assessment experiments and the change in the orientation of the pre-filter (Explained in 2.4) resulted in the minimum leaks in the system.

The leaks in the system for $PM_{2.5}$ and PM_{10} are shown in Figure 17. It was observed that in the initial phase of the system; the percentage of leaks present in the system was <2% for $PM_{2.5}$ and 10% for PM_{10}. As the number of operation hours increases, the percentage of leaks was found to be increased to 45% and 35% for $PM_{2.5}$ and PM_{10} respectively except in some cases where the leaks were found to be approximately 60% and 45% for $PM_{2.5}$ and PM_{10}. Once the system was rectified in January 2023, the percentage of the leaks was reduced to 30% for $PM_{2.5}$ and <30% for PM_{10} expect in some cases where it was approximately 40% which is shown in

[1] Leak in the system can be defined as the amount of unfiltered air by-passed from the filters. The leaks in the system can be due to the gaps between two filters, gaps between filters and filter frame or from end plates.

Figure 17 Regular maintenance is required to reduce the ingression of the pollutants along with floor dust cleaning and sealing of the leaks inside the system.

It was observed that the mostly $PM_{2.5}$ leak rate is higher than that of PM_{10} in most cases, as shown in Figure 17. This may be due to the escaping of smaller particles from the gaps compared to the bigger-sized particles. Baron et al. (2002) studied the filtration phenomenon for smaller size particles (0.6-1.9 µm); it was reported that the smaller size particles can pass around the filter (bypass leak). Some larger particles (>2 µm) can also bounce from the filter surface, penetrate through the leak or maybe re-entrained by impacting particles and enter the leak carried by the high-velocity airflow (Baron et al., 2002). These leaks are caused by the cardboard structure of the pre-filter, which is not rigid in the 3M filters. The gaps between the filter frame and the filters were restricted by using the cascade tape in the system. The gaps between the pre-filers were sealed by pasting the pre-filters together using adhesive tape. The quality of the material used for leak sealing work, such as cascade and adhesive tape, also affects the system's effectiveness in arresting leaks. Moreover, it was also observed that the continuous operation of the system at higher fan capacity had generated new leaks in the system. Therefore, it is necessary to have regular maintenance in the system to reduce the leak in the system.

4.6 Dust loading on the filters

The dust loading on the filters was assessed by the gravimetric method. The dust-loaded pre and fine filter samples were taken out from the filter bank at different periods of operations, as shown in Table 12. The system was operated for approximately four months at different fan capacities, and the operational time was according to the experimental plan. It should be noted that the dust loss occurred while uninstalling and re-installing the filters, and dust falling out from the filters is not accounted for in these calculations. The dust deposited on the filters was calculated by Equation 2.

$$\text{Mass deposited}\left(\frac{g}{m^2}\right) = \frac{I_F - I_I}{\text{Area of filter}} \text{ ………………….. Equation 2}$$

Where,

I_F = Final weight of the loaded filter
I_I = Initial weight of the filter
Area of filter: 0.3 m^2 (For pre-filter) and 3.3 m^2 (For fine filter)

Table 12. Dust loading on the pre-filters and fine filters samples during the winter months.

Date	**Fan Capacity**	**Flow Rate**	**Pressure Drop**	**Dust Loading (g/m^2)**			
				Pre-filter		**Fine filter**	
	(%)	m^3/s	in-H_2O	g	g/m^2	g	g/m^2
01-11-2022	50	508.26	0.17	5.00	16.67	13.37	4.05
08-12-2022	75	793.31	0.40	42.75	142.50	28.85	8.74
23-01-2023	100	890.86	1.49	53.35	177.83	34.95	10.59
27-02-2023	100	969.83	1.33	57.25	190.83	38.85	11.77

It was observed that the dust deposited on the pre-filter sample during November 2022 was lesser than the fine filter samples, as shown in Table 12. However, for the rest of the months in the winter period, the dust deposited observed on pre-filter samples was higher than that on fine-filter samples; which is due to the cake formation phenomenon. Since the media porosity is not finer in the pre-filter, the particles are expected to escape to the fine filter. As shown in section 2.6, the dust particles start to deposit on pre-filters after a few days of the operation. Once sufficient cake was formed on the pre-filters, the particles began to get deposited on the pre-filter, and a thick cake was formed, as shown in to Figure 21. It was also observed that once a sufficient amount of dust was collected on the pre-filters, the dust on the filter started falling out from the pre-filters and accumulated on the floor while operating the system at higher fan capacity, as shown in Figure 49.

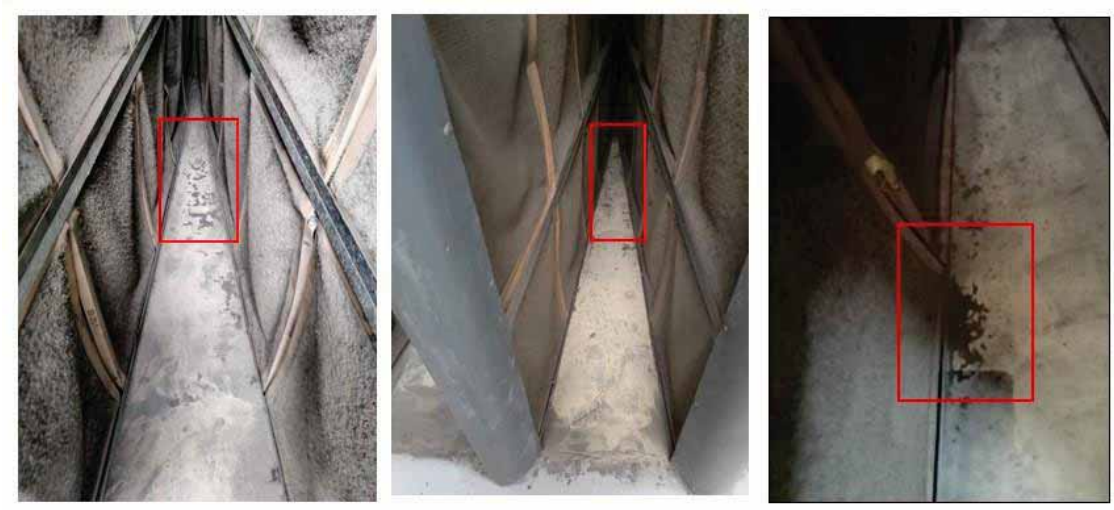

Figure 49. Dust fallen out from the pre-filters on the floor.

The cumulative dust load on pre and fine-filters in g/m^2 at different operational hours throughout MSACS operation are shown in Figure 50. It was observed that the cumulative dust load on the pre-filter samples was ~ 191g/m^2, and it was ~ 12 g/m^2 on fine filter samples.

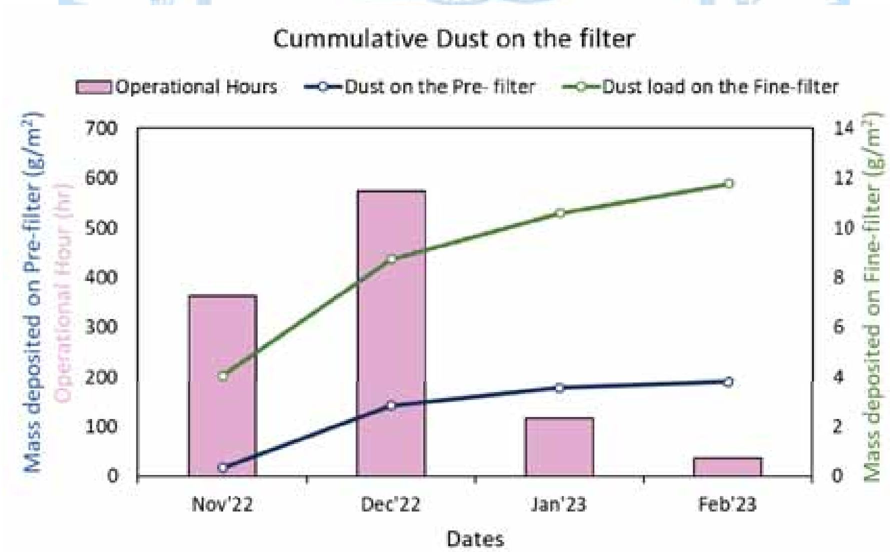

Figure 50. Cumulative dust load on the filter at different operational hours[2].

At the end of February 2023, the cumulative dust deposited on pre-filters approached its maximum capacity i.e., 200 g/m^2. The dust load on the fine filters was lesser than its maximum

[2] Number of operating hours mentioned for each month is total of the hours the fan was operated at various fan capacities.

dust load capacity i.e., 80 g/m^2. Having a high dust loading on the pre-filter samples indicated the replacement of pre-filters. Therefore, at the end of February 2023, it was recommended to replace the loaded pre-filters with new pre-filters. The maximum dust loading achieved by the fine filter depends on Relative Humidity (RH). As per the technical document number shared by UoM, the maximum dust loading of ~ 80 g/m^2 can be achieved for the RH between 50-70%. For the RH <50%, the fine filters can have a maximum loading of ~ 40 g/m^2. During the operation, most of the time RH was > 50%. Therefore, the fine filters installed in MSACS can be used till the dust loading reaches its maximum limit, i.e., ~ 80 g/m^2. The maximum dust load collected for the winter operation period (October 2022 - February 2023) through the total installed 4800 pre-filters and 4800 fine filters were 275 kg and 187 kg respectively.

The results from these measurements indicate that during the initial period of operation, most of the dust is captured by fine filter, and then as the dust accumulation increases the particles' capturing is dominated by pre-filter due to cake formation. This clearly indicates only pre-filters need to be replaced, and the fine filters can be used for a longer period of time. Another important implication of these results is that moderately loaded pre-filters can be used as fine filters in the future while replacing the pre-filters. It will help in reducing the cost as the cost of fine filters are approximately four times the pre-filter.

4.6.1 Effect of dust loading on pressure drop

To understand the effect of particulate matter loading on pressure drop, a scatter plot was plotted for 50% fan capacity as shown in Figure 51 and Figure 52 for pre-filters and fine filters. Since, we had the total pressure drop of the filters and not the pressure drops contributed by each filter, a standardized pressure drop with respect to face velocity was considered. The total pressure drop with no loading condition was found ~ 0.05 in-H_2O. The filter samples were weighted by gravimetric sampling method after operating the MSACS system for many days, as explained in Section 4.6. A polynomial fit of order two was used to understand the relationship between the parameters. It was observed from Figure 51 that there is a steep rise in pressure drop once the loading increases beyond 100 g/m^2 for pre-filters and 7.5 g/m^2 for fine-filters.

The details on dust loading, pressure drop, corresponding flow rate and operational hours are shown in Table 12. The recommended pressure drop for changing the filters was 1.1 in-H_2O at 1000 m^3/s flow rate. For MSACS, the maximum system pressure drop was achieved at ~ 0.48 in-H_2O for a flow rate of 483 m^3/s which agreed with the designed capacity indicating strong approval in theoretical and experimental data. As per the technical dossier shared by UoM, the maximum particulate deposition on the pre-filter for RH ranging between ~ 50-70% is 200 g/m^2 and for fine-filter, it is 80 g/m^2. However, for the RH between 30-50%, the maximum particulate deposition on the pre-filter would be 100 g/m^2, and for fine-filters it would be 40 g/m^2. During the operation of MSACS, the RH was mostly between 50-70%, and hence, the 200 g/m^2 and 80 g/m^2 for pre-filters and fine-filters values were considered.

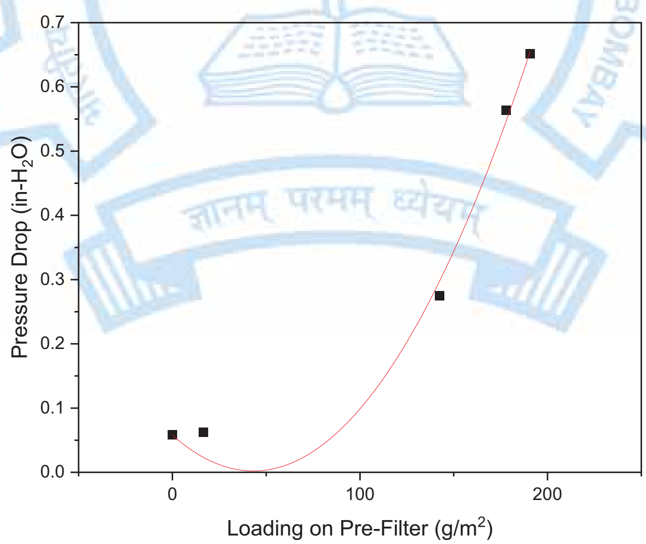

Figure 51. Effect of loading on pressure drop for Pre-Filters.

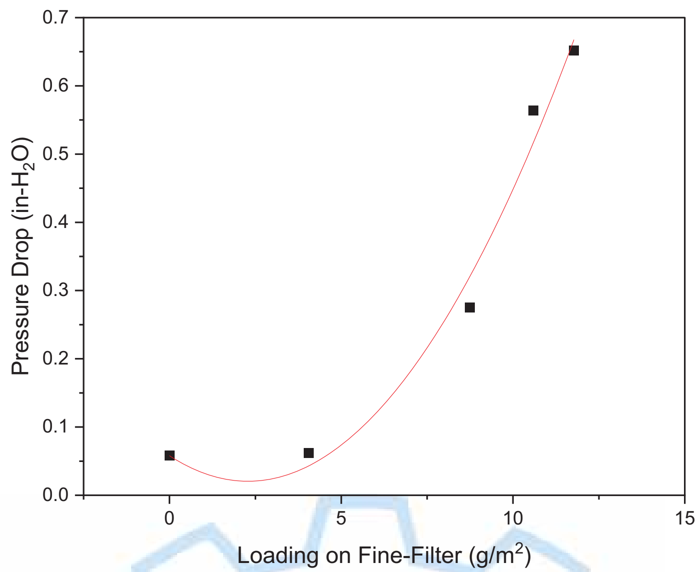

Figure 52. Effect of loading on pressure drop for Fine-Filters.

5 Background PM Concentration and Meteorology Around the MSACS

The background PM concentrations and the historical data of PM, wind speed and wind direction are reported here to assess the air quality in the nearby area of MSACS. The historical wind speed and wind direction data is referred to identify the different monitoring locations around the MSACS.

5.1 Historical pollution load and meteorology

Connaught Place is residential cum commercial area in Delhi. The average monthly $PM_{2.5}$ concentration at the Mandir Marg site for 2016-2020 is shown in Figure 53. It was found that in the winter months (November, December, January and February), the mean $PM_{2.5}$ concentration was 179.17 µg/m^3, while in monsoon months (June, July and August), it decreased and was found to 41.71 µg/m^3. Further, the mean concentration of $PM_{2.5}$ was found to be 70.94 µg/m^3 during the summer (March, April and May), which indicated a significant seasonal effect on the ambient concentration of $PM_{2.5}$.

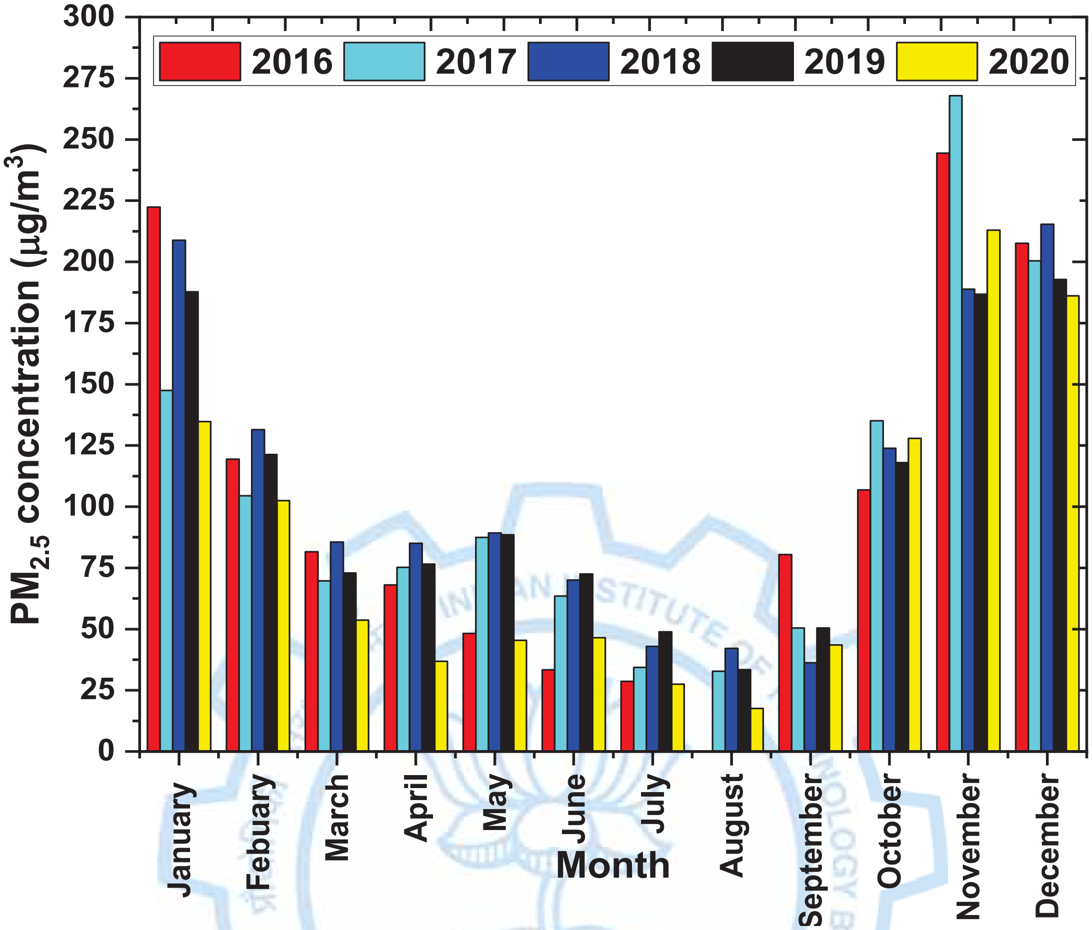

Figure 53. Average Monthly $PM_{2.5}$ concentrations from 2016-2020.

As per the historical wind-rose data for Mandir Marg station for 2016-2021, it was found that the wind comes from the West direction for the summer (March-May) and the winter (October-February) season (Figure 54 and Figure 55). The historical wind rose data was used to identify suitable monitoring locations to assess the MSACS performance in the ambient domain. The monitoring locations were selected based on the historical data of the upwind and downwind directions at the locations.

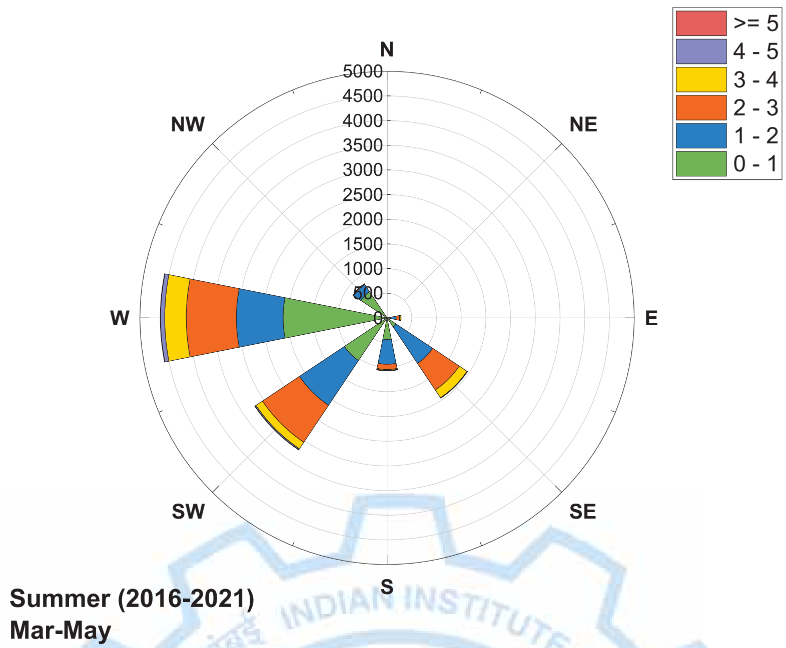

Figure 54. Windrose for Summer (2016-2021).

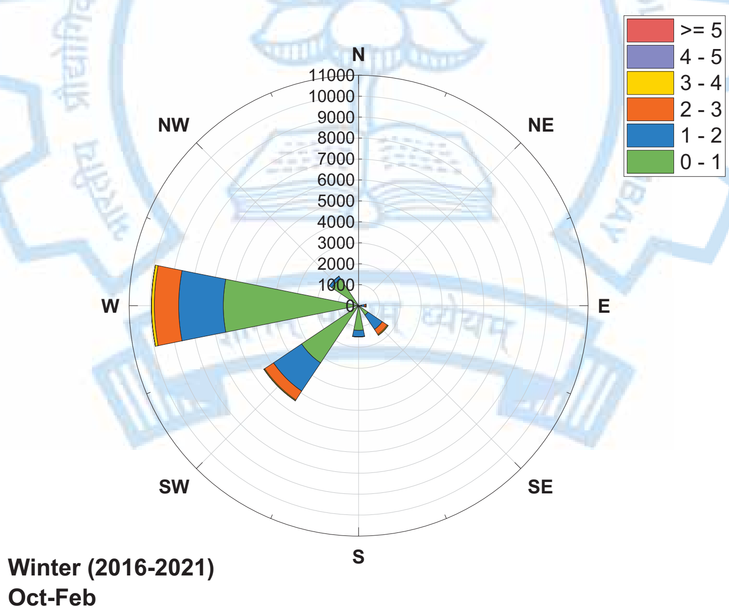

Figure 55. Windrose for Winter (2016-2021).

5.2 PM Concentration during winter (October 2022 - February 2023)

The weekly average concentration for PM_{10} and $PM_{2.5}$ during the winter period at the Mandir Marg is shown in Figure 56 and Figure 57. It was found that in the winter months (October, November, December, January and February), the mean $PM_{2.5}$ concentrations were 130.92 µg/m^3 and the mean PM_{10} was 227.97 µg/m^3 indicated by a red dotted line. An increasing trend was seen from the beginning of October until the second week of January. The highest weekly concentration of $PM_{2.5}$, i.e., ~ 240 µg/m^3 was observed during the second week of January 2023 While the PM_{10} concentration was observed highest in the first week of November 2022, i.e., ~ 340 µg/m^3. This indicated that the fractional load for the PM also varied in different winter months. A high pollutant load was observed during the peak winter months, and it gradually starts decreasing from the third week of January till February 2023.

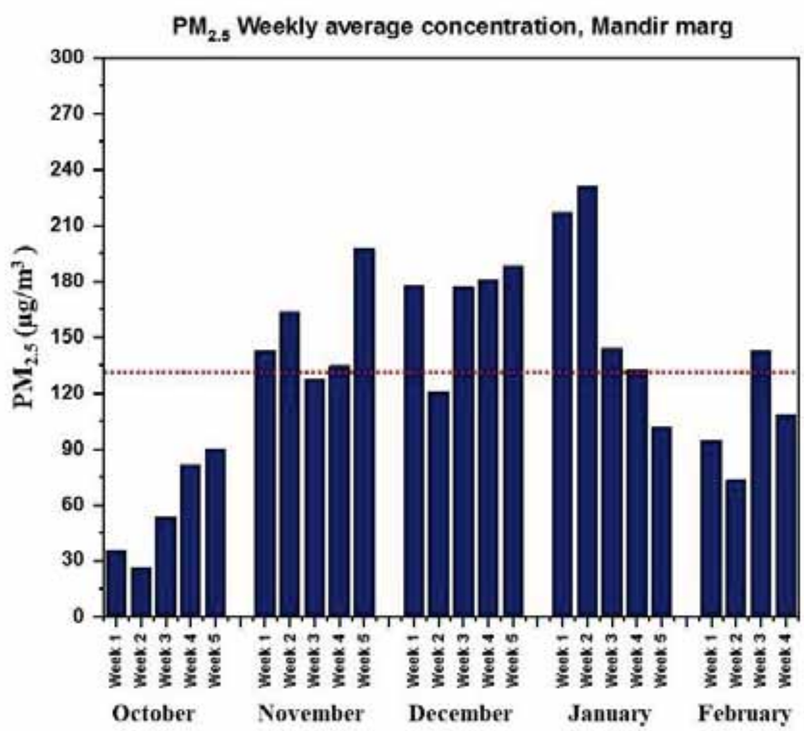

Figure 56. $PM_{2.5}$ concentration during the winter period (October 2022 - February 2023).

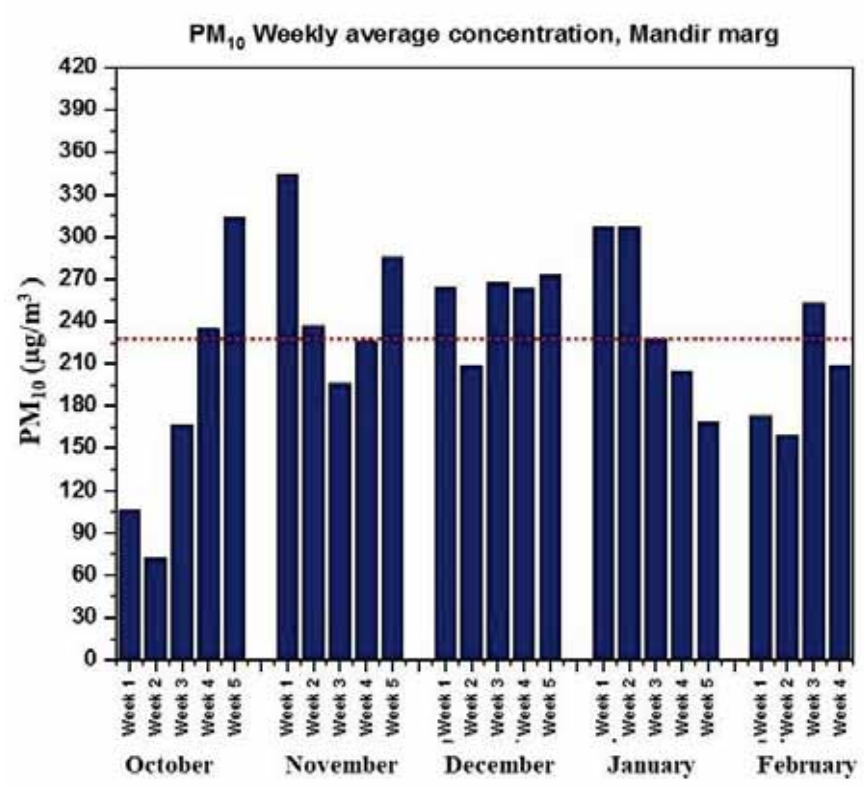

Figure 57. PM_{10} concentration during the winter period (October 2022 - February 2023).

5.3 Wind speed and wind direction (October 2022 - January 2023)

The wind speed and wind direction are the meteorological parameters that significantly affect pollutant transportation and its concentration. The wind rose was plotted for the winter seasons October 2022- January 2023. The variation of wind speed and wind direction at Mandir Marg monitoring station during the winter season are shown in Figure 58. It was found that during the winter season, the wind comes from mostly the West & South-West directions. However, the directions except the North direction are showing significant variation. The most common wind speed falls in the range of 0-0.8 m/s, which was ~ 70% of the total wind.

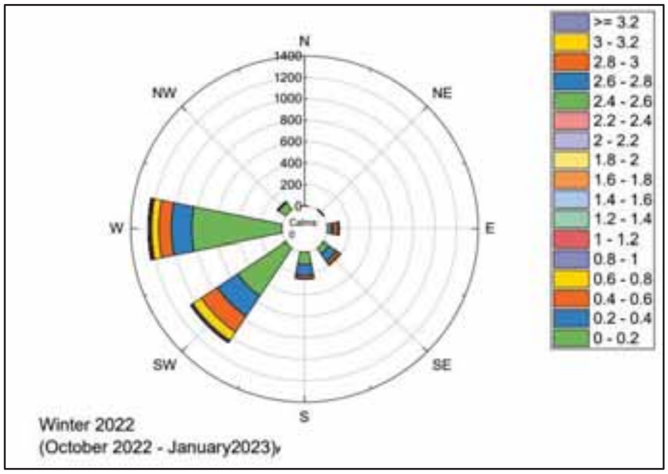

Figure 58. Wind rose for winter 2022 (Oct 2022-Jan 2023).

It was also observed that the wind direction and wind speed varied in different months of the winter period. The wind was found mostly blowing from the West direction in October and January. While in November and December, most of the wind was blown from the South-West and South directions. The monthly wind-rose plots for Mandir Marg station are shown in Figure 59.

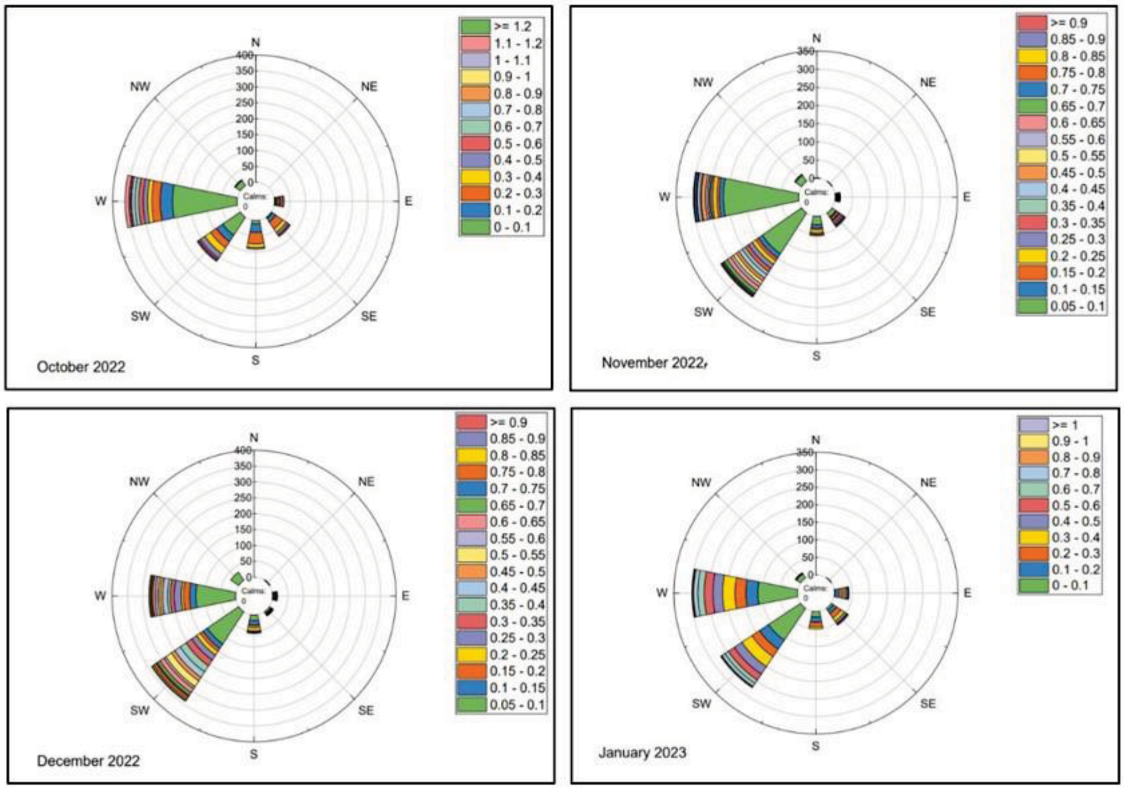

Figure 59. Monthly wind rose for winter 2022 (Oct 2022-Jan 2023).

Moreover, a significant variation in wind speed and wind direction was also observed on a daily basis. A few examples of wind-rose plots for the daily variations are shown in Figure 60. It must be noted that most of the wind was blown from the South-West direction on 23/11/2022, while on 24/11/2022 and 29/11/2022, most of the wind was found to be blown from the South-West and West directions. However, it was also observed that wind speed also varied on an hourly basis. Therefore, the effect of wind variations and wind directions need to be carefully considered while interpreting the MSACS effect in the ambient domain, since these parameters are dynamic in the ambient environment.

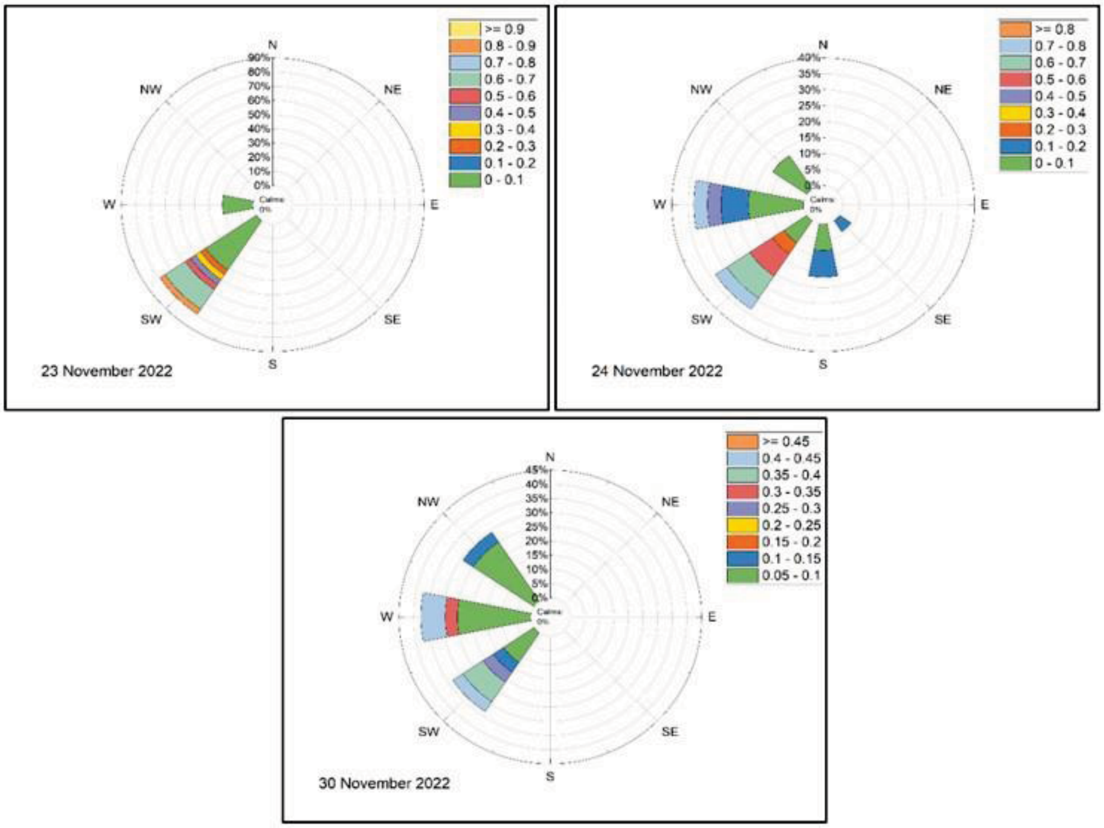

Figure 60. Illustrations for daily variations of wind speed and direction.

6 MSACS Performance in the Ambient Domain

The effectiveness of the MSACS system in the ambient domain was evaluated by measuring the PM_{10} and $PM_{2.5}$ concentrations at different distances from the MSACS to identify the clean air zone. The "OFF-ON-OFF" methodology was adopted to assess the reduction in ambient PM concentration with and without MSACS operations (Bächler et al., 2021). The methodology of OFF-ON-OFF strategy and OFF-ON strategies are reported in detail in previous Interim reports. Several OFF-ON-OFF measurements were conducted each month to examine the effectiveness of the MSACS system at different meteorological conditions and pollution loads. The measurements were carried out using various monitoring instruments, which includes a reference grade monitor, i.e., E-BAM, and multiple research-grade instruments (DustTrak and OPS, TSI, USA). The continuous measurement was recorded using the Low-Cost Sensor (LCS) installed around the MSACS. The E-BAM recorded the PM concentrations at 50 m distances from the MSACS, while the research-grade monitoring instruments were used for farther distances.

For assessing the MSACS effectiveness at farther distances, firstly the ambient PM concentrations were measured in the MSACS OFF condition for 30-60 minutes. Thereafter, measurements were taken at MSACS ON condition for ~ 90 minutes. The longer monitoring durations were planned for OFF-ON-OFF measurements since the clean air from MSACS takes some time to reach farther distances in stable and calm atmospheric conditions. However, in some cases, the measurement was also taken for 30-90 minutes in MSACS OFF conditions depending on different meteorological conditions. These field measurements were conducted in the morning, afternoon, early morning and late night sessions to assess the effectiveness of the MSACS at different periods of the day.

6.1 Monitoring location and choice of location

The monitoring locations and choice of locations are critical for analysing MSACS performance in the ambient domain. The MSACS is situated in a residential cum public hotspot location. To measure the MSACS' clean air effect in the ambient domain, several mobile monitoring locations were selected up to 700 m in all possible directions, as shown in Figure 61 and Figure 62.

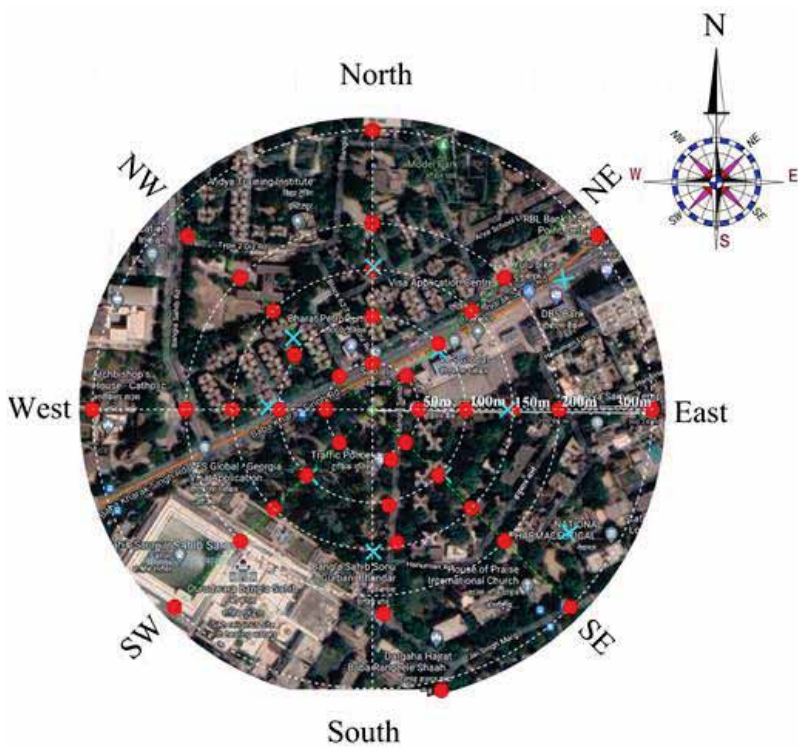

Figure 61. Nodes for the field sampling.

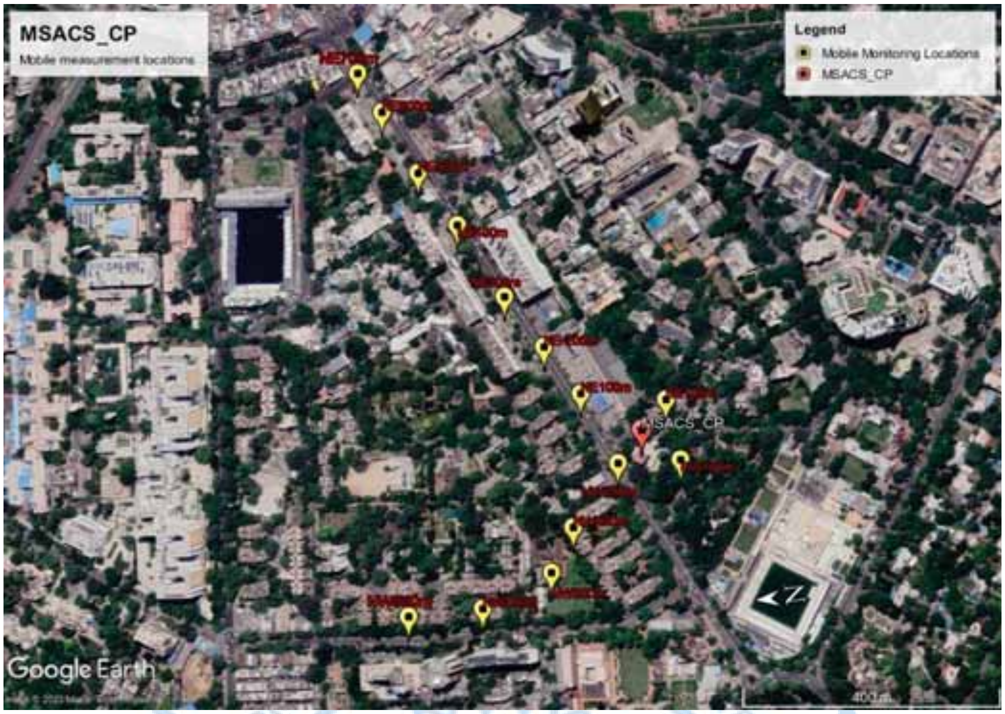

Figure 62. Monitoring locations around the MSACS.

The monitoring locations were selected based on the historical wind profile and feasibility of the suitable locations around the MSACS. The monitoring locations were selected in the MSACS jet direction in all four directions i.e., South-East (SE), North-East (NE), North-West (NW) and South-West (SW). However, these locations were delineated in an off-jet direction due to restricted places such as residential infrastructure, hotspot places, etc. During the winter measurement, several monitoring locations were identified at different distances from 50 m to 700 m in all four directions. The details for all possible monitoring locations and their characteristics are mentioned in Table 13. However, considering the minimum hindrance to clean air jet in the NE direction, several measurements were taken in the NE direction up to 700 m distances. The monitoring locations in the NE directions at different distances, such as 300 m, 400 m and 500 m are shown in Figure 63. It is to be noted that measurement in some directions was not feasible due to the restricted entry or hindrance by the buildings around the MSACS.

Figure 63. Monitoring location in NE direction at (a) 200 m (b) 300 m (c) 400 m (d) 500 m (e) 700 m distance from MSACS.

Table 13. Identified monitoring locations and characteristics for mobile measurements.

Sr.No.	Direction and Distance (m)		Location	Site Characteristics
1	North-East	100	Boundary of CPWD quarters (Block 87). Opposite to Shivaji metro station	• In the line of sight of the tower • Both fan & tower are visible. • Heavy traffic on road lying between tower and sampling point. • Trees causing an obstruction. • Road dust during turbulence • Under tree canopy
2		200	Nagaland Sales Emporium, Near Baba Khadag Singh Marg	• Both fan & tower are visible. • In the line of sight of the tower • Trees and building causing the obstruction. • Road dust during turbulence at 50m • Under tree canopy
3		300	Cauvery Sales Emporium, Near Baba Khadag Singh Marg	• In the line of sight of the tower • Both fan & tower are not visible. • Trees and building causing the obstruction. • Road dust during turbulence at 50m • Under tree canopy
4		400	Under States Emporium boundary, Near Baba Khadag Singh Marg	• In the line of sight of the tower • Both fan & tower are not visible. • Trees and building causing the obstruction. • Road dust during turbulence at 50m • Under tree canopy
5		500	Outside Delhi tourism office	• In the line of sight of the tower • Both fan & tower are not visible. • Trees and building causing the obstruction. • Road dust during turbulence at 50m • Under tree canopy
6		700	Delhi development co-operation boundary	• In the line of sight of the tower • Both fan & tower are not visible. • Trees and building causing the obstruction. • Road dust during turbulence at 50m • Under tree canopy
7	South-East	100	CPWD Quarter, back of Block-2, near boundary wall	• In the line of sight of the tower • Both fan & tower are not visible. • High-rise building causing the obstruction. • Road dust during turbulence

				• Under tree canopy
8		200	Near, Gurudwara Bangla Saheb parking	• Not in the line of sight of the tower • Both fan & tower are visible. • Road dust during turbulence • Under tree canopy
9		300	Near YWCA Gate	• Not in the line of sight of the tower • Both fan & tower are not visible. • High-rise building causing the obstruction. • Road dust during turbulence • Under tree canopy
10		400	Near NHPC Camp office	• Not in the line of sight of the tower • Both fan & tower are not visible. • High-rise building causing the obstruction. • Road dust during turbulence • Under tree canopy
11		500	Near ECI-HQ	• Not in the line of sight of the tower • Both fan & tower are not visible. • High-rise building causing the obstruction. • Road dust during turbulence
12	**North-West**	100	CPWD quarter boundary, opposite to tower on the left of the petrol pump	• Present in the line of sight to the jet stream with respect to the fan facing the main road. • Site under the canopy of trees. • Dry leaves are present on the barren ground. • No source of emission
13		200	Inside CPWD quarter park, opposite to tower on the left of the petrol pump	• In the line of sight with respect to the tower • Site under the canopy of trees. • Dry leaves are present on the barren ground. • No source of emission
14		300	Near Kali Temple just besides the roadway	• In the line of sight with respect to the tower but no visibility • Site under the canopy of trees. • Dry leaves are present on the barren ground.

				• Heavy traffic hotspot
15		400	The front gate of Tata Communication	• In the line of sight with respect to the tower but no visibility • Site under the canopy of trees. • Dry leaves are present on the barren ground. • Heavy traffic hotspot
16		500	The front gate of WHO	• In the line of sight with respect to the tower but no visibility • Site under the canopy of trees. • Dry leaves are present on the barren ground. • Heavy traffic hotspot
17	**South-West**	100	Boundary of the Traffic Training Park	• In the line of sight to the tower but slightly shifted to the left towards fan F1 and F2. • Both fan & tower are visible • Obstruction to the jet stream of the tower due to trees in the park. • No source of emission
18		200	SPYM Bangla sahib center	• Not in the line of sight with respect to the tower but no visibility • Dry leaves are present on the barren ground • Heavy traffic hotspot
19		300	YSCO	• Not in the line of sight with respect to the tower but no visibility • Heavy traffic hotspot
20		400	Near Gurudwara Bangla Saheb Front gate	• In the line of sight of the tower • Both fan & tower are not visible. • High-rise building causing the obstruction. • Road dust during turbulence • Under tree canopy
21		500	Morarji Desai National Institute of Yoga	• In the line of sight of the tower • Both fan & tower are not visible. • High-rise building causing the obstruction. • Under tree canopy

6.2 MSACS performance at different distances

The effectiveness of the MSACS system in the ambient domain was evaluated at different distances from the MSACS. The MSACS was operated for several OFF-ON-OFF conditions. The PM_{10} and $PM_{2.5}$ concentrations were recorded in the system OFF condition followed by the system ON condition at different selected monitoring locations up to 700 m distances around the MSACS. For an OFF-ON-OFF cycle of the MSACS, the percentage reduction in ambient PM concentration was calculated using Equation 3.

$$\%\ \text{Reduction}(\eta) = \frac{\text{Concentration}_{\text{OFF}} - \text{Concentration}_{\text{ON}}}{\text{Concentration}_{\text{OFF}}} \times 100 \ldots\ldots\ldots \text{Equation 3}$$

Before analyzing the data, the outliers were eliminated. Considering the multivariable nature of the data and its dependency on different meteorological factors, three methods were evolved for calculating the percentage reduction in ambient PM concentration, i.e., Average method, Maximum impact method and Consistent/persistent method.

In the average method, average PM concentrations were considered for complete durations in MSACS OFF and ON conditions, giving an overall estimation for the percentage reduction for PM concentration. The maximum impact method was intended to assess the maximum reduction for PM concentration, which would occur if the diurnally varying wind direction directly passed through the sampling point and lasted for sufficient time to reach the sampling point. In this method, an average of a set of trough values of concentration in the ON condition and the average values during the OFF condition were used in Equation 3 to obtain the efficiency. Also, to account for PM concentration variation around the MSACS due to continuous pollution sources, a consistent/persistent method was selected. In the consistent/persistent method, percentage reduction was calculated using the average PM concentration for the stable condition only during the MSACS ON and OFF condition. The different methodologies served the purpose of ensuring that any systematic effects occurring in the midst of ambient fluctuations in concentrations due to uncontrolled local sources randomly varying wind directions, etc. are not missed but get captured in a qualitative way. The final efficiency reported for each measurement was estimated by a representative average of the efficiencies obtained from the above methods.

The MSACS performance was examined at various times of the day, such as early morning, afternoon, evening and late night. Further, a detailed analysis is described below to assess the MSACS clean air jet effect in MSACS OFF and ON conditions. Several experiments were conducted for the OFF-ON-OFF cycle. The percentage reduction for PM_{10} and $PM_{2.5}$ was analysed in the MSACS OFF condition, then MSACS ON condition, followed by another OFF condition. Approximately 145 minutes of OFF-ON-OFF cycle experiment was conducted, i.e., 25 minutes of OFF, 70 minutes of ON and 50 minutes of OFF. The purpose of including the 2nd OFF condition was to assess how the ambient PM concentrations return to the higher concentration levels once the system is in the OFF condition.

For example, the results for the performance of the MSACS for the OFF-ON-OFF cycle at 50% fan capacity are shown in Figure 64. A notable drop in the PM_{10} and $PM_{2.5}$ concentration was observed at 50 m, 70 m and 100 m when the MSACS was switched ON, and the PM_{10} and $PM_{2.5}$ concentration levels increased once the MSACS switched OFF. A reduction of 40-43% for PM_{10} and 35-36% for $PM_{2.5}$ is observed at 50 m in the SE direction (Table 15, Case 5). Similarly, in the SE direction at 70 m, a reduction of 33-37% and 30-34% was observed for PM_{10} and for $PM_{2.5}$ respectively. At 100 m in NW direction, a reduction of 8-17% for PM_{10} and 12-18% for $PM_{2.5}$. It was found that the PM_{10} and $PM_{2.5}$ concentration levels significantly decreased in the MSACS ON condition, and the PM concentration level started to regain its level in the MSACS OFF condition, which clearly indicated that the PM concentration level decreased in the MSACS ON condition.

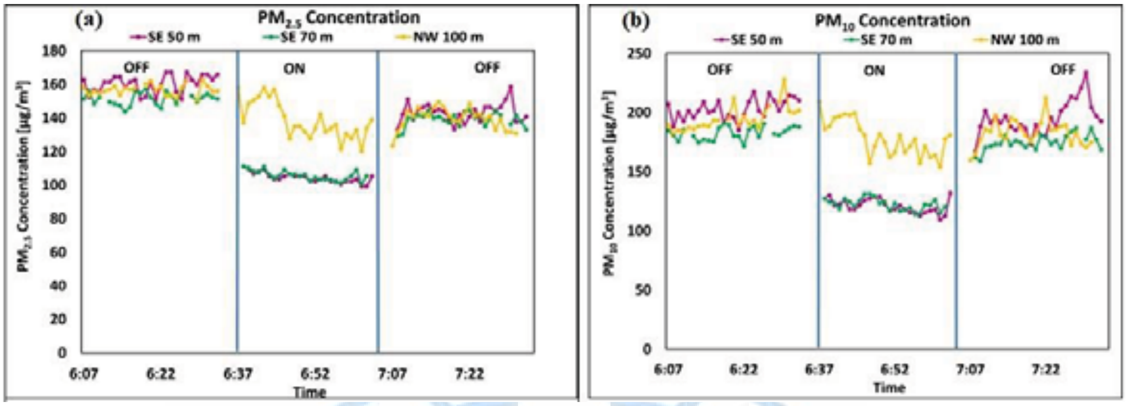

Figure 64. The concentration variations for (a) $PM_{2.5}$ (b) PM_{10} in the MSACS OFF-ON-OFF conditions for 50 m (SE), 70 m (SE) and 100 m (NW) at 50% fan capacity.

The MSACS performance in the ambient domain was also found to be affected by atmospheric conditions such as ambient PM concentration, temperature and relative humidity along with the wind speed and wind direction. Since the ambient condition in the field is dynamic, the wind speed and wind direction are also crucial for the system performance, as stable wind speed and downwind measurements may favour the MSACS performance positively. The maximum reported reduction in PM concentration at different distances from the MSACS was observed when the contributing factors, such as wind speeds and wind direction, favoured the clean air jet of the MSACS. The effect of these contributing factors on MSACS' performance is described in detail below with specific cases.

6.2.1 Effect of wind speed: Low wind vs High wind

The concentration variations for PM_{10} at different distances in MSACS ON and OFF conditions are shown in Figure 65 (a) at the low wind speed and Figure 65 (b) at the high wind speed. Considering test 26 of Table 15, when the ambient wind speed was 0.5 – 0.7 m/s, a significant reduction was observed PM_{10} i.e., ranging from 25%-42% at 100 m, 27%-54% at 200 m, 26%-40% at 300 m and 21%-45% at 400 m distance from the MSACS. At high wind speed of ~ 1.3-

1.6 m/s in test 30 of Table 15, the percentage reduction for PM_{10} was found to be ranging from 15%-34%; 8%-26%; and 5%-22% at 200 m, 400 m and 500 m distances, respectively. This indicates that a higher PM_{10} percentage reduction was observed at low wind speed conditions as compared to the high wind speed conditions around the MSACS. Thus, MSACS performance in the ambient domain is significantly affected by the wind speed.

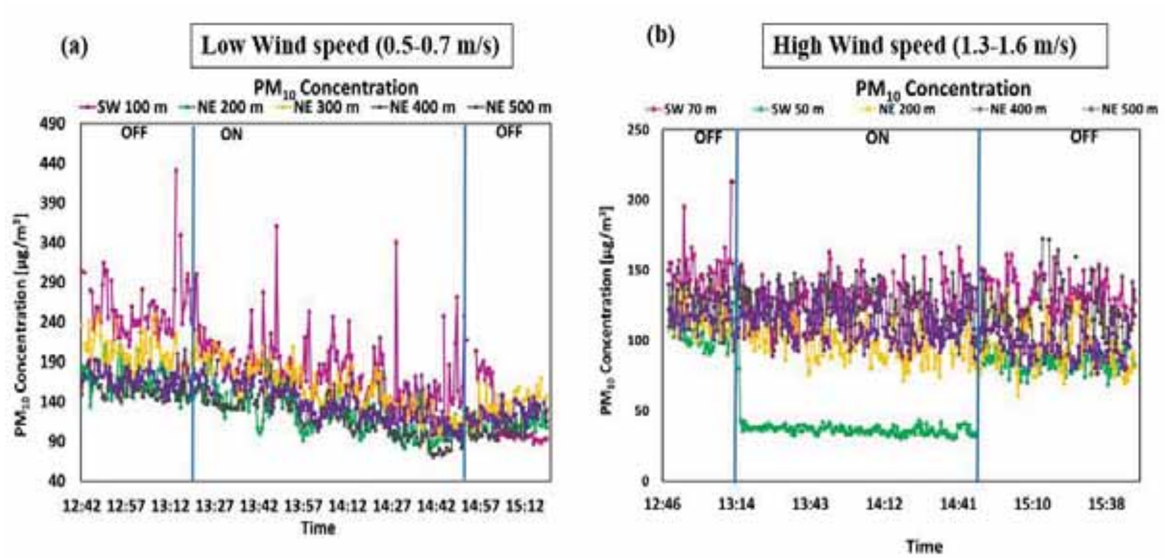

Figure 65. The concentration variations for PM_{10} at different distances in MSACS ON and OFF conditions at (a) Low wind speed and (b) High wind speed conditions.

6.2.2 Effect of wind direction: Downwind vs Upwind

The concentration variations for PM_{10} at different distances in the MSACS ON and OFF conditions are shown in Figure 66 (a) Downwind and (b) Upwind. Considering Test 29 of Table 15, when the wind was found to be blowing from the South-West (SW) direction, the maximum percentage reduction was observed in the downwind direction, i.e., North-East (NE) direction. The percentage reduction for PM_{10} was found to be ranging from 28% - 57% at 200 m, 23% to 51% at 300 m, and 23% to 40% at 400 m distance from the MSACS. When the wind was also blowing from the North direction, i.e., Test 31 of Table 15, the percentage reduction for PM_{10} in the upwind direction, i.e., NE direction, was found to be comparatively lesser. The percentage reduction for PM_{10} in the upwind direction ranged from 1% -21% at 200 m, 5% - 26% at 400 m, and 3%-15% at 500 m. While on the same day, in the downwind direction, i.e., SE at 50 m, it was found to be ranging from 56% to 61% and it was 25% to 51%, at 70 m in SE. This indicates that a higher PM_{10} percentage reduction was observed at the downwind condition as compared to the upwind condition. Therefore, a significant impact of wind direction was observed on the performance of MSACS in the ambient domain.

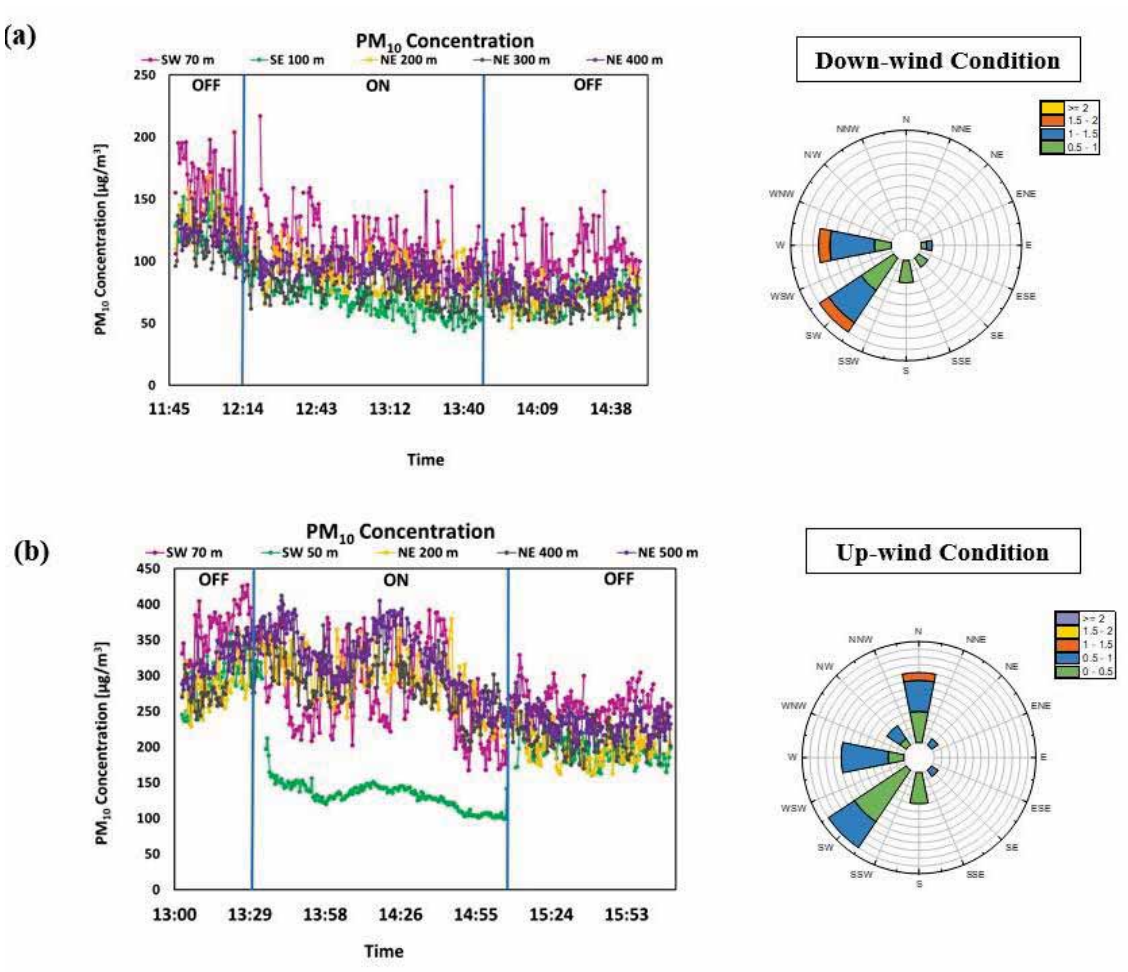

Figure 66. The concentration variations for PM_{10} at different distances in MSACS ON and OFF conditions at (a) Downwind and (b) Upwind conditions.

.

6.2.3 MSACS performance (October 2021- August 2022)

The measurements were taken during October 2021- August 2022 at several distances, such as 20 m, 50 m, 100 m, 150 m and 300 m. The percentage reduction of PM_{10} and $PM_{2.5}$ levels (Range) of the few experimental cases for the October 2021- August 2022 period at different distances in the vicinity of the MSACS system are briefly included here and summarised in Table 14. The detailed analysis of MSACS performance for October 2021- August 2022 was discussed in detail in the Interim Report-2.

6.2.4 MSACS performance (October 2022-February 2023)

A new set of filters were replaced with the loaded filters, and the MSACS was kept ready for the winter period (October 2022-February 2023) study. Several experiments were performed during the winter of 2023 with various fan capacities, distances, and times of day (Early morning, Late night, Evening and Afternoon). For the winter season (October 2022-February 2023), all experiments were analysed for assessing the MSACS performance with respect to the percentage reduction of PM_{10} and $PM_{2.5}$ in the ambient. The percentage reduction of PM_{10} and $PM_{2.5}$ levels (Range) of the few experimental cases for the winter season (October 2022-February 2023) at different distances in the vicinity of the MSACS system are summarised in Table 15.

Two late-night measurements were performed at NE 700 m distance to know the impact of MSACS. The wind speed in both the measurements was approx. <0.5 m/s and the wind direction was West (Refer to case 33, Table 15) and East for case 34, Table 15. From the results it was observed that the average reduction obtained from all the three methods described in the section 6.2 was 7±7%, indicating some reduction even at higher distances. Since the number of data points is limited more data needs to be collected for a strong indication.

Table 14. The percentage reduction of PM_{10} and $PM_{2.5}$ levels (Range) at different distances in the vicinity of the MSACS system (October 2021- August 2022).

Tests	**Measurement time**	**Fan Capacity**	**CADR (m³/s)**	**Humidity**	**Wind Speed**	**Wind Direction**		**% Reduction for $PM_{2.5}$ at different distances**						**% Reduction for PM_{10} at different distances**				
1*	Evening	50%	150		0.3	NW	**Direction, Distances in meters**	SE 50	SE 100	SE 300				SE 50	SE 100	SE 300		
							Percentage Reduction (%)	**22-28**	**30-33**	**13-20**				**33-40**	**43-45**	**16-23**		
2*	Forenoon	50%	175		1.3	SW	**Direction, Distances in meters**	SW 50	SW 100	SW 300				SW 50	SW 100	SW 300		
							Percentage Reduction (%)	**28-30**	**8-12**	**8-11**				**31-34**	**6-11**	**7-10**		
3*	Forenoon	50%	201		1.97	SW	**Direction, Distances in meters**	NW 50	NW 100					NW 50	NW 100			

							Percentage Reduction (%)	**21-31**	**7-13**					**31-48**	**14-24**			
4*	Afternoon	50%	201		0.75	SW	**Direction, Distances in meters**	SE 50	SE 100					SE 50	SE 100			
							Percentage Reduction (%)	**23-41**	**10-21**					**33-66**	**16-42**			
5*	Afternoon	50%	201		0.58	WSW	**Direction, Distances in meters**	W 50	W 100					W 50	W 100			
							Percentage Reduction (%)	**36-47**	**29-38**					**34-49**	**26-37**			
6*	Afternoon	50%	200		1.8	WSW	**Direction, Distances in meters**	S 50	S 100	S 300				S 50	S 100	S 300		
							Percentage Reduction (%)	**17-23**	**9-22**	**5-17**				**21-31**	**3-20**	**0-15**		
7*	After noon	50%	200		1.7	WSW	**Direction,**	NW 50	NW 150					NW 50	NW 150			

							Distances in meters											
							Percentage Reduction (%)	**42-52**	**29-35**					**51-64**	**28-37**			
8*	Afternoon	50%	184		1	SW	**Direction, Distances in meters**	NW 20	NW 50	NW 100	NW 150			NW 20	NW 50	NW 100	NW 150	
							Percentage Reduction (%)	**37-47**	**34-44**	**6-16**	**7-22**			**59-63**	**49-61**	**7-26**	**7-26**	
9*	Afternoon	50%	184		0.47	W	**Direction, Distances in meters**	SW 50	SW 100					SW 50	SW 100			
							Percentage Reduction (%)	**29-37**	**17-24**					**47-59**	**28-42**			
10*	Afternoon	50%	206		0.18	WSW	**Direction, Distances in meters**	SW 50	SW 100					SW 50	SW 100			
							Percentage Reduction (%)	**47-56**	**23-36**					**52-60**	**12-32**			

11*	Afternoon	50%	189		2.73	WSW	**Direction, Distances in meters**	SE 20	SE 50	SE 100	SE 150			SE 20	SE 50	SE 100	SE 150	
							Percentage Reduction (%)	**47-57**	**29-30**	**20-32**	**8-30**			**61-69**	**31-35**	**16-32**	**16-35**	
12*	Morning	50%	296		1.77	SW	**Direction, Distances in meters**	SW 20	SW 50	SW 100				SW 20	SW 50	SW 100		
							Percentage Reduction (%)	**68-71**	**55-62**	**47-57**				**79-80**	**62-71**	**39-49**		
13*	Forenoon	50%	266		1.94	ESE	**Direction, Distances in meters**	NW 20	NW 50	NW 100				NW 20	NW 50	NW 100		
							Percentage Reduction (%)	**50-56**	**50-65**	**3-26**				**57-62**	**50-70**	**7-27**		
14*	Morning	75%	393		1.63	SSE	**Direction, Distances in meters**	NW 20	NW 50	NW 100				NW 20	NW 50	NW 100		

							Percentage Reduction (%)	**62-66**	**48-59**	**16-25**				**65-70**	**43-58**	**16-29**		
15*	Forenoon	75%	417		1.9	ESE	**Direction, Distances in meters**	NE 20	NE 50	NE 100				NE 20	NE 50	NE 100		
							Percentage Reduction (%)	**41-51**	**25-47**	**8-20**				**53-61**	**21-50**	**0-29**		
16*	Afternoon	100%	501		1.48	ESE	**Direction, Distances in meters**	SW 20	SW 50	SW 100				SW 20	SW 50	SW 100		
							Percentage Reduction (%)	**55-61**	**37-47**	**10-27**				**74-81**	**43-56**	**8-30**		
17*	Morning	100%	721		3.9	SW	**Direction, Distances in meters**	SW 20	SW 50	SW 100				SW 20	SW 50	SW 100		
							Percentage Reduction (%)	**55-67**	**48-62**	**11-25**				**57-65**	**49-61**	**8-22**		
18*	Mor ning	100%	603		1.8	SW	**Direction,**	NW 20	NW 50	NW 100				NW 20	NW 50	NW 100		

							Distances in meters											
							Percentage Reduction (%)	**53-68**	**57-71**	**0-5**				**52-71**	**58-73**	**0-3**		

* indicates the experiments were performed for two OFF and the reduction given was for the first OFF-ON; - indicates no reduction was observed in that direction.

Table 15. The percentage reduction of PM_{10} and $PM_{2.5}$ levels (Range) at different distances in the vicinity of the MSACS system (October 2022- February 2023).

Tests	Measurement time	Fan Capacity	CADR (m^3/s)	Humidity	Wind Speed	Wind Direction		% Reduction for $PM_{2.5}$ at different distances						% Reduction for PM_{10} at different distances				
1*	Morning	50%	322				**Direction, Distances in meters**	SE 50	SE 70	N 20	N 150			SE 50	SE 70	N 20	N 150	
							Percentage Reduction (%)	**0.7-11**	**29-41**	**35-41**	**0-32**			**21-32**	**33-43**	**43-48**	**0-39**	
2*	Evening	50%	322				**Direction, Distances in meters**	SE 50	SE 70	NW 100	NW 150			SE 50	SE 70	NW 100	NW 150	
							Percentage Reduction (%)	**22-30**	**0-3**	**-**	**-**			**33-43**	**0-9**	**0-10**	**-**	
3*	Early Morning	50%	326				**Direction, Distances in meters**	SE 50	SE 70	NW 100	NW 150			SE 50	SE 70	NW 100	NW 150	

							Percentage Reduction (%)	**27-33**	**22-32**	**0-7**	**1-7**			**23-38**	**24-37**	**0-4**	**1-7**	
4*	Evening	50%	326				**Direction, Distances in meters**	SE 50	SE 70	NW 100	NW 150			SE 50	SE 70	NW 100	NW 150	
							Percentage Reduction (%)	**13-27**	**0-11**	**7-15**	**-**			**39-51**	**5-20**	**9-23**	**-**	
5*	Early Morning	50%	333				**Direction, Distances in meters**	SE 50	SE 70	NW 100	NW 150			SE 50	SE 70	NW 100	NW 150	
							Percentage Reduction (%)	**35-36**	**30-34**	**12-18**	**3-12**			**40-43**	**33-37**	**8-17**	**2-11**	
6*	Evening	50%	333				**Direction, Distances in meters**	SE 50	SE 70	NW 100	NW 150			SE 50	SE 70	NW 100	NW 150	
							Percentage Reduction (%)	**3-16**	**-**	**-**	**-**			**19-34**	**0-24**	**0-5**	**-**	
7	Late Night	50%	184		1.5-2		**Direction,**	NW 50	NW 200	NW 300	NW 400			NW 50	NW 200	NW 300	NW 400	

							Distances in meters											
							Percentage Reduction (%)	**16-21**	**-**	**0-3**	**-**			**32-37**	**-**	**0-7**	**-**	
8	Early Morning	50%	184		0-1		**Direction, Distances in meters**	NE 200	NE 300	NE 400	NE 500			NE 200	NE 300	NE 400	NE 500	
							Percentage Reduction (%)	**7-18**	**0-2**	**1-8**	**0-2**			**8-18**	**0-2**	**3-11**	**0-8**	
9	Afternoon	75%	314	44			**Direction, Distances in meters**	E-BAM 50	NE 200					NE 200				
							Percentage Reduction (%)	**17**	**0-31**					**0-37**				
10	Afternoon	75%	189	44	4-5		**Direction, Distances in meters**	E-BAM 50	NE 200	NE 400				NE 200	NE 400			

							Percentage Reduction (%)	**41**	**20-35**	**22-41**				**17-34**	**22-42**			
11	Late Night	75%	325	71	~ 0		**Direction, Distances in meters**	E-BAM 50	NE 200	NE 300	NE 400	NE 500		NE 200	NE 300	NE 400	NE 500	
							Percentage Reduction (%)	**63**	**11-14**	**18-24**	**7-15**	**2-7**		**14-17**	**15-22**	**9-17**	**4-15**	
12	Early Morning	75%	325	80	~ 0	NW	**Direction, Distances in meters**	E-BAM 50	NE 200	NE 300	NE 400	NE 500		NE 200	NE 300	NE 400	NE 500	
							Percentage Reduction (%)	**48**	**6-13**	**12-18**	**12-19**	**6-15**		**2-12**	**8-20**	**6-20**	**5-16**	
13	Afternoon	75%	253	67	1.75		**Direction, Distances in meters**	E-BAM 50	NE 200	NE 300	NE 500			NE 200	NE 300	NE 500		
							Percentage Reduction (%)	**46**	**33-46**	**33-43**	**30-15**			**31-50**	**33-49**	**25-51**		

14	Late Night	75%	311	76-82	2	E	**Direction, Distances in meters**	E-BAM 50	NE 200	NE 300	NE 500			NE 200	NE 300	NE 500		
							Percentage Reduction (%)	**44**	**11-21**	**11-12**	**14-15**			**13-17**	**13-19**	**9-21**		
15	Early Morning	75%	311	82-84	2	W	**Direction, Distances in meters**	E-BAM 50	NE 200	NE 300	NE 500			NE 200	NE 300	NE 500		
							Percentage Reduction (%)	**15**	**0-8**	**-**	**-**			**0-16**	**0-6**	**0-7**		
16	Afternoon	75%	276	45.7	0.13 - 1.25	NW	**Direction, Distances in meters**	NE 100	NE 200	NE 400	NE 500			NE 100	NE 200	NE 400	NE 500	
							Percentage Reduction (%)	**0-6**	**0-4**	**-**	**0-13**			**0-10**	**0-5**	**-**	**0-20**	
17	Afternoon	75%	300	37-38			**Direction, Distances in meters**	E-BAM 50	NE 100	NE 200	NE 400			NE 100	NE 200	NE 400		

							Percentage Reduction (%)	**36**	**5-27**	**13-25**	**9-22**			**3-29**	**8-28**	**6-26**		
18	Late Night	75%	452	60			**Direction, Distances in meters**	E-BAM 50	NE 100	NE 300	NE 400	NE 500		NE 100	NE 300	NE 400	NE 500	
							Percentage Reduction (%)	**21**	**0-13**	**7-21**	**4-18**	**1-14**		**10-29**	**14-33**	**8-22**	**9-28**	
19	Early Morning	75%	452	65			**Direction, Distances in meters**	E-BAM 50	NE 200	NE 300	NE 400	NE 500		NE 200	NE 300	NE 400	NE 500	
							Percentage Reduction (%)	**-**	**-**	**-**	**-**	**-**		**-**	**-**	**-**	**-**	
20	Afternoon	75%	237	48.5 - 61.2	~ 0.5		**Direction, Distances in meters**	E-BAM 50	NE 200	NE 300	NE 400	NE 500		NE 200	NE 300	NE 400	NE 500	
							Percentage Reduction (%)	**41**	**32-52**	**27-44**	**24-36**	**20-37**		**33-66**	**21-45**	**20-28**	**18-38**	

21	Late Night	75%	326	>95	0-0.52	SSW-NNE	**Direction, Distances in meters**	E-BAM 50	S 100	NE 100	NE 200	NE 300		S 100	NE 100	NE 200	NE 300	
							Percentage Reduction (%)	**44**	**9-33**	**20-31**	**15-27**	**15-29**		**11-33**	**21-33**	**17-31**	**17-29**	
22*	Afternoon	75%	334	76	0.53-1.4	NW-NE	**Direction, Distances in meters**	E-BAM 50	SE 50	NE 100	NW 500	NW 500		SE 50	NE 100	NW 100	NW 150	
							Percentage Reduction (%)	**17-25**	**3-14**	**-**	**-**	**-**		**3-20**	**-**	**-**	**-**	
23*	Afternoon	75%	303	62-68	0.6-1.39		**Direction, Distances in meters**	E-BAM 50	SE 50	NE 150	NW 150	SW 75		SE 50	NE 150	NW 150	SW 75	
							Percentage Reduction (%)	**36**	**29-39**	**20-22**	**15-19**	**-**		**18-28**	**12-15**	**13-24**	**-**	
24*	Afternoon	75%	376	60-72	0.69-2.2	Wind direction	**Direction, Distances in meters**	E-BAM 50	NW 70	NE 200	NE 300	NE 400	NE 500	NW 70	NE 200	NE 300	NE 400	NE 500

							Percentage Reduction (%)	**9-18**	**0-9**	**0-6**	**0-8**	**0-4**	**0-4**	**0-11**	**0-10**	**0-11**	**0-4**	**0-7**
25	Afternoon	75%	394	54-58	1.25	N-SE	**Direction, Distances in meters**	NE 200	NE 300	NE 400	NE 500			NE 200	NE 300	NE 400	NE 500	
							Percentage Reduction (%)	**7-14**	**6-12**	**3-8**	**2-9**			**1-14**	**6-13**	**6-11**	**0-10**	
26*	Afternoon	100%	649	38-40	0.52 - 0.72	SW-WNW	**Direction, Distances in meters**	E-BAM 50	SW 100	NE 200	NE 300	NE 400	NE 500	SW 100	NE 200	NE 300	NE 400	NE 500
							Percentage Reduction (%)	**81**	**26-39**	**28-41**	**26-34**	**23-41**	**20-37**	**25-42**	**27-54**	**25-40**	**21-45**	**20-35**
27*	Afternoon	100%	542	39-41			**Direction, Distances in meters**	E-BAM 50	SE 100	NE 200	NE 300	NE 400	NE 500	SE 100	NE 200	NE 300	NE 400	NE 500
							Percentage Reduction (%)	**27**	**22-38**	**11-21**	**7-17**	**3-17**	**3-15**	**25-28**	**13-32**	**7-20**	**3-23**	**7-25**

28	Afternoon	100%	392	34.8	0.28	N	**Direction, Distances in meters**	E-BAM 50	SW 100	NE 300	SE 100	NE 400	NE 500	SW 100	NE 300	SE 100	NE 400	NE 500
							Percentage Reduction (%)	**24**	**42-50**	**31-42**	**44-55**	**31-43**	**43-34**	**48-59**	**29-44**	**44-66**	**32-51**	**27-50**
29*	Afternoon	100%	650	31	0.52 - 0.89	SW S-W	**Direction, Distances in meters**	E-BAM 50	SW 70	SE 100	NE 200	NE 300	NE 400	SW 70	SE 100	NE 200	NE 300	NE 400
							Percentage Reduction (%)	**49**	**34-57**	**42-26**	**32-50**	**23-41**	**21-33**	**31-49**	**45-62**	**28-57**	**23-51**	**23-40**
30*	Afternoon	100%	611	35-37	1.25 - 1.64	SSE -SW	**Direction, Distances in meters**	E-BAM 50	SW 70	SW 50	NE 200	NE 400	NE 500	SW 70	SW 50	NE 200	NE 400	NE 500
							Percentage Reduction (%)	**35**	**19-43**	**47-57**	**27-42**	**14-28**	**12-28**	**13-43**	**62-73**	**15-35**	**8-27**	**5-23**
31*	Afternoon	100%	611	44.2	0.89	NNE	**Direction, Distances in meters**	E-BAM 50	SW 70	SW 50	NE 200	NE 400	NE 500	SW 70	SW 50	NE 200	NE 400	NE 500

							Percentage Reduction (%)	**26**	**27-43**	**40-45**	**10-21**	**10-18**	**9-16**	**25-51**	**56-61**	**1-21**	**5-26**	**3-15**
32	Afternoon	100%	553	40	1.08	SE	**Direction, Distances in meters**	E-BAM 50	SW 50	NE 200	NE 400	NE 500		SW 50	NE 200	NE 400	NE 500	
							Percentage Reduction (%)	**Error in data**	**31-47**	**15-25**	**11-22**	**11-20**		**62-70**	**9-27**	**0-30**	**5-23**	
33	Late Night	100%	553	80	0-1.44	Wind Speed varies	**Direction, Distances in meters**	E-BAM 50	NE 200	NE 400	NE 500	NE 700		NE 200	NE 400	NE 500	NE 700	
							Percentage Reduction (%)	**47-53**	**11-17**	**8-13**	**9-14**	**10-18**		**14-28**	**10-20**	**13-18**	**11-18**	
34*	Late Night	100%	603	68-83	~ 0	N-E	**Direction, Distances in meters**	E-BAM 50	SW 70	NE 200	NE 400	NE 500	NE 700	SW 70	NE 200	NE 400	NE 500	NE 700
							Percentage Reduction (%)	**-**	**28-32**	**0-8**	**-**	**0-3**	**0-4**	**60-65**	**10-40**	**0-13**	**4-28**	**1-28**

* indicates the experiments were performed for two OFF and the reduction given was for the first OFF-ON; - indicates no reduction was observed in that direction.

6.3 MSACS performance by E-BAM

The MSACS performance in the ambient domain was also assessed using the E-BAM in the MSACS ON and OFF conditions. E-BAM is a standard reference grade instrument that is widely accepted and used for measuring real-time ambient particulate matter ($PM_{2.5}$ or PM_{10}). Installation of the E-BAM was aimed to measure the concentration at a fixed location for 24 hr. E-BAM was installed in the North-East (NE) direction at ~ 50 m of distance from the MSACS.

The $PM_{2.5}$ concentrations recorded by the E-BAM in the MSACS OFF and ON conditions at different fan capacities, such as 50%, 75% and 100%, were analysed to assess the MSACS. Several experiments have shown a significant reduction of $PM_{2.5}$ concentrations in the MSACS ON conditions compared to OFF conditions. The percentage reduction of $PM_{2.5}$ for different fan capacities, seasons and meteorological conditions is summarised in Table 15. Further few examples of the $PM_{2.5}$ concentration variation recorded by E-BAM during the OFF-ON experiments are discussed in this section.

For example, the $PM_{2.5}$ concentration recorded by E-BAM in the MSACS OFF and ON conditions at 75% fan capacity is shown in Figure 67. The average $PM_{2.5}$ concentration during the MSACS OFF condition (at 22:45-23:45 hours) was ~ 272 µg/m^3, while the $PM_{2.5}$ concentration was reduced to ~ 154 µg/m^3 in MSACS ON condition (at 00:30-01:30 hours), indicating a significant reduction, i.e., ~ 44% in $PM_{2.5}$ concentration in the MSACS ON condition.

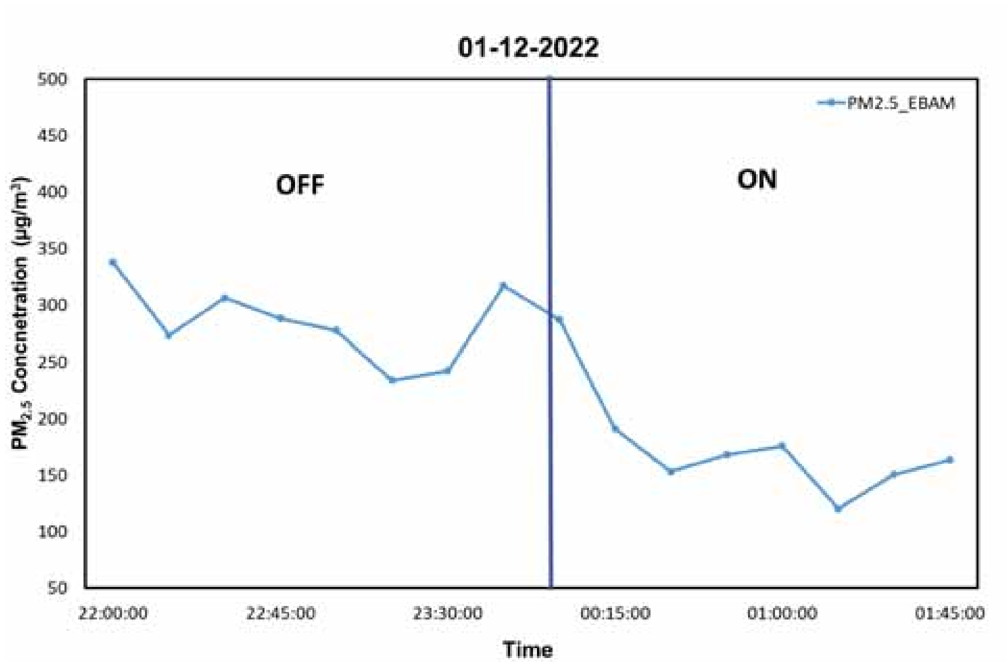

Figure 67. $PM_{2.5}$ concentration variation recorded by E-BAM in MSACS OFF-ON condition at 75% fan capacity.

Likewise, the $PM_{2.5}$ concentration recorded by E-BAM in the night-time in the MSACS OFF and ON conditions at 100% fan capacity is shown in Figure 68. The average $PM_{2.5}$ concentration during the MSACS OFF condition (at 22:00-23:00 hours) was observed to be ~ 114 $\mu g/m^3$. While the average $PM_{2.5}$ concentration was ~ 62 $\mu g/m^3$ in the MSACS ON condition (at 23:45-01:00 hours). Around 45% reduction of $PM_{2.5}$ concentration level was observed for this experiment, indicating a notable reduction in the $PM_{2.5}$ level during MSACS ON condition compared to when MSACS was in OFF condition.

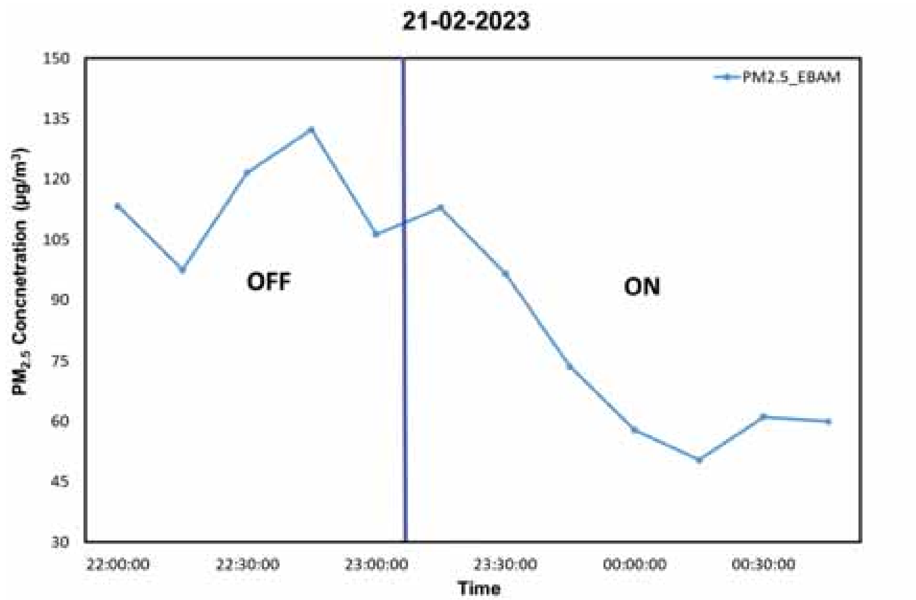

Figure 68. $PM_{2.5}$ concentration variation recorded by E-BAM in the MSACS OFF-ON condition at 100% fan capacity.

Another OFF-ON-OFF experiment performed in the afternoon time at 100% fan capacity is shown in Figure 69. The average $PM_{2.5}$ concentration during the 1st OFF condition was found to be ~ 30 µg/m^3, and it was decreased significantly, i.e., ~ 15 µg/m^3 in the MSACS ON condition. Further, the average $PM_{2.5}$ concentration again increased to ~ 30 µg/m^3 during the 2nd OFF condition, followed by the ON condition, which indicated a clear effect of MSACS in the ambient $PM_{2.5}$ concentration level in the MSACS ON condition. Since the $PM_{2.5}$ level started building up once the MSACS in switched OFF, as shown in Figure 69.

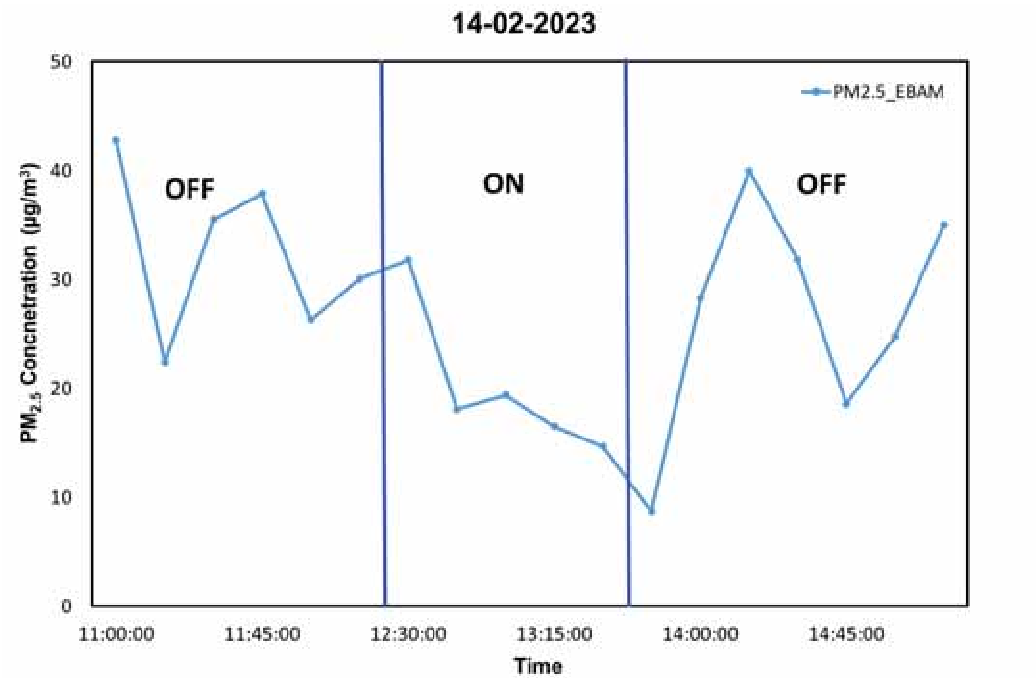

Figure 69. $PM_{2.5}$ concentration variation recorded by E-BAM in the MSACS OFF-ON-OFF condition at 100% fan capacity.

The impact of MSACS's clean air jet was further analysed for the $PM_{2.5}$ concentration trend recorded from E-BAM and the MSACS operation hours. For example, $PM_{2.5}$ data recorded from E-BAM was analysed for the high pollution conditions in the winter season, i.e., November 01, 2022, to February 28, 2023. It was observed that the $PM_{2.5}$ concentration was significantly decreased when the MSACS was operated for a more extended period as compared to days when the MSACS was kept OFF or operated for a shorter duration. The effect of MSACS' operational hours on $PM_{2.5}$ concentration is shown in Figure 70. The result indicated that when the MSACS was operated for 24 hours, it led to a significant reduction in the $PM_{2.5}$ concentration. While less reduction was observed when the MSACS operated between 8 hours to 15 hours, as compared to the days when it was operated for approximately 24 hours. It was found that the $PM_{2.5}$ concentration decreased significantly when the MSACS was operated for a longer duration as compared to days when the MSACS was kept OFF or operated for a shorter duration.

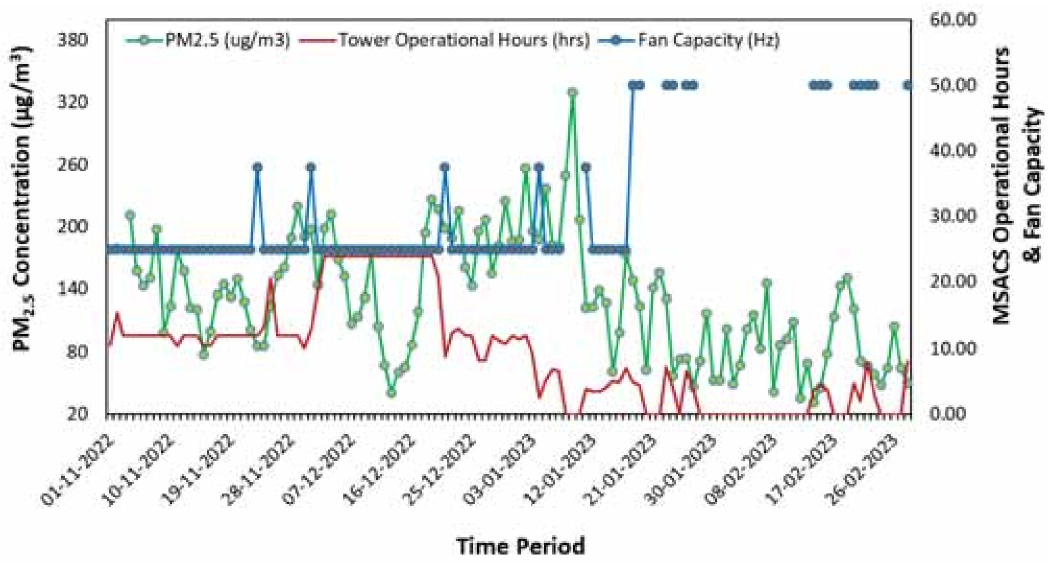

Figure 70. Effect of MSACS operational hours on $PM_{2.5}$ concentration recorded by E-BAM.

In summary, the recorded PM concentration data by the E-BAM in the MSACS ON condition has clearly shown a significant impact of MSACS clean air jet on the PM concentration level at a distance of ~ 50 m. The OFF-ON-OFF experiment are discussed above with examples of the $PM_{2.5}$ concentration variation recorded by E-BAM. The percentage reduction of $PM_{2.5}$ calculated using the E-BAM recorded concentrations data was found to be ranging from 9% to 53% depending upon different meterological and operating conditions, which was found quite similar to the percentage average reduction of $PM_{2.5}$ calculated using mobile monitoring devices (i.e., DustTrak), i.e, 1% to 36%, at 50 m distance from the MSACS.

6.4 MSACS Performance using LCS

Ten LCS were installed near the tower vicinity to monitor the continuous and whole-day trends of $PM_{2.5}$ and PM_{10} concentrations at different distances from the MSACS. The PurpleAir PA-II SD model, a popular device for measuring outdoor air quality in residential areas, schools, and public spaces, were installed at different distances from MSACS. The PA-II SD uses laser particle sensors to measure the air's concentration of $PM_{2.5}$ and PM_{10} particles. These LCS can be connected to WiFi networks to get continuous real-time data and it also include sensors for temperature and humidity. The LCS provides the high time resolution data of 2-min, which is well-versed to capture the ambient variation at the micro level. The data recorded by the LCS installed around the MSACS at different distances are used to evaluate the continuous ambient background concentrations of $PM_{2.5}$ and PM_{10}. The LCS locations around the MSACS are enlisted in Table 16.

Table 16. LCS locations in MSACS vicinity.

Sensor Nomenclature	**Distance(m) and direction from MSACS center**	**Landmark**
P 1	SE 100 m	CPWD Qtrs. Block 5 (65-80)
P 2	SE 150 m	CPWD Qtrs. Lobby.
P 3	NE 50 m	Near CPWD Qtrs. Entry Gate
P 4	E 500 m	Outside Delhi tourism office
P 5	NE 100 m	Boundary of CPWD quarters (Block 87). Opposite to Shivaji metro station
P 6	NE 200 m	Nagaland Sales Emporium, Baba Kharak Singh Marg
P 7	N 150 m	CPWD Qtrs. Block 90(A-T)
P 8	NW 100 m	CPWD Qtrs. Block 101 (A-T)
P 9	W 150 m	CPWD Qtrs. Block 108 (A-T)
P 10	W 50 m	Traffic School Entrance Gate.

The 24-hr continuous data recorded using the LCS was used for assessing the MSACS performance in the ambient domain during the OFF and ON conditions of the MSACS and few of the OFF-ON experiments are discussed in this section. For example, the $PM_{2.5}$ and PM_{10} concentrations data recorded by the LCS, installed in the South-East direction at 50 m distance, for ON-OFF conditions for the late night to morning hours is shown in Figure 71. A significant decrease was observed in the $PM_{2.5}$ and PM_{10} concentrations at 50 m distances in MSACS ON condition at 75% fan capacity. The concentrations of $PM_{2.5}$ and PM_{10} was found to be risen up significantly, in MSACS OFF condition. However, the phenomena of concentration reduction for $PM_{2.5}$ and PM_{10} was found to be repeated in every MSACS ON condition.

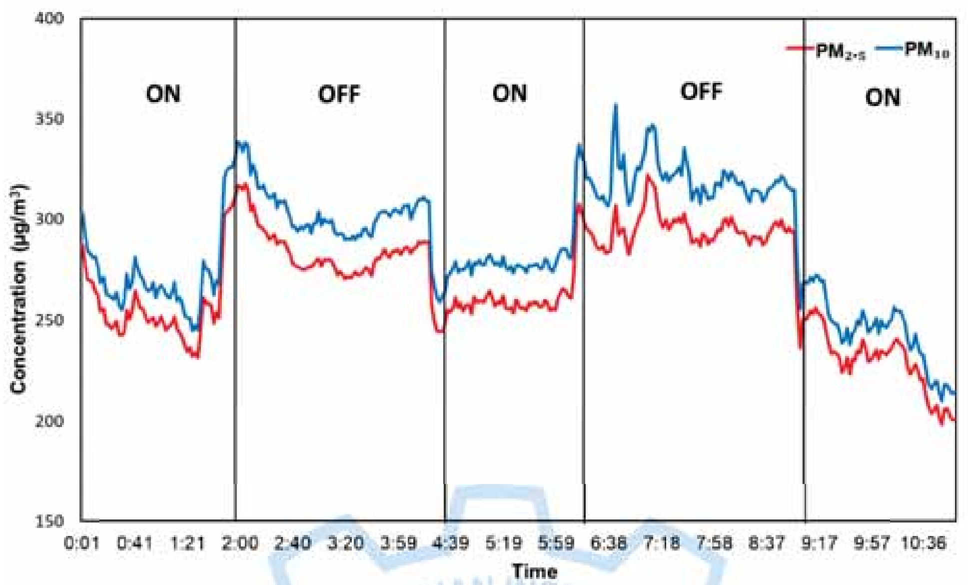

Figure 71. PM concentrations variation for MSACS ON-OFF conditions at 75% fan capacity (50 m SE).

The time series graphs were plotted to understand the PM concentration variation trends of the installed sensors. $PM_{2.5}$ and PM_{10} data were collected from the installed LCS. The LCS recorded concentration data at 2-minute intervals. The collected data was resampled to hourly and daily averages for long-term series analysis. The continuous data recording by all LCS was challenging due to frequent power disruption issues at different locations and some LCS were stolen. Therefore, LCS could not record the data continuously for some locations. Few LCS supported with battery backup were also installed to overcome the power supply issues to record the continuous PM data at multiple locations. The available continuous data was preprocessed and analysed for all the sensor data installed at different distances. It was assumed that there is a sound effect of the MSACS at the nearest distance and little effect at a large distance. To test this hypothesis, the LCS data recorded by two LCS, 1- installed nearby MSACS at 150 m distance in SE direction (SE150) and 2- installed at 250 m distance in NW direction (NW250) was analysed.

The hourly average time series data recorded from November 23, 2022, to December 26, 2023, was analysed for the concentration variation of $PM_{2.5}$ and PM_{10} at two locations, i.e., SE150 and NW250. The time series concentration data recorded from these two LCS are shown in Figure 72 for $PM_{2.5}$ and Figure 73 for PM_{10}. The time series plot clearly showed that the SE150 sensor has a significantly lower concentration as compared to the NW250, which showed an impact of the clean air jet of MSACS in spite of the construction site.

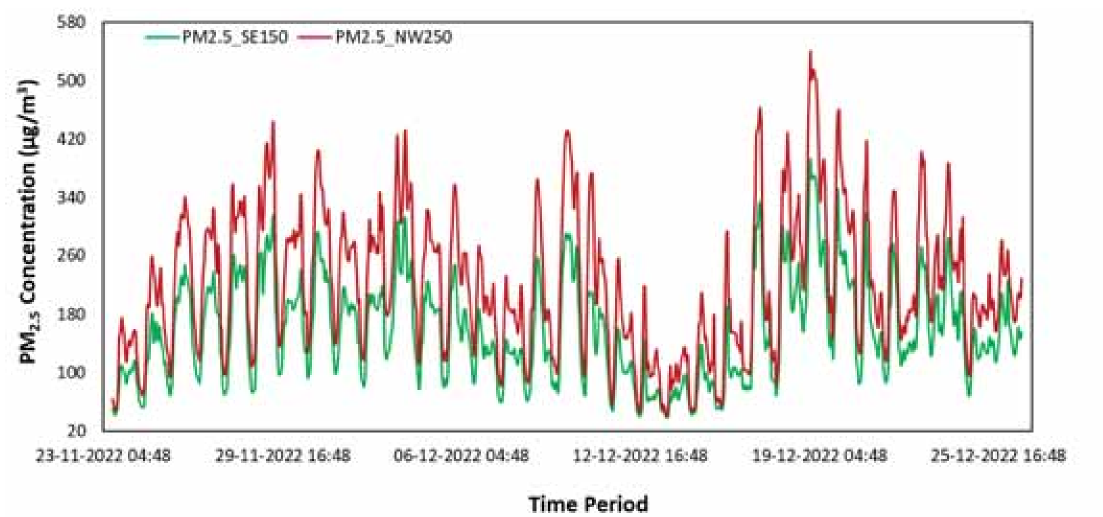

Figure 72. $PM_{2.5}$ concentration recorded by the LCS installed at 150 m and 250 m away from MSACS.

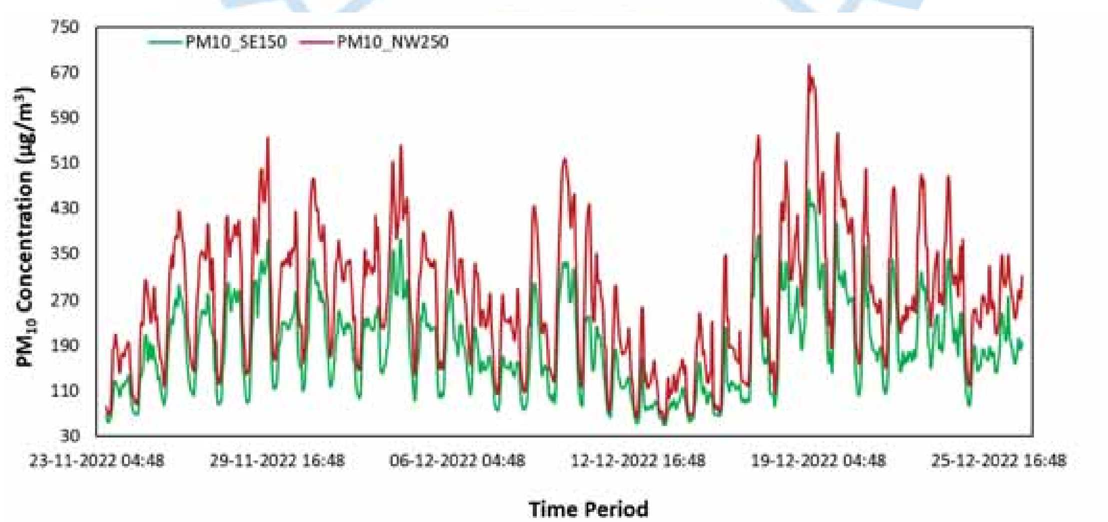

Figure 73. PM_{10} concentration recorded by the LCS installed at 150 m and 250 m away from MSACS.

Similarly, the hourly average time series data recorded from LCS from December 01, 2022, to December 04, 2022, was analysed for the concentrations variation of $PM_{2.5}$ and PM_{10} at four different locations using LCS, i.e., NE50, SE50, NW100 and NE150. The time series concentration data recorded from these four LCS are shown in Figure 74 for $PM_{2.5}$ and Figure 75 for PM_{10}. The LCS located at 50 m distance (NE50 & SE50) from the MSACS showed more reduction as compared to the NW100 and NE150. The LCS NE50 and SE50 located near the roadside, where still more reduction was observed.

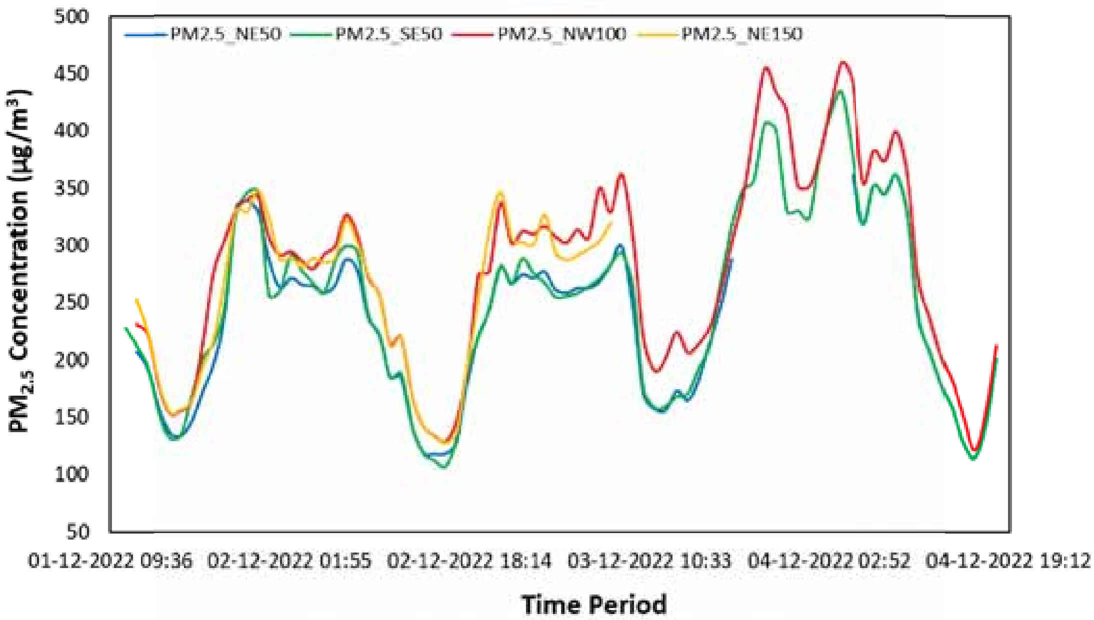

Figure 74. $PM_{2.5}$ concentration recorded by the LCS installed at a distance of 50 m, 100 m and 150 m.

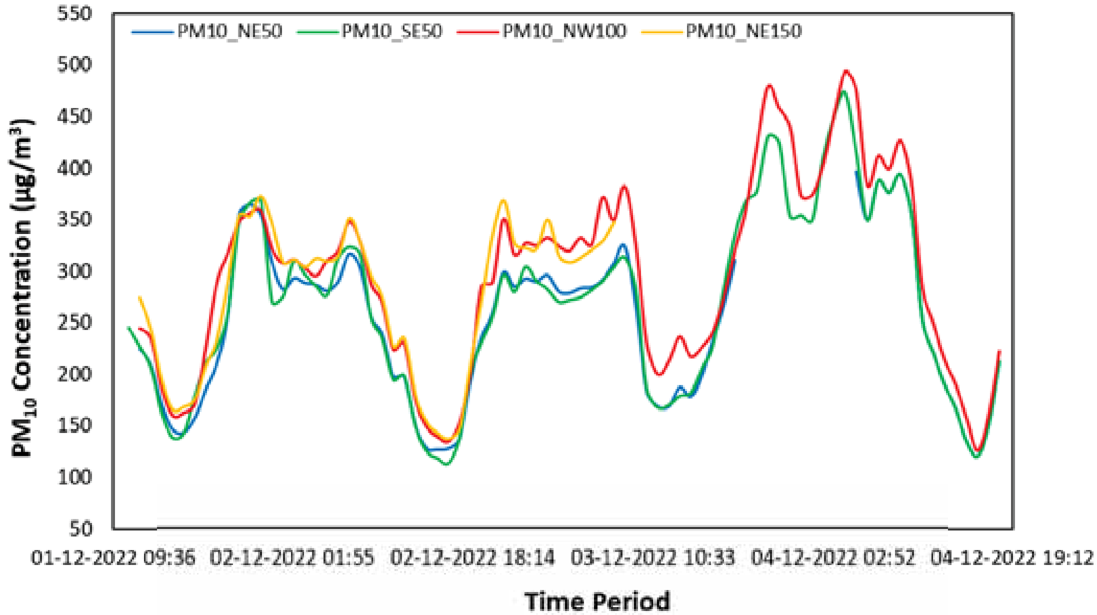

Figure 75. PM_{10} concentration recorded by the LCS installed at a distance of 50 m, 100 m and 150 m.

7 Overall System Performance in the Ambient Domain

To evaluate the performance of MSACS in the ambient domain, all the collected data from the various OFF-ON cycles from Oct’21-Feb’23 was summarized and classified into various categories to understand the influencing parameters on the performance of the MSACs system in the ambient domain. The methodology used to calculate the performance is explained in detail in Section 6.2. The average of all three methods was taken to evaluate the performance of the MSACS. The overall system performance in terms of the percentage reduction of PM concentrations is summarized in this section.

7.1 MSACS performance under various operating and meteorological Conditions

A total of 408 and 426 data points were collected for two years of monitoring for PM_{10} and $PM_{2.5}$ concentrations around the MSACS. The $PM_{2.5}$ data also includes results from the reference grade instrument, E-BAM. The overall efficiency of the system as a percentage reduction in PM_{10} and $PM_{2.5}$ concentration at various distances, irrespective of the wind speed, wind direction, and pollution load, is shown in Figure 76. The data was classified into various bins of reduction efficiency and distances. A summarized Table was generated by pooling all sets of data. The MSACS performance at different distance ranges (i.e., 21-99 m, 100-199 m, 200- 399 m and >400 m (includes data for 500 m and 700 m)) and their corresponding number of times % reduction in PM_{10} and $PM_{2.5}$ range (i.e., <1, 1-10, 10-20, 20-30,….. and >80%) is shown in Table 17. The average percentage reduction was calculated by including all the data collected for two years. The average percentage reduction of 56% and 48% was obtained for PM_{10} and $PM_{2.5}$, respectively, at a 20 m distance from the MSACS. The percentage reduction for PM_{10} and $PM_{2.5}$ at a distance range of 21-99 m was found to be 34% and 30%, respectively. Similarly, the percentage reduction at a distance range of 100-199 m, 200-399 m, and >400 m for PM_{10} was 13%, 13%, and 14%, respectively; and for $PM_{2.5}$ it was found to be 12%, 13%, and 13% respectively.

For curve fitting purposes, the performance data points that are not physically meaningful, such as zero impact were removed. 64 data points out of a total of 408 data points for PM_{10} and 75 data points out of a total of 426 data points for $PM_{2.5}$ were excluded for the curve fitting purpose. The data removed are summarised in

Table *18*. It is observed from Figure 76 and Figure 77, that there is no significant difference between the results with and without including the non-physical meaningful performance data points. For non-physically meaningful data that were excluded, the average percentage reduction of 62% and 52% was obtained for PM_{10} and $PM_{2.5}$, respectively, at a 20 m distance from the MSACS. The percentage reduction for PM_{10} and $PM_{2.5}$ at a distance range of 21-99 m was found to be 37% and 32%, respectively. Similarly, the percentage reduction at a distance range of 100-199 m, 200-399 m, and >400 m for PM_{10} was 17%, 16%, and 16%, respectively; and for $PM_{2.5}$ it was found to be 16%, 16%, and 16%, respectively.

Table 17. Overall summary of PM_{10} and $PM_{2.5}$ reduction at different distances from MSACS.

	Number of counts for reduction ranges at different distances (m)									
Reduction Range (%)	PM_{10}					$PM_{2.5}$				
	20	**21-99**	**100-199**	**200-399**	**>400**	**20**	**21-99**	**100-199**	**200-399**	**>400**
<1	5	8	35	14	7	6	14	37	15	12
1-10		7	29	18	9	1	13	25	12	8
10-20	2	15	40	12	19	2	15	42	18	13
20-30	1	18	13	7	5	2	28	16	3	7
30-40	1	20	6	6	4	2	22	5	7	5
40-50	5	18	3	2	1	11	21	2	2	
50-60	7	18	4			15	19	3		
60-70	25	11				17	3			
70-80	11	1				1				
>80	1					1	1			
Total N	**58**	**116**	**130**	**59**	**45**	**58**	**136**	**130**	**57**	**45**
Average	**56±22**	**34±19**	**13±13**	**13±13**	**14±11**	**48±22**	**30±18**	**12±12**	**13±13**	**13±12**

Table 18. Overall summary of PM_{10} and $PM_{2.5}$ reduction at different distances from MSACS excluding non-physically meaningful data.

Reduction Range (%)	Number of counts for reduction ranges at different distances (m)									
	PM_{10}					$PM_{2.5}$				
	20	**21-99**	**100-199**	**200-399**	**>400**	**20**	**21-99**	**100-199**	**200-399**	**>400**
0-10		7	31	20	10	2	15	26	15	10
10-20	2	15	40	12	19	2	15	42	18	13
20-30	1	18	13	7	5	2	28	16	3	7
30-40	1	20	6	6	4	2	22	5	7	5
40-50	5	18	3	2	1	11	21	2	2	
50-60	7	18	4			15	19	3		
60-70	25	11				17	3			
70-80	11	1				1				
>80	1					1	1			
Total N	**53**	**108**	**97**	**47**	**39**	**53**	**124**	**94**	**45**	**35**
Average	**62±15**	**37±18**	**17±12**	**16±12**	**16±11**	**52±17**	**32±17**	**16±11**	**16±12**	**16±11**

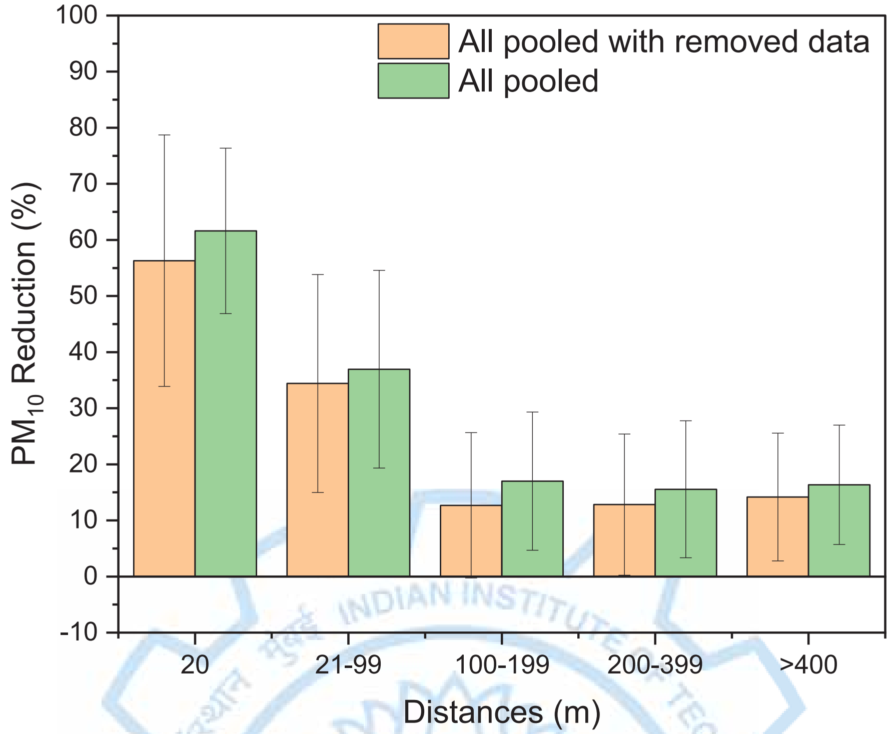

Figure 76. Percentage reduction of PM_{10} at different distances from the MSACS for all pooled no reduction data removed and all pooled results.

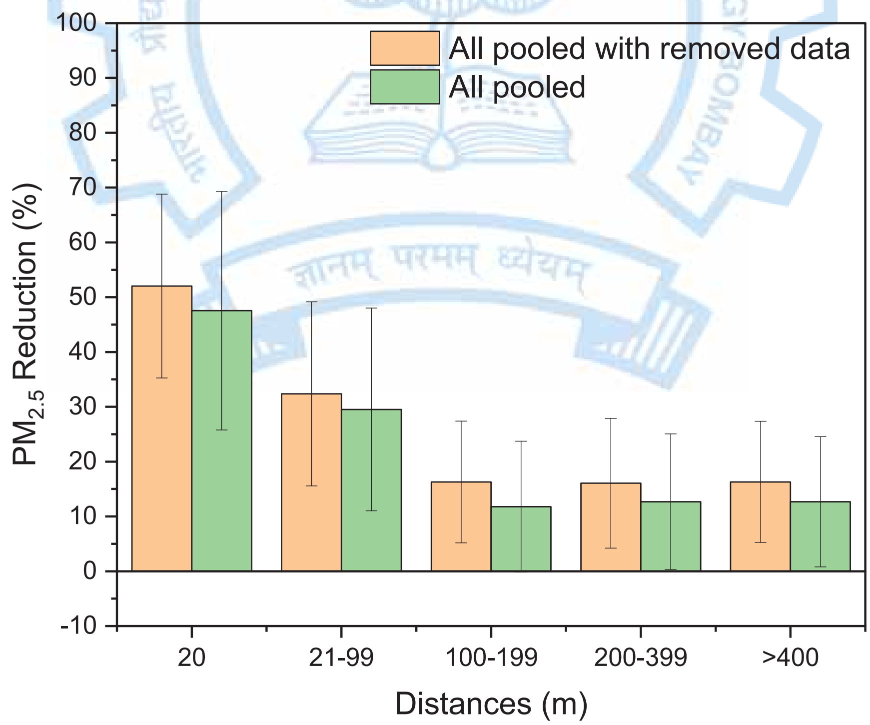

Figure 77. Percentage reduction of $PM_{2.5}$ at different distances from the MSACS for all pooled no reduction data removed and all pooled results.

It was also observed from Figure 76 that the rate of decay from 20 m to 100 m was by approx. 60% and from 100 m to 200 m was approx. 35%. However, beyond 200 m the decay rate in reduction was almost similar. A similar trend in the decay rate was also observed from the modelling results. It was also observed that the reduction in efficiency for PM_{10} is high as compared to $PM_{2.5}$ up to 100 m and after 100 m the reduction efficiencies are almost similar.

7.2 Performance comparison for two winter periods (2021-22 vs 2022-23)

The MSACS system was commissioned in September 2021. After several days of operation, few dislodging of filters from the filter assembly was observed and many leak points were identified. Filter frame strengthening work was performed to avoid dislodging, and many leaks were sealed continuously during the winter period. After leak proofing, the system performance was significantly improved. Overall, during the first winter (Oct'21-Feb'22) the system was not leakproof, all the leak sources in the system were rectified by March 2022. So, the results from the first winter 2021-2022 are to be interpreted cautiously. A comparison of the percentage reduction for PM_{10} and $PM_{2.5}$ between Winter 1 (Oct'22-Feb'22) and Winter 2 (Oct'22- Feb'23) is shown in Figure 78 and Figure 79. The total number of data points analysed for the Winter 1 was 123 while for Winter 2, it was 134 for PM_{10}. Similarly, the data points for Winter 1 were 123 while for Winter 2, it was 154 for $PM_{2.5}$.

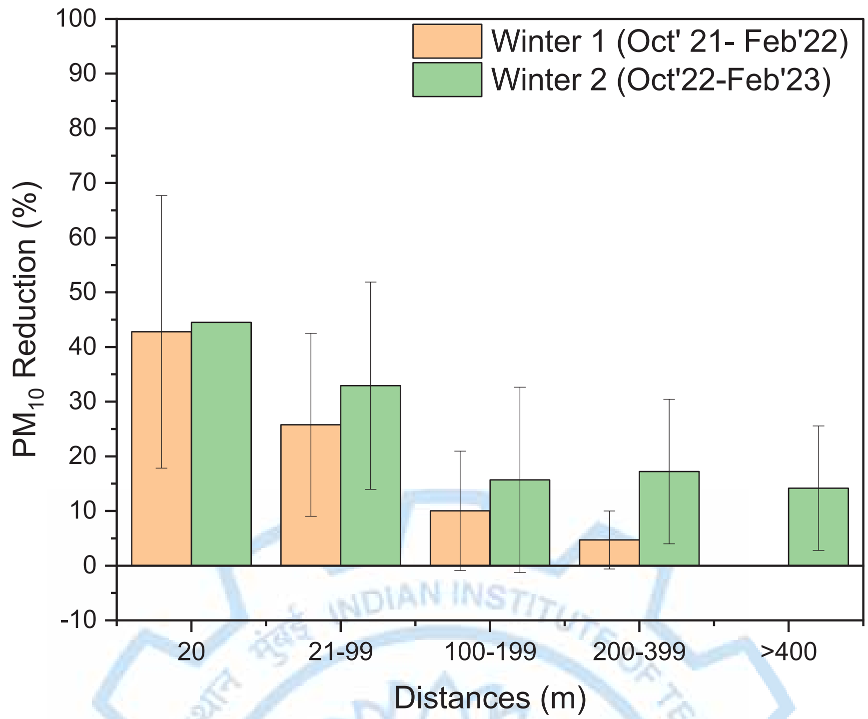

Figure 78. Reduction efficiency for PM_{10} for Winter 1 and Winter 2 at various distances from the MSACS.

It was found that the MSACS performance during the Winter 2 was better than the Winter 1.The average concentration reduction at a distance range of 20 m, during Winter 1 was found to be 43% for PM_{10} and 29% for $PM_{2.5}$. While for Winter 2, the reduction efficiency was found to be 45% for PM_{10} and 37% for $PM_{2.5}$. For 21-99 m, Winter 1 showed a reduction of 26% and 19% for PM_{10} and $PM_{2.5}$ respectively and for Winter 2 it showed a reduction of 33% and 28% for PM_{10} and $PM_{2.5}$ respectively. Similarly, for 100-199 m and 200- 399 m, Winter 1 showed a reduction efficiency of 10% and 5% for PM_{10} and 9% and 5% for $PM_{2.5}$. For 100-199 m and 200- 399 m, Winter 2 showed a reduction efficiency of 16% and 17% for PM_{10} and 13% and 17% for $PM_{2.5}$ respectively. The details on the classified winter 1 and winter 2 for PM_{10} and $PM_{2.5}$ are shown in Table 19 and Table 20.

Table 19. Overall summary of PM_{10} reduction: comparison of two winter seasons at different distances.

Reduction Range (%)	Number of counts for reduction ranges at different distances (m)									
	Winter 1 (Oct'21-Feb'22)					Winter 2 (Oct'22-Feb'23)				
	20	**21-99**	**100-199**	**200-399**	**>400**	**20**	**21-99**	**100-199**	**200-399**	**>400**
<1	1	5	17	8				8	6	7
1-10		3	12	10			3	5	6	9
10-20		9	15	1			2	6	11	19
20-30	1	10	3	1			5	4	6	5
30-40		7	3				6	3	6	4
40-50	2	6	2			1	2		2	1
50-60	1	4					1	3		
60-70	2						3			
70-80										
>80										
Total N	**7**	**44**	**52**	**20**		**1**	**22**	**29**	**37**	**45**
Average	**43±25**	**26±17**	**10±11**	**5±5**		**45**	**33±19**	**16±17**	**17±13**	**14±12**

Table 20. Overall summary of $PM_{2.5}$ reduction: comparison of two winter seasons at different distances.

Reduction Range (%)	Number of counts for reduction ranges at different distances (m)									
	Winter 1 (Oct'21-Feb'22)					Winter 2 (Oct'22-Feb'23)				
	20	**21-99**	**100-199**	**200-399**	**>400**	**20**	**21-99**	**100-199**	**200-399**	**>400**
<1	1	7	18	9			4	10	6	12
1-10		7	13	6			5	5	6	8
10-20	1	7	15	5			4	6	13	13
20-30	2	15	3				9	3	3	7
30-40	1	6	3			1	10	2	7	5
40-50	1	1					7	2	2	
50-60	1	1					2	1		
60-70										
70-80										
>80							1			
Total N	**7**	**44**	**52**	**20**		**1**	**42**	**29**	**37**	**45**
Average	**29±18**	**19±13**	**9±10**	**5±6**		**37**	**28±18**	**13±16**	**17±13**	**13±12**

A significant improvement was observed in Winter 2. One of the reasons for such significant improvement in MSACS performance may be attributed to increased CADR. The average CADR for Winter 1 was 180±28 m^3/s, as the system was mostly operated at 50% fan capacity due to the possibility of dislodging of the filters when operated at higher fan capacity. After the improvement and the strengthening of the filter frame, in Winter 2, the MSACS was operated mostly at 75% and 100% fan capacity and had an average CADR of 398±140 m^3/s. This signifies, that for improvement in the performance of the MSACS, all the possible leaks should be sealed.

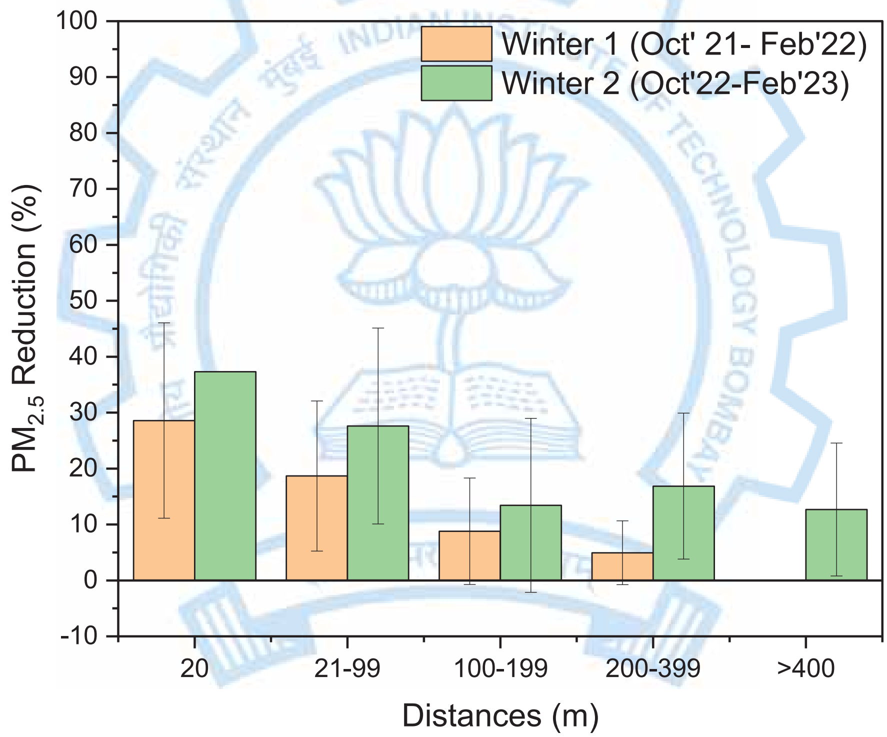

Figure 79. Reduction efficiency for $PM_{2.5}$ for Winter 1 and Winter 2 at various distances from the MSACS.

7.3 Effect of CADR on performance

To understand the effect of CADR on the performance of the MSACS, the dataset was divided into two categories CADR>300 m^3/s and CADR <300 m^3/s. The total number of data points for CADR>300 m^3/s was 200 for PM_{10} and 218 for $PM_{2.5}$. While for CADR<300 m^3/s, the total number of data points was 206 for PM_{10} and 208 for $PM_{2.5}$. From Figure 80 and Figure 81, it was observed that as CADR increases, the performance at higher distances improves significantly. For 20 m distance from MSACS at CADR >300 m^3/s and CADR<300 m^3/s the reduction in concentration were almost similar 59% and 54% for PM_{10} and 51% and 44% for $PM_{2.5}$. For distances between 21-99 m, the cleaning efficiency of MSACS observed for CADR >300 m^3/s and CADR <300 m^3/s were 40% and 30% for PM_{10} and 34% and 25% for $PM_{2.5}$. For distances 100-199 m, 200-399 m, and >400 m the reduction efficiency for CADR >300 m^3/s and CADR<300 m^3/s for PM_{10} were 15%, 17%, 12% and 12%, 9%, and 17% respectively. Similarly, the reduction efficiencies for CADR >300 m^3/s and CADR<300 m^3/s at 100-199 m, 200-399 m, and >400 m distances for $PM_{2.5}$ were 14%, 17%, 17% and 10%, 9% and 17% respectively.

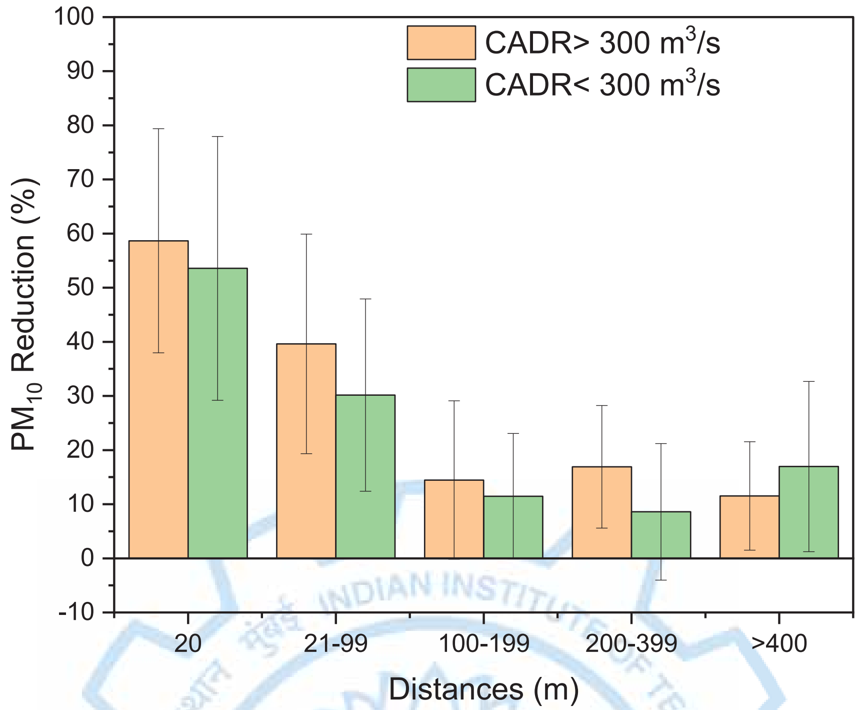

Figure 80. Reduction efficiency for PM_{10} for CADR>300 m^3/s and CADR<300 m^3/s at various distances from the MSACS.

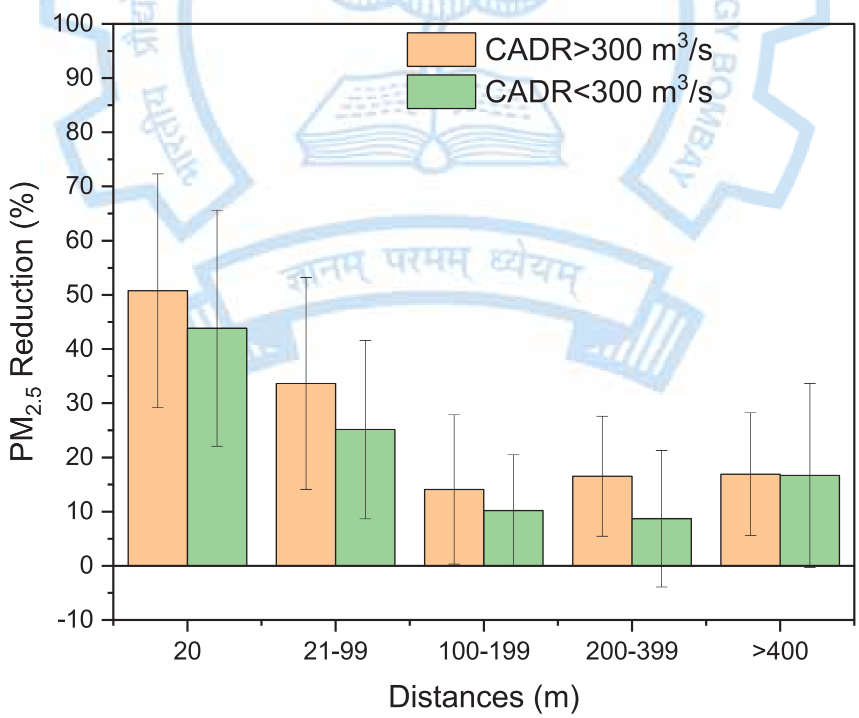

Figure 81. Reduction efficiency for $PM_{2.5}$ for CADR>300 m^3/s and CADR<300 m^3/s at various distances from the MSACS.

Table 21 and Table 22, corresponding to Figure 80 and Figure 81 show the removal efficiencies for CADR >300 m^3/s and CADR <300 m^3/s PM_{10} and $PM_{2.5}$. The mean removal efficiencies for majority of locations are higher for CADR >300 m^3/s as compared to CADR <300 m^3/s. Not much significance needs to be attached to the case of >400 m since the difference in the efficiencies for higher and lower flow rates are well within their error bars. On the whole, not withstanding the large error bars, the data indicates a trend of superior performance at higher CADR.

Table 21. Comparison of performances of MSACS for CADR>300 m^3/s and CADR<300 m^3/s at various distances for PM_{10}.

Number of counts for reduction ranges at different distances (m)										
Reduction Range (%)	**CADR> 300 m^3/s**					**CADR< 300 m^3/s**				
	20	**21-99**	**100-199**	**200-399**	**>400**	**20**	**21-99**	**100-199**	**200-399**	**>400**
<1	2	3	13	3	5	3	5	22	11	2
1-10		4	11	5	6		3	18	11	3
10-20	1	2	17	11	19	1	13	23	1	
20-30		6	6	5	2	1	12	7	2	3
30-40	1	10	2	5	3		10	4	1	1
40-50	3	7				2	11	3	2	1
50-60	2	9	4			5	9			
60-70	14	10				11	1			
70-80	7	1				4				
>80	1									
Total N	**31**	**52**	**53**	**29**	**35**	**27**	**64**	**77**	**28**	**10**
Average	**59±21**	**40±21**	**15±15**	**17±11**	**12±11**	**54±24**	**30±18**	**12±12**	**9±13**	**17±16**

Table 22. Comparison of performances of MSACS for CADR>300 m^3/s and CADR<300 m^3/s at various distances for $PM_{2.5}$.

Reduction Range (%)	Number of counts for reduction ranges at different distances (m)									
	CADR> 300 m^3/s					**CADR< 300 m^3/s**				
	20	**21-99**	**100-199**	**200-399**	**>400**	**20**	**21-99**	**100-199**	**200-399**	**>400**
<1	3	7	15	2	9	3	7	22	13	3
1-10	1	6	7	6	6		7	18	6	2
10-20		4	15	13	13	2	11	27	5	
20-30		10	10	2	5	2	18	6	1	2
30-40	1	13	2	6	2	1	9	3	1	3
40-50	7	14	2			4	7		2	
50-60	8	12	2			7	7	1		
60-70	9	3				8				
70-80	1									
>80	1	1								
Total N	**31**	**70**	**53**	**29**	**35**	**27**	**66**	**77**	**28**	**10**
Average	**51±22**	**34±20**	**14±14**	**17±11**	**17±11**	**44±22**	**25±17**	**10±11**	**9±13**	**17±17**

7.4 Effect of different seasons on the performance of the MSACS

To evaluate the performance of MSACS in different seasons, an evaluation was made when the MSACS was leak-proofed. For comparison purposes, Winter 2 was evaluated against the data collected for summer and monsoon'22. The data points for Winter 2 were 134 and 154 for PM_{10} and $PM_{2.5}$ and for summer, monsoon was 150 for $PM_{2.5}$ and PM_{10}. From Figure 82 and Figure 83, a reduction in efficiency in summer and monsoon and Winter 2 are shown. At 20 m the data point for Winter 2 is only 1 as compared to 53 and 50 data for PM_{10} and $PM_{2.5}$ for the summer and monsoon. Because of less number of data points the comparison between different seasons at 20 m distance should not be made. Similarly, for the 21-99 m distance, the data points for Winter 2 are 22 and 42 for PM_{10} and $PM_{2.5}$ respectively, while the data points for summer and monsoon are 53 and 50 for PM_{10} and $PM_{2.5}$ respectively. Since the data points between two seasons vary, no comparison should be made between various seasons. The less number of data points in Winter 2 at a nearby distance is because the measurements were mostly carried at further distances. For distances between 100-199 m, Winter 2 showed a reduction of 16% and 13% for PM_{10} and $PM_{2.5}$ respectively. And for summer and monsoon, a reduction of 14% and 14% for PM_{10} and $PM_{2.5}$ respectively. Since, no far measurements >200 m were conducted in the summer and monsoon season, the effect on MSACS performance season-wise comparison is difficult to make.

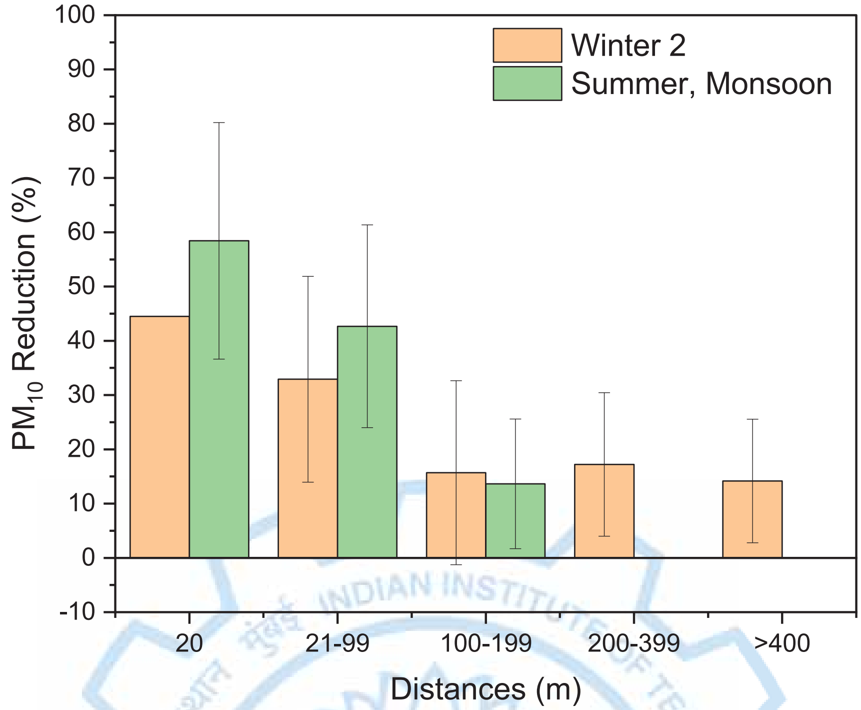

Figure 82. Reduction efficiency for PM_{10} for winter 2 and Summer, Monsoon at various distances from the MSACS.

The results for performance comparison against the second winter and summer and monsoon for PM_{10} and $PM_{2.5}$ are summarised in Table 23 and Table 24. Due to low windspeed in winter, winter has more stable and calm conditions as compared to summer and monsoons favouring the performance at a distance between 100-199 m. The concentration in the summer and monsoon is very low as compared to winter and mostly below the NAAQS limit, hence it is not advisable to operate the MSACS at low concentration.

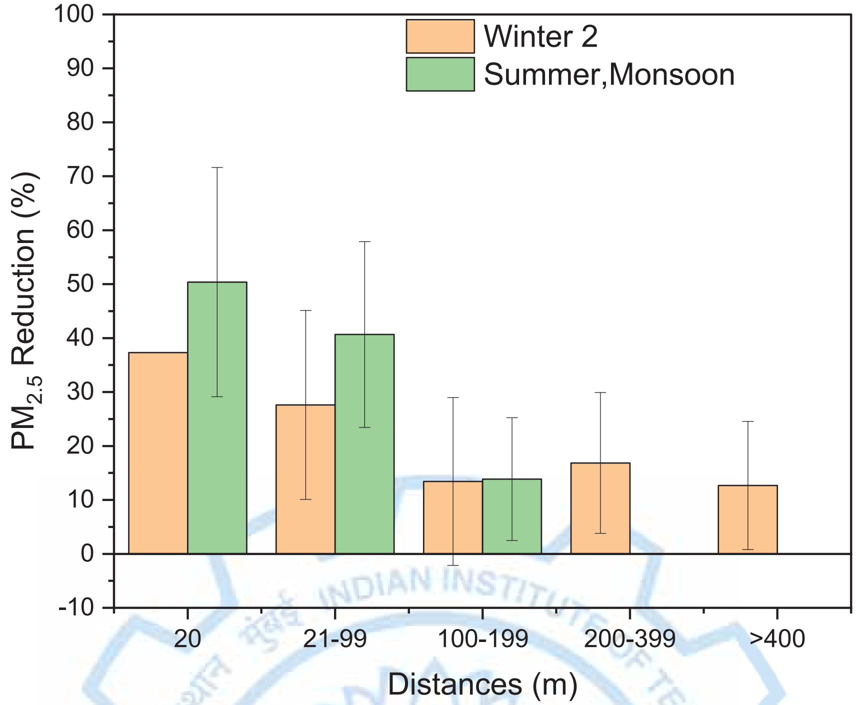

Figure 83. Reduction efficiency for $PM_{2.5}$ for winter 2 and Summer, Monsoon at various distances from the MSACS.

Table 23 Comparison of performances of MSACS for Winter 2 with Summer and Monsoon seasons at various distances for PM_{10}.

	Number of counts for reduction ranges at different distances (m)									
Reduction Range (%)	**Winter 2**					**Summer and Monsoon**				
	20	**21-99**	**100-199**	**200-399**	**>400**	**20**	**21-99**	**100-199**	**200-399**	**>400**
<1			8	6	7	4	3	10		
1-10		3	5	6	9		1	12		
10-20		2	6	11	19	2	4	19		
20-30		5	4	6	5	3	6			
30-40		6	3	6	4	1	7			
40-50	1	2		2	1	2	10	2		
50-60		1	3			6	13	1		
60-70		3				23	8			
70-80						11	1			
>80						1				
Total N	**1**	**22**	**29**	**37**	**45**	**53**	**53**	**44**		
Average	**45**	**33±19**	**16±17**	**17±13**	**14±12**	**59±22**	**43±19**	**14±12**		

Table 24 Comparison of performances of MSACS for Winter 2 with Summer and Monsoon seasons at various distances for $PM_{2.5}$.

	Number of counts for reduction ranges at different distances (m)									
Reduction Range (%)	**Winter 2**					**Summer, Monsoon**				
	20	**21-99**	**100-199**	**200-399**	**>400**	**20**	**21-99**	**100-199**	**200-399**	**>400**
<1		4	10	6	12	5	3	10		
1-10		5	5	6	8	1	1	7		
10-20		4	6	13	13	1	4	21		
20-30		9	3	3	7		4	10		
30-40	1	10	2	7	5		6			
40-50		7	2	2		10	13			
50-60		2	1			14	16	2		
60-70						17	3			
70-80						1				
>80		1				1				
Total N	**1**	**42**	**29**	**37**	**45**	**50**	**50**	**50**		
Average	**37**	**28±18**	**13±16**	**17±13**	**13±12**	**50±21**	**41±17**	**14±11**		

8 CFD Modelling

8.1 Summary of important findings from previous simulations

As discussed earlier in previous Interim reports, the performance of the MSACS is influenced by both system parameters such as (Filtration efficiency, Fan capacity, CADR) and environmental parameters (meteorological conditions, topographical features surrounding the area, various sources present, etc). The summary of the impact of some key parameters are described below.

- Effect of wind direction and wind speed:

In the previous report, various parameters that affect cleaning efficiency have been discussed in detail. These include wind speed, wind direction, fan capacity, and other important parameters. By analysing these parameters, it is possible to optimize the cleaning process and improve MSACS' efficiency. The results of plain terrain simulations showed that the direction of wind plays a very essential role to provide the cleaning zone in various directions. It was found that different cleaning areas were obtained in various directions depending upon the direction of the wind as well as the obstructions present in its path. However, it was found that if there are no obstacles present, the cleaning pattern would be the same for all the cases with respect to the prominent wind direction. In all the cases of plain terrain simulations with changing wind directions, the cleaning was observed to be going beyond 500 m in the downstream side. However, the presence of different structures in the prominent wind direction affects the cleaning pattern as well as the area covered and reduces the cleaning efficiency in the downwind direction.

Both measurements and simulation indicated that there is a significant impact of wind direction and wind velocity on the effective cleaning zone. From previous study (referring to Interim report-2), it was found that, if the system is performed at its full capacity and highest filtration efficiency, a favourable wind direction would cover the maximum measurement locations in different directions. However, with higher wind speeds, the upwind and crosswind jets were observed to cover smaller distances in their respective directions and then started bending towards the downstream jet and covers large distance in the downwind direction. This shows the significance of the wind speed and wind direction, as it plays a major role in cleaning the air in the specific area and far distances from the MSACS.

- Effect of fan capacity:

The effect of varying fan capacities was observed for plain terrain simulations and it was found that, although there is no change in the behaviour of efficiency with respect to operating fan capacity along the wind direction of flow i.e. upwind and downwind, the crosswind efficiency was influenced by the operating fan capacity i.e. correspond to clean air delivery rate (CADR). It was observed that as operating fan capacity increases, the width for a specific efficiency level increases in all other three directions. This is the major advantage of operating at higher fan capacities as this would increase the overall area of impact.

8.2 Importance and need of winter simulations

The CFD numerical models were developed, analysed, and comparisons for data were being made with respect to monitoring results for the summer and rainy seasons of the year 2022. As the MSACS is basically meant for high air pollution loads or scenarios such as winter, its operation at low concentrations in summer and rainy seasons was not found to be fully useful. Large uncertainties were also seen in measurements which were supported by various simulations. Thus, there was need for measurements during the winter season that would provide real efficiency of the system.

To draw a definite conclusion more data and information was acquired, especially the performance during the winter when the pollution load is high. Also, it is important to understand the performance during night-times as the influence of other sources will be minimal and meteorological conditions are typically of low wind conditions without much fluctuations. This typically represents the high load PM conditions. One of the shortcomings of the measurements this far was the exclusion of the night-time data, where it is expected that the system would perform better due to the prevalence of no-wind conditions. Thus, the next phase of the study included essentially focusing on determining the range of air cleaning including the data of night-time as well as early-morning measurements along with afternoon measurements during winter season under different operating scenarios of the MSACS. This study has been carried out and its result and analysis has been described in the current report.

9 CFD Modelling and Monitoring Comparison

It is important to compare the modelling results with the monitoring results to validate the modelling approach so that the validated model can be used for simulating various scenarios and optimized operating scenarios conditions of MSACS can be found for maximum benefit.

9.1 Methodology

Different measurements were carried out by monitoring team during different time intervals of the day at the Connaught Place site, to observe the actual effects of MSACS on reducing the concentration of particulate matter in the surrounding area. In this section of the report, we are focusing more on the performance of MSACS during 2022-23 winter season through modelling. The measurements performed in the months from November 2022 to February 2023 were considered for comparison and validation with monitoring. Few of these cases have been described in the upcoming sections given below.

The mobile measurements were carried out by using research-grade instruments to find out the absolute concentration at various locations when the air cleaning system is operated at different fan capacities. The local concentrations at the upstream and downstream sides of the filter array were obtained for finding the filtration efficiency of the air cleaning system. The local concentration is measured for MSACS ON/OFF conditions for getting air pollution reduction efficiency at different locations using Equation 4 given below.

The air pollution reduction efficiency can be calculated by using Equation 4.

$$\text{Air pollution reduction efficiency} = 1 - \frac{\text{Local PM concentration}}{\text{Ambient PM concentration}} \text{ ..... Equation 4}$$

Local point or area sources change the local pollutant concentrations which may lead to an increase or decrease in air pollution. In the absence of local point or area sources, the clean air coming out of the air cleaning system should have a lower PM concentration within an effective reduction zone. The numerical model of the air cleaning system is assumed with a uniform distribution of air pollution in the confined domain without any source.

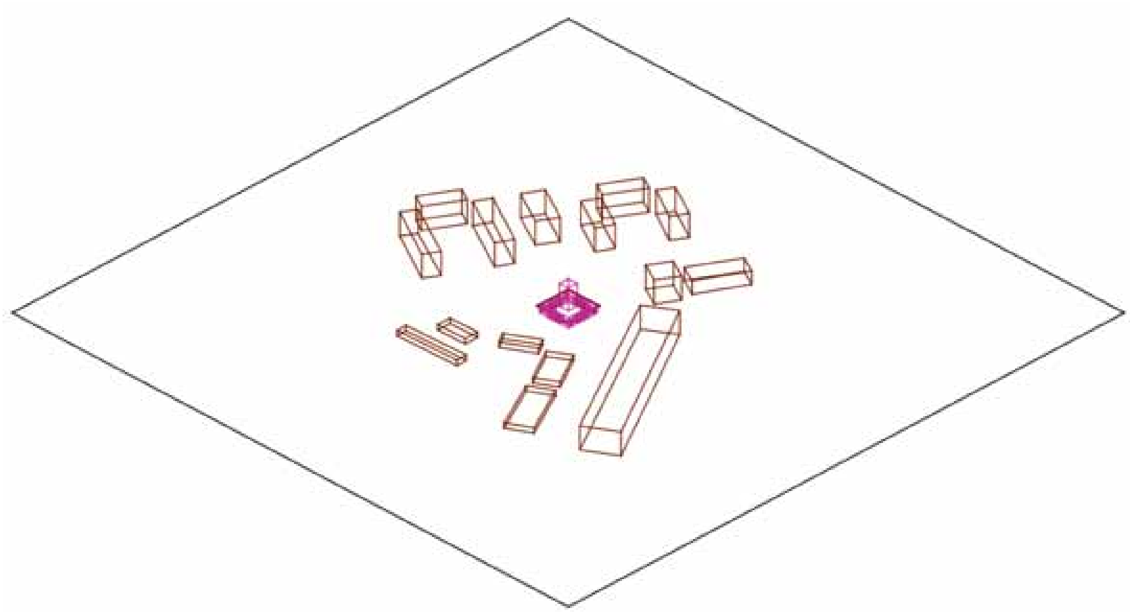

Figure 84. Simplified geometry of MSACS with nearest existing buildings/structures/obstacles considered for CFD simulations. (Domain not to scale)

With reference to the actual site scenario, the geometry including the MSACS, building structures and other obstacles was prepared using the software. The domain size considered for this study was 5 km by 5 km. After this, the mesh was prepared accordingly. Mesh independency test was also performed to get the optimum mesh required for accuracy and to reduce the time period of the simulations. An unstructured tetrahedral mesh with approximately 3.42 million elements was obtained for the geometry prepared. To validate the monitoring measurements, the required boundary conditions were given for a domain in the CFD modelling simulation. The background concentration is assumed to be uniformly distributed in the CFD domain. Background concentration is considered as 100 $\mu g/m^3$ to easily correlate with air pollution reduction efficiency. The local concentration at the position is compared with the uniformly distributed background concentration to find out the air pollution reduction efficiency using numerical method.

The presence of obstacles or buildings as solid structures restricts the clean air from going far from the MSACS. The porosity given for buildings is zero while performing the simulation. Roughness height is taken as 0.25 m. Considering the topography of the area and the presence of various buildings and obstacles in the actual site, roughness height has to be considered while performing the simulations. For areas or landscapes having scattered obstacles at relative distances of 8 to 12 m obstacle heights for low solid objects (e.g. buildings), it has been suggested to use roughness height of 0.25 m for such type of terrain (Davenport et al., 2000).

Stability class F (i.e. stable) was used while performing the simulations, as during winter season the wind speed on the site was observed to be < 2 m/s and the atmosphere is stable with very less turbulence. Further, the temperature during winters is usually low with very slight day solar insolation. Also, the night cloudiness (fraction of sky covered by clouds) was observed to be less, and since most of our measurements were performed in late night time and early mornings, which suggested us to use stability class F in the simulations (Masters and Ela, 2008).

The numerical scheme used for the study is UDS (Upwind Discretization Scheme). k-epsilon turbulence model was used and steady-state simulations were performed. Mesh independence test was also performed to get the optimum mesh. After giving all the boundary conditions, the simulations were started. The results didn’t alter much after reaching to a residual value in the order of 10^{-4} and convergence was said to be achieved. Then, in post-processing, the modelling results were extracted and visualized to compare and validate them with the monitoring data.

The CFD simulation results are compared with the monitoring data for the different dates mentioned in the Table 25. In the months of November 2022 to February 2023, afternoon as well as late night and early morning measurements were carried out. Several weather station factors were considered throughout the simulation, and the findings were validated against the monitoring results under various scenarios.

9.2 Modelling and monitoring comparison scenarios

The various simulation scenarios that are considered and compared with the monitoring data of respective dates are given in the Table 25, and they are described further in detail.

As already discussed in the Interim Report- 1, during the winter season calm weather conditions are there i.e. wind velocity is generally low and has mostly been found within 1 m/s. The cases given below have been categorised into two categories on the basis of wind speed, low and high. The wind speeds < 1 m/s were considered as low and > 1 m/s was taken as high wind speed.

Table 25. Parameters used for different simulation scenarios based on monitoring data of the respective days.

Case No.	**Nature of wind**	**Date**	**Wind Direction**	**Wind Speed (m/s)**	**System Flow Rate (m^3/s)**	**Filtration Efficiency (%)**	**CADR (m^3/s)**	**Objectives/ Remarks**
1	**Low wind speed**	Monitoring and modelling comparison for 24th Nov 2022 (Late night)	NW	0.3	739.73	43.9	324.74	To compare monitoring measurements with modelling in NE direction
2		Monitoring and modelling comparison for 25th Nov 2022 (Early morning)	NW	0.3	739.73	42.9	317.34	To compare monitoring measurements with modelling in NE direction
3		Monitoring and modelling comparison for 22nd Dec 2022 (Late night)	NNE	0.52	799.39	40.8	326.15	To compare monitoring measurements with modelling in S and NE directions
4		Monitoring and modelling	WNW	0.52	1136	57	647.52	To compare monitoring measurements with

		comparison for 18th Jan 2023 (Afternoon)						modelling in SW and NE directions
5	**High wind speed**	Monitoring and modelling comparison for 11th Jan 2023 (Afternoon)	NNE	1.25	791.12	49.8	393.97	To compare monitoring measurements with modelling in NE direction
6		Monitoring and modelling comparison for 15th Feb 2023 (Late night)	SW	1.64	1006.36	60.7	610.86	To compare monitoring measurements with modelling in SW and NE directions

9.2.1 Case – 1: The simulation scenario as per the monitoring measurements carried out on 24th November 2022, Late night in North-East direction (Wind speed: low)

In this case, the modelling results are compared with the monitoring performance results for the sampling conducted in the late night of 24th November 2022. The average wind speed measured by the weather station during that particular time period was 0.3 m/s and the wind direction was North-West . The system flow rate measured was 739.73 m^3/s and the buffer zone efficiency in the downstream of filter bank measured using research-grade instrument was 43.9% on 24th November 2022. The CADR for this case is calculated as 324.74 m^3/s. For CFD simulation, similar boundary conditions have been used for individual fan jets in each direction. Based on the unavailability of the locations for the measurement due to huge hindrances provided by the buildings and structures in other directions, only North-East direction measurements were carried out in the late night of 24th November 2022. Figure 85 below shows the contours of the concentration profile for this case.

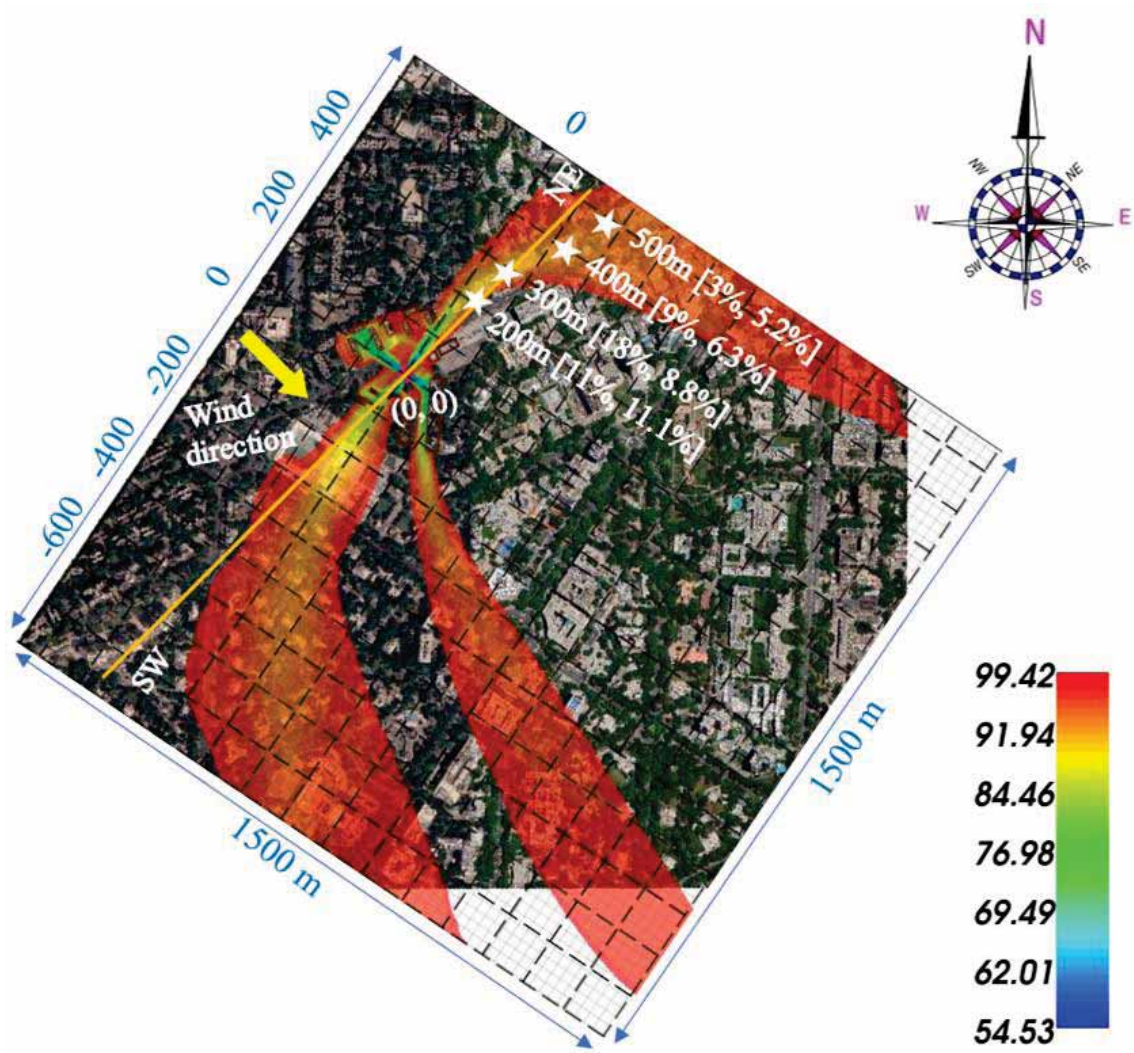

*Star-points indicate: Measurement distance from MSACS in shown direction along with [monitoring, modelling] values of % Air pollution reduction efficiency.

Figure 85. Filled contours of concentration profile (1500 m x 1500 m) dated 24th November 2022, Late night (Considered parameters are: wind speed = 0.3 m/s, wind direction = North-West, filtration efficiency = 43.9%, fan capacity = 739.73 m^3/s and CADR = 324.74 m^3/s).

Based on the meteorological parameters and clean air delivery rate from an individual fan, contours are shown in Figure 85. The star points indicate the location of the measurements at various distances from MSACS, along with values of air pollution reduction efficiency (%) as per the monitoring data collected and modelling data observed. As already discussed in the experimental section that the monitoring data was collected in the non-operating (OFF) and in operating (ON) conditions of the MSACS. In non-operating conditions, it provides background concentration and in operating conditions gives the change in the concentration, which is measured using a research-grade instrument. It allows us to find the air pollution reduction efficiency for a specific period of time and at different locations.

The yellow line (SW to NE) shown gives the modelling results at different locations from the MSACS in the respective directions. There are slight deviations in monitoring and modelling point locations due to the presence of various structures and local sources present in the actual scenario.

As the wind direction is North-West, the spread of the jet is more in the South-West and South directions as shown in the concentration contours above. The maximum concentration reduction is obtained at the outlet of each jet while the background concentration is 100 μg/m^3. Cleaning efficiency is maximum at the fan outlet and decreases away from fans position. The results from field measurements and CFD simulation are compared in Table 26. One important thing to note here is, for comparison with modelling, the monitoring values obtained with Average method were used for all the cases. The Average method for calculating the percentage reduction in ambient PM concentration has already been described in the Section 6.2 of the report.

Table 26. Comparison of results of air pollution reduction efficiency between measurements and modelling in North-East direction dated 24th November 2022, Late night (Considered parameters are: wind speed = 0.3 m/s, wind direction = North-West, filtration efficiency = 43.9%, fan capacity = 739.73 m^3/s and CADR = 324.74 m^3/s).

Measurement Direction		**North-East**			
Distance from MSACS (0,0) in m		200	300	400	500
Particle size		$PM_{2.5}$	$PM_{2.5}$	$PM_{2.5}$	$PM_{2.5}$
Air pollution reduction efficiency (%)	From monitoring	11	18	9	3
	From CFD Modelling	11.1	8.8	6.3	5.2

From Table 26, it is observed that the CFD simulation results match well with the monitoring results for most of the distances. At 200 m distance North-East, the reduction efficiency was observed to be 11% from both monitoring as well as modelling. CFD results show a decrease in reduction efficiency as we move away from MSACS, however, the monitoring results were observed to be having slight contradiction, i.e. 11% at 200 m and 18% at 300 m. At 200 m downwind, a lesser value of reduction efficiency was observed than at 300 m distance. It has been found that at farther distances, sometimes, due to local concentration variations and various activities at the site, the concentration was not stable. This might be the reason behind the slight contradiction.

With modelling, slightly lesser values of % air pollution reduction efficiencies were observed as compared to monitoring. The reduction efficiencies in the North-East direction observed through modelling at 200, 300 and 400 m were 11%, 8.8% and 6.3% respectively. More than 5% efficiency even up to distances of 500 m from MSACS was observed through modelling.

The plot of air pollution reduction efficiency along with the monitoring and modelling comparison at various distances from MSACS Centre (0,0) is shown in Figure 86. The blue line in the graph below shows the varying trend of the air pollution reduction efficiencies obtained from modelling at different distances from MSACS from South-West to North-East direction. The orange coloured dots show the values of air pollution reduction efficiencies at various measurement locations obtained from monitoring. Also, the green coloured dots in the plot represent the reduction in the air pollution reduction efficiency at respective measurement locations observed with the help of modelling.

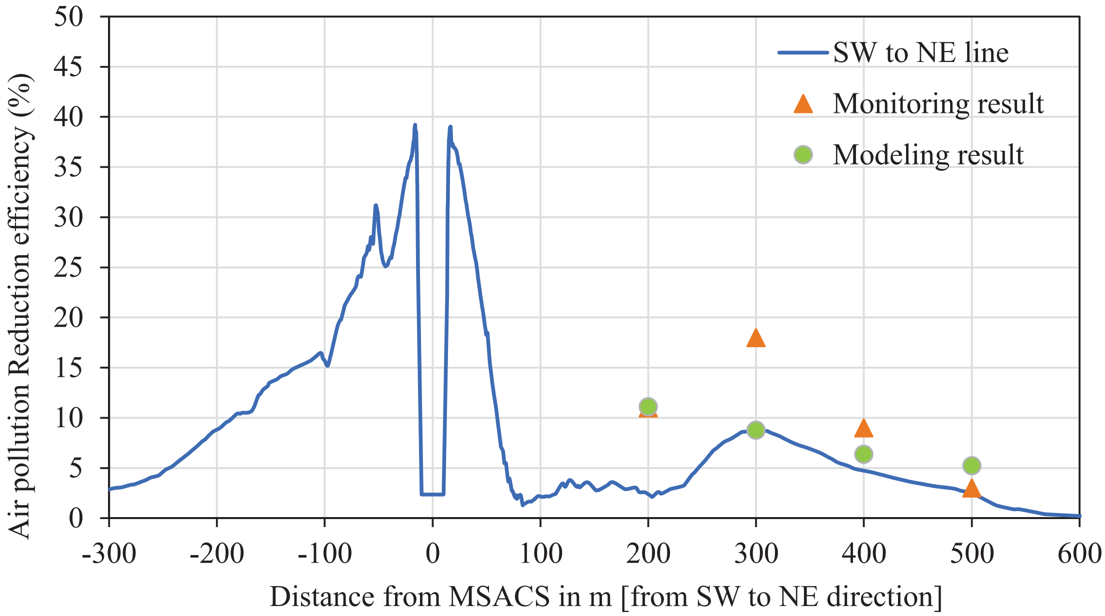

Figure 86. Monitoring and Modelling comparison of Air pollution reduction efficiency at various distances from MSACS dated 24th November 2022, Late night (Considered parameters are: wind speed = 0.3 m/s, wind direction = North-West, filtration efficiency = 43.9%, fan capacity = 739.73 m^3/s and CADR = 324.74 m^3/s).

Due to the unavailability of locations, measurement points are not exactly in NE direction but slightly away from NE direction. And due to this reason, a slight deviation in the results has been observed which can be easily seen from the contours as well as blue line shown in Figure 86. The blue line showing the trend of modelling results of clean air stream in North-East direction (right-hand side of centre (0,0)) shows a drastic decrease in reduction efficiencies up to 200 m, as the peak flow of clean air jet is slightly away from measuring points of SW to NE line as shown in Figure 85. The values from monitoring and modelling show good agreement. A slight variation in the values obtained from modelling and monitoring are acceptable due to the effect of local sources and obstacles present in the actual scenario and other metrological aspects, which are not incorporated during the simulation.

The cleaning efficiency of the South-West stream trend (on the left side of the MSACS centre) gradually decreases as shown in the plot above. At 100 m distance from the MSACS, the cleaning efficiency 15%, while at 200 m distance it is between 8-10%.

9.2.2 Case – 2: The simulation scenario as per the monitoring measurements carried out on 25th November 2022, Early morning in North-East direction (Wind speed: low)

In this case, the air pollution reduction efficiency along different directions for the North-West wind is simulated. The parameters considered for simulation were the same as for the sampling date of 25/11/2021 carried out in early morning. This case is similar to Case 1, except there is a slight change in filtration efficiency. The filtration efficiency in this case was found to be 42.9%. The average wind speed measured by the weather station during that particular time period was 0.3 m/s and the wind direction was North-west . The system flow rate was 739.73 m^3/s (same as Case 1). The CADR for this case is calculated to be 317.34 m^3/s. For CFD simulation filtration efficiency was taken as 42.9%. North-East measurements were taken in the early morning at the distances of 200 m, 300 m, 400 m and 500 m. The measurement locations were not available in directions other than North-East due to the presence of the buildings and structures. Simulations were performed and concentration contours were obtained with respect to the above-mentioned parameters for this case.

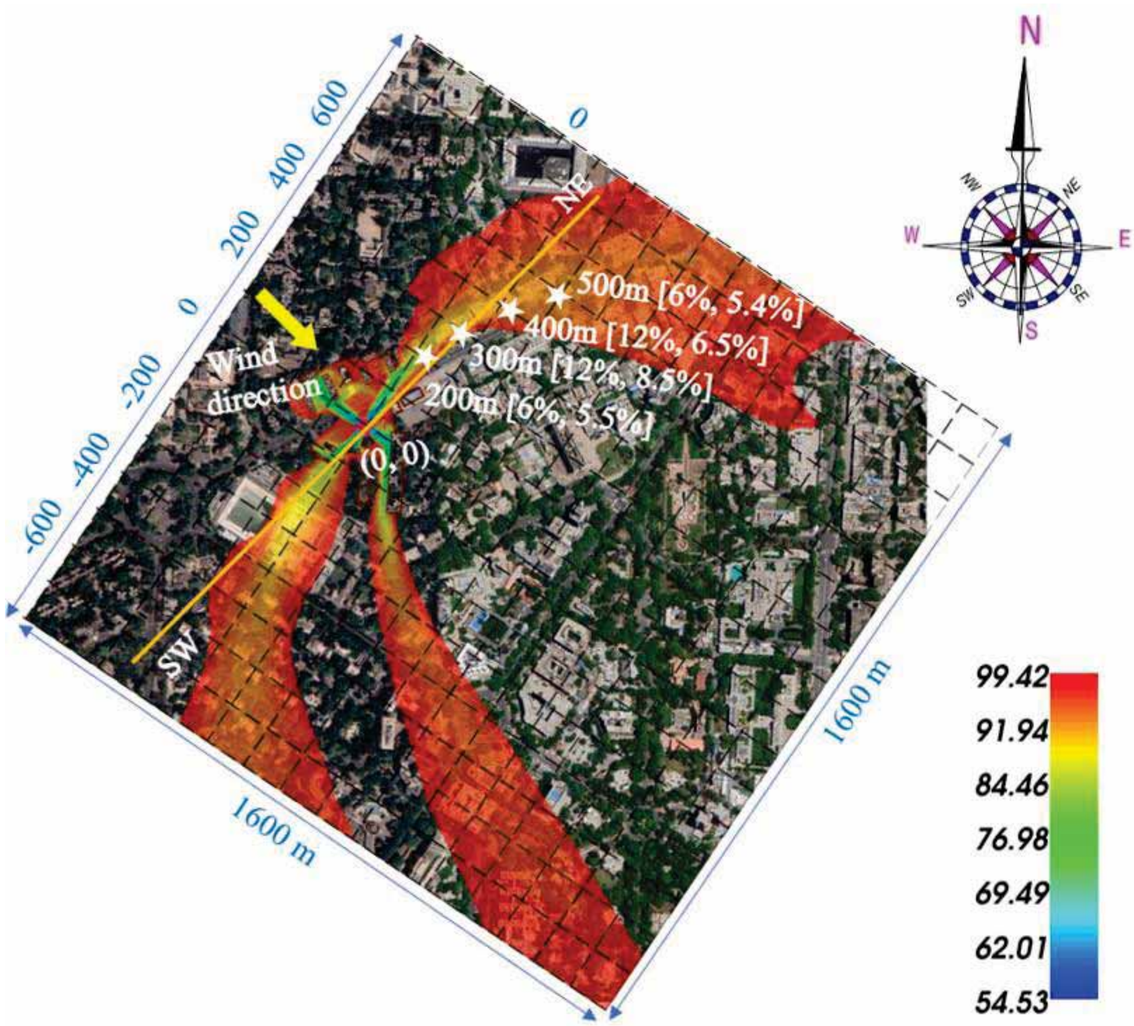

*Star-points indicate: Measurement distance from MSACS in shown direction along with [monitoring, modelling] values of % Air pollution reduction efficiency.

Figure 87. Filled contours of concentration profile (1600 m x 1600 m) dated 25th November 2022, Early morning (Considered parameters are: wind speed = 0.3 m/s, wind direction = North-West, filtration efficiency = 42.9%, fan capacity = 739.73 m^3/s and CADR = 317.34 m^3/s).

The maximum reduction in concentration was obtained at the outlet of the jet while the background concentration considered is 100 μg/m^3. As shown in *Star-points indicate: Measurement distance from MSACS in shown direction along with [monitoring, modelling] values of % Air pollution reduction efficiency.

Figure *87*, a large spread of clean air was obtained up to longer distances in the South-West and North-East directions i.e., in the crosswind direction of the wind flow, whereas due to the presence of the buildings, the clean air spread was lesser in upstream and downstream wind directions. Since the wind speed is low, the crosswind jets travel more distance in their respective directions. The monitoring results and simulation results are compared in Table 27.

Table 27. Comparison of results of air pollution reduction efficiency between measurements and modelling in North-East direction dated 25th November 2022, Early morning (Considered parameters are: wind speed = 0.3 m/s, wind direction = North-West, filtration efficiency = 42.9%, fan capacity = 739.73 m^3/s and CADR = 317.34 m^3/s).

Measurement Direction		**North-East**			
Distance from MSACS (0,0) in m		200	300	400	500
Particle size		$PM_{2.5}$	$PM_{2.5}$	$PM_{2.5}$	$PM_{2.5}$
Air pollution reduction efficiency (%)	From monitoring	6	12	12	6
	From CFD Modelling	5.5	8.5	6.5	5.4

From the above Table 27, at 200 m distance North-East, the reduction efficiency from monitoring was observed to be 6% only. In the same direction, the values of air pollution reduction efficiency through measurements were found to be 12% at distances of 300 m as well as 400 m. The reduction efficiency then decreased to 6% at 500 m. One important point has been observed here that the pollution reduction efficiency near the tower is lower at 200 m than at 300 m. Due to the wind direction being northwest, the North-East and South-West jets travel some distance and start bending along the wind direction. Furthermore, the width of clean air jet is lesser at locations nearer to MSACS and it then spreads over distances. As a result, the near monitoring points do not fall exactly at the peak flow and fall slightly away from the clean air jet, and thus reporting lower air pollution efficiency. This is the reason why at a distance of around 200 m, a lesser air pollution reduction efficiency of 6% was obtained, as the measurement point location is slightly different from the location of center of the jet where maximum cleaning would have been obtained. This concept can be clearly visualized with the help of Figure 88 and Figure 89 shown below.

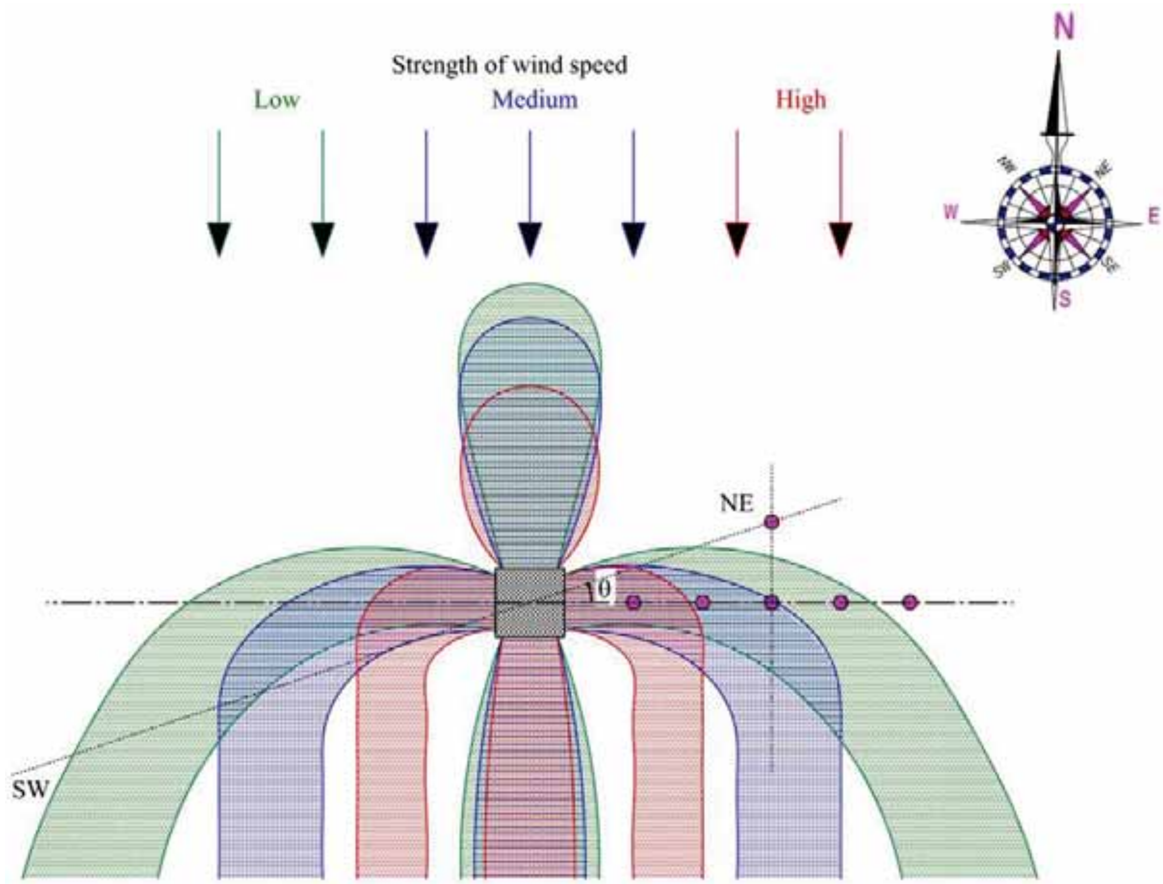

Figure 88. Bending of clean air jets due to the effect of wind speed.

Figure 88 and Figure 89 explain well how the strength of wind speed and effect of wind direction leads to bending of the jets. Due to this phenomenon, some of the measurement points fall out of the peak flow region of jets, and thus lesser air pollution reduction efficiency was obtained. Similar behaviour was also observed with the modelling, where a reduction efficiency of 5.5% was obtained at 200 m, since the observation point does not lie in the region of clean air jet. The points after this were falling within the clean air jet region and gave an efficiency of around 8.5% at 300 m distance and 6.5% at 400 m distance. Cleaning efficiency of more than 5% was obtained even at a distance of 500 m with modelling.

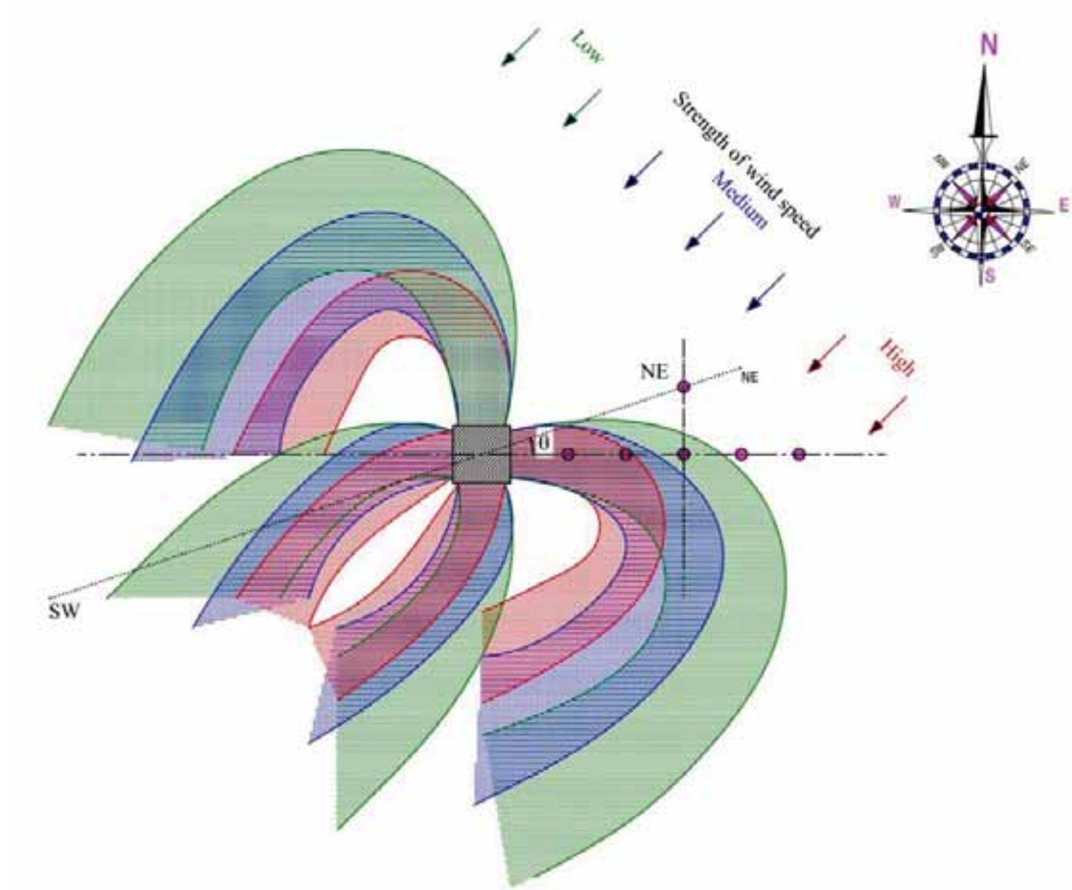

Figure 89. Bending of clean air jets due to the effect of wind direction.

The plot shown below describes the comparison of monitoring and modelling values of % air pollution reduction efficiency for Case 2.

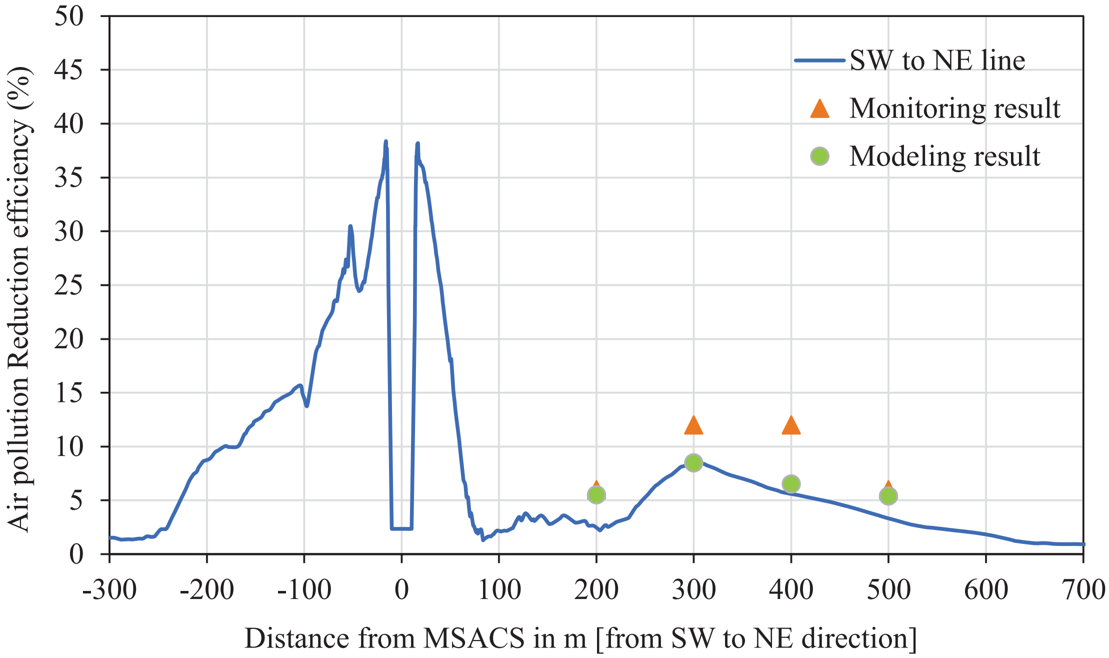

Figure 90. Monitoring and Modelling comparison of Air pollution reduction efficiency at various distances from MSACS dated 25th November 2022, Early morning (Considered parameters are: wind speed = 0.3 m/s, wind direction = North-West, filtration efficiency = 42.9%, fan capacity = 739.73 m^3/s and CADR = 317.34 m^3/s).

The trend of values observed through modelling can be seen with the blue line shown above. Both the sides are showing a decreasing trend with some irregularities in between. In South-West direction (represented by left-hand side of the plot from the center (0, 0)), we observe reduction efficiency of 15% at a distance of 100 m, and 10% at 200 m. In North-East direction (right side of plot from (0, 0)), there is a sudden fall in the reduction efficiency up to 200 m which is due to deviation of clean air jet from the line plotted to observe modelling values. After 200 m distance, the clean air jet and the measurement locations align with each other to give proper values at respective locations. With modelling, cleaning efficiencies of 5-10% were observed in North-East direction up to distances of 500 m.

9.2.3 Case – 3: The simulation scenario as per the monitoring measurements carried out on 22nd December 2022, Late night in North-East and South directions (Wind speed: low)

In this case, the monitoring measurements conducted on 22/12/2022 are compared with the CFD simulation results. The measured meteorological conditions, flow rate and efficiency were used as inputs to the CFD model. Buffer zone efficiency is 40.8%, wind speed measured was 0.52 m/s with a wind direction of 32.6° (N-NE wind). The system flow rate was measured to be 799.39 m^3/s. The CADR for this case was found to be 326.15 m^3/s. North-East and South direction measurements were carried out on the late night of 22nd December 2022. For CFD simulation, the filtration efficiency considered is 40.8%, and the simulations were performed to find the effective reduction zone and to compare the results with the monitoring data obtained for this case. The contours for PM concentration contours along different directions for the North-North-East wind measured on late night of 22/12/2022 is shown in *Star-points indicate: Measurement distance from MSACS in shown direction along with [monitoring, modelling] values of % Air pollution reduction efficiency.

Figure *91*.

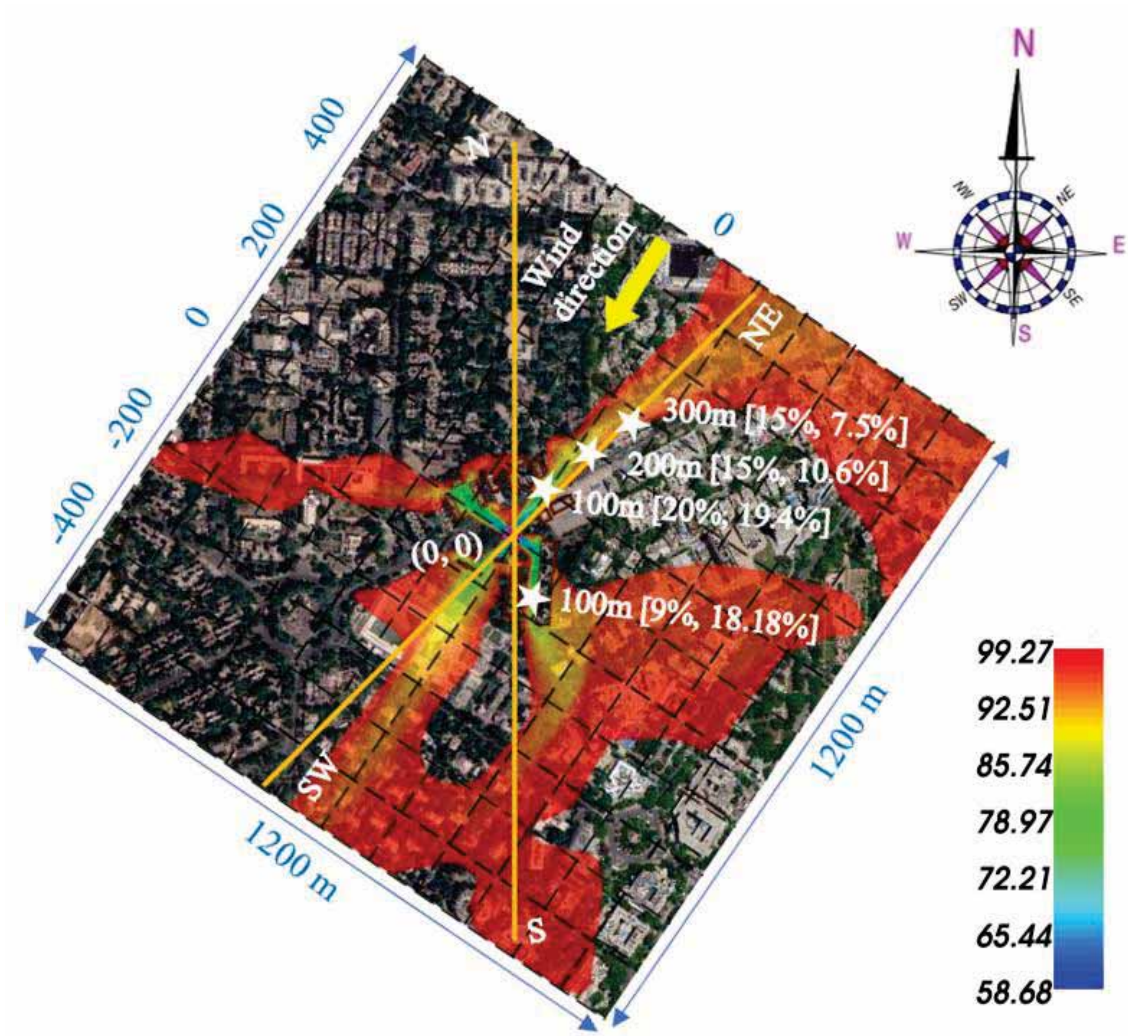

*Star-points indicate: Measurement distance from MSACS in shown direction along with [monitoring, modelling] values of % Air pollution reduction efficiency.

Figure 91. Filled contours of concentration profile (1200 m x 1200 m) dated 22nd December 2022, Late night (Considered parameters are: wind speed = 0.52 m/s, wind direction = North-North-East, filtration efficiency = 40.8%, fan capacity = 799.39 m^3/s and CADR = 326.15 m^3/s).

The concentration contours are shown in *Star-points indicate: Measurement distance from MSACS in shown direction along with [monitoring, modelling] values of % Air pollution reduction efficiency.

Figure *91* considering meteorological parameters and clean air delivery rate from individual fans. The star points shown in the above figure indicate the measurement locations at various distances from MSACS. The yellow lines indicate the values obtained in the given directions with respect to CFD modelling. The clean air streams in North-West and South-East directions strike the building structures and after that, they pass through either side of the structures and then travel further with a decrease in their cleaning efficiencies.

The maximum reduction in concentration was obtained at the outlet of the jets with a background concentration of 100 µg/m^3. Cleaning efficiency is highest at the fan outlet and decreases away from the fan position in all directions. For this case, the clean air spread was observed to be more and also the streams covered larger distances as seen in the above figure.

Table 28. Comparison of results of air pollution reduction efficiency between measurements and modelling in North-East and South directions dated 22nd December 2022, Late night (Considered parameters are: wind speed = 0.52 m/s, wind direction = North-North-East, filtration efficiency = 40.8%, fan capacity = 799.39 m^3/s and CADR = 326.15 m^3/s).

Measurement Direction		**North-East**			**South**
Distance from MSACS (0,0) in m		100	200	300	100
Particle size		$PM_{2.5}$	$PM_{2.5}$	$PM_{2.5}$	$PM_{2.5}$
Air pollution reduction efficiency (%)	From monitoring	20	15	15	9
	From CFD Modelling	19.4	10.6	7.5	18.18

The results from monitoring as well as modelling showed around 20% air pollution reduction efficiency at a distance of 100 m from MSACS in North-East direction. The efficiency decreased as distance from MSACS increased and 15% reduction efficiency was observed at 200 m as well as 300 m. CFD modelling results showed slight variation from the monitoring data obtained, with 10.6% reduction efficiency at 100 m and 7.5% at 200 m North-East. The monitoring measurements were also carried out in South direction and around 9% reduction efficiency was observed at a distance of 100 m. At the same location, the cleaning efficiency with modelling was observed to be around 18%. This variation is considered acceptable due to many different reasons, such as in modelling the background concentration is considered uniform but in the actual scenario it is not. Different real-time point sources are there in actual scenarios which have not been considered in the modelling. There may also be a possibility of less pollution concentration near the tower compared to farther distances, which results in more cleaning efficiency as compared to the modelling results. Further, the effect of temperature inversion was not considered in the simulation. These are all some of the limitations of the modelling simulations, which need to be improved to enhance the methodology.

Figure 92 gives the comparison of results obtained at measurement locations with monitoring and modelling, as well as with the modelling results at various locations obtained from the lines plotted in actual South-West to North-East direction.

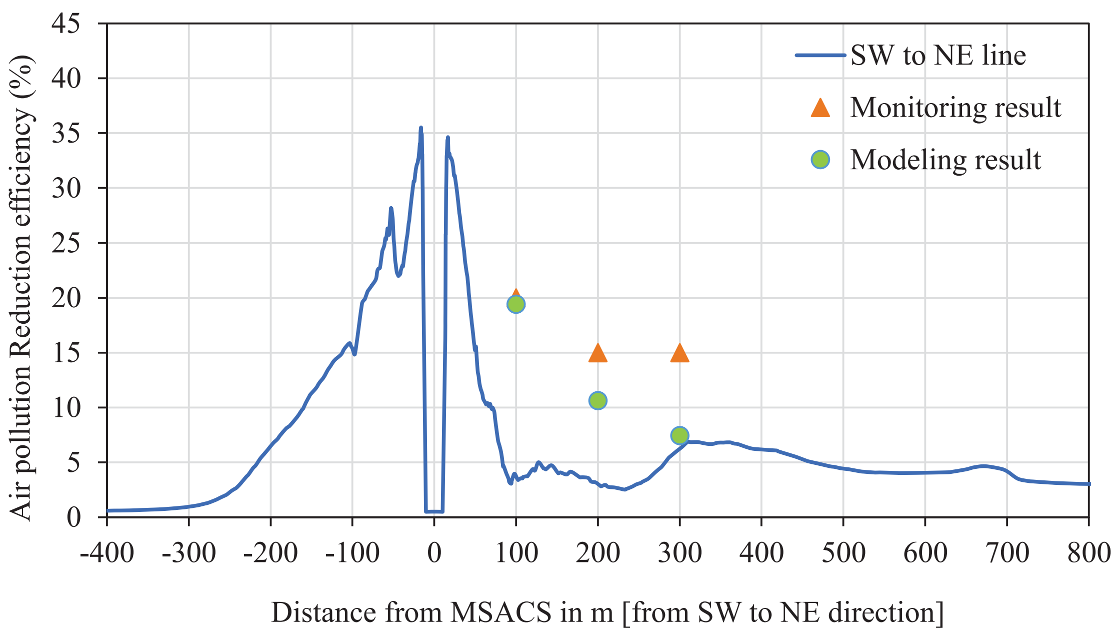

Figure 92. Monitoring and Modelling comparison of Air pollution reduction efficiency at various distances from MSACS dated 22nd December 2022, Late night (Considered parameters are: wind speed = 0.52 m/s, wind direction = North-North-East, filtration efficiency = 40.8%, fan capacity = 799.39 m^3/s and CADR = 326.15 m^3/s).

The plot shows % air pollution reduction efficiencies obtained from modelling compared with some measurement locations of monitoring. The blue trendline indicates results from modelling plotted for South-West to North-East direction. CFD modelling results obtained here show good agreement with monitoring results for distances nearer to MSACS. However, slight variations were observed in the values for distances far from MSACS. It can be observed from the above plot that, a sudden fall in the reduction efficiency in the actual North-East direction was obtained (indicated by right-hand side of blue line), since the line drawn does not align with the peak flow of the clean air jet (see *Star-points indicate: Measurement distance from MSACS in shown direction along with [monitoring, modelling] values of % Air pollution reduction efficiency.

Figure *91*). After a certain distance, the efficiency increased slightly and an almost constant reduction efficiency of 5% was obtained even up to and beyond 700 m distance from MSACS.

9.2.4 Case – 4: The simulation scenario as per the monitoring measurements carried out on 18th January 2023, Afternoon in South-West and North-East directions (Wind speed: low)

Air pollution reduction efficiency is compared with CFD simulation results for validating performance at specific sampling locations, for the measurement conducted on 18/01/2023. In this case, buffer zone efficiency was observed to be 57%. Wind speed observed from the weather station was 0.52 m/s and wind direction West-North-West  . With a fan capacity of 100%, the flow rate was found to be 1136 m^3/s. Hence the CADR for this case was calculated to be 647.52 m^3/s. For CFD Simulation, filtration efficiency of 57% was considered, and the simulations were performed considering the above-mentioned conditions. Measurements were carried out in South-West and North-East directions at specific sampling locations on the afternoon of 18th January 2023.

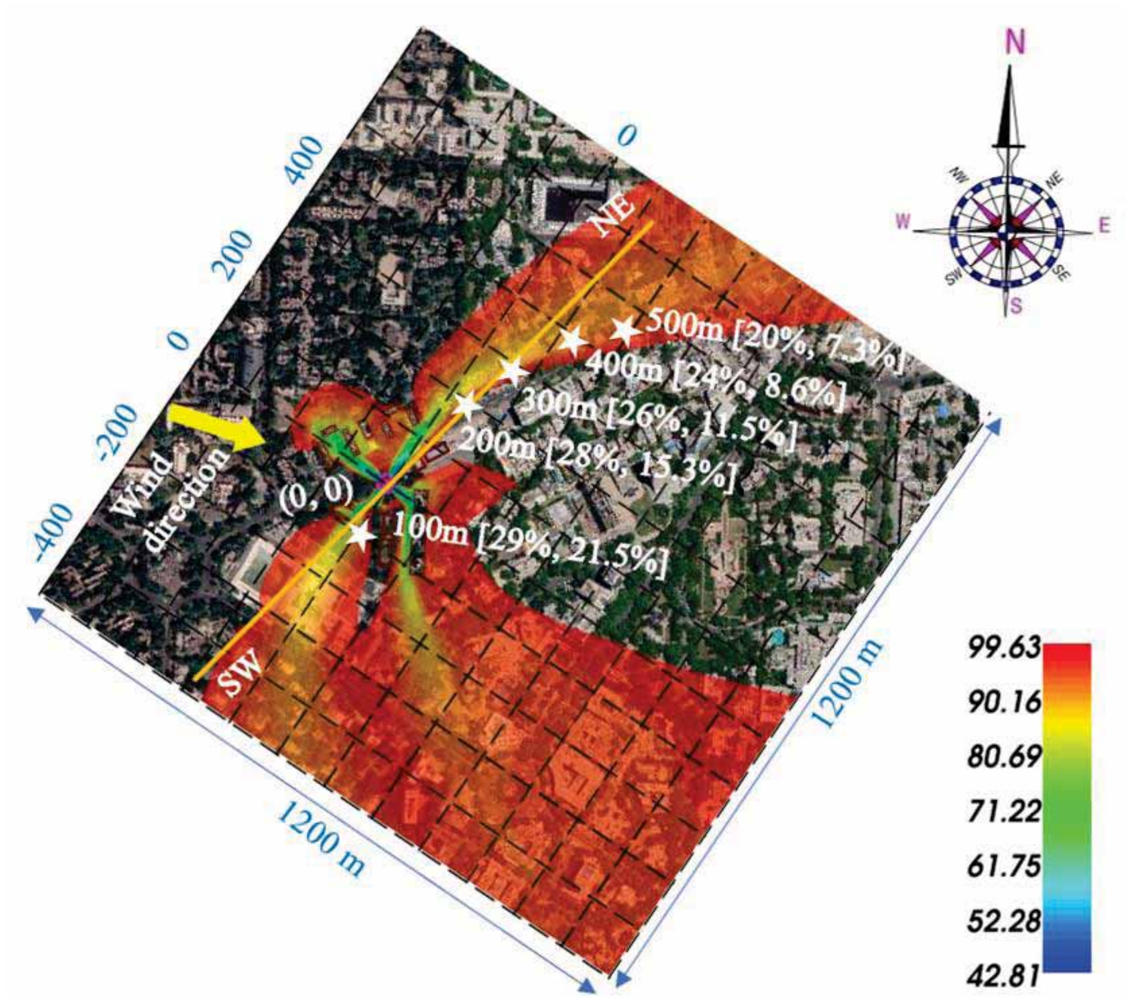

*Star-points indicate: Measurement distance from MSACS in shown direction along with [monitoring, modelling] values of % Air pollution reduction efficiency.

Figure 93. Filled contours of concentration profile (1200 m x 1200 m) dated 18th January 2023, Afternoon (Considered parameters are: wind speed = 0.52 m/s, wind direction = West-North-West, filtration efficiency = 57%, fan capacity = 1136 m^3/s and CADR = 647.52 m^3/s).**Star-points indicate: Measurement distance from MSACS in shown direction along with [monitoring, modelling] values of % Air pollution reduction efficiency.*

Figure 93 shown above gives the PM concentration contours based on the various parameters stated above. Due to higher fan capacity in this case, we observed much more spread of the clean air in the considered area and the locations. Also, the filtration efficiency of 57% was obtained in this case, which along with a higher fan capacity of 1136 m^3/s gave the CADR of 647.52 m^3/s, which was observed to be more than rest of the cases discussed previously.

It can be seen that due to the effect of upcoming wind, the clean air streams in crosswind and upwind directions travel a distance of about 200 m in their direction and then start bending in South-East direction along with the wind flow. Table 29 shows all the measured and modelled results obtained in different directions at various locations from MSACS for this case.

Table 29. Comparison of results of air pollution reduction efficiency between measurements and modelling in South-West and North-East direction dated 18th January 2023, Afternoon (Considered parameters are: wind speed = 0.52 m/s, wind direction = West-North-West, filtration efficiency = 57%, fan capacity = 1136 m^3/s and CADR = 647.52 m^3/s).

Measurement Direction		**South-West**	**North-East**			
Distance from MSACS (0,0) in m		100	200	300	400	500
Particle size		$PM_{2.5}$	$PM_{2.5}$	$PM_{2.5}$	$PM_{2.5}$	$PM_{2.5}$
Air pollution reduction efficiency (%)	From monitoring	29	28	26	24	20
	From CFD Modelling	21.5	15.3	11.5	8.6	7.3

The results from monitoring showed air pollution reduction efficiency of 29% at a distance of 100 m in South-West direction. In the North-East direction, gradually decreasing air pollution reduction efficiencies of 28%, 26% and 24% were obtained at 200 m, 300 m and 400 m respectively. At 500 m North-East, 20% efficiency was observed from measurements. The results from modelling gave 21.5% reduction efficiency at a distance of 100 m in South-West direction. At a distance of 200 m North-East, cleaning efficiency of 15% was observed. After this point, in North-East direction, reduction efficiency of 11.5% was observed at 300 m, 8.6% at 400 m and > 7% up to distance of 500 m. This much difference in modelling and monitoring results is acceptable due to sources variation as well as terrain variation in the actual scenario. Some other reasons for this deviation have already been discussed in previous cases.

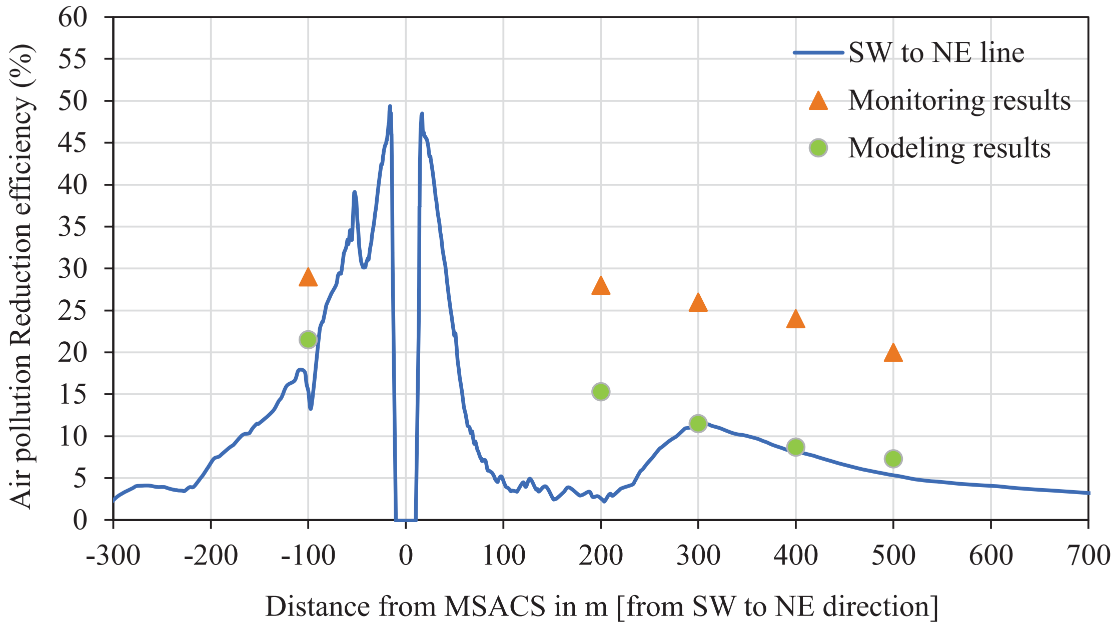

Figure 94. Monitoring and Modelling comparison of Air pollution reduction efficiency at various distances from MSACS dated 18th January 2023, Afternoon (Considered parameters are: wind speed = 0.52 m/s, wind direction = West-North-West, filtration efficiency = 57%, fan capacity = 1136 m^3/s and CADR = 647.52 m^3/s).

The above plot shows the air pollution reduction efficiencies in South-West and North-East directions. The left side of the plot from centre (0, 0) indicates the South-West and right side indicates North-East direction. The trend of modelling in South-West direction shows a decrease in the air pollution reduction efficiency after the clean air is released from the fan. The cleaning efficiency of around 40%, 15% and 8% were observed at distances of 50 m, 100 m and 200 m respectively. However, the modelling values obtained in the exact North-East direction showed a sudden decrease in cleaning efficiency up to 200 m, and then starts increasing up to 300 m as it coincided with the peak flow of clean air jet. However, after a distance of 300 m in North-East, due to bending of clean air jets, it gets deviated from NE line and thus lesser values of reduction efficiencies are obtained.

9.2.5 Case – 5: The simulation scenario as per the monitoring measurements carried out on 11th January 2023, Afternoon in North-East direction (Wind speed: high)

For this case, the simulation results are compared with the monitoring performance results for the sampling conducted in the afternoon of 11th January 2023. On this day, the average wind speed measured by the weather station during that particular afternoon time period was 1.25 m/s and the wind direction was North-North-East wind. The system flow rate measured was 791.12 m^3/s and the buffer zone efficiency measured using research-grade instrument was 49.8%. The CADR for this case is calculated as 393.97 m^3/s. For CFD simulation, similar boundary conditions have been used for individual fan jets in each direction. The concentration contours for this case are shown in *Star-points indicate: Measurement distance from MSACS in shown direction along with [monitoring, modelling] values of % Air pollution reduction efficiency.

Figure *95*, based on the meteorological parameters and system flow rate stated above.

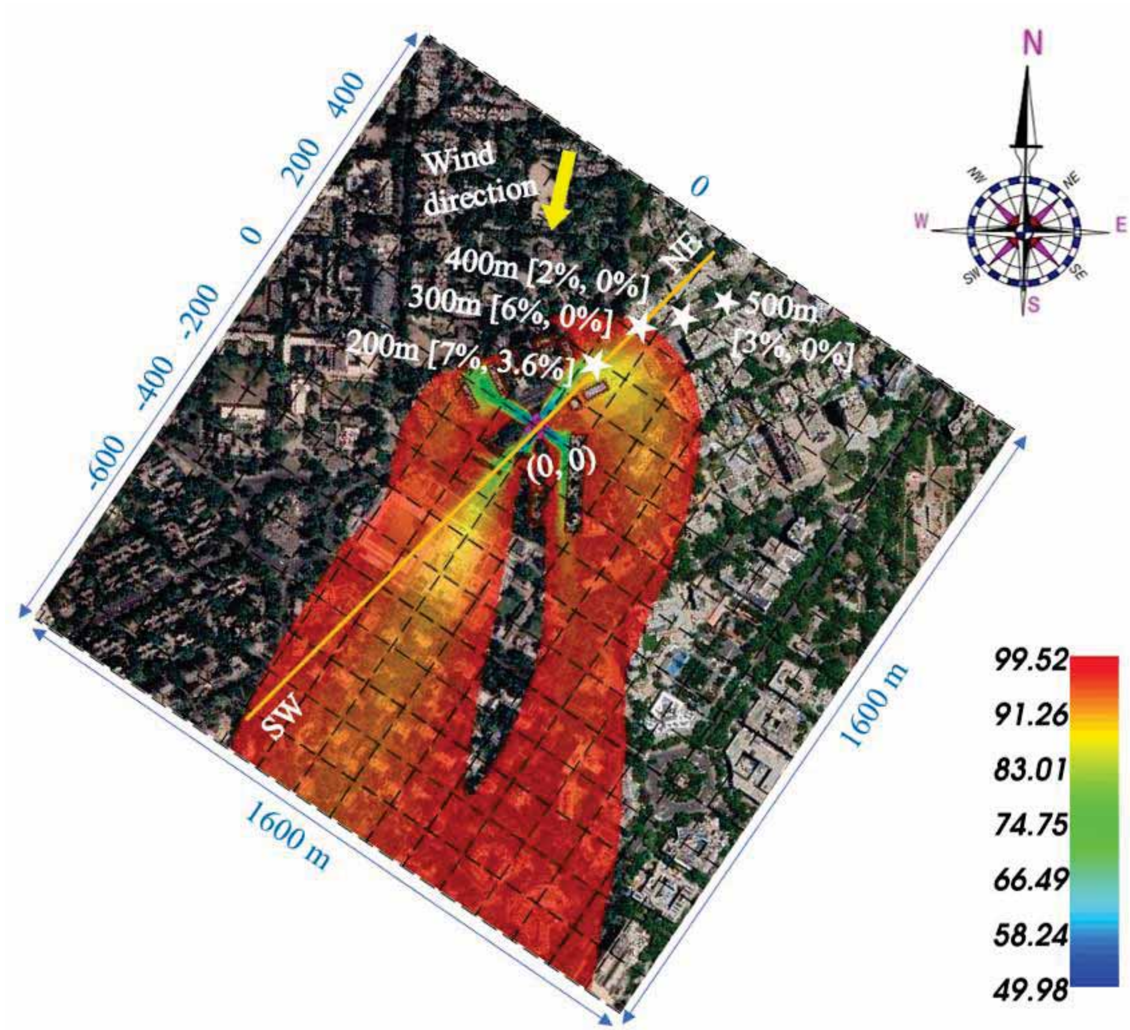

*Star-points indicate: Measurement distance from MSACS in shown direction along with [monitoring, modelling] values of % Air pollution reduction efficiency.

Figure 95. Filled contours of concentration profile (1600 m x 1600 m) dated 11th January 2023, Afternoon (Considered parameters are: wind speed = 1.25 m/s, wind direction = North-North-East, filtration efficiency = 49.8%, fan capacity = 791.12 m^3/s and CADR = 393.97 m^3/s).

Filter efficiency is maximum at the fan outlet and decreases with increasing distance from MSACS. The maximum reduction in concentration at the fan outlet is 50 μg/m^3 and the background concentration is 100 μg/m^3. The fans were operated at 75% capacity and the system flow rate was 791.12 m^3/s for each fan jet. As the wind is coming from NNE direction with velocity of 1.25 m/s, which is quite high, it was observed that after travelling a certain distance in their respective jet directions, all of the clean air streams bend and start travelling along with the wind flow, towards one same direction i.e. South-West. This clearly shows the effect of local or existing wind flow on the clean air streams released from different jet directions.

Table 30. Comparison of results of air pollution reduction efficiency between measurements and modelling in North-East direction dated 11th January 2023, Afternoon (Considered parameters are: wind speed = 1.25 m/s, wind direction = North-North-East, filtration efficiency = 49.8%, fan capacity = 791.12 m^3/s and CADR = 393.97 m^3/s).

Measurement Direction		**North-East**			
Distance from MSACS (0,0) in m		200	300	400	500
Particle size		$PM_{2.5}$	$PM_{2.5}$	$PM_{2.5}$	$PM_{2.5}$
Air pollution reduction efficiency (%)	From monitoring	7	6	3	2
	From CFD Modelling	3.6	0	0	0

At 200 m North-East from the MSACS, the air pollution reduction efficiency was reported as 7% from monitoring. With modelling it was observed to be 3.6% at the same location. At distances of 400-500 m, the reduction efficiency was found to be 2-3% from monitoring and almost near to 0% from modelling, as these locations were falling in the shadow region of clean air jet in this direction. Thus, one can say that the results of monitoring and modelling are in good agreement and the model is validating well with the experiments.

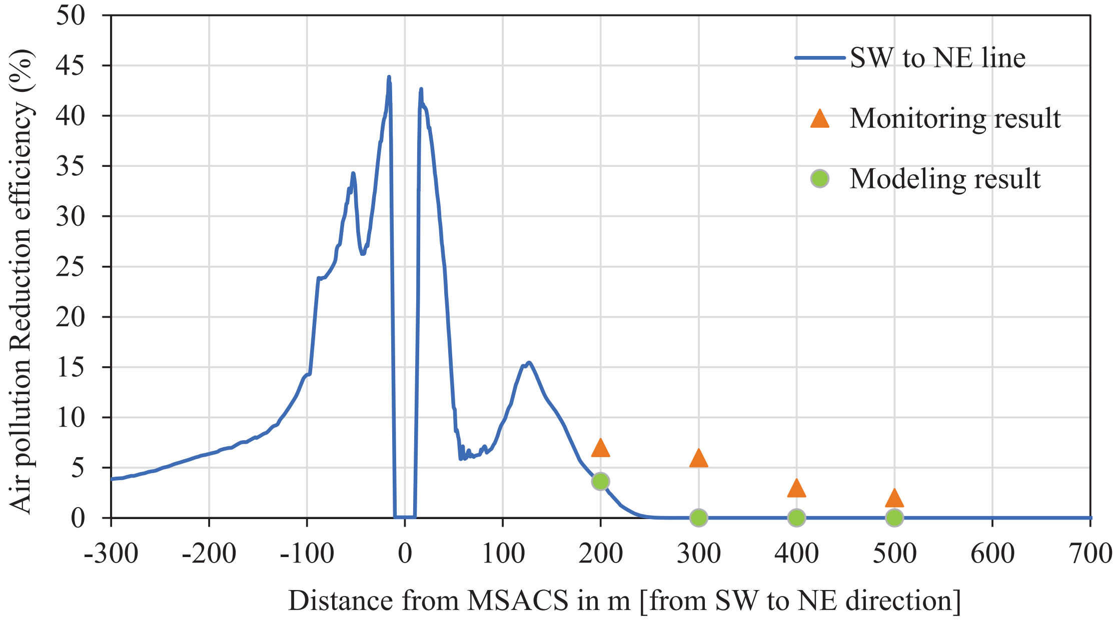

Figure 96. Monitoring and Modelling comparison of Air pollution reduction efficiency at various distances from MSACS dated 11th January 2023, Afternoon (Considered parameters are: wind speed = 1.25 m/s, wind direction = North-North-East, filtration efficiency = 49.8%, fan capacity = 791.12 m^3/s and CADR = 393.97 m^3/s).

In the above plot, the blue line representing modelling values at various locations from MSACS shows decrease in the trend with distances away from MSACS. In South-West direction, which is downstream of wind flow, the plot shows reduction efficiency of 20% at 100 m, 6% at 200 m and around 5% up to 300 m distance. The results for reduction efficiencies in North-East direction have already been discussed and compared with the monitoring values in the previous Table 30. However, some monitoring values for distances nearer to the tower (less than 200 m) are also required, to have a clear and better comparison with modelling.

9.2.6 Case – 6: The simulation scenario as per the monitoring measurements carried out on 15th February 2023, Late night in South-West and North-East directions (Wind speed: high)

For this case, the simulation results are compared with the monitoring performance results for the sampling conducted in the afternoon of 15th February 2023. On this day, a high wind speed of 1.64 m/s was observed by the weather station during afternoon time period and the wind direction was South-West wind . The system flow rate measured was 1006.36 m^3/s and the buffer zone efficiency measured using research-grade instrument was 60.7%. The CADR for this case is calculated as 610.86 m^3/s, with a high fan capacity of 100%. For CFD simulation, similar boundary conditions have been used for individual fan jets in each direction. The concentration contours for this case are shown in *Star-points indicate: Measurement distance from MSACS in shown direction along with [monitoring, modelling] values of % Air pollution reduction efficiency.

Figure *97*, based on the meteorological parameters and system flow rate stated above.

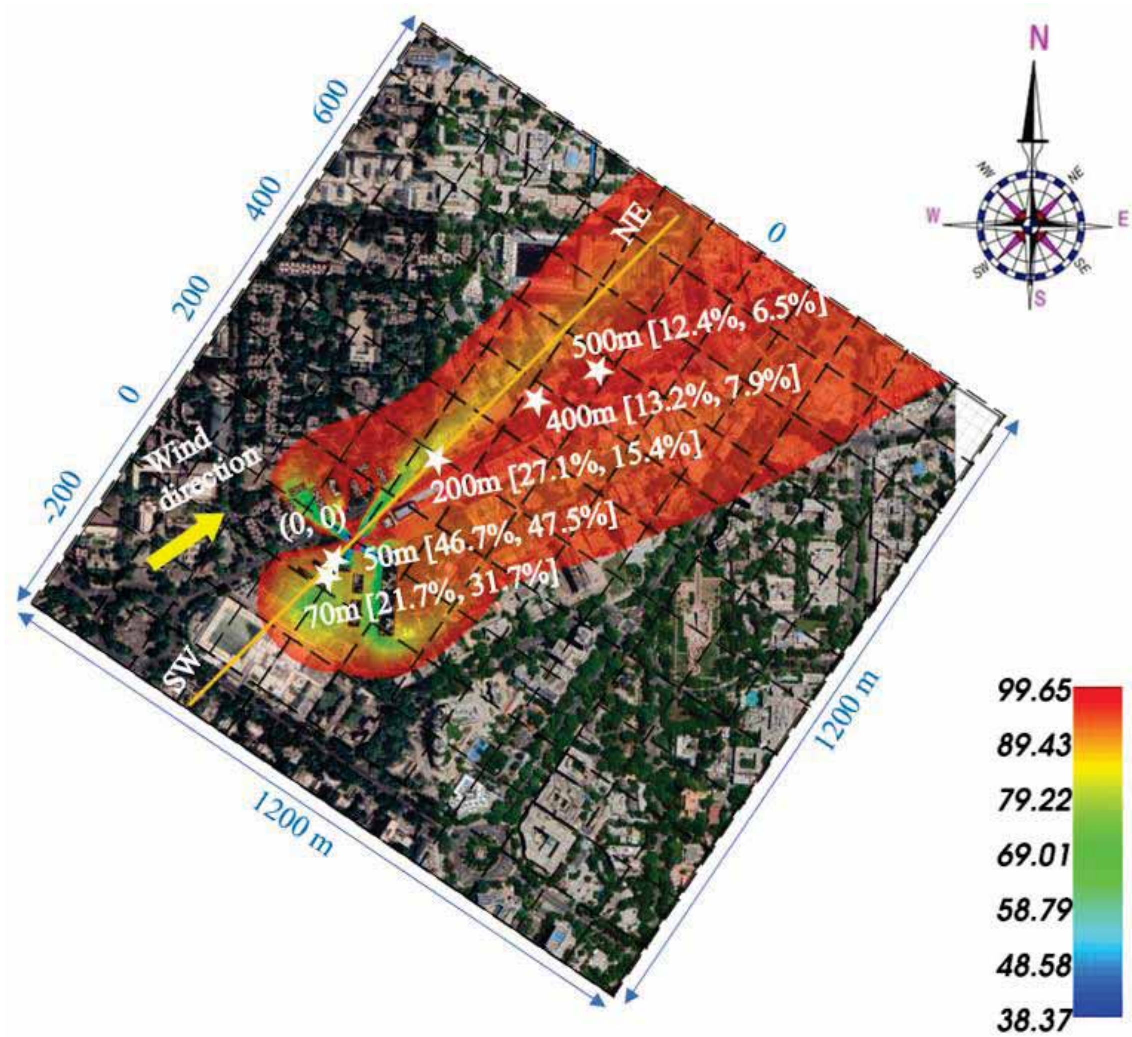

*Star-points indicate: Measurement distance from MSACS in shown direction along with [monitoring, modelling] values of % Air pollution reduction efficiency.

Figure 97. Filled contours of concentration profile (1200 m x 1200 m) dated 15th February 2023, Late night (Considered parameters are: wind speed = 1.64 m/s, wind direction = South-West, filtration efficiency = 60.7%, fan capacity = 1006.36 m^3/s and CADR = 610.86 m^3/s).

The contours in above *Star-points indicate: Measurement distance from MSACS in shown direction along with [monitoring, modelling] values of % Air pollution reduction efficiency.

Figure *97* show the PM concentration profiles in different directions. The maximum concentration reduction was obtained at the outlet of each fan. The background concentration was 100 $\mu g/m^3$. Maximum cleaning efficiency is observed at the fan outlet and decreases away with increasing distance from MSACS. It was observed that the spreading of the clean air obtained was higher in the North-East direction only i.e., the direction downstream of the wind flow. Whereas, the clean air spread was much lesser in the rest of the directions. A higher wind speed of 1.64 m/s was observed on this day, which influenced the clean air streams in other directions. These streams travelled some distance and then bend along with the direction of incoming high-speed wind flow. The monitoring and modelling results are given and compared in Table 31.

Table 31. Comparison of results of air pollution reduction efficiency between measurements and modelling in South-West and North-East directions dated 15th February 2023, Late night (Considered parameters are: wind speed = 1.64 m/s, wind direction = South-West, filtration efficiency = 60.7%, fan capacity = 1006.36 m^3/s and CADR = 610.86 m^3/s).

Measurement Direction		**South-West**		**North-East**		
Distance from MSACS (0,0) in m		50	70	200	400	500
Particle size		$PM_{2.5}$	$PM_{2.5}$	$PM_{2.5}$	$PM_{2.5}$	$PM_{2.5}$
Air pollution reduction efficiency (%)	From monitoring	46.7	21.7	27.1	13.2	12.4
	From CFD Modelling	47.5	31.7	15.4	7.9	6.5

The results showed air pollution reduction efficiency of 46.7% from monitoring and 47.5% from modelling at a distance of 50 m in South-West direction. After this, a reduction in efficiency was observed at 70 m from both monitoring as well as modelling. In the North-East direction, which is downstream of the upcoming wind flow, gradually decreasing air pollution reduction efficiencies of 27.1%, 13.2% and 12.4% were obtained at 200 m, 400 m and 500 m respectively. The results from modelling gave 15.4% reduction efficiency at a distance of 200 m in North-East direction. After this point, in the same direction, reduction efficiency of 7.9% was observed at 400 m, and 6.5% at 500 m. Thus, one can see that the model is validating quite well with the monitoring results in all the considered directions.

The plot of air pollution reduction efficiency comparing modelling and monitoring values at various distances in different directions with MSACS as centre (0,0) is shown in Figure 98.

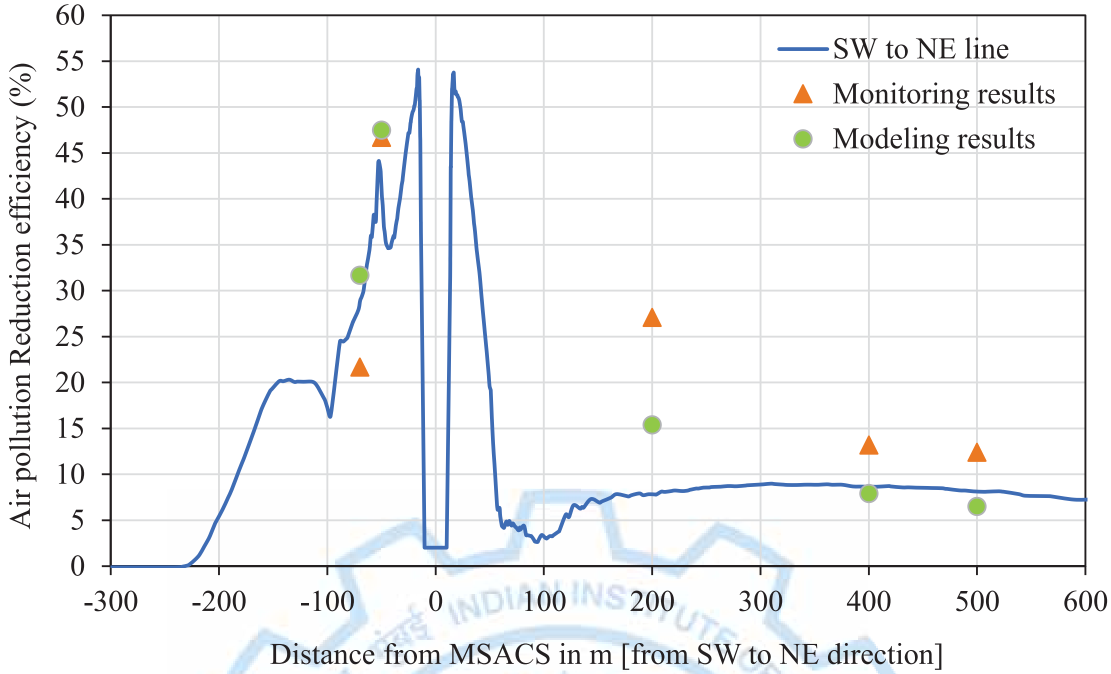

Figure 98. Monitoring and Modelling comparison of Air pollution reduction efficiency at various distances from MSACS dated 15th February 2023, Late night (Considered parameters are: wind speed = 1.64 m/s, wind direction = South-West, filtration efficiency = 60.7%, fan capacity = 1006.36 m^3/s and CADR = 610.86 m^3/s).

The blue line showing the trend of modelling results of clean air stream in South-West direction (left-hand side of (0,0)) shows decrease in reduction efficiencies with some abrupt changes. This might be due to the presence of various building structures present in between. Also, a high wind speed led to bending of South-West jet along with it in downwind direction.

In North-East direction, a sudden decrease in the modelling values obtained was observed up to 100 m, since the peak flow of North-East jet was not aligning with the considered North-East line (shown in *Star-points indicate: Measurement distance from MSACS in shown direction along with [monitoring, modelling] values of % Air pollution reduction efficiency.

Figure *97*). After this distance, an efficiency of 5-10% was obtained up to and even beyond 800 m North-East.

- **Additional simulations summarized along with the results:**

Some more monitoring measurements were validated with the modelling for different dates at different scenarios, and the results of both along with the comparison are given in Table 32. These simulations are done for different scenarios compared to previously described cases in various winter months. The methodology followed are same as the previous modelling cases. However, the modelling and monitoring comparison are very similar to previous modelling findings.

Table 32. Results and comparison of Air pollution reduction efficiency obtained from monitoring and modelling considering various parameters for different dates.

Date		Parameters						Measurement location	Results of Air pollution reduction efficiency (%)	
	Nature of wind	Wind speed (m/s)	Wind direction	System flow rate (m^3/s)	Filtration Efficiency (%)	CADR (m^3/s)	Relative humidity (%)		From Monitoring	From Modelling
23/01/23 Afternoon	Low wind speed	0.28	NNE	890.86	44	391.98	34.8	SW 100	42	17.8
								SE 100	44	17.8
								NE 300	31	8.3
								NE 400	31	3.2
								NE 500	29	1.4
02/11/22 Early morning		0.5	W	470.2	39	183.38	80	NE 200	18.3	10.6
								NE 300	1.7	8.8
								NE 400	7.8	7.3
								NE 500	1.7	6.6

21/02/23 Late night		0.5	S	994.58	55.6	552.98	80	SW 50	54	44.2
								NE 200	11	15.9
								NE 400	8	9.7
20/02/23 Afternoon	**High wind speed**	1.08	SE	994.58	55.6	552.98	40	SW 50	30.6	44.3
								NE 200	14.8	15.1
01/12/22 Late night		2	E	739.73	42.1	311.42	80	NE 200	15	1.1
								NE 300	11	0
								NE 500	6	0

The contours obtained for above mentioned cases are given below along with the monitoring and modelling values of air pollution reduction efficiencies obtained at different measurement locations.

9.2.7 Case – 7: The simulation scenario as per the monitoring measurements carried out on 23rd January 2023, Afternoon in South-West, South-East and North-East directions (Wind speed: low)

Air pollution reduction efficiency was compared with CFD simulation results for validating the performance at specific sampling locations, for the measurement conducted on 23/01/2023. In this case, buffer zone efficiency was observed to be 44%. Wind speed observed from the weather station was 0.28 m/s and wind direction was North-North-East. The flow rate was found to be 890.86 m^3/s, and the CADR for this case was calculated to be 391.98 m^3/s. For CFD Simulation, filtration efficiency of 44% was considered, and the simulations were performed considering the above-mentioned conditions. Measurements were carried out in North-East, South-East and South-West directions at specific sampling locations on the afternoon of 23rd January 2023.

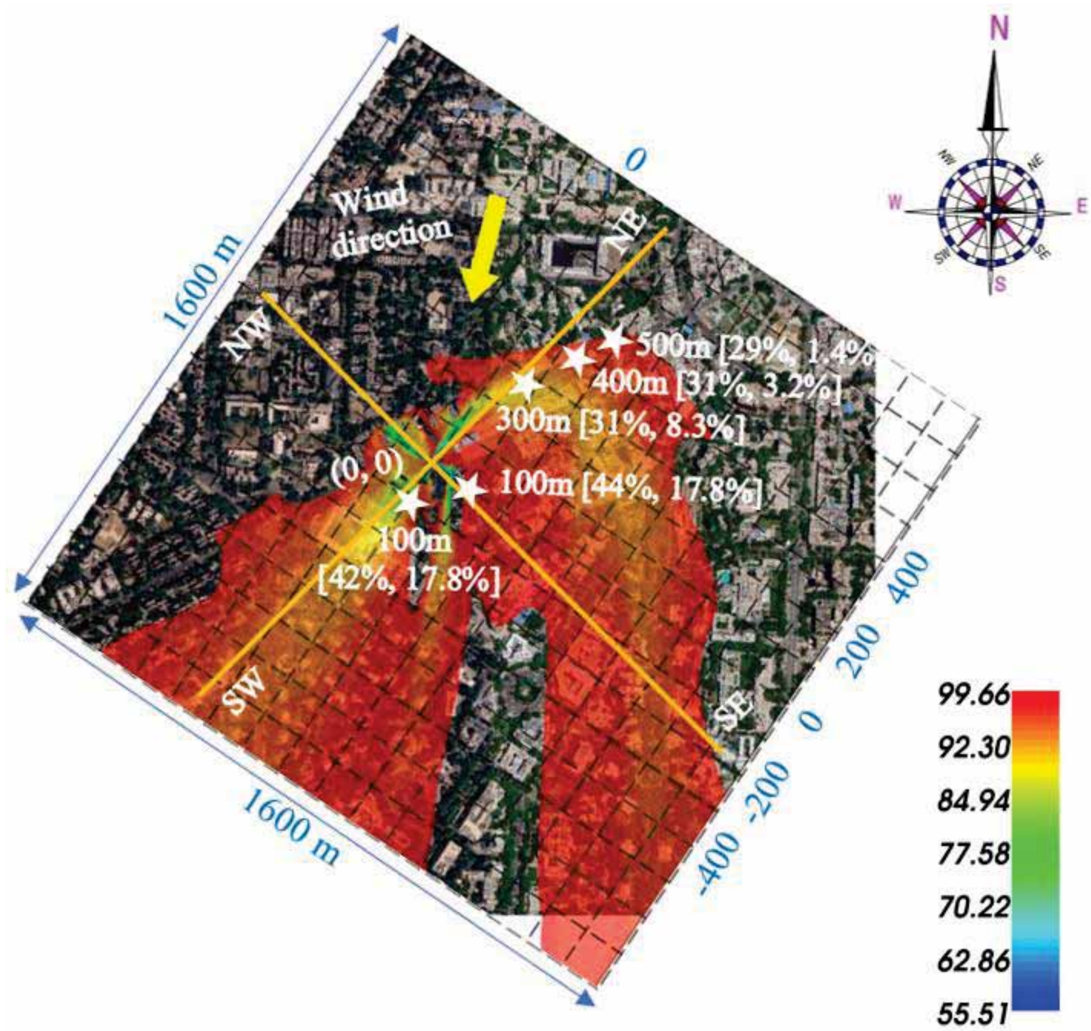

*Star-points indicate: Measurement distance from MSACS in shown direction along with [monitoring, modelling] values of % Air pollution reduction efficiency.

Figure 99. Filled contours of concentration profile (1600 m x 1600 m) dated 23rd January 2023, Afternoon (Considered parameters are: wind speed = 0.28 m/s, wind direction = North-North-East, filtration efficiency = 44%, fan capacity = 890.86 m^3/s and CADR = 391.98 m^3/s).

A low wind speed of 0.28 m/s resulted in the spreading of clean air up to longer distances in all directions. In one of the crosswind directions due to presence of obstruction the clean air jet got restricted. However, in the upwind direction there are no or very less obstructions present, which along with the effect of very low wind speed led to more spreading of clean air in this direction.

9.2.8 Case – 8: The simulation scenario as per the monitoring measurements carried out on 2nd November 2022, Early morning in North-East direction (Wind speed: low)

In this case, the modelling results are compared with the monitoring performance results for the sampling conducted on the early morning of 2nd November 2022. On this day, the buffer zone efficiency was observed to be 39%. The average wind speed measured by the weather station during the afternoon time period was 0.5 m/s with wind direction of West. The flow rate was measured as 470.2 m^3/s. The CADR for this case was calculated to be 183.38 m^3/s. For CFD simulation, the filtration efficiency was considered as 39%, and the simulations were performed to find the effective reduction zone. North-East direction measurements were carried out in the early morning of 2nd November 2022. *Star-points indicate: Measurement distance from MSACS in shown direction along with [monitoring, modelling] values of % Air pollution reduction efficiency.

Figure *100* below shows the contours of PM concentration profile for this case.

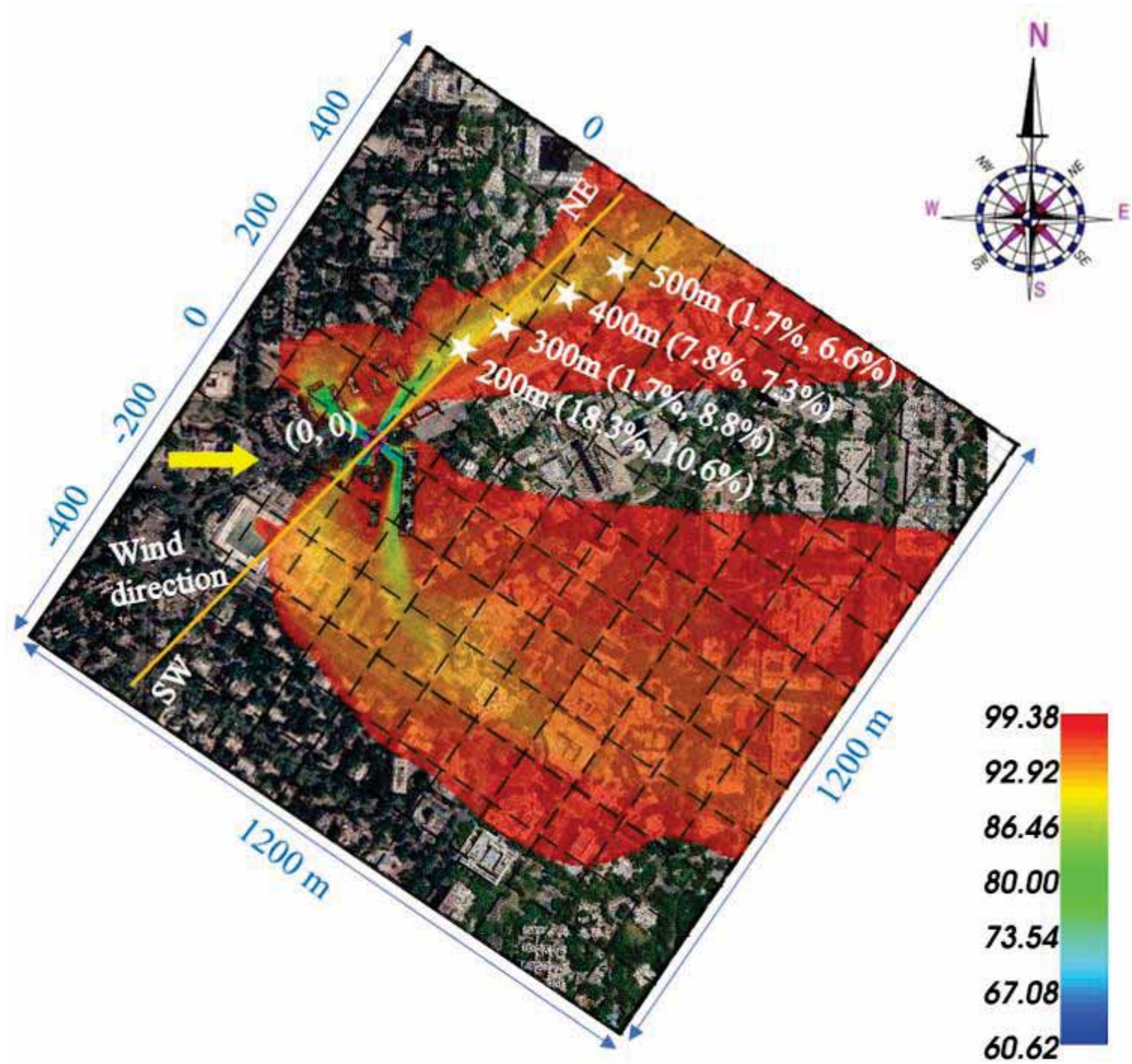

*Star-points indicate: Measurement distance from MSACS in shown direction along with [monitoring, modelling] values of % Air pollution reduction efficiency.

Figure 100. Filled contours of concentration profile (1200 m x 1200 m) dated 2nd November 2022, Early morning (Considered parameters are: wind speed = 0.5 m/s, wind direction = West, filtration efficiency = 39%, fan capacity = 470.2 m^3/s and CADR = 183.38 m^3/s).

From the above figure, it is observed that monitoring and modelling values are showing good agreement. However, one important thing to note here is in North-East direction at a distance of 300 m, the value of reduction efficiency obtained was less than that at 400 m. The reason behind this has already been described in Case 2 (section 9.2.2) that, sometimes the monitoring points do not fall exactly at the peak flow and fall slightly away from the clean air jet. From the contours in *Star-points indicate: Measurement distance from MSACS in shown direction along with [monitoring, modelling] values of % Air pollution reduction efficiency.

Figure *100*, one can clearly observe that the measurement location of 300 m NE is falling out of peak flow of clean air jet in this direction and thus reporting a lower air pollution efficiency.

9.2.9 Case – 9: The simulation scenario as per the monitoring measurements carried out on 21st February 2023, Late night in South-West and North-East directions (Wind speed: low)

For Case 9, the simulation results were compared with the monitoring performance results for the sampling conducted in the late night of 21st February 2023. The average wind speed measured by the weather station during that particular time period was 0.5 m/s and the wind direction was South. The system flow rate measured was 994.58 m^3/s and the buffer zone efficiency in the downstream of filter bank measured using research-grade instrument was 55.6%. The CADR for this case was calculated as 552.98 m^3/s. For CFD simulation, filtration efficiency input was taken as 55.6%, and simulations were performed for this case. The monitoring measurements were carried out in South-West and North-East directions.

The resulting contours of concentration profiles for this case are shown in Figure 101 below.

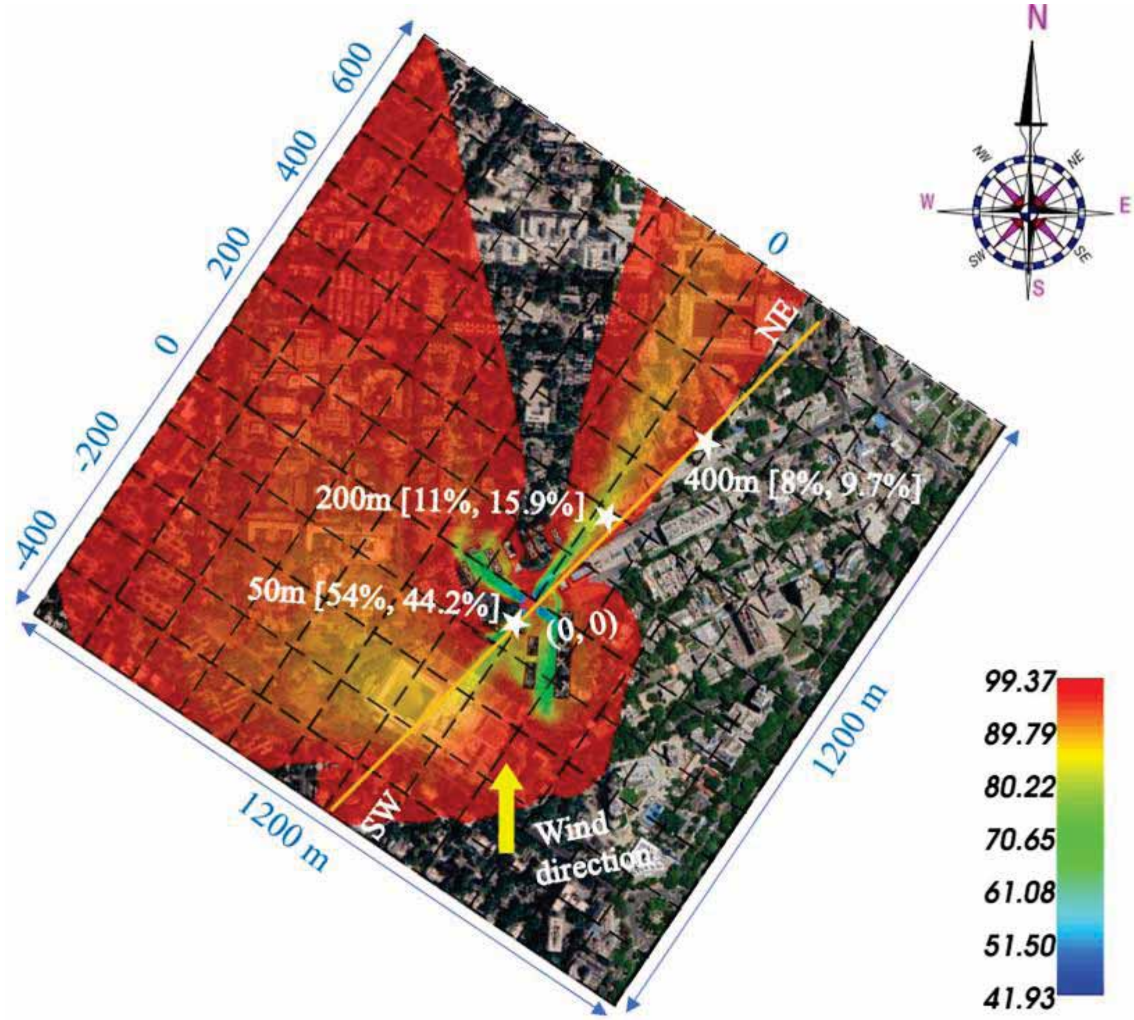

*Star-points indicate: Measurement distance from MSACS in shown direction along with [monitoring, modelling] values of % Air pollution reduction efficiency.

Figure 101. Filled contours of concentration profile (1200 m x 1200 m) dated 21st February 2023, Late night (Considered parameters are: wind speed = 0.5 m/s, wind direction = South, filtration efficiency = 55.6%, fan capacity = 994.58 m^3/s and CADR = 552.98 m^3/s).

The effect of low wind speed can be clearly observed with the contours shown above. A higher effective reduction zone was obtained in all the directions, as compared to the cases with high wind speed. The values of air pollution reduction efficiency show that the model is validating well with the monitoring results.

9.2.10 Case – 10: The simulation scenario as per the monitoring measurements carried out on 20th February 2023, Afternoon in South-West and North-East directions (Wind speed: high)

In this case, the monitoring measurements conducted on 20/02/2023 are compared with the CFD simulation. The measured meteorological conditions, flow rate and efficiency were used as inputs to the CFD model. The average wind speed measured by the weather station during that particular time period was 1.08 m/s with wind direction of South-East wind. Buffer zone efficiency is 55.6% and flow rate is 994.58 m^3/s. The CADR for this case was found to be 552.98 m^3/s. South-West and North-East direction measurements were carried out in the afternoon time. For CFD simulation, similar boundary conditions have been used for individual fan jet in each direction to find the effective reduction zone and compare the results with the monitoring data obtained in this case. The contours for PM concentration profiles along different directions for the East wind measured in the afternoon of 20th February 2023 are shown in *Star-points indicate: Measurement distance from MSACS in shown direction along with [monitoring, modelling] values of % Air pollution reduction efficiency.

Figure *102*.

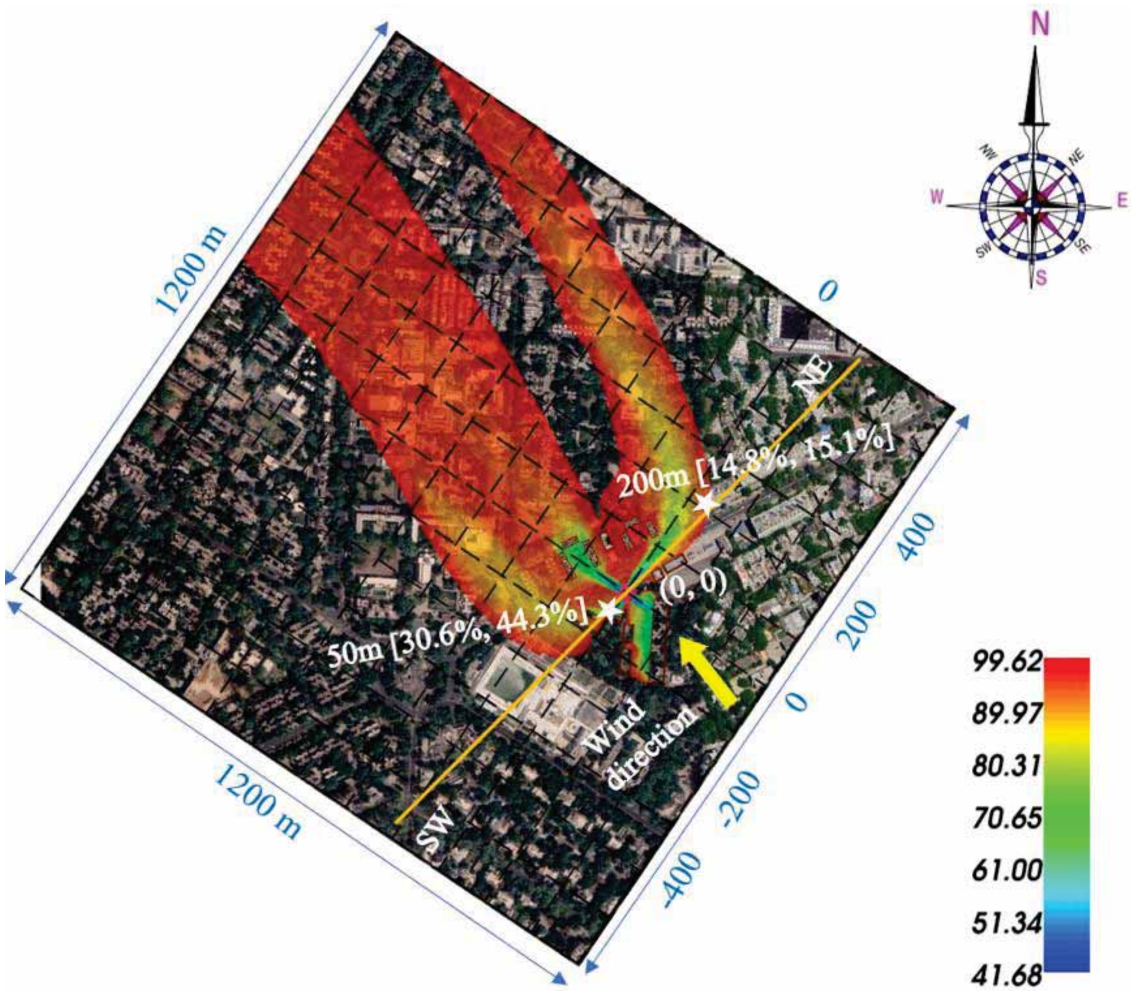

*Star-points indicate: Measurement distance from MSACS in shown direction along with [monitoring, modelling] values of % Air pollution reduction efficiency.

Figure 102. Filled contours of concentration profile (1200 m x 1200 m) dated 20th February 2023, Afternoon (Considered parameters are: wind speed = 1.08 m/s, wind direction = South-East, filtration efficiency = 55.6%, fan capacity = 994.58 m^3/s and CADR = 552.98 m^3/s).

The values in the above contour show that the model is validating very well with the monitoring results for distances up to 200 m. However, high wind speed led to bending of crosswind jets as well as upwind jets with the upcoming wind in one single downwind direction (North-West here). The presence of building structure along with the upcoming high wind speed from South-East restricted the upwind jet from traveling further as shown in *Star-points indicate:

Measurement distance from MSACS in shown direction along with [monitoring, modelling] values of % Air pollution reduction efficiency.

Figure *102*.

9.2.11 Case – 11: The simulation scenario as per the monitoring measurements carried out on 1st December 2022, Late night in North-East directions (Wind speed: high)

In this case, the modelling results are compared with the monitoring performance results for the sampling conducted in the late night of 1st December 2022. On this day, the buffer zone efficiency was observed to be 42.1%. The average wind speed measured by the weather station was 2 m/s with wind direction of East. The flow rate was measured as 739.73 m^3/s. The CADR for this case was calculated to be 311.42 m^3/s. For CFD simulation, the filtration efficiency was considered as 42.1%, and the simulations were performed to find the effective reduction zone. North-East direction measurements were carried out in the late night of 1st December 2022. *Star-points indicate: Measurement distance from MSACS in shown direction along with [monitoring, modelling] values of % Air pollution reduction efficiency.

Figure *103* below shows the contours of PM concentration profile for this case.

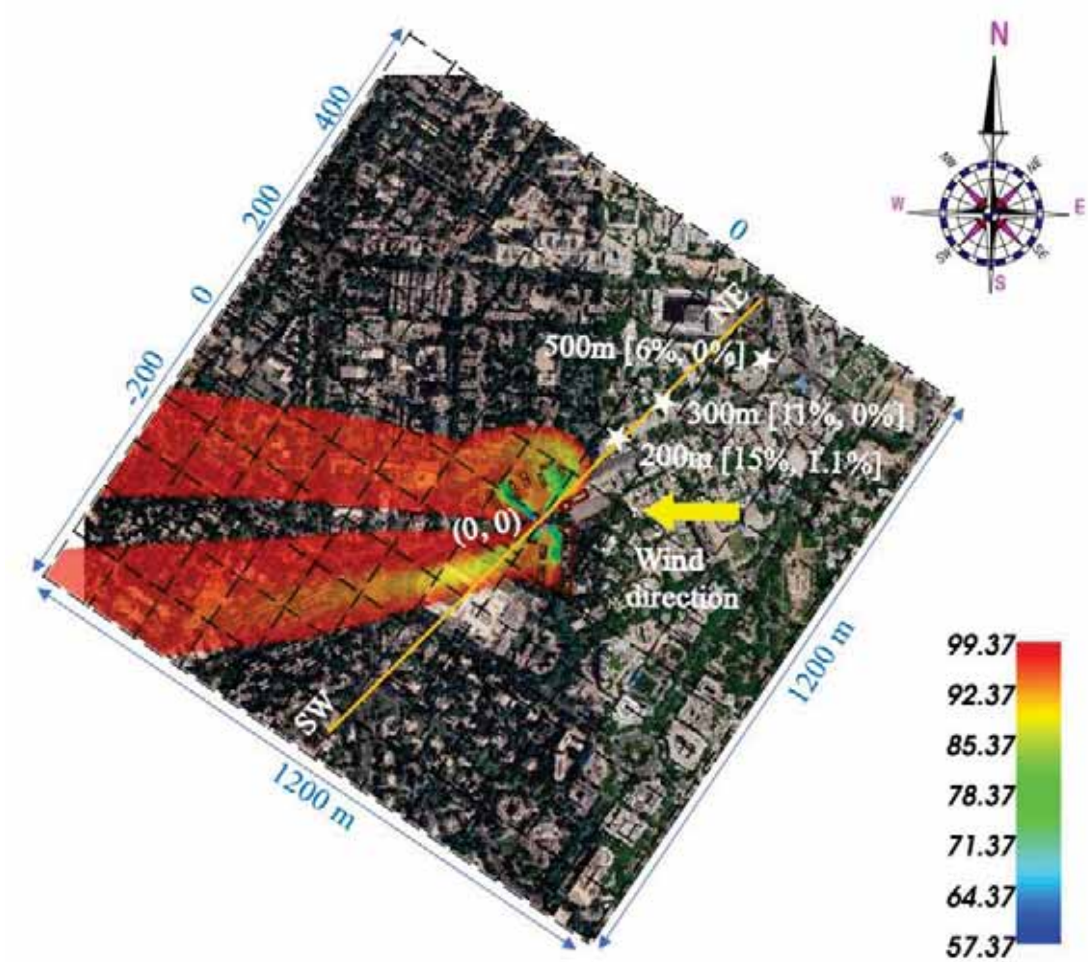

*Star-points indicate: Measurement distance from MSACS in shown direction along with [monitoring, modelling] values of % Air pollution reduction efficiency.

Figure 103. Filled contours of concentration profile (1200 m x 1200 m) dated 1st December 2022, Late night (Considered parameters are: wind speed = 2 m/s, wind direction = East, filtration efficiency = 42.1%, fan capacity = 739.73 m^3/s and CADR = 311.42 m^3/s).

A high wind speed of 2 m/s influenced all the jets into downwind direction as shown in *Star-points indicate: Measurement distance from MSACS in shown direction along with [monitoring, modelling] values of % Air pollution reduction efficiency.

Figure *103*. All the measurement points are observed to be lying in the shadow region of clean air zone. Thus, it is expected that no reduction efficiency would be obtained at these locations which stands true with the modelling values obtained. However, the monitoring values at these locations show some considerable cleaning. This might be because of presence of various sources in the actual scenario and possibly after some time due to the effect of wind dispersion, self-cleaning happened and thus considerable reduction efficiency values at distances of 200-300 m were obtained as shown.

9.3 Effect of low and high wind speed on the area of impact

To observe the effect of changing the wind speed from low to high, two cases from the above simulated cases were considered, Case 4 (section 9.2.4) having a low wind speed of 0.52 m/s and Case 6 (section 9.2.6) with a high wind speed of 1.64 m/s. Rest of the parameters for these cases such as filtration efficiency, fan capacity and CADR were almost the same. The figures below show the contours for both cases.

Figure 104. Contours for (a) Low wind speed (0.52 m/s)   (b) High wind speed (1.64 m/s).

From the Figure 104 shown above, one can clearly see that with low wind speed case, a higher spread of clean air was obtained, while with high wind speed, the area of cleaning i.e. effective reduction zone was much lesser. The crosswind jets covered a much larger distance with low wind speed. Whereas for high wind speed flow, it was observed that the crosswind jets, after covering a short distance in their respective direction, start bending along with the upcoming high-speed wind flow and then join with the downstream jet. Also, the downstream jet was observed to be going up to much more distance with the high-speed wind flow. Hence, it can be concluded that the system will give better cleaning performance in the winter period under the conditions of low wind speeds.

10 Pooling of Modelling Data and its Comparison with Pooled Monitoring Results (for Winter 2022-23)

To compare the modelling results with monitoring and to find the difference between values obtained from both, the pooling of the whole data was also carried out as shown in Table 33. For this analysis, the data from winter 2022-23 measurements was used. The data from both modelling and monitoring was segregated on the basis of various ranges of air pollution reduction efficiency. Total number of data points were extracted as per the respective distances of measurement locations. After this, the weighted average was calculated for different ranges of distances from MSACS. The standard deviation values were also calculated for the monitoring data obtained.

Table 33. Pooling of modelling data and its comparison with pooled monitoring results (for winter 2022-23)

Reduction Range	**Number of counts as per distance**					
		21-99	**100-199**	**200-399**	**400-599**	
<1					3	
1-10				9	16	
10-20			4	9		
20-30			1			
30-40		1				
40-50		3				
50-60						
60-70						
70-80						
80-90						
	Total N	**4**	**5**	**18**	**19**	**= 46**
Modelling	Average	41.93	18.94	9.06	5.89	
Monitoring	Average	29.52	11.77	12.68	12.68	
	Std. deviation	18.49	11.94	12.39	11.89	

From the above Table 33, the comparison of results showed that for distances up to 100 m, modelling and monitoring values show a slight deviation from each other. However, these small deviations are acceptable considering the source and terrain variations in the actual scenario as discussed previously. The analysis showed that for all the distances up to 600 m, the modelling values lie well within the standard deviation calculated with monitoring. It can clearly be seen from the Table 33 that the modelling data for various ranges of distances lies well within the range of monitoring values obtained, and thus it can be stated that our model is validating very well with monitoring measurements.

11 Summary and Conclusions

The overall summary of the Pilot study project at Connaught Place, and its findings and major conclusions based on the two years of operational experience, are as follows.

11.1 Initiation of the Project

Outdoor air cleaning as a feasible concept was proposed by the University of Minnesota around 2016 to offer a technological solution to combat urban air pollution in rapidly developing economies. The idea was to purify polluted air through a suitable technology and re-inject the clean air into the breathing zone of the general public. It was important to test this idea and its suitability to the Indian context, through experimentation in severely polluted regions such as Delhi. It is in this context that a conversation between IITB and University of Minnesota experts took place and the idea of a pilot study was mooted. The focus of the study was to install a medium-scale pump-filtration-based outdoor air cleaning device, study its performance and examine its range of impact in ambient regions under various environmental and operating conditions. Following the Honourable Supreme Court order to install two towers, one at Anand Vihar under CPCB funding and another at Connaught Place site under DPCC funding, the latter project at Connaught Place took shape through a tripartite MoU signed between DPCC, Tata-projects Limited (TPL) and IIT Bombay. With this MoU, signed on 7th August 2020, MSACS was installed and commissioned in September 2021 at Connaught Place. As per MoU, its performance evaluation was planned for the subsequent two-year period till August 2023. However actual performance evaluation was conducted only for the period September 2021 to February 2023 in view of the withdrawal of O&M maintenance support after February 2023. Large amount of experience was gained both during installation and performance evaluation in this world-pioneering study. In view of different topographical features the experience with the Connaught Place air cleaner complemented the air cleaner at

Anand Vihar. The details of the installation, challenges faced in rendering the satisfactory operation of the Connaught Place air cleaner, after its commissioning and the results obtained have been presented in this and previously submitted reports. The preceeding pages of this final report have specifically focused on the details of the performance evaluation and estimates of the region of impact of MSACS in mitigating air pollution in the ambient domain. In this concluding section, we summarise a collective view of this experience and the achievements made, in a concise manner.

11.2 Strategic Achievements

Given the importance of air cleaning technology in the Indian context, it is beneficial to take stock of the strategic gains made in this project. These are given below.

11.2.1 Successful Mission Mode Collaboration

The completion of the installation of the smog tower within the time frame of 10 months stipulated by the Honourable Supreme Court, was a major milestone achievement of the project**.** This was made possible by a synergistic collaboration between the various partners participating in the project. Tata Projects Limited, IIT Bombay and DPCC along with the foreign agency, Clean-Air Care Limited (CCL), a start-up company of the faculty of the University of Minnesota (UoM), collaborated with each other on a mission mode basis to meet this target. As the installation period coincided with the period of lockdown due to COVID-19, the various meetings, both among the Indian collaborators as well as meetings with faculty of UoM were all held online. The entire concept drawing of the structure and the NGFS (Novel Geometry Filtration System) filter arrangement shared by UoM in the course of online meetings were analysed, understood and converted to shovel-ready drawings within a month through concerted efforts of TPL and IITB collaborators. In spite of the severe constraint of COVID-19, the project partners led by TPL, constructed the structure, fabricated various components, imported the necessary filters from 3M company, made purchases of fans, and control systems along with other accessories and successfully installed the system within the stipulated deadline. At the same time, IITB collaborators acquired the monitoring instrumentation and worked on developing mathematical models and measurement methodologies, at considerable speed. This project stands out as a success story of a novel technological collaboration between governmental, academic and private organisations executed under extremely difficult circumstances to meet a commitment of National importance.

The successful execution of the Supreme Court Mandated Project in mission mode to meet the specified time frame through multi-institutional collaborations may be considered as the first achievement of the project.

11.2.2 Acquisition of know-how

Although Indian academia trained in aerosol science and engineering is familiar with the principles of air cleaning technologies from a theoretical standpoint and laboratory scale perspective, there was no prior experience in designing and installing an outdoor air cleaning system with a very large Clean Air Delivery Rate (CADR) of the order of 860 m^3/s. Considering the importance of developing technologies, among a mix of options, to mitigate air pollution in Indian urban settings, this project has gone a long way in internalising the know-how of building large-scale air cleaners, among the project partners. The development of high through put, low resistance filtration arrangement, choice of appropriate tower structure, understanding of the design of the system, acquisition of the right type of critical components, operational experience, development of mathematical software, evolving the designs of performance evaluation and execution methods, has provided a significant learning experience to the faculty of IITB and the engineers of TPL associated with the project.

An important outcome of this study is the building of human resource capital and technical capacity towards setting up of future air cleaner systems, if the need arises, suitable for different Indian urban ecosystems. Specific mention should be made of (i) expertise gained by Indian air pollution community through this project in the area of aerosol science and engineering for pollution control and (ii) the development of the CFD model to predict the impact of the air cleaner in the ambient domain, which is a new development in the Indian context for the air pollution applications. On the whole, the pilot study imparted a corpus of valuable knowledge to the Indian project teams for future articulations on the need for such systems in the country and concurrent technological developments to meet these needs.

The internalisation of the knowledge and practical experience by the project partners is another major achievement of this project in the crucial area of air pollution technology.

11.2.3 Capacity building for Self-Reliance

This project has leap-frogged several progressive steps towards achieving self-reliant capacity building to take up futuristic applications of customised air cleaner systems for different geographical regions of India. The capacity has been built at various levels namely, concept developments, design calculations, particle filtration engineering, computational and experimental experiences, shovel-ready design and installation. This is in accordance with the original vision of the project wherein it was perceived that the collaboration with UoM served the purpose of hand-holding to acquire in-house experience in the area of low resistance, high through-put filtration systems and the engineering aspects related to an efficient structure to house them. The experience serves the purpose of national self-reliance for working towards the setting up similar systems customised to suit specific challenges of spatial domain of impact, operational and establishment costs. Some areas where customised air cleaners might find future applications are: densely populated marketplaces, school and hospital premises, stadiums of national importance, residential campuses and possibly other strategically important locations. Customised air cleaner systems could also serve a crucial role in empowering the general public living in housing society communities to provide themselves with relatively cleaner air through the concept of 'willingness to pay' the cost of installation as well as operation.

Self-reliance towards the development of customised future air cleaners is the third significant achievement of this project.

11.3 Technical Achievements in the post-installation phase

11.3.1 Preparations of documents and SOPs

As soon as the MoU was signed, IITB prepared a technical document for TPL to provide a concept overview of air pollution issues and scientific basis of the proposed technology. Subsequently, several SOPs, protocols and methodological documents were prepared for the smooth execution of the operations and measurements during the project. This included documents on the measurements of flow rates, pressure drop, fan operation guidelines, experimental protocol, scoping document for modelling, filter replacement strategy and Time Between Replacements (TBR), start-up and stopping guidelines. Other related developments included instrument calibration procedures, establishments of methods for intrinsic and buffer zone efficiencies.

11.3.2 System evaluation and leak testing after commissioning

Troubleshooting, leak tests and rectification using the seek-seal method, strengthening of filter supports and arriving at solutions on the optimal fan speed to minimize dislodging of filters, arriving at operational limits, were some of the tasks undertaken by the study immediately post-commissioning. Some of these activities were also repeated after the dust-loaded filters were replaced with fresh filters, in the period 2022-2023.

a) Seek and seal method of leaks: During the initial evaluation phase, large number of leaks were detected. An elaborate survey with photography was undertaken to examine various joints in the structure and in the filter frames to detect potential leak paths. The rectification of the leaks was made by following seek and seal approach and protocols such as buffer zone and intrinsic efficiency measurement techniques were devised for assessing the effectiveness of sealing the leaks. Introduction of the concept of buffer zone efficiency was particularly useful for estimating the fractional leak rates thereby providing a quantitative measure of the effectiveness of the seek and seal approach. While the original designers had only envisaged intrinsic filtration efficacy as measure of system performance, the leaks through the gaps in the structure components or between the gaps in the 4800 filters do actually reduce the overall efficiency of the clean air in the corridor region between the filter and fan assemblies. The measurement of efficiency in this region directly gave indications of the presence of leaks and this information was utilised to assess the adequacy of sealing. Typically, while the intrinsic efficiencies attained more than 90%, the maximum buffer zone efficiencies up to 75-80% have been realised. When the fresh filters are loaded, both intrinsic and buffer zone efficiencies show decrease initially and then increase to optimum levels and these are as per the well-known behaviour of charged fibrous filters.

b) Dislodging of the filters: Initial testing of the system was started at 50% capacity. Before increasing the operation at higher fan capacity, the corrective measures such as frame strengthening was done to avoid dislodging of filters from the frames. This was done based on the dislodging experience gained by operating the tower at 100% capacity at Anand Vihar site.

11.3.3 Filter loading and Pressure drop

The criteria for replacing the filters specified by Clean Air Care Limited are based on the maximum pressure drop developed across filters due to accrual of dust load during the MSACS operations. It was recommended that the filter replacement activity should be initiated when the pressure drop exceeds 1.1 in-H_2O across the filter system which as per the original estimate, corresponds to a limit of 200 g/m^2 for pre-filter and 80 g/m^2 on fine filter. These limits were arrived at from limited laboratory studies of low levels of dust loading on the filters and it was recognised to be of tentative nature. It was expected to be strengthened by the experience gained from operating the MSACS. The large body of pressure drop data reported herein from the actual operating experience of the MSACS during this pilot study is a valuable tool at arriving at the limits to be set for replacing the filters. A summary plot of the pressure drop vs dust load data showed a maximum pressure drop (Figure 51) of 0.65 in-H_2O for a dust loading about 200 g/m^2 on coarse filter (12.5 g/m^2 on the fine filter, Figure 52) corresponding to a mean flow rate of ~ 500 m^3/s. Linear extrapolation to the original design flow rate of 1000 m^3/s yields a pressure drop of 1.3 in-H_2O, which is rather close to the actual measured pressure drop of 1.4 in-H_2O at flow rate of 1005 m^3/s. In view of this, the original design estimate of 1.1 in-H_2O at 1000 m^3/s stands reasonably validated within uncertainties of measurements. Hence considering the huge difference in the environmental conditions and the laboratory conditions, the present field data may be considered nearly consistent with the original estimates. Mainly, the present data constitutes a real field validation of the long-term behaviour of the filters deployed in the MSACS. For practical purposes, one may retain the pressure drop of about 1.1 in-H_2O across Pre-filters + Fine filter bank as a guiding index for initiating filter replacement.

11.3.4 Flow rates and fan capacities

The stated maximum operating capacity of the system at the highest frequency of 50 Hz corresponds to the delivery of designed air flow rate of 1000 m^3/s. The flow rates are expected to decrease proportionally at the lower operational capacities. Several measurements of flow rates at 50%, 75% and 100% operational capacity have been made and the measured flow rates (Table 10) are in conformity with predicted ratings within 5-10% difference. If there is a need to operate the system even if the pollution levels are within the regulatory limits, then it is advisable to operate it at lower fan capacities in order to conserve power and unwanted loading of the system, as well as to safeguard the potential dislodging of the filters. Also, as an operational philosophy, the system should not be turned on abruptly at high capacities but is required to be gradually raised in discrete steps from lower capacities to higher capacities.

11.3.5 Intrinsic efficiency measurement for performance assessment of filters

It is a common practice in air cleaners to specify the efficiency of the filter element by spreading a piece of it in a test facility and make measurement of filtration efficiency at specified pressure drops, flow rates and temperature using standard protocol. Since CADR estimate depends on the efficiency of the filter installed in the facility, it was felt necessary to measure the intrinsic filter efficiency directly from the installed filters by in-situ measurements under specified fan capacity. Periodic data were collected on in-situ measurements conducted using specially made iso-kinetic sampling arrangements, and particles were counted using DustTrak PM monitor. Large data was collected on the size-wise efficiency, its variation with dust loading characteristics and its dependency on fan capacity and environmental conditions. The patterns of dependencies observed, such as the initial fall in efficiency with dust loading, followed by an increase upto ~ 90% were consistent with the information supplied by the Clean-Air Care Limited. The satisfactory intrinsic efficiency data thus obtained, clearly demonstrated that the MSACS filters were performing as per the design expectations.

11.4 The impact of MSACS in the ambient domain

The idea of installing an outdoor air cleaner system was conceived for the purpose of providing a technological option to combat urban air pollution by creating a clean air zone of reasonable extent that would benefit the general public. While its implementation in public domain depends upon various socio-economic and local considerations, the most crucial aspect would be its performance in the ambient domain evaluated using scientific principles. Thus, the key aspect of this pilot study is the assessment of impact of the air cleaner system towards mitigating PM pollution levels in the ambient domain. To achieve this assessment, extensive experimental study designs were instituted to measure the extent of reduction in the pollution levels at various distances from the Air cleaner system, considering its dependence on the operating parameters of the MSACS, ambient pollution load, meteorological and environmental parameters prevailing at the time of the measurements. As is written out in details in the various sections in this report, this was a Herculean task, conducted meticulously by the project team using various study designs, measurement protocols, precision equipment in conjunction with mathematical models and statistical methods. The study conducted in the past two years after installation have yielded a vast amount of data and insights on these variables. These are presented in the report in considerable detail. Here salient results are highlighted.

11.4.1 OFF/ON sequence methodology for assessment of impact

A major challenge in assessing whether the operation of the facility has brought about reduction of pollution at certain location or not, is to overcome the difficulties of statistical fluctuations in pollutant concentrations due to fugitive sources coupled with the variations in the meteorology. To minimise the influence of these fluctuations, a series of measurements were made by keeping MSACS OFF for a certain period of time followed by measurements when the tower is switched ON. These OFF/ON sequences of measurements have largely yielded reliable estimates of performance.

Hundreds of measurements were made over the past 2 years to arrive at a reliable estimate of the impact of MSACS. These included measurements (i) downstream, upstream and transverse directions with respect to wind directions, (ii) round the year, especially during severely polluted days in winter, (iii) different times of the day, (iv) under varying wind speed conditions, (v) for different operating capacity of the tower, (vi) at different locations and distances using OFF/ON method. The obtained concentration data were analysed for location-specific cleaning efficiency by averaging over several types of estimates and statistical methods. Over all, about 426 measured estimates of cleaning efficiency covering all situations were made. The detailed analysis of the dependency of these data on the above mentioned parameters has been presented in the preceeding pages of the report.

11.4.2 Measures of Performance

In order to appreciate the complex nature of the task of providing summary measures of performance culled from the large amount of measured data, it is necessary to go back and look at the principle of how the air cleaner is expected to clean the ambient domain. The principle of this device is that the polluted air sucked from a height of 24 meters at the tower mouth, is forced through the filter assembly by 40 fans and the clean air is delivered at ground level up to a height of 5 meters into the ambient domain at velocities of about 2.5 metres per second. The released clean air jet travels significant distances depending on the normal wind speed and direction and then gradually loses its clean air quality by mixing with the polluted ambient air. In this process, it creates a "clean air zone" in the ambient domain there by averting a certain quantum of $PM_{2.5}$ exposures to populations present in that domain. As the number of people exposed increases approximately as square of the distance from the tower, a reach of clean air at farther distances even at a smaller level of air cleaning efficiency of say, 1-5% would potentially avert significant "population-exposures". This may be considered as a beneficial impact of the MSACS. Along with this, associated metrics namely "Effective Reduction Zone" (ERZ), and the "Averted Population Exposures" due to the operation of the air cleaner system would also be useful in assessing the impact, especially during the period of severe pollution episodes.

A back of the envelope calculation of the maximum possible ERZ may be made as follows. We note that the MSACS is designed to deliver 75 million cubic meters of clean air per day which is equivalent to 50% cleaning an area of about 1 km^2 in a day or equivalently a radius of impact of about 600 meters, assuming a still atmosphere and a mixing height of 75 meters and an aerosol residence time of 1 day. This is similar to the situation that exists in Delhi during severely polluted winter seasons. This however is only an idealised upper bound estimate and the real range will be lower due to wind flows, building obstructions and the presence of turbulence in the atmospheric flows.

11.4.3 Qualitative highlights of performance

Summer vs Winter: As noted in section 7.4, upto a distance of about 200 m, performance data available for both the seasons indicate similar air cleaning efficiencies. From intuitive reasoning one can argue that due to higher wind speed and greater turbulence, the performance is expected to be lower in summer and rainy seasons especially at far off locations. In fact large number of available data have convincingly shown significant air cleaning efficiency at distances upto 500 meters in winter season. In this season, the PM concentrations were in excess of 250 $\mu g/m^3$, and the observed PM reductions at 500 meter distance were about 13%. Numerical modelling results also indicate that the cleaning efficiencies are higher for low wind speeds as is the case in winter and are lower at higher wind speeds which is often the case in summer. In summer and rainy seasons, the PM concentrations are generally lower and hence there is no need to operate the MSACS. Besides, due to operational reasons, it is not advisable to operate the system during rain. The present data conclusively establishes that the air cleaner system performs well in the winter season, which is also desirable since it coincides with severe pollution period. In summer and rainy seasons the pollution levels are low, and it is not required to operate the air cleaner.

11.4.4 The range of impact

We now come to the most important question on the range of impact of the air cleaner. As mentioned, the large body of the data presented in the report provides information on the range of clean air ejected from the tower under various conditions. To provide an overall index of the range of performance, we average over the entire set of data (Section 7), regardless of directionality, wind speed, season etc., keeping only the distance of the measured location from the tower as the independent variable. This metric offers a robust measure of a representative average or "overall air cleaning efficiency" of the tower as a function of distance. To strengthen statistics, all the physically valid data points (351 points for $PM_{2.5}$ and 344 points for PM_{10}) have been distributed in five distance categories. The bars around each data point indicate the standard errors in the measured efficiencies. Figure 105 below shows the summary of the averaged air cleaning efficiencies for PM_{10} plotted as a function of distance from the MSACS. The figure shows that the 'Overall air cleaning efficiency' decreases as one moves away from the MSACS, which is consistent with our understanding of degradation of the clean air jet released into polluted air. The decrease is rapid initially but slows down at distances beyond 150 meters. In fact, the overall efficiencies are around 16% both at 300 m and 500 m distances thereby indicating a tendency of the clean air jet to persist at longer distances. Very similar spatial decay behaviour is seen for the overall air cleaning efficiency for $PM_{2.5}$ as well, as shown in Figure 106. The average values are only indicative numbers with significant standard errors around them and hence specific meanings cannot be attached to the small differences in the efficiencies in $PM_{2.5}$ and PM_{10}. It is however, remarkable that both the cases show almost identical patterns of behaviour, namely, slow decay at large distances. It may not be out of place to note that the slow decay behaviour is in accordance with the classical jet propagation theory which indicates rapid initial degradation followed by near saturation phenomena of fluid entrainment due to momentum flux conservation.

It is a mathematical fact that slow variations with distance are generally indicative of power-law behaviour. Accordingly, we perform non-linear regression fits to the experimentally obtained 'overall efficiency' data, to reciprocal power functions of the type, $\eta = \frac{1}{(a+bx)^c}$. The fitted parameters for both PM_{10} and $PM_{2.5}$ are given in the Figure 105 and Figure 106 along with the best fit plots. The obtained R^2 values namely, 0.97, 0.96 in the two cases, are quite close to unity and hence the fits may be deemed excellent within the range of the distances examined. However, one should be careful in extending the predictive power of the fits to large distances. The prevalence of unpredictable fluctuation due to fugitive pollution sources, meteorological parameters and building obstructions render the predictive power of the fits unreliable beyond about 500 m. Hence we limit the applicability of the fits to distances within 500 m. Within this distance, one may conclude that an improvement of ambient air quality to the extent of 50%-16% has been found during the operation of the air cleaner. In other words, it may be safely ascertained based on an analysis of large body of data, that the installed outdoor air cleaner system at Connaught Place has made a definite impact over significant distances in the ambient domain around it. This is a major take away from this pilot study.

It may be pointed out here, that the trends and results obtained for Anand Vihar MSACS show very similar performance. This fact confirms the intrinsic capability of the air cleaner system in delivering clean air in the ambient domain.

PM$_{10}$ All pooled results, (344)

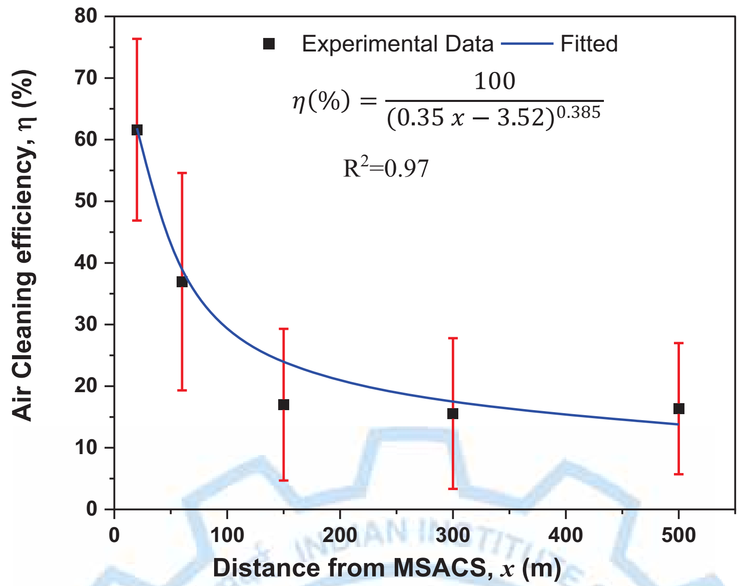

Figure 105. Variation of the average air cleaning efficiency with distance of the monitoring site from MSACS for PM_{10}.

PM$_{2.5}$ All pooled results, (351)

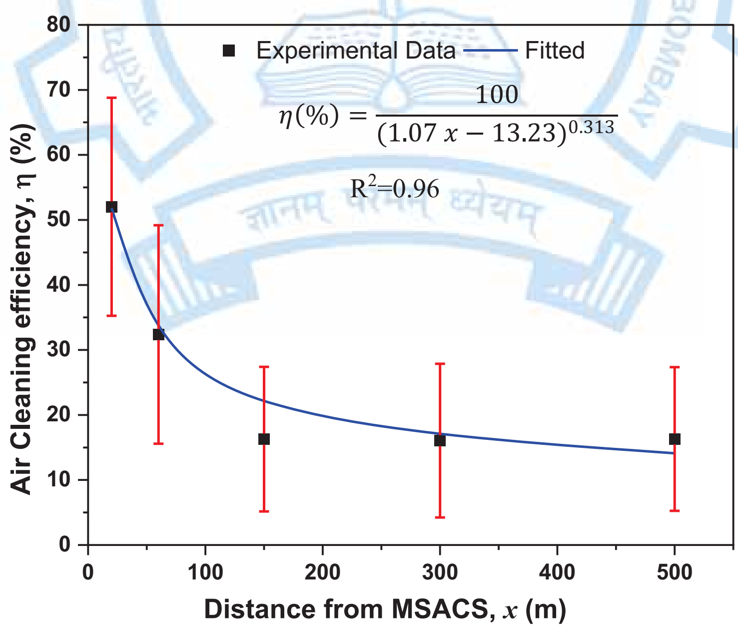

Figure 106. Variation of the average air cleaning efficiency with distance of the monitoring site from MSACS for $PM_{2.5}$.

"Effective Reduction Zone (ERZ)" estimate

An estimate of the ERZ may be carried out by using the nonlinear regression models, which are found to follow the data very closely. We present the results only for PM_{10}; those for $PM_{2.5}$ are very close to these. From the weighted area integration of the nonlinear fits for the observed range of 500 m, it is found that the effective reduction zone (ERZ) is $0.78\ km^2$ having an area weighted average of air cleaning efficiency of 18% for PM_{10}. General public present within this ERZ is expected to be benefitted by the deployed air cleaner as follows. The population within the range of 500 meters ($ERZ = 0.78\ km^2$) will be breathing on the average 18% purer air as compared to the air they would have breathed in the absence of the air cleaner.

Assuming a population density of about $25{,}000\ persons/km^2$ for Delhi in the Connaught Place area, we may say that on an average a population of about 0.78x25,000=19,500 persons will be benefitted by about 18% reduction of PM levels by the operation of the tower. This is a statistically averaged number: those who live closer to the MSACS will experience higher clean air benefits and those living farther will experience less. Although the benefit is lower at larger distances, it must be borne in mind that the number of persons increases quadratically with distance and hence large population will experience benefit at larger distances albeit at lower levels. For example, during severe pollution episodes with PM_{10} levels exceeding $350\ \mu g/m^3$, this will amount to an averted population exposure of $\sim 10^6\ person.\mu g/m^3$ considering 500 m as the range of impact. This is a significant averted exposure benefitting general public due to the clean air delivered by MSACS. In other words, we can say that the air cleaner impacts the general public as a whole by averting significant collective PM exposure to the population.

To sum up, the data obtained from this comprehensive pilot study programme has clearly shown that the installed air cleaner system at Connaught Place has reduced the ambient PM pollution levels to a significant extent in its vicinity upto an average range of impact of about 500 meters. The effective (weighted average) air cleaning efficiency within this region is about 18%. This is the most important knowledge that has emerged from this pilot study. It provides a crucial input for performing detailed studies on cost-benefit analysis in the future, considering the levels of air pollution, the population density vis-à-vis the cost of installation and operation of the tower. These studies have to be carefully conducted with considerable thought and detail, and are outside the scope of this project. For the present, the pilot study has successfully achieved its objective of (i) installing an outdoor air cleaner system at Connaught Place, (ii) conducting a comprehensive scientific study to assess its impact and (iii) arriving at a conclusive estimate of the range of impact of the air cleaner in the ambient domain from the extensive data obtained from measurements combined with mathematical modelling approaches.

12 Recommendations

Based on the results of the pilot study the following recommendations may be made for future purposes.

1. **Use in Winter, not in Summer**: It was inferred from the large data obtained from the pilot study that the outdoor air cleaner system installed at Connaught Place in Delhi possesses a range of impact of about 500 meters having an area weighted air cleaning efficiency of 18%. It performs best specifically in the winter season. This is mainly because of low wind speed and turbulent conditions during which the clean air jet travels to large distances. Since winter is a season when severe pollution episodes occur (~ 350 $\mu g/m^3$ for PM_{10}) in Delhi and elsewhere the air cleaner system is indeed useful in providing relief within its zone of influence in these places. In contrast the pollution levels are generally low in summer and rainy seasons (less than the regulatory limits) and hence there is no need for operating the MSACS in these seasons. This would also reduce the cost of operation of the MSACS, and help reduce the unnecessary loading of the filters. Hence, it is recommended to limit the use of air cleaner essentially to the *'winter season'* to combat severe air pollution episodes and conserve resources.

2. **Deploy as Zonal units, not city scale**: It may be emphasized that the present pilot study investigated a technological feasibility of establishing clean air zones within a certain range in locations of high population density for combating severe urban air pollution. These zones of high impact refer to places where large number of people are likely to benefit from the deployed air cleaner: Transport hubs, Urban residential clusters, market places, school & hospital complexes, play grounds & parks etc. The outdoor air cleaners may be deployed in specific contexts on a case by case basis. However they

should not be replicated in large numbers for the purpose of cleaning large regions of cities as it will not only be inefficient but also may not be cost-effective.

3. **Optimise with respect to Energy-Cost-Performance Efficiency**: The MSACS installed in Delhi is based on UoM design acquired on payment through their Start-up company, Clean air care LLC (CCL). It is not necessarily the most optimised model for the Indian urban scenario. It was taken up as a pilot study essentially to investigate the feasibility of large-scale filtration for achieving large clean air delivery rates and estimate the range of impact in the ambient domain. There exists considerable scope for improvement of this device in future designs in terms of making such systems *energy-cost-performance* efficient. As the feasibility of air cleaning effectiveness of this device stands demonstrated in this pilot study, it is recommended that attention be paid towards reengineering the system to make it more efficient. The cost benefit analysis should also be carried out by considering the installation cost and the cost of operation and maintenance vis-à-vis the overall benefit gained including population health because of technologically averted exposures. The overall optimisation may also take into consideration the concept of *'willingness to pay'* by communities by setting up air ceaner systems in their residential areas to enjoy clean air benefits.

4. **Indigenize filters and filter frames**: The pilot study demonstrated the importance of making the filtration system more robust and cost effective. The experience of MSACS operation at Anand Vihar alerted us about the possibility of filter dislodging at Connaught Place also. Based on this experience, caution was exercised in the Connaught Place MSACS operation to ensure minimal dislodging events. However, on the whole, dislodging is a real possibility at 100% operation as the filters get loaded

with the currently used 3M filters leading to large leaks. Also, the cost of import of the filters added significantly to the operational cost of the facility. Hence the development of indigenous filters and more robust filter frames will go a long way in reducing the operational cost and improving performance. It is thus recommended to initiate the process of '*development of robust filter'* frames using locally available filters.

5. **Reduce Size, Scale and Footprint**: The use of 40 fans of 25 HP each for driving the air in the system through a large array of the filters housed in a civil structure is the main factor responsible for the space requirement and the cost of the installation. The fans were designed to operate at 1000 m^3/s. However, it may not be always necessary to deploy such a high through put system. Depending upon the context in which air cleaner has to be deployed one may reconsider the design with smaller number of fans, lower height of the tower and smaller foot print. This will help in the reduction of installation cost and the operational cost by a factor of more than two and greatly render the system suitable for cities where availability and cost of the land is a critical factor in governing considerations for the deployment. Hence it is recommended to customise the '*more compact designs'* of the air cleaner systems.

6. **Hybridise:** There are several principles for air cleaning, apart from filtration. In order to lower the substantial cost of replacement of filters, the system could be reengineered by judiciously integrating '*filterless air purging technologies'* to reduce the load on fine filters. Filterless technologies could incorporate ionisation and electrostatic precipitation principles or a combination of both. It is recommended that research should be directed towards the realisation of these ideas.

7. **MSACS as national facility:** The system installed at Connaught Place is second of its kind (after MSCAS at Anand Vihar) downdraft type outdoor air cleaning facility in the world. It is a unique national achievement in the complex area of large-scale clean air delivery technology. Studies conducted so far have been essentially limited for its performance evaluation and proof-of-concept in a real-scale ambient domain. In the future, it motivates avenues for improvements and development of new devices by academia and industrial partners. In this context, this facility would be extremely useful for conducting specific experiments as well as testing future control technologies. Specific examples are: Testing of hybridization concepts, new filter development, modified geometries for enhancing clean air jet propagation and several other possibilities. In view of all this, the MSACS facility at Connaught Place should be maintained as a National facility. This will go a long way in achieving self-reliant technological solutions to the urban air pollution problems.

References

Baron, P. A., & Bennett, J. S. (2002). Calculation of leakage and particle loss in filter cassettes. *Aerosol Science & Technology*, *36*(5), 632-641.

Baron, P. A., Khanina, A., Martinez, A. B., & Grinshpun, S. A. (2002). Investigation of filter bypass leakage and a test for aerosol sampling cassettes. *Aerosol Science & Technology*, *36*(8), 857-865.

Bächler, P., Müller, T. K., Warth, T., Yildiz, T., & Dittler, A. (2021). Impact of ambient air filters on PM concentration levels at an urban traffic hotspot (Stuttgart, Am Neckartor). Atmospheric Pollution Research, 12(6), 101059.

Tang, M., Chen, S. C., Chang, D. Q., Xie, X., Sun, J., & Pui, D. Y. (2018). Filtration efficiency and loading characteristics of PM2. 5 through composite filter media consisting of commercial HVAC electret media and nanofiber layer. Separation and Purification Technology, 198, 137-145.

Davenport, A. G., Grimmond, C. S. B., Oke, T. R., & Wieringa, J. (2000, May). Estimating the roughness of cities and sheltered country. In *Preprints, 12th Conf. on Applied Climatology, Asheville, NC, Amer. Meteor. Soc* (Vol. 96, p. 99).

Masters, G. M. & Ela, W. P., (2008). *Introduction to Environmental Engineering and Science: Pearson New International Edition*. Pearson Education, Incorporated.

Shi, B., Ekberg, L. E., & Langer, S. (2013). Intermediate air filters for general ventilation applications: An experimental evaluation of various filtration efficiency expressions. *Aerosol science and Technology*, *47*(5), 488-498.

Tien, C. Y., Chen, J. P., Li, S., Li, Z., Zheng, Y. M., Peng, A. S., ... & Chen, S. C. (2020). Experimental and theoretical analysis of loading characteristics of different electret media with various properties toward the design of ideal depth filtration for nanoparticles and fine particles. *Separation and Purification Technology*, 233, 116002.

Acknowledgements

Funding support provided by Delhi Pollution Control Committee (DPCC) is gratefully acknowledged. The authors are thankful to the (i) UoM experts for providing the technical advice from time to time (ii) Support provided by O&M team of Tata Projects Ltd, (iii) IIT Delhi team for their help in field sampling. The authors acknowledge the encouragement and support provided by Director IIT Bombay and other senior functionaries.

APPENDIX-I

Leaks in the MSACS: Action items to be attended by DPCC & TPL

Observations from Field visit: Medium Scale Air Cleaning System (MSACS) at Connaught Place, Dt. 14/12/2021 – 16/12/2021

In this note, the following aspects to which attention is required to be given by DPCC are described. The salient action items are:

(1) The possibility of filter dislodging during full operation exists. DPCC may Initiate with TPL-AMC, the filter frame reinforcement strategy as is being done for Anand Vihar,

(2) All Leak paths of polluted air bypassing the filter have to be identified and sealed.

The details are mentioned below.

During the site visit of PI, IITB, it was observed that there were some signs of filter dislodging at a couple of places however the dislodging may happen while running the system at 100% fan capacity. Dislodging of filters from the filter frame has happened at the CPCB sites at 100% capacity when the system was running for a long duration. These issues of possibility of dislodging, TPL O&M team may discuss with UoM experts.

In the meantime, the visit of PI also brought forth some other shortcomings which also need to be rectified. These pertain to leaks of unfiltered air from various openings into the buffer zone, bypassing the filter assembly, resulting in the degradation of the quality of the clean air ejected into the atmosphere. Plugging these leaks is as important as the reinforcement of filters against dislodging to ensure that the buffer zone air consists of only the filtered air ($PM_{2.5}$ removal efficiency >80%) and is not sullied by external polluted air. To help the TPL/O&M team to plug these gaps, the observations made during the site visit were discussed with the O&M team during the visit and are presented below. The TPL O&M team is also requested to look for other leak paths, if any, and plug them as well.

Identified Leak Path in the System by Systematic Survey within the facility

Several leaks have been identified in the system (Figure 107 to Figure 113). The major leaks in the system are highlighted using a red arrow on the images below. The flow through the leaks is different based on the size of the openings. Some of the major leaks are through

(a) Between filters due to distorted edges,

(b) Leak through cut-outs in the roof of the tower

(c) Leak through the main door of the tower,

(c) Leak through the opening in the door inside the tower & door remain open many times during fan on condition,

(e) Leak through cut-outs in the pillar,

(f) Leak through the openings at the corners inside the tower & openings in the pillars inside the tower,

(g) Leak through cut-outs in the walls inside the tower,

Velocity measurements of the air coming through these leaks were taken using research-grade instrument. The flow through the leaks are different based on the size of the openings and flow through that regions.

Figure 107. Leak between filters due to the distorted edge.

Figure 108. Leak through the cut-outs in the roof and pillar.

Figure 109. Leak through the main door of the tower.

Figure 110. Leak through the opening in the door inside the tower and sometimes when the door remains open.

Figure 111. Leak through cut-outs in the pillar.

Figure 112. Leak through openings in the pillars inside the tower.

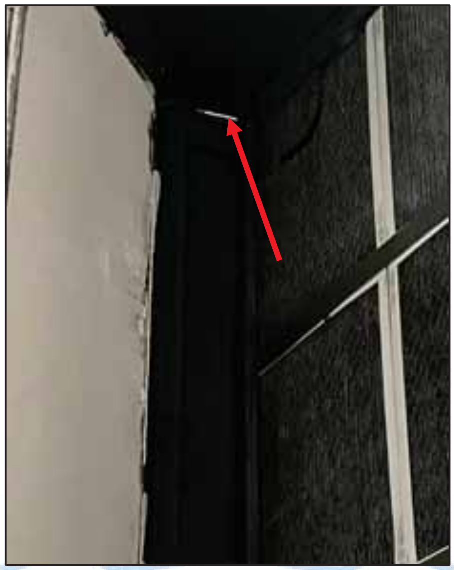

Figure 113. Leak through cut-outs near the walls inside the tower.

By working backwards from the observed $PM_{2.5}$ concentrations in the buffer we may estimate that the possible bypass in airflow due to the leak of polluted air from gaps could be as high as 20-25%. It is expected that these leaks will increase as the pressure drop builds up across filters with time due to dust loading and/or at higher operating fan capacity. It is a clear indication that plugging the leaks inside the tower will help increase the system's efficiency and deliver a higher clean air flow rate to the atmosphere.

Figure 114. IIT Bombay team site visit.

Measurements & Observations

1. Checking the Filter replacements & associated components

Observation: The filter replacement might be done as there is no dislodged filter present in the filter frame. It is difficult to see the replaced filters as dust collection is initiated on new filters and visualization is not possible to identify replaced filters. There is no issue associated with the replacement of the filter.

Figure 115. Filter replacements & available strips in the filter frame.

2. Route cause analysis (RCA) of dislodging filters

Observation: Filter dislodging might be because only one vertical strip is present in the filter frame. This may be because of the unfollowed UoM drawing which was received along with the technical dossier document.

Figure 116. Bending of the fine filter inside the MSACS.

3. Root Cause Analysis Leaks in the System

Several leaks have been identified in the system. The major leaks in the system are highlighted using a red arrow in the images below. The flow through the leaks is different based on the size of the openings. Some of the major leaks are through (a) Between filters due to the distorted edge, (b) Leak through cut-outs in the roof of the MSACS (c) Leak through the opening in the door inside the MSACS & door remains open many times as fan started, (d) Leak through the main door of the MSACS, (e). Leak through cut-outs in the pillar, (f). Leak through the openings at the corners inside the MSACS, (g). Leak through openings in the pillars inside the MSACS, (h). Leak through cut-outs in the walls inside the MSACS, (i). Leak due to the missing bolts of the fans inside the MSACS.

Figure 117. Leak between filters due to distorted edge.

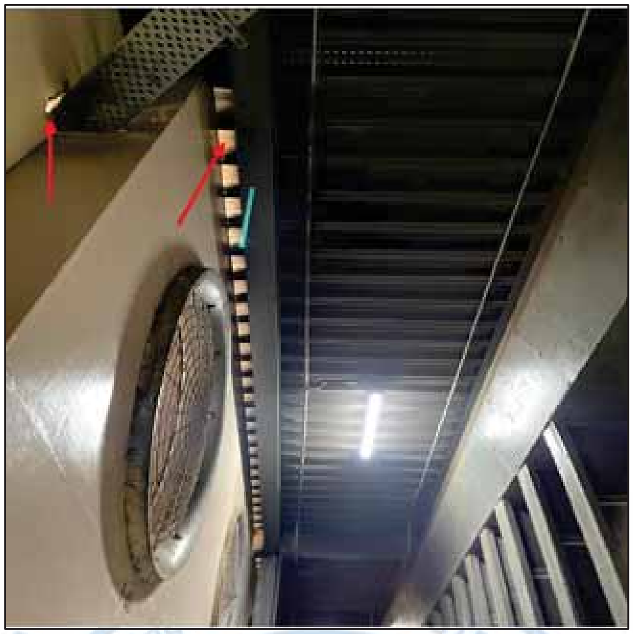

Figure 118. Leak through the cut-outs in the roof and pillar.

Figure 119. Leak through the main door of the MSACS.

Figure 120. Leak through the opening in the door inside the MSACS.

Figure 121. Leak through cut-outs in the pillar.

Figure 122. Leak through the openings at the corners inside the MSACS.

Figure 123. Leak through openings in the pillars inside the MSACS.

Figure 124. Leak through cut-outs in the walls inside the MSACS.

Figure 125. Leak due to the missing bolts of the fans inside the MSACS.

Observations from Field visit: Medium Scale Air Cleaning System, Delhi at Connaught Place, Dt. 27/05/2022 – 31/05/2022

In this note, the following aspects to which attention is required to be given by NBCC/DPCC are described. The salient action items are:

(1) All Leak paths of polluted air bypassing the filter have to be identified and sealed.

The details are mentioned below.

During the site visit, it was observed that epoxy flooring is done to avoid air bypass through the gap on the floor and filter frame. The majority of the leaks identified and reported in the previous site visit has been addressed except for few small leakages. It is to be noted that after addressing all these leaks, the buffer zone efficiency has improved for both $PM_{2.5}$ and PM_{10} as reported in Monthly report. However, the measurements indicate that there are still leaks and/or maybe new leaks are in the system. Due to leaks, unfiltered air from various openings enter into the buffer zone, bypassing the filter assembly, resulting in the degradation of the quality of the clean air ejected into the atmosphere. Plugging these leaks is important to ensure that the buffer zone air consists of only the filtered air and is not sullied by external polluted air. It is also requested to NBCC as the co-ordinating and project management agency to coordinate with the concerned stakeholders to address these issues on an urgent basis. Additionally, it is observed that supporting strips currently installed are slightly off placed to the filter array in many places and may not be able to provide adequate support to the filter frame to avoid filter dislodging in all conditions. The observations made during the site visit and the details about various leaks found are discussed below.

Root Cause Analysis of Leaks in the system

Several leaks have been identified in the system shown in the following Figure 126 to Figure 131. The major leaks in the system are highlighted using a red arrow on the images below. The flow through the leaks is different based on the size of the openings. Some of the major leaks are as follows:

(a) Leak through the bottom edge of the filter frame
(b) Leak through the main door of the tower,
(c) Leak through the opening in the door inside the tower. (Upstream opening to internal door is requested),
(d) Leak between filters due to edge gaps and gap at end plate,
(e) Leak through endplate,
(f) Leak through the openings at the distorted endplate,
(g) Leak through the top edge of filter frame,
(h) Leak through the top corner of the walls and plywood inside the tower.

The filter frame is mounted between the floor and the shroud of the system. At both these edges, the air is passing without passing through the filter media. There is the total of 160 filter frames (40 filter frames per side) are available in the system, hence at the 320 edges due to the filter array of the filter frame need to be sealed to avoid air bypassing. It is clearly shown in Figure 126 and Figure 131 that the top and bottom edges of the filter frame are not sealed properly. It should be sealed on a priority basis. The other leaks identified are shown below in pictures.

Figure 126. Leak through the bottom edge of the filter frame.

Figure 127. Leak between filters due to edge gaps and gap at end plate.

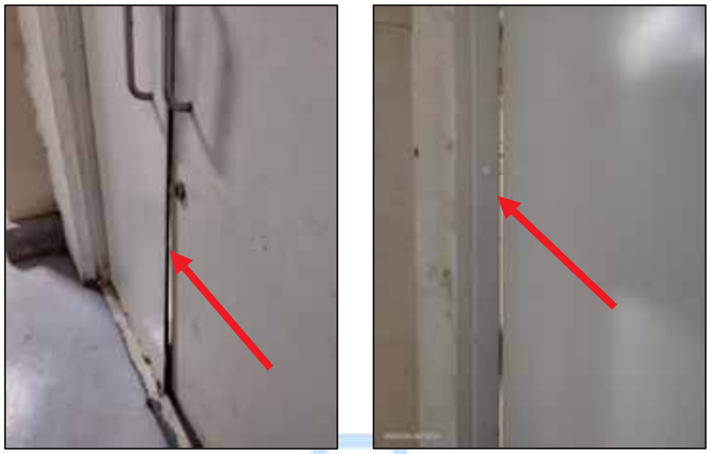

Figure 128. Leak through the main door of the tower.

Figure 129. Leak through the opening in the door inside the tower. *(Upstream opening to internal door is requested)*

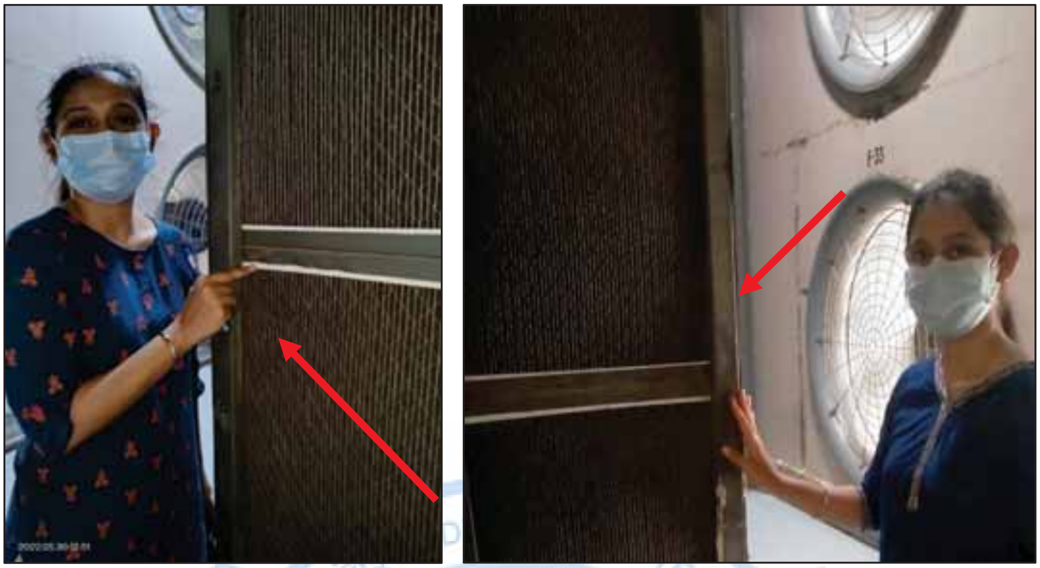

Figure 130. Leak through the openings at the distorted endplate.

Figure 131. Leak through the top edge of the filter frame.

Figure 132. Actual air coming through filter ~ 0.27 m/s.

Figure 133. Air coming through gap between filter and filter frame ~ 7.53 m/s.

Figure 134. Leak through the openings at the distorted endplate ~ 10.87 m/s.

It is expected that the backflow air bypass rate inside the system will increase significantly when the system will be operated at a higher fan capacity. Plugging of previously identified leaks has improved the buffer zone efficiency results which is an indicator to identify leaks. It is a clear indication that plugging the leaks and openings inside the tower will help increase the system's efficiency and deliver a higher flow rate of cleaner air to the atmosphere. It is requested to address all the leaks and any other additional leaks in the system on a priority basis.

Site visit by UoM

Figure 135. Site visit by University of Minnesota (UoM) and IIT B experts.

APPENDIX-II

Flow Rate Measurement Protocol

The step by step procedure for measuring flow rate using VelociCalc-9565-P-NB (Make: TSI) Instrument is given below:

1. Before measurements: Check the frequency of the Axial fans from the SCADA system. Ensure that all fans are operating at the same capacity. In case of maintenance of fan has to be noted in datasheet.
2. Make sure that an AA battery is available in the instrument and start the VelociCalc-9565-P-NB instrument.
3. Ensure required parameters are selected in the instrument for measurement.
    a. Flow measurement: Velocity, Flow Rate, and Temperature
4. Ensure that area of the fan outlet 1.3725 m^2 is entered as duct outlet area to calculate flow rate internally by measuring velocity using different probes.
5. To measure velocity it has two probes available as follows:
    a. Hotwire probe, model: 964 (Shown in Figure 136)
        - This probe has a sensor for measuring velocity, temperature and relative humidity.

    b. Rotating vane probe, model: 495 (Shown in Figure 136)
        - This probe gives flow rate and velocity.

Note: Rotating vane probe to be used at the outlet of the axial fan. Other location in the ACS one has to use hotwire probe. (Vane probe is not possible to measure velocity at below the doors or between the filters) Decision to be taken based on the location of the measurements and feasibility of the area available for measurements.

6. Check the units of measurements such as velocity (m/s), flow rate (m^3/s), and temperature (Degree Celcius).
7. Carry Rotating vane probe along with the instrument for measuring flow rate for axial fan outlet at the time of measurements. Attach rotating vane probe with the VelociCalc-9565-P-NB instrument (As shown in Figure 136).

(a) (b)

Figure 136. VelociCalc 9565-P-NB instrument along with (a) hot wire probe and (b) rotating vane probe.

8. Note down the fan number and location of the fan in datasheet for measuring flow rate at the outlet of the axial fan.
9. Note down the measurement location for different nodes as shown in Figure 137.

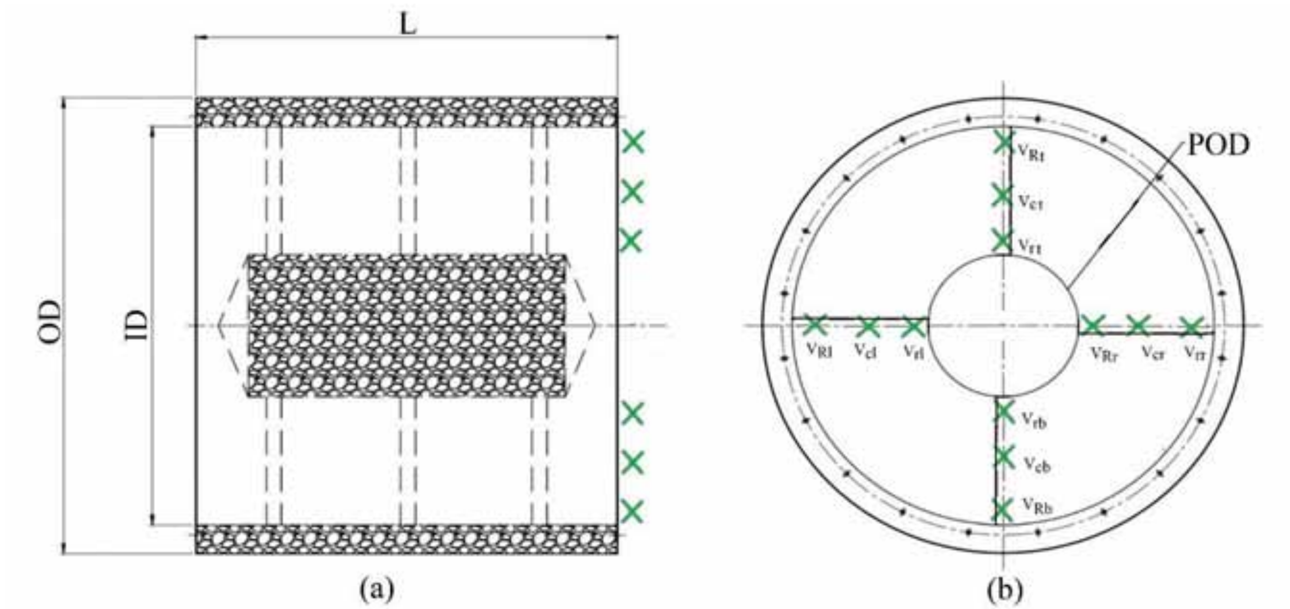

Figure 137. The silencer with nodes for vane probe locations (a) side view (b) front view.

Nomenclature for flow rate and velocity measurement in a radial manner at the outlet of the fan using rotating vane-probe of velometer instrument and same has been given in the attached datasheet such that

V_r: velocity at the nearest centre for an offset of 25 cm

V_c: velocity at the average radius or ~ (r+R)/2

V_R: velocity at the extreme edge of the fan i.e., 70 cm from centre

Again used the second subscript for circumferential manner such that if we are facing towards the fan then the center of the fan, one should be top, right, left and bottom

V_{rt}, V_{ct}, and V_{Rt}: velocity at the vertically top from the centre at the nearest edge, average radius and extreme edge of silencer drum respectively

V_{rr}, V_{cr}, and V_{Rr}: velocity at the horizontally right side at the nearest edge, average radius and extreme edge of silencer drum respectively

V_{rl}, V_{cl}, and V_{Rl}: velocity at the horizontally left side at the nearest edge, average radius and extreme edge of the silencer drum respectively

V_{rb}, V_{cb}, and V_{Rb}: velocity at vertically bottom side at the nearest edge, average radius and extreme edge of the silencer drum respectively

Total 12 node points from each fan.

10. To measure velocity with the help of a rotating vane probe to be placed at the initiated node point as per the airflow direction arrows given on the rotating vane probe. (Airflow directions are marked at the sides of the rotating vane probe.)

11. Wait for two minutes or more till the variation in the readings gets stable.

12. Keep observing reading on the display of the instrument for the velocity and flow rate. Wait for the stable reading. Start VelociCalc-9565-P-NB instrument for measurements. (Select 30 seconds per measurement for the particular node). Take measurements for all 12 nodes precisely if possible.

13. After the stable reading for 30 seconds, note down the velocity and flow rate shown on the instrument.

14. At selected each node, at least three readings at Vcr or Vcl (as shown in Figure 137) for velocity (flow rate calculated internally) should be done and noted in the datasheet.

15. Fill the data sheet with the measured values.

16. This procedure has to be repeated for all forty fans available in the air cleaning system.

17. After completion of the measurements stops VelociCalc-9565-P-NB instrument.

18. Follow this procedure at least twice a week.

Static Pressure Drop Measurement Protocol

The step by step procedure for measuring static pressure drop using VelociCalc-9565-P-NB (Make: TSI) Instrument is given below:

1. Before measurements: Check the frequency of the Axial fans from the SCADA system. Ensure that all fans are operating at the same capacity.
2. Make sure that an AA battery is available in the instrument and start the VelociCalc-9565-P-NB instrument.
3. Ensure required parameters are selected in the instrument for measurement.
    a. Flow measurement: Velocity, Flow Rate, and Temperature
    b. Static/Dynamic Pressure measurements: Pressure and Barometric/Atmospheric Pressure, and Temperature
4. Check the units of measurements such as velocity (m/s), flow rate (m^3/s), pressure drop (in-H_2O), barometric/atmospheric pressure drop (in-H_2O) and temperature (Degree Celcius).
5. Carry Neoprene rubber pipe and static pressure probe along with the instrument for measuring static pressure at the time of measurements. Attach static probe with neoprene rubber tubing and another end of neoprene rubber tubing with the positive port (as per the markings given on the instrument) of the VelociCalc-9565-P-NB instrument (As shown in Figure 139).

Figure 138. VelociCalc-9565-P-NB instrument.

Figure 139. Static pressure probe and neoprene rubber tubing.

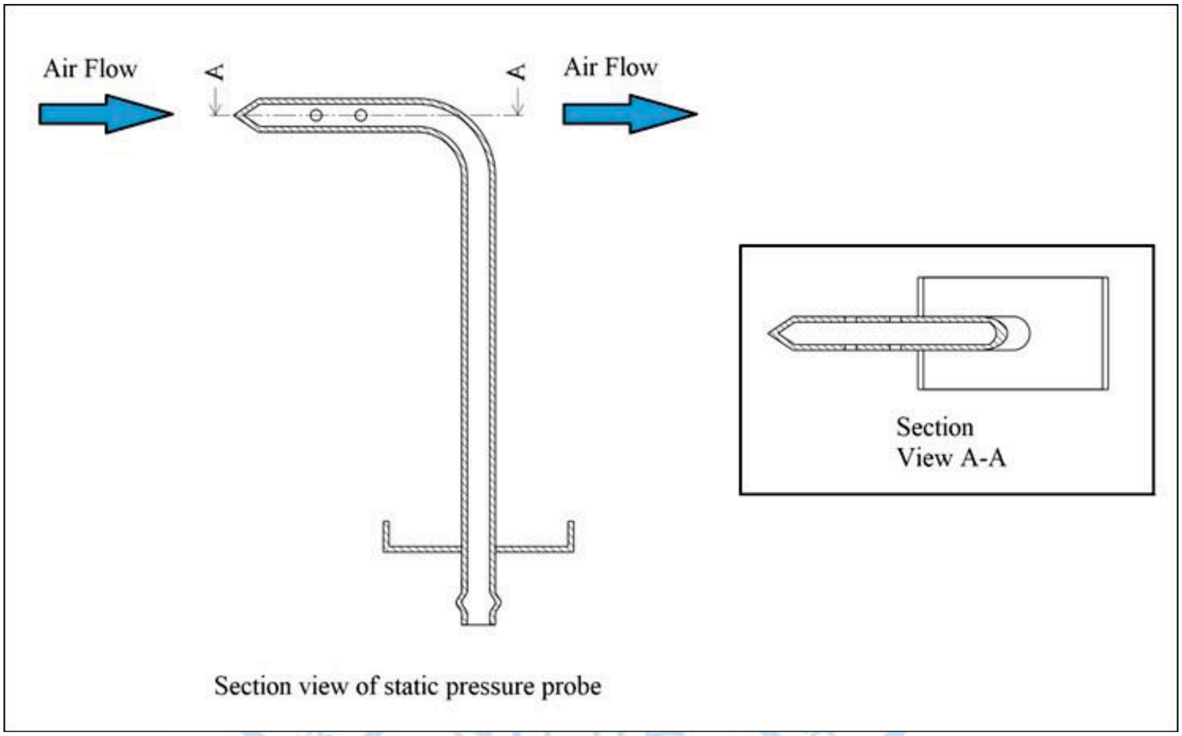

Figure 140. Section view of static pressure probe with airflow direction for measurements.

6. Select multiple locations from the filter frame (note the frame number and height) for measuring static pressure drop from the downstream side of the filter frame. (The selected filter frame should not be bend/dislodged filters).
7. The following figure shows the locations of the measurements of the static pressure drop for one side. Similar positions have to select for all four sides of the ACS.

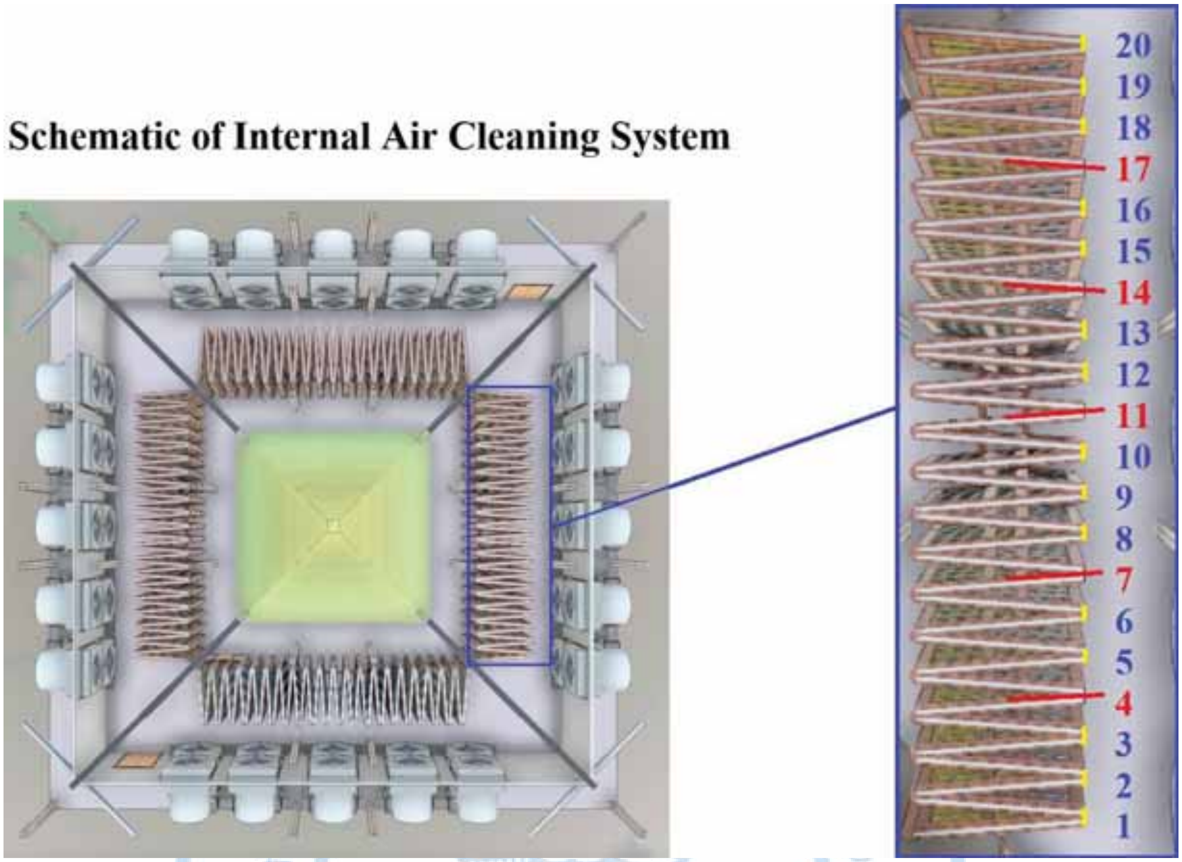

Figure 141. Top view of the locations for measuring the static pressure drop in the MSACS.

8. Note down the location inside the air cleaning system with respect to fan number and filter frame number. Make sure that the selected location is the same as measurements are done previously.

9. For all measurements of static pressure drop, the measurement locations should be the same for all times.

10. The following figure is given for understanding the locations of the measurements of the static pressure drop across filter bank, pre-filter and fine filter.

The static pressure drop across filter bank

The static pressure drop across the filter bank/array has to be measured as shown in the following figure. The location of the neoprene rubber tubing is adjacent to the filter media of the pre-filter available at the middle filter of the third row from the bottom.

Figure 142. Side view showing the height of the location of the end of neoprene rubber tube of setup for measuring the static pressure drop across filter bank.

Note: The one end of the neoprene rubber tubing is on the upstream side of the airflow (before filter bank) and another end is on the downstream side of the airflow (after filter bank).

II. The static pressure drop across pre-filter and fine filter

The static pressure drop across the pre-filter and fine filter have to be measured by keeping the static pressure probe as shown in the following figure. The location of the static pressure probe is passing through the gap of two pre-filters in the filter frame.

Static pressure drop across pre-filter: The Instrument has directly connected to the static pressure probe on the upstream side of the filter bank.

Static pressure drop across fine filter: The Instrument has connected to the static pressure probe on the downstream side of the filter bank as shown in the following figure.

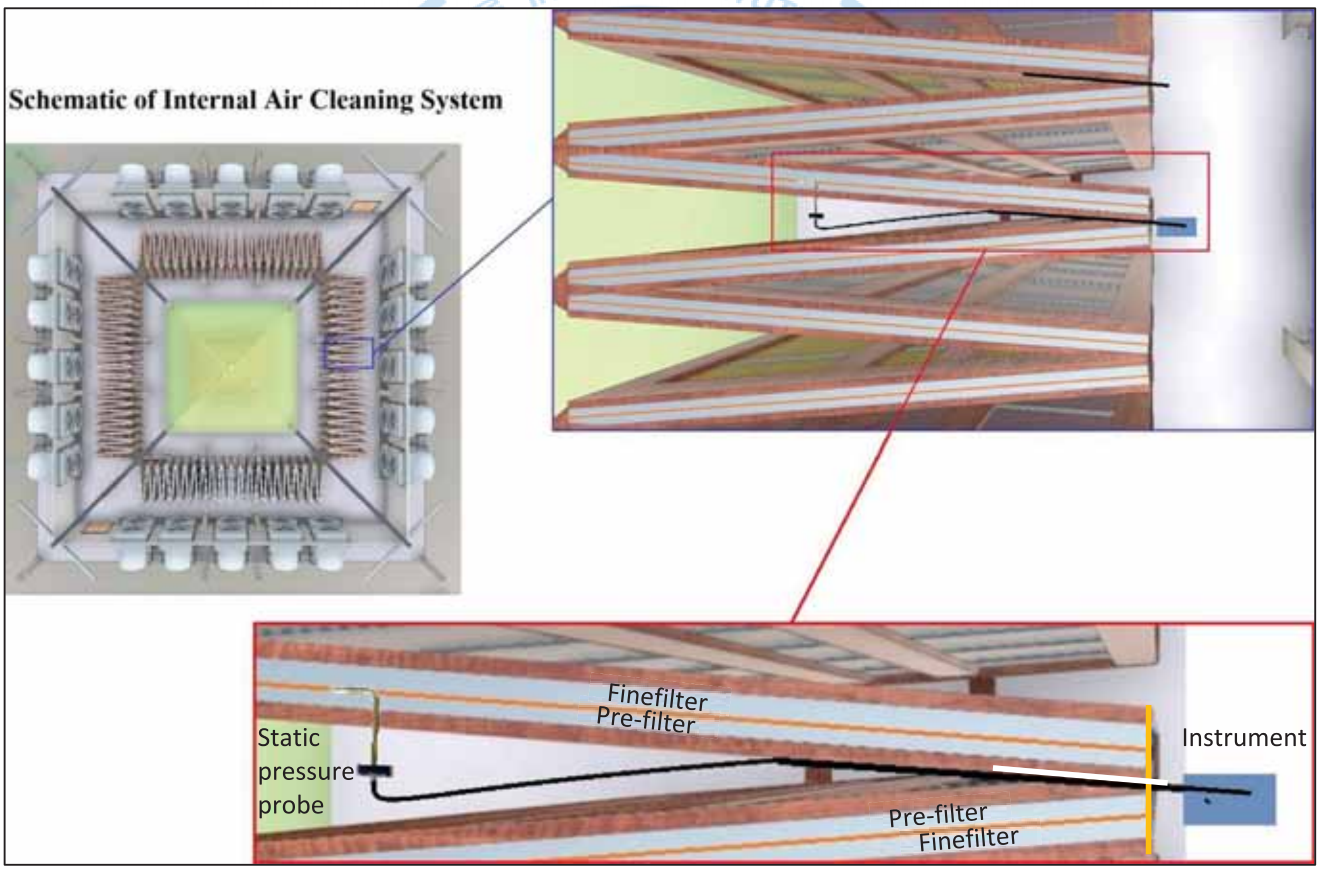

Figure 143. Top view of the location of the static pressure probe of setup for measuring the static pressure drop across the fine filter.

Note: While doing all the measurements the neoprene rubber tubing should not be blocked or pinched or bent throughout the length from one end to another end of the tube.

11. The filters should not be disturbed while inserting the static pressure probe between the two pre-filters for static pressure drop measurements across the pre-filter or fine filter as shown in the above Figure.

Figure 144. Side view showing the height of the location of the static probe of the setup for measuring the static pressure drop across the fine filter.

Note: For static pressure drop across pre-filter the instrument should be on the upstream side of the airflow (before filter bank). The static probe should be at the same position as measuring for the static pressure drop across the fine filter.

12. Make sure that the air is flowing over the holes as shown in Figure 140 for the static pressure probe.

13. At selected each location, at least three readings for pre-filter, fine filter and filter array (total static pressure drop) should be done to measure static pressure drop.

14. Wait for one / two minutes till the variation in the readings gets stable.

15. Keep observing the reading on the display of the instrument for the pressure drop and wait for the stable reading. Start VelociCalc-9565-P-NB instrument for measurements. (Select 30 seconds per measurement for the particular location). Take measurements for all four sides with maximum locations shown in Figure 141.

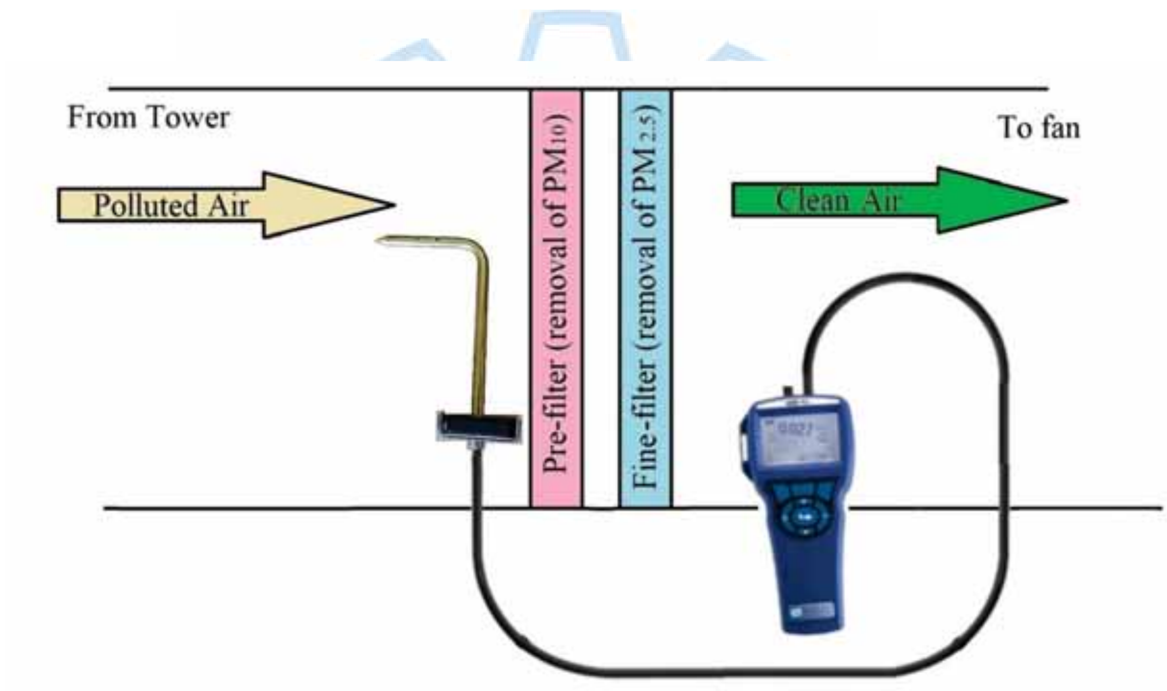

Figure 145. Schematic setup for measuring the static pressure drop across filter bank.

16. After the stable reading for 30 seconds, note down the pressure drop shown on the instrument. Also, note down the barometric/atmospheric pressure and temperature.

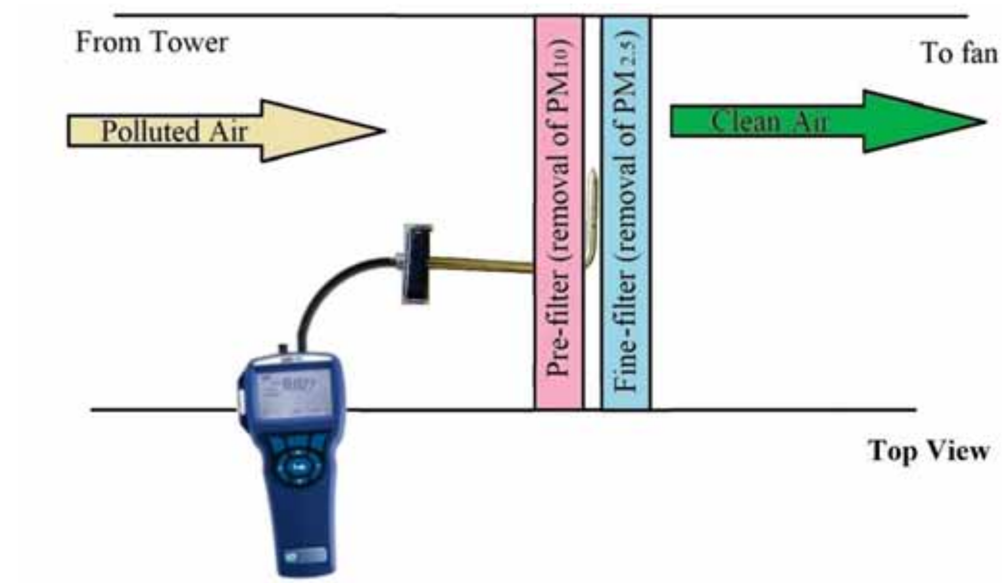

Figure 146. Schematic setup for measuring the static pressure drop across pre-filter.

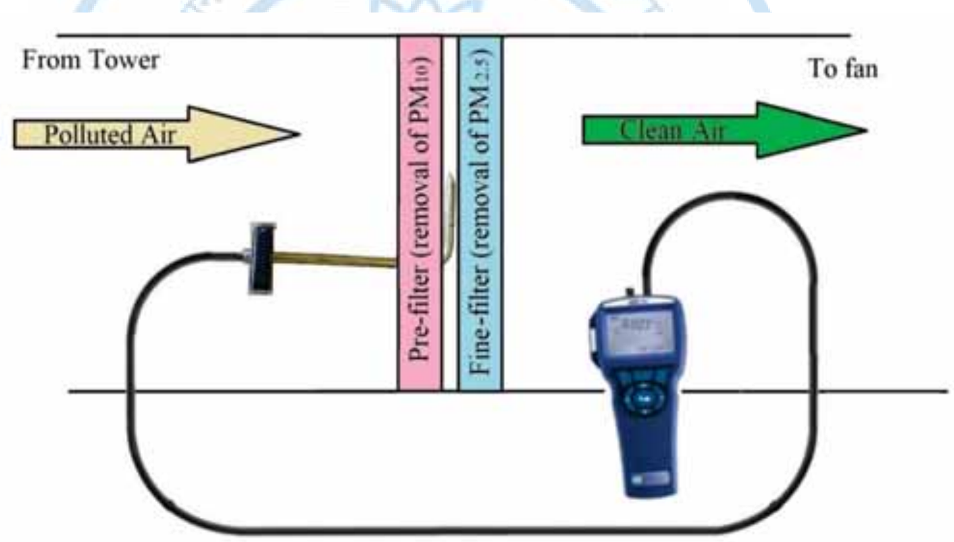

Figure 147. Schematic setup for measuring the static pressure drop across the fine filter.

17. Fill the data sheet with the measured values. (It should be shared with IIT Bombay for further analysis of the data)

18. After completion of the measurements stops the VelociCalc-9565-P-NB instrument.

19. Follow this procedure at least twice a week.

Data Sheet for Static Pressure Drop:

Static Pressure Drop (in-H_2O)

DPCC (Connaught Place)						
Person In-charge:- *At a centre for the side of filter bank						
Name:-				Instruments:- VelociCalc-9565-P-NB		
Date:				VelociCalc-9565-P-NB Instrument for ΔP		
Barometric Pressure: (in of H_2O)						
Direction	Location / Frame No.	Sr. No.	Pre-Filter (in-H_2O)	Fine Filter (in-H_2O)	Filter Array (in-H_2O)	Fan Operating Capacity (Hz)
SE	4	1				
		2				
		3				
SE	7	1				
		2				
		3				
SE	11	1				
		2				
		3				
SE	14	1				
		2				
		3				
SE	17	1				
		2				
		3				
NE	24	1				
		2				
		3				
NE	27	1				
		2				
		3				
NE	31	1				
		2				
		3				
NE	34	1				
		2				
		3				
NE	37	1				
		2				
		3				
NW	44	1				
		2				
		3				
NW	47	1				
		2				
		3				
NW	51	1				
		2				
		3				

	NW	54	1				
			2				
			3				
	NW	57	1				
			2				
			3				
	SW	64	1				
			2				
			3				
	SW	67	1				
			2				
			3				
	SW	71	1				
			2				
			3				
	SW	74	1				
			2				
			3				
	SW	77	1				
			2				
			3				

APPENDIX-III

Filter replacement work inside the MSACS

Figure 148. Filter replacement from filter bank.

Figure 149. Filter frame assembly cleaning prior to fresh filters placement.

Figure 150. Fine filter installation.

Figure 151. Fine filter installation in the filter bank.

Figure 152. (a) Fine and (b) Pre-filter installation work completed.

Air Quality Monitoring - Inside and outdoor

Figure 153. Inside Tower- Filter Measurement.

Figure 154. Outdoor Measurement.

Figure 155. Night time measurement.

Site Visit by IITB team

Figure 156. IIT Bombay team site visit.

Figure 157. Night-time measurements by the team.

Figure 158. Velocity & flow Measurement.

Figure 159. Moblie LCS Box for monitoring.

Maintenance of Monitoring Devices

E-BAM Maintenance

Figure 160. E-BAM Maintenance.

Figure 161. E-BAM shaft cleaning.

Figure 162. E-BAM assembly after cleaning.

Optical Aerosol Monitor cleaning

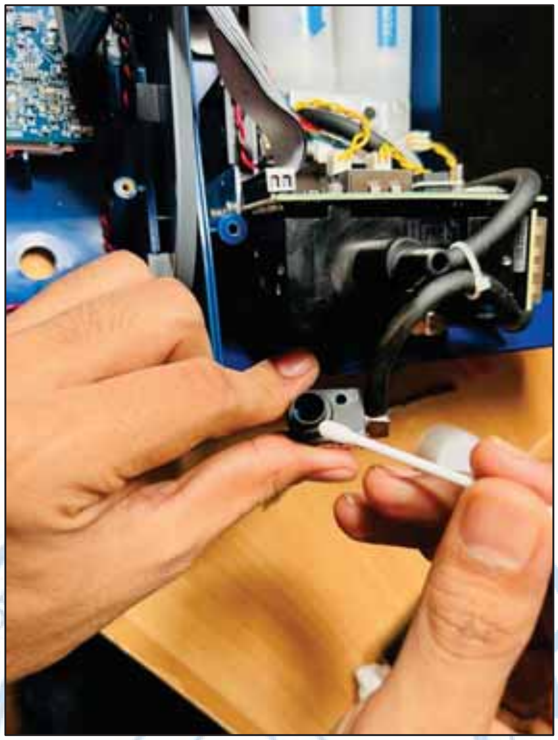

Figure 163. Inlet cleaning.

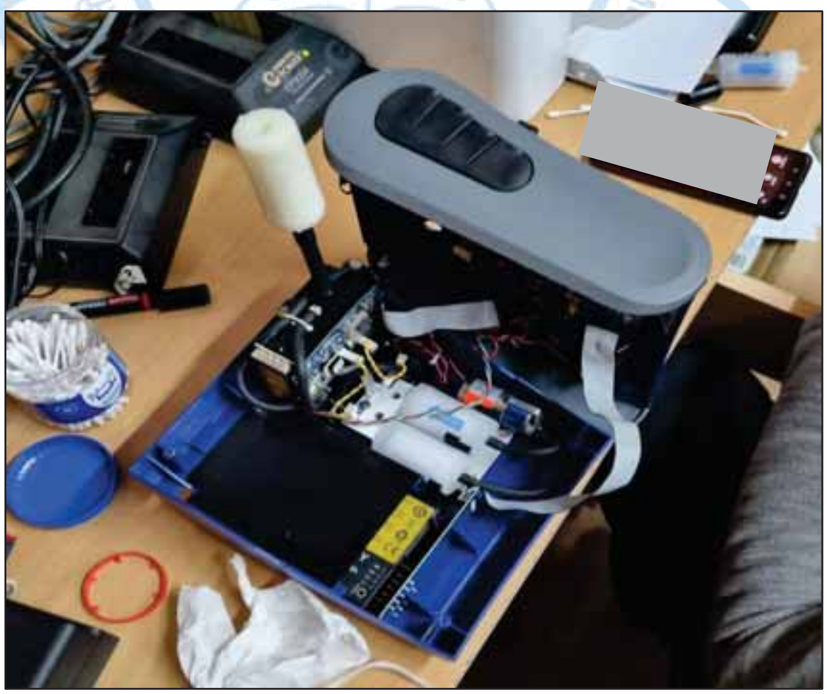

Figure 164. Calibration after device cleaning.

Figure 165. Optical particle sizer cleaning.

Figure 166. Fixed LCS Maintenance.

Figure 167. Filter weighing.

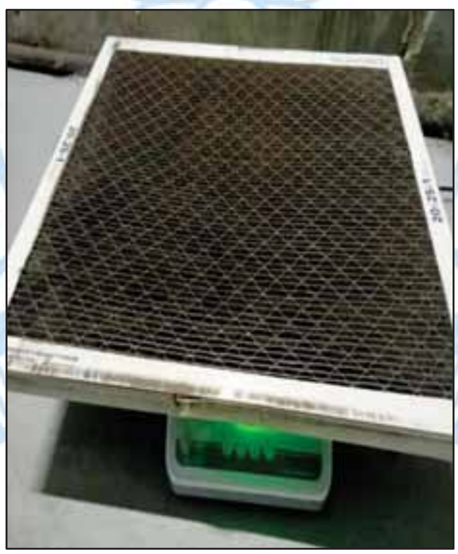

Figure 168. Dust load measurement on Fine filter sample.

Figure 169. Saturated pre and fine filter sample.

Figure 170. Filter sample collection.

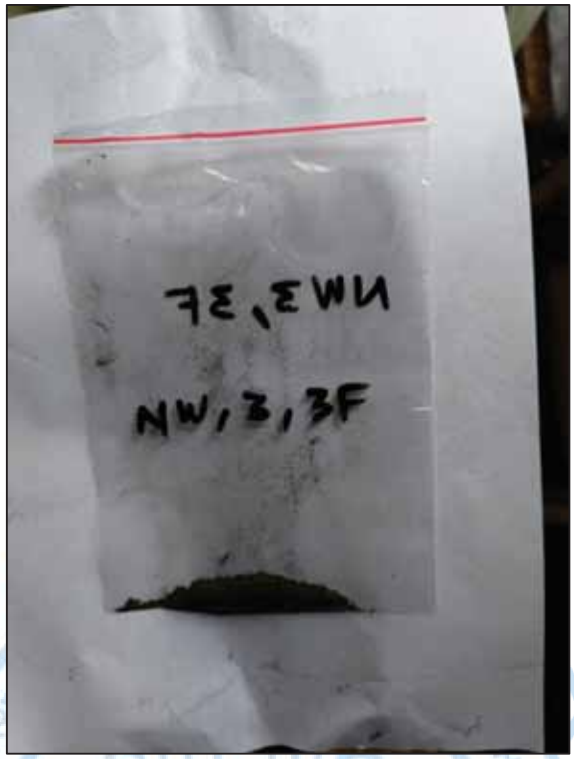

Figure 171. Collected dust sample.